

COMSAT

Technical Review

Volume 23 Number 1, Spring 1993

Advisory Board Joel R. Alper
Joseph V. Charyk
John V. Evans
John S. Hannon

Editorial Board Richard A. Arndt, *Chairman*
Olaleye A. Aina
S. Joseph Campanella
Dattakumar M. Chitre
Calvin B. Cotner
Allen D. Dayton
Russell J. Fang
Ramesh K. Gupta
Michael A. Hulley
Edmund Jurkiewicz
Lewis R. Karl
Ivor N. Knight
Amir I. Zaghoul

Past Editors Pier L. Bargellini, 1971–1983
Geoffrey Hyde, 1984–1988

Editorial Staff MANAGING EDITOR
Margaret B. Jacocks
TECHNICAL EDITOR
Barbara J. Wassell
PRODUCTION
Barbara J. Wassell
N. Kay Flesher, *Composition*
Virginia M. Ingram, *Graphics*
CIRCULATION
Merilee J. Worsey

COMSAT TECHNICAL REVIEW is published by COMSAT Corporation. Subscriptions, which include the two issues published for a calendar year, are: one year, \$20 U.S.; two years, \$35; three years, \$50; single copies, \$12; article reprints, \$3. Overseas airmail delivery is available at an additional cost of \$18 per year. Make checks payable to COMSAT and address to: Records Department, COMSAT Corporation, 22300 COMSAT Drive, Clarksburg, MD 20871-9475, U.S.A.

ISSN 0095-9669

© COMSAT CORPORATION 1993
COMSAT IS A TRADE MARK AND SERVICE MARK
OF COMSAT CORPORATION

COMSAT TECHNICAL REVIEW

Volume 23 Number 1, Spring 1993

- 1** ARCHITECTURES FOR INTELSAT COMMUNICATIONS SYSTEMS IN THE ISDN ERA
D. M. Chitre AND **W. S. Oei**
- 35** DESIGN AND VALIDATION OF THE ITALSAT AOCS FLIGHT SIMULATOR
A. Ramos, R. L. Minciotti, T. Hampsch, G. Allison, E. W. Hare AND **J. W. Opiekun**
- 61** THE EUTELSAT IN-ORBIT TEST SYSTEM
K. D. Fullett, B. J. Kasstan, W. D. Kelley, V. E. Riginos, P-H. Shen, S. L. Teller AND **Y. Tharaud**
- 101** MICROWAVE MEASUREMENT SYSTEM SOFTWARE
K. D. Fullett, W. D. Kelley, V. E. Riginos, P-H. Shen AND **S. L. Teller**
- 139** CTR NOTE: GEOSTATIONARY COMMUNICATIONS SATELLITE LOG FOR YEAR-END 1992
L. W. Kemp AND **D. C. May**
- 207** TRANSLATIONS OF ABSTRACTS
FRENCH 207 SPANISH 210
- 213** AUTHOR INDEX, CTR 1992
- 215** INDEX OF 1992 PUBLICATIONS BY COMSAT AUTHORS

Architectures for INTELSAT communications systems in the ISDN era

D. M. CHITRE AND W. S. OEI

(Manuscript received November 15, 1991)

Abstract

A series of INTELSAT satellite system architectures that support narrowband and broadband integrated services digital network (ISDN) services is presented. These architectures define an evolutionary path for the INTELSAT system, from its traditional role as a physical transmission medium, to more elaborate ISDN switching and signaling functions. By using the information available in ISDN signaling messages and performing certain enhanced functions within the satellite system as a subnetwork, system-specific technologies and inherent strengths can be exploited for better network functional support. In addition, possible deficiencies due to propagation delay can be removed. For broadband ISDN (BISDN), a separate migration path is described which fully matches the synchronous optical network and synchronous digital hierarchy transmission technologies. This approach can potentially evolve toward onboard processing of BISDN asynchronous transfer mode functions.

Introduction

A worldwide revolution is under way in the telecommunications environment, stimulated by rapid advances in digital technology and explosive growth in the information marketplace. Progress in information technology has led to significant changes in the generation and communication of information—both qualitative and quantitative, as well as verbal, pictorial, and numerical. The coupling of local area networks (LANs) with global communications networks can make information, database, and processing power available anywhere in the world. The essential infrastructure to realize

this vision of the "global village" is the integrated services digital network (ISDN).

The motivation behind the ISDN concept is the application of innovative technologies that promote competition among equipment vendors, improve and enhance service quality and diversity for carriers, and improve service for subscribers at lower total cost.

Narrowband ISDN (NISDN) will provide additional network features (supplementary services) such as calling and called party identity presentation; service and bandwidth flexibility; improved quality and network responsiveness; higher information transfer speed; network-based message handling (user-to-user signaling); and greater control by end users over their calls, including end-to-end terminal interworking. To evolve through transitional periods with communications over dissimilar networks, a number of interworking solutions have been devised which support interfaces between the ISDN and networks such as the public switched telephone network, the packet-switched public data network, the circuit-switched public data network, and other ISDNs.

The above ISDN service features and network functions rely on network information contained in stored-program-controlled exchanges, combined with enhanced subscriber and interoffice common channel signaling. Within the network, the ISDN will use Common Channel Signaling System No. 7 (SS7), with the ISDN user part (ISUP), the signaling connection control part (SCCP), the transaction capability application part for enhanced services such as 800 service, and the operations and maintenance application part for signaling network management. At the subscriber access level, the common channel signaling is Digital Subscriber Signaling System No. 1 (DSS1) over either a 16-kbit/s (basic access) or 64-kbit/s (primary access) D-channel. Apart from signaling, the D-channel can also be used for relatively low-speed data communications (e.g., credit card validation).

Another new network service is the software-defined virtual private network for use by multinational subscribers. This is an innovative network-based alternative to private networks interconnected by permanent leased lines. The telecommunications deregulation that is spreading globally will stimulate the interest in such value-added network service for inter-corporate private networking on an international basis. Both non-ISDN services and virtual private networks employ remotely controllable network facilities (e.g., digital cross-connects and multiplexers), as well as stored program control capabilities in public network exchanges.

The prospect of fiber optic technologies replacing copper-wire subscriber loops will open up a considerable amount of end-to-end bandwidth, preparing

the way for future broadband ISDN (BISDN). In parallel, advances in very large-scale integration technology are creating new possibilities for the design and implementation of multigigabit-per-second switches for BISDN nodes. The BISDN is expected to be based on a new form of fast packet switching known as asynchronous transfer mode (ATM), which is an innovative network transport concept that employs a single switching fabric common to all narrowband and broadband telecommunications services. ATM is a cell-based transport system in which each cell is of constant size (53 bytes) and has a 5-byte header that includes routing information.

Recently, alternative network technologies have emerged which, given their current level of maturity, are likely to be implemented to meet more immediate service needs prior to the time when BISDN ATM becomes a commonly accepted network solution. These pre-BISDN technologies are inter-LAN communications that employ frame relay network services at T1 and E1 bit rates, and switched multimegabit data service (SMDS) operating at 45 Mbit/s in the U.S. The SMDS technology is based on switching and multiplexing short, 53-byte cells, and can be seen as a predecessor to the ATM technique for BISDN. These two candidate network technologies are geared toward intra-corporation, high-speed data communications over higher bit rate, high-quality leased digital connections. They are being advertised as the vehicle for higher throughput and faster network transport of bursty data communications traffic. Metropolitan area networks operating at 100-Mbit/s rates represent a third network technology, which is expected to integrate data and voice communications over a common ATM-like transport network composed of high-speed internetwork nodes and leased digital connections. The faster cross-network times of these new technologies are a direct result of the high quality of modern transmission media. Very low error occurrences permit considerable reduction of processing within the networks, especially the elimination of node-to-node error handling by acknowledgment and retransmissions protocols. This in turn leads to a need for effective congestion-control mechanisms to handle traffic surges.

Effects on international satellite systems

Most of the new network services described above will present themselves to the INTELSAT system as an increase in demand for digital satellite leased connections. Growth will also occur in existing and future connections that are part of public switched networks (digital PSTN and public ISDN). For almost any new development in telecommunications networks, conventional wisdom has assumed that the only role for satellites will be to provide higher

bit rates and better bit-transparent transmission facilities for both PSTN and leased connections.

It is frequently stated that the geographical advantage of satellites facilitates the provision of network services on a global basis. However, further investigation has shown that the provision of digital transmission (open systems interconnection [OSI] layer 0) capability alone is insufficient. Offering traditional, static transmission pipes without additional features has several drawbacks and consequences.

Certain ISDN and non-ISDN (data) services will experience discernible quality-of-service (QOS) degradation due to the inherently long satellite delay. Also, early and frequent congestion is experienced on satellite fixed-capacity connections, especially on the more dispersed thin routes and high-bandwidth services. Alternatively, satellite routes may be engineered to achieve acceptable QOS levels, although this would result in inefficient use of the system. The resource efficiencies that could be achieved with any form of call concentration, point-to-point switching, and (for selected communications types) point-to-multipoint mode would remain unexploited. The multipoint/multidestination features of satellites could be offered as value-added network support for specific communications service connectivities and network capability requirements not easily met with terrestrial connection.

This paper evaluates the design philosophies of satellite communications systems in view of current telecommunications network developments. Specifically, for INTELSAT, new alternatives are presented for retaining the role of the system as the international communications interconnection between the national networks of signatories and users. This process does not preclude system functional enhancements in terms of architectural makeup, functional integration or separation, level of intelligence, technology compositions, and so forth. As an international network interconnection facility, INTELSAT's adaptations to these network trends should not be customized to specific network services, but instead should be able to accommodate and support a large spectrum of telecommunications services with virtual service transparency.

Based on current and projected telecommunications and network service needs, the overall impact of the latest technical developments on public and private telecommunications networks is assessed. Three key requirements must be satisfied by the satellite system: connectivity, adaptability to the various bandwidths of ISDN services, and QOS. These requirements translate into functional determinants for the satellite system architectural design, and for migration of the INTELSAT satellite communications systems. The five functional determinants identified for future enhanced satellite systems are described below.

Transmission quality and bandwidth

On heavy traffic routes, quality and bandwidth requirements for satellite connections will tend to be determined by the submarine fiber optic cables sharing these routes. These cables will be used for high transmission bit rate connections (e.g., synchronous digital hierarchy [SDH]) supporting a range of low- and high-bandwidth services, from voice to digital video. It is expected that such connections will have a bit error rate (BER) of 1×10^{-9} or better. High-bit-rate services will always demand high transmission quality.

It is also prudent to establish the quality requirements for lower bit rate satellite transmission links on medium and thin routes at the same levels as for thick routes. From a service viewpoint, the accuracy and integrity of the resulting end-to-end, user-perceivable QOS parameter information should not be route- or destination-dependent.

Resource time- and space-sharing

For satellite systems, the available absolute bandwidth, power, and orbital slots are limited. The large service area typical of satellite systems amplifies these limitations on a per-link basis. Sharing time and space resources within the satellite system enables more efficient use of these valuable resources, while supporting new service applications with a higher bit rate per service. The efficiency is gained by exploiting the statistical independence of various sources of calls, and through call concentration and call switching. Such techniques are especially effective on lower rate satellite connections.

Dispersed network connectivities

Satellite systems have an advantage over terrestrial systems in terms of their flexibility in interconnecting networks at any geographical location and network hierarchical switching level within their coverage area. The multicapability ISDN, as a network, may benefit from this satellite-dispersed networking feature for optimum, nonhierarchical network structuring. The concept, based on small earth stations spread over a larger number of terrestrial network "landing points," is more acceptable in today's evolving deregulated telecommunications environment.

Delay effect compensation

Independence from the transmission medium is a criterion for the virtual transparency of the network as a whole to telecommunications services. The long cross-network signal transfer time encountered over satellite connections often manifests itself as end-user-perceived degradation of data communications

protocol throughput. These protocols are used in certain telecommunications services, such as those based on packet switching, and QOS degradation is incurred when the protocol operating parameters are selected improperly. The relative throughput degradation is proportional to the connection bit rate under an error-free environment.

Techniques to compensate for the effect of satellite delay on data protocols are currently in use in dedicated (private) data networks. Service transparency of the ISDN requires selective application of protocol conversion or adaptation techniques internal to the network, possibly as part of the satellite subnetworks.

Multipoint network connection structure

The multipoint value of certain ISDN teleservices or bearer services, as well as multiparty and conference call ISDN supplementary services, normally requires special arrangements (*e.g.*, bridges, and the signaling procedures to activate them) of the ISDN exchanges in the essentially point-to-point-oriented ISDN. The satellite transmission system is well-suited to wide-area bridging, with considerably less network resources and facilities than would be necessary with terrestrial systems. The per-call establishment of satellite-based multipoint connectivities would need to be controlled by appropriate network signaling procedures.

NISDN-compatible INTELSAT satellite communications subnetwork

In the architecture described below, the satellite system provides nonswitched point-to-point transmission for international transit links between national NISDNs. In this role, the earth segment of the satellite system does not need ISDN call-addressing information, as no call routing is performed. Thus, the satellite network appears to be a point-to-point link between two switching centers carrying ISDN traffic. The satellite system essentially provides the transmission function of either a national or international transit connection element. The switching center connected to the earth station contains the functions necessary to interpret call-addressing information according to the ISDN international numbering plan, and any interworking functions needed to connect dissimilar ISDNs. Dedicated trunks must be established between each communicating pair of switching centers "logically extended" through the satellite subnetwork. In addition, trunk groups must be provisioned to match service characteristics, because service-related information is not available directly to the earth station due to the lack of ISDN signaling capability.

Categories of functions

Two new categories of functions are incorporated into this architecture to enhance the support of ISDN services, and one support function category results from the other two.

CATEGORY 1: SINGLE AND MULTIRATE CIRCUIT-MODE BEARER SERVICE SUPPORT FUNCTIONS

To efficiently support unrestricted ISDN circuit-mode bearer services such as 2×64 kbit/s, 384 kbit/s, 1,544 kbit/s, and 1,920 kbit/s in this architecture, the satellite subnetwork performs call concentration on a wide-area-network (WAN) basis, whereby appropriate satellite capacity is assigned on demand, call by call. ISDN traffic pertaining to services such as 64-kbit/s unrestricted transfer, and services requiring $N \times 64$ kbit/s capacity, are accommodated efficiently using a pool of 64-kbit/s channels accessible to all earth stations in the community.

CATEGORY 2: PROTOCOL CONVERSION FUNCTION

Packet-mode bearer services, frame-mode bearer services, and teleservices that use packet protocols employing circuit-mode bearer services may experience general performance degradation due to the long propagation delay introduced by the satellite system. This degradation results mainly from the use of suboptimum protocol parameters for operation within a satellite environment. Protocol conversion techniques are used to overcome these drawbacks.

The protocol conversion function (PCF) is an ISDN facility logically associated with routing decisions in ISDN exchanges. It is activated selectively, depending on the ISDN call type and call routing. The process can be considered an internal ISDN interworking function. The PCF ensures transparency to ISDN services when calls are routed over satellite connections. The protocols involved include ISDN communications protocols contained in-band, with delay-sensitive operating parameters at OSI layers 2 and 3 associated with some ISDN bearer services and/or end terminals. Also included are delay-sensitive ISDN protocols and network-provided interworking (or OSI) lower layer interworking procedures. The undesired effects of satellite delay are poor performance, or even failure, of these protocols when operated over 64 kbit/s or $N \times 64$ -kbit/s connections (H11 and H12 connections). The PCF essentially converts such protocols into one of a small number of satellite-optimized common protocols used over the satellite connection segment.

CATEGORY 3: SIGNALING SUPPORT FUNCTIONS

Some signaling capabilities are necessary within the satellite subnetwork to support category 1 and 2 functions. The degree of access to ISDN SS7 network signaling and satellite system internal signaling capabilities depends to a great extent on the satellite system's functional architecture and on the way the two supported functionalities are implemented.

For concentrating or switching ISDN calls over the subnetwork, per-call handling of connection within the satellite subnetwork requires connection control, either as part of, or derived from, ISDN signaling. Two basic approaches are conceivable. The first consists of full functional integration of satellite subnetwork signaling into the SS7 network, with the SS7 signaling point codes assigned to the satellite subnetwork acting as a transit exchange. In the second approach, connection control is derived from the ISDN signaling network through the ISDN exchanges "suspended" by the satellite subnetwork. The first method is appropriate when true switching is performed by the satellite subnetwork, while the second is more suitable if the subnetwork under consideration is performing a wide area concentration function without call switching and routing.

For PCF, a number of implementations are conceivable. Stand-alone PCF can occur, either remotely (*e.g.*, in the earth stations) or collocated with ISDN exchanges. This approach would require call information exchange over a dedicated signaling arrangement between the ISDN exchange and the stand-alone PCF, based on principles similar to those employed in the international switching center (ISC) digital circuit multiplication equipment (DCME) signaling system defined in International Telegraphy and Telephony Consultative Committee (CCITT) Recommendation Q.50. In a more integrated approach, tight functional interactions could occur with internal ISDN exchange functions.

Access to ISDN SS7 messages is required in any case so that the network interworking function associated with satellite routing and PCF can detect, during call setup, known delay-sensitive ISDN in-band communications protocols (*e.g.*, those currently encoded in the ISDN DSS1 and those under discussion in international standards committees), as well as delay-sensitive ISDN protocols. Access is also necessary to invoke the PCF that terminates the protocol locally, selects and inserts one of a small number of satellite-optimized common protocols, and requests that the other end of the link perform the reverse processes.

Subnetwork functional architecture

Figures 1 and 2 are composite functional block diagrams of the satellite subnetwork and earth stations, respectively. All new functionalities for enhanced

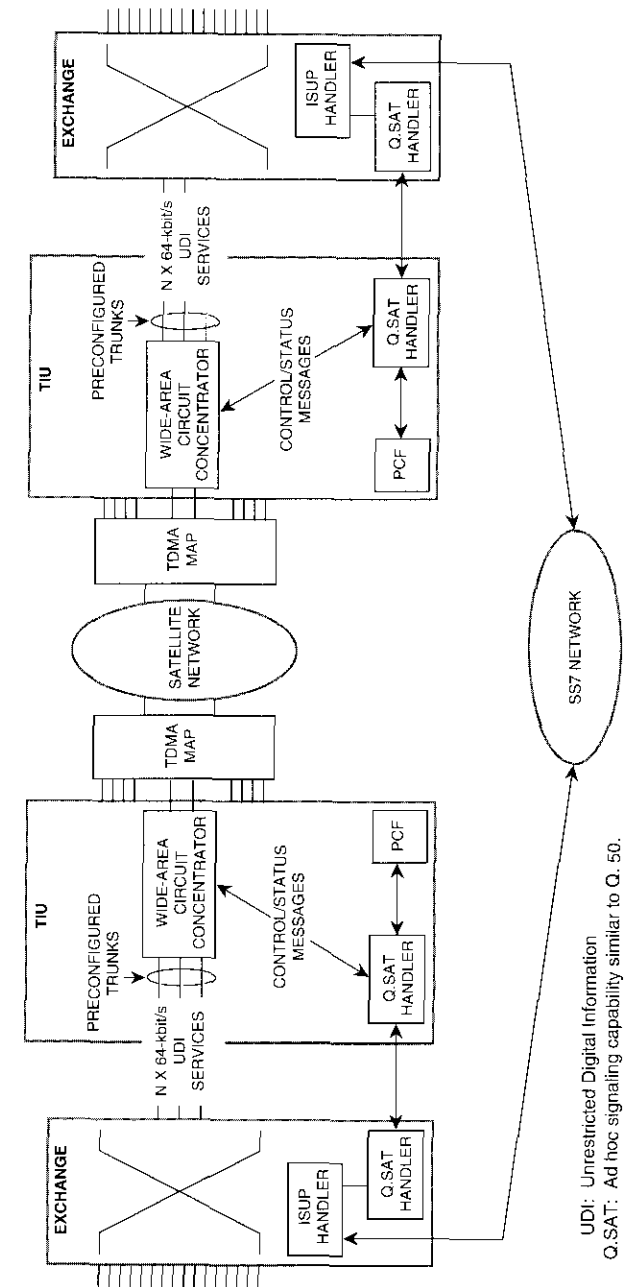


Figure 1. NISDN-Compatible Subnetwork Architecture

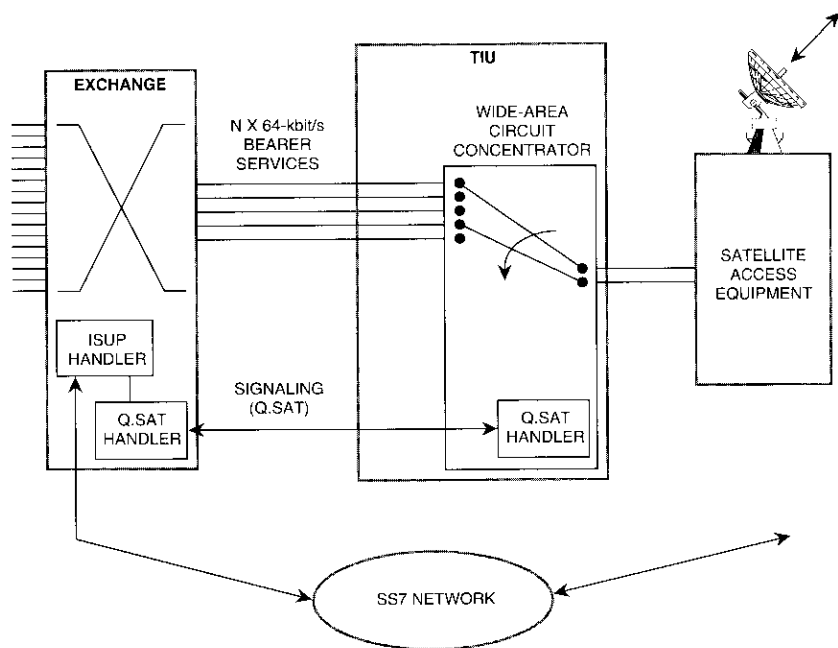


Figure 2. Satellite Access to Exchange Interfacing via Earth Station TIU

NISDN service support are collected in a functional grouping called the terrestrial interface unit (TIU). The interfaces to a TIU are as follows:

- Terrestrial trunk interface from the switching center
- Internetwork signaling subsystem
- Time-division multiple access (TDMA) capacity manager
- Intranetwork signaling subsystem
- Satellite protocol conversion subsystem.

Operation of the wide-area circuit concentration in the TIU centers on the fact that the terrestrial switches do not make full use of trunk capacity when supporting $N \times 64$ -kbit/s services. When dedicated satellite trunks are preallocated to connect terrestrial trunks, valuable satellite capacity may remain unused. Therefore, sharing the satellite channels among the terrestrial trunks will result in more efficient use of satellite resources. The amount of satellite capacity saved will depend on the service mix and the service-provisioning techniques used in the terrestrial network to support these services.

A stand-alone PCF is located remotely in the earth station TIU functional grouping in order to relieve the terrestrial network exchanges of additional satellite subnetwork functions.

Subnetwork signaling support

The subnetwork architectural design and functional grouping determine the signaling support functions and interfaces. Overall, subnetwork signaling is divided into three segments:

- Segment 1. External Signaling* among terrestrial switching centers external to the satellite network.
- Segment 2. Internal Signaling* among earth stations and the satellite network controller.
- Segment 3. Dedicated Internetwork Signaling* between a terrestrial switching center and an earth station.

Figure 3 depicts the relationship among the three signaling groups.

SEGMENT 1: EXTERNAL SIGNALING

External signaling here refers to ISDN signaling capability (*i.e.*, SS7). The terrestrial switching centers use the message transfer part (MTP) protocol (refer to the Appendix, CCITT Rec. Q.701–Q.704) to exchange ISUP signaling messages over point-to-point signaling links. For international signaling, the links may be provided by the satellite network transparently, or by terrestrial or undersea cables. In either case, the ISUP signaling messages and information are normally not accessible to the earth station.

The ISUP in the SS7 protocol provides the signaling functions required to support basic bearer services and supplementary services for voice and non-voice applications in an ISDN. The ISUP uses the MTP (and in some cases the SCCP) to transfer signaling and control information between network switching and signaling nodes.

The ISUP messages are carried in the signaling information field of the MTP signaling units. A message may consist of the following parts:

- Routing label
- Circuit identification code (CIC)
- Message type code
- Mandatory fixed part

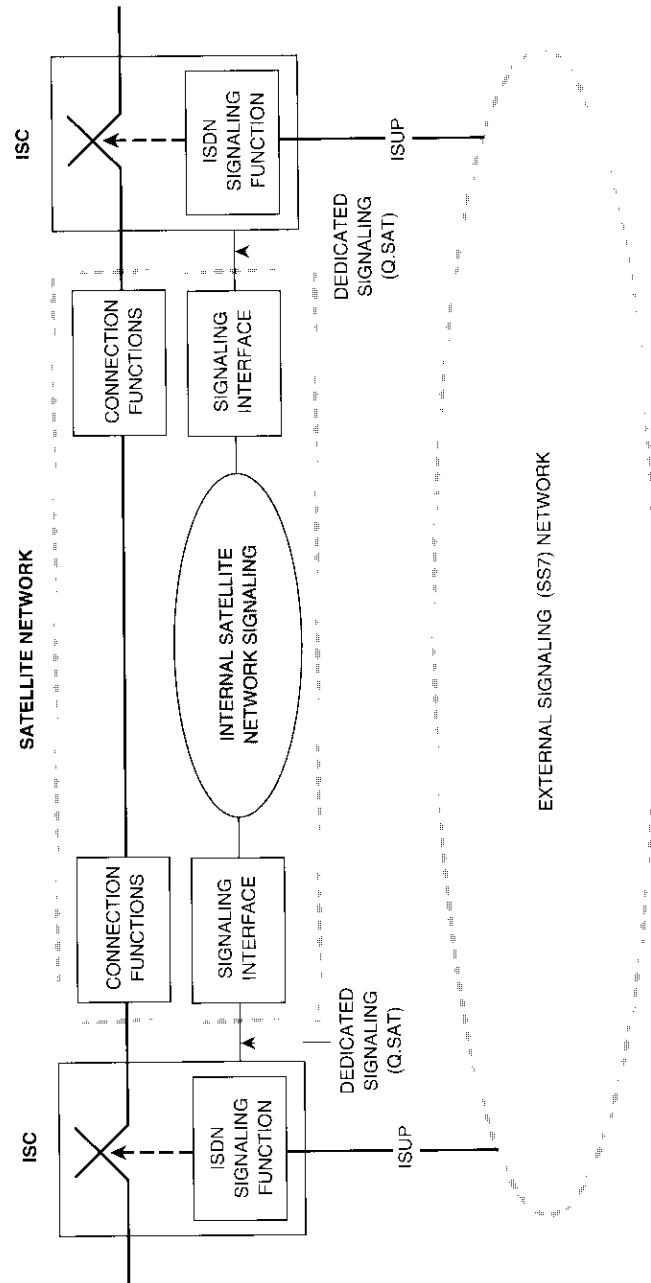


Figure 3. Signaling Requirements of a Satellite System to Support ISDN Services

- Mandatory variable part
- Optional part (which may contain fixed- and variable-length parameter fields).

A set of signaling procedures is defined for the setup and release of national and international ISDN connections. The basic call-control procedure is divided into three phases: call setup, data/conversation, and call clear-down. When an originating switching center has received complete selection information from the calling party and has determined that the call is to be routed to another switching center, it selects a suitable, available, interswitching center circuit and sends an initial address message (IAM) to the succeeding center. The CIC field of this ISUP message carries the identifier of the available circuit. The routing information either is stored locally or can be obtained from a remote database. The setup message also contains bearer capability information, which is analyzed by the originating switching center to determine the correct connection type and network signaling capability. This information is then mapped into the user service information parameter of the IAM.

Information received from the access interface is used to set the transmission medium requirement (TMR) parameter, while the bearer information received is used to set the initial mode of the connection. The connection types allowed are speech, 3.1-kHz audio, 64-kbit/s unrestricted, alternate speech/64-kbit/s unrestricted, and alternate 64-kbit/s unrestricted/speech. The IAM conveys that the indicated circuit has been seized.

When $N \times 64$ kbit/s ($N \geq 2$) connections are required, the basic procedures for single 64-kbit/s connections are used to control contiguous 64-kbit/s channels between exchanges.

SEGMENT 2: INTERNAL SIGNALING

The internal (or network) signaling of the satellite network consists of signaling functions related to ISDN connection control and satellite network management. For network management, internal system signaling is used to coordinate (infrequent) capacity reassignments to traffic terminals, under supervision of the Network Control Center (NCC). The initiation of such reassignments depends on the traffic load distribution across the various communicating traffic terminals, and can be done either automatically (based on local load measurements and some cooperative decision algorithms) or manually by the system operator at the NCC.

For ISDN per-call connection control, internal system signaling between ISDN entities in correspondent traffic terminals is used to coordinate, on a call-by-call basis, the terrestrial-channel-to-satellite-channel assignments (including

time slot groupings) for $N \times 64$ -kbit/s connections between pairs of traffic terminals. It is also used for call-by-call coordination of the identification and invocation of appropriate satellite protocol conversion functions for certain types of ISDN communications protocols.

The specifics of the per-call signaling mechanism will depend on the internal satellite subnetwork system selected. A low-rate TDMA system is considered below to illustrate intranetwork signaling issues. This signaling capability can be achieved by one of two methods. The first employs the satellite common channel signaling system, in which signaling information from a source TIU to a destination TIU passes through the NCC. The earth stations send this information using inbound (to NCC) orderwire channels available in the signaling/status burst (SB) assigned to that earth station. The source earth station sends a (forward) channel assignment inbound orderwire message containing the value of N , time slot sequence integrity information, and destination trunk identification information. The NCC relays this message to the destination earth station after validating and logging it locally for statistical and monitoring purposes. The destination earth station acknowledges the assignment by sending an explicit acknowledgment message containing reverse channel assignment messages (effectively lengthening the call setup time).

Call setup time may be reduced by eliminating the acknowledgment and letting the source earth station select both the forward and reverse channels based on information accumulated in a local database. This introduces a finite probability that the destination earth station will assign overlapping forward or reverse channels to an incoming call. With the use of well-protected bursts, a feed-forward signaling system may be employed which does not require explicit acknowledgment of assignment messages. The SBs could use forward error correction to introduce sufficient redundancy in signaling information. Use of a feedback signaling system increases call setup time.

A second method for conveying inter-TIU signaling is to use a direct signaling channel that carries all channel assignment information. In this case, the SB channel carries signaling information directly between the earth stations. By proper selection of burst time plans (BTPs), SBs can be made receivable by a set of earth stations. As a broadcast burst, the SB can be received by a group of correspondent earth stations, in addition to the network controller, and can be used to carry call setup-related signaling among earth stations, with the NCC as a passive monitor (e.g., gathering call statistics) in the process. This scheme introduces a single-hop delay in call setup time and offers better delay performance than the previous scheme, which used the satellite common channel signaling system.

SEGMENT 3: DEDICATED INTERNETWORK SIGNALING

To control satellite system functions on a call-by-call basis, the earth station equipment must have access to a subset of ISDN signaling information from the SS7 network. The switching centers can provide this information by extracting relevant signaling parameters from ISDN messages, as described later. The center then uses separate standard and/or proprietary signaling protocols to communicate this information to the earth station equipment.

To support ISDN services such as speech, 3.1-kHz audio, and especially on-demand 64-kbit/s unrestricted digital information transfer via DCME, dedicated signaling is provided using an international standard given in CCITT Rec. Q.50. The switching center uses a Q.50 signaling link to the DCME to transmit circuit seizure and release messages for on-demand connections, receive acknowledgments and circuit status from the DCME, and perform maintenance functions. At the earth station, this Q.50 link is terminated within the DCME. Therefore, the signaling procedures used to support these services are transparent to the rest of the earth station equipment. The DCME communicates with remote DCMEs at other earth stations via an inter-DCME assignment signaling channel.

In the NISDN satellite subnetwork architecture, a small number of satellite channels are allocated on demand to a large number of incoming terrestrial channels, based on system engineering and traffic analysis. It is assumed that the service profile of the traffic on each route within the coverage area will provide sufficient burstiness to make efficient use of satellite resources through call concentration. This also means that there may not always be sufficient satellite capacity available to meet the incoming demand, leading to blocking in the satellite system.

Efficient support of ISDN multirate services ($N \times 64$ -kbit/s UDI transfer) can be provided by an arrangement similar to the DCME case described above, using signaling between a switching center and an earth station TIU to indicate service requests. This signaling can be used to perform multirate call setup and release, perform satellite protocol conversion on links supporting other data transfer services, communicate resource availability for these services to the switching center, and so forth. Since there is currently no CCITT standard for the exchange of such information, an ad hoc signaling capability similar to Q.50 is identified and referred to here as Q.sat.

Messages

A number of messages are necessary for the Q.sat signaling capability to accomplish the functions listed above. The first group of messages conveys

channel availability information, and the corresponding acknowledgments, from the TIU to the switching center. This message group contains information about the number of 64-kbit/s channels available for unrestricted information transfer. An acknowledgment message from the switching center confirms correct receipt of the status information. A reliable communications protocol is necessary between the switching center and the TIU to ensure correct transmission and reception of this vital information.

The second set of messages consists of the $N \times 64$ -kbit/s call setup/disconnect information flow and corresponding acknowledgments, which result in the assignment of satellite capacity to a call. These messages are similar to the call setup/disconnect messages and their acknowledgments specified in Rec. Q.50.

Since this architecture does not support switching capability in the satellite network, these services are supported over dedicated trunks that are preconfigured between the switching center and the earth station at network configuration time. The trunks' fixed correspondence between the switching center and the earth station allows for the unambiguous CIC used in the ISUP message.

The Q.sat seizure request message carries the following information:

- Incoming trunk/channel identification (corresponding to the CIC of the IAM).
- Number of incoming channels (corresponding to the TMR of the IAM).
- Lower-layer protocol information for satellite protocol conversion.

The earth station sends the following information to the switching center over a Q.sat link:

- Accept/reject (blocked) message in response to a circuit seizure message received from the switching center.
- Acknowledgment of circuit release message status information consisting of duplex channel availability within the satellite system between this earth station and its correspondent earth stations (updated periodically).
- Maintenance-related messages for trunks.

The third set of messages consists of those required for maintenance. They describe the status (out of service/in service) of individual terrestrial and space channels, loopback test pass/fail, link status, error performance on the space segment, new capacity allocation within the space segment resulting from time plan changes, and so forth. These messages may also require acknowledgment.

A fourth set of messages is used to administer protocol conversion functions within the satellite system.

Q.sat message communications protocols

A message-based protocol can be used to support Q.sat signaling information transfer. For a message-based protocol at the physical level, a 64-kbit/s digital channel could control a sizable number of trunks. At the link level, a point-to-point, error-correcting, high-level data link control (HDLC)-class protocol will provide the expected performance.

For communication over short distances, better performance can be obtained without error-correcting protocols. Since the signaling messages in question are independent of each other, a datagram transport service may be appropriate, as opposed to a connection-oriented scheme. An architecture based on an MTP-like protocol provides the features required for such a transport link.

Call processing

Figure 4 depicts a successful ISDN call setup and disconnect phase to support $N \times 64$ -kbit/s unrestricted bearer services that use a TIU in a satellite network. The following sequence describes the end-to-end call setup signaling.

STEP A: USER/LOCAL EXCHANGE SIGNALING (REC. Q.931)

When a user initiates a call, the terminal equipment sends a Q.931 SETUP message to the local switching center. This message contains such information elements as bearer capability (and optionally transit network selection), low-layer capability, called party number, and called party subaddress.

STEP B: LOCAL EXCHANGE/INTERMEDIATE EXCHANGE SIGNALING (REC. Q.763)

When the originating (local) switching center receives complete selection information from the calling party and determines that the call is to be routed to another switching center, a suitable and available interexchange circuit is selected. An IAM is then generated and sent to the succeeding switching center. Appropriate routing information is available at the originating switching center, or can be obtained by querying a remote database. Selection of the route will depend upon the called party number, connection type required, and signaling capability of the network. The bearer capability information in the Q.931 SETUP message is analyzed by the originating switching center to determine the correct connection type and network signaling capability. This information is then mapped into the user service information parameter of the IAM ISUP message.

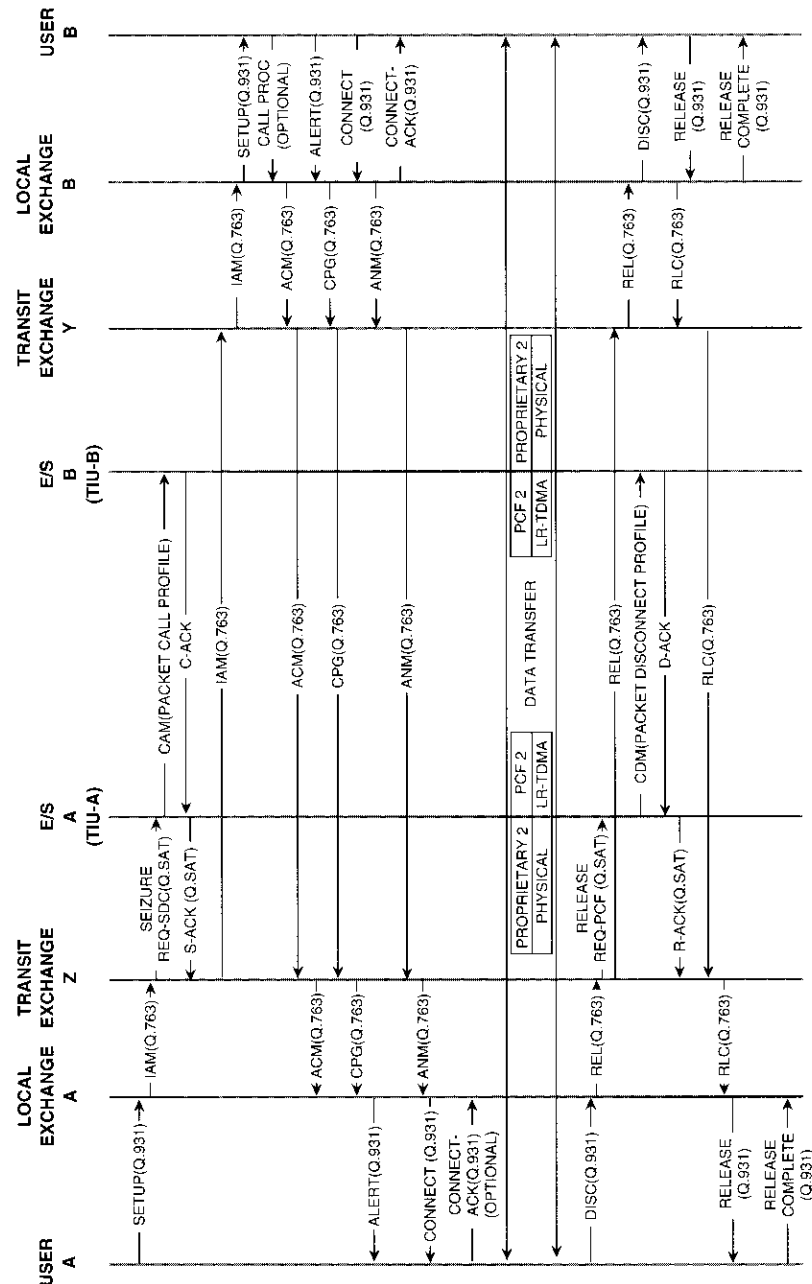


Figure 4. Call Setup and Disconnect Procedure for Packet Protocols (Use of PCF)

Information received from the access interface is used to set the value of the TMR parameter, and information used by the originating switching center to determine the routing of the call is included in the IAM (as TMR and forward call indicators) to enable correct routing at the intermediate exchanges. The IAM implicitly indicates the circuit that has been seized. If subaddress information is received from the calling user, it is passed unchanged to the destination switching center in the access transport parameter of the IAM. This forms the first signaling segment.

STEP C: INTERMEDIATE EXCHANGE/EARTH STATION (TIU) SIGNALING (Q.sat)

At an intermediate switching center, the IAM is analyzed to determine the routing of the call based on the called-party number. For an incoming call, the switching center forms a Q.sat signaling message when satellite channels are available to meet the call setup request. (Duplex channel availability within the satellite network is periodically sent to the switching center by an earth station connected to the center.) Otherwise, the call is rerouted using alternate paths, or blocked by the switching center.

Based on the call destination, TMR parameter, and availability of channels through the TIU, the intermediate switching center generates a Q.sat seizure message to the earth station TIU. (The Q.sat messages discussed here are a set of signaling messages.) The TIU acknowledges this message (Q.sat S-ACK) while forwarding a channel assignment message (CAM) to the correspondent TIU. The CAM contains the value of N in the $N \times 64$ -kbit/s request, the placement and order (time slot sequence integrity) of N channels within the satellite network, and the destination trunk and channel identification.

STEP D: SATELLITE CHANNEL ALLOCATION

Terrestrial channels are mapped into satellite channels in support of $N \times 64$ -kbit/s services, to efficiently utilize satellite capacity.

Through the Q.sat signaling link manager, the TIU receives an $N \times 64$ -kbit/s seizure request containing the value of N , the identification of the destination earth station, and the placement of the incoming call within the switching center/TIU trunk. The TIU has information regarding available time slots within the subburst designated for the destination of interest. As discussed earlier, the subburst configuration is preassigned in this basic role. The TIU uses its system-wide resource status database to ensure that adequate capacity exists to carry the call with its required directionality (full- or half-duplex). When reverse channel capacity is available (in the case of a full-duplex call), the TIU assigns forward channels from the subburst designated for the destination.

The TIU must inform the destination TIU of this (forward) channel assignment, using a signaling method explained below. Based on this signaling information, the destination TIU maps satellite channels back to the original terrestrial channel format and thus completes the call through the satellite system. The call may be blocked at the destination TIU due to lack of satellite capacity for the reverse channels, or due to glare conditions (simultaneous seizure of identical time slots). Further, the switching center may have to overcome its own glare conditions for the call. These issues will be discussed later.

When the call is disconnected, the switching centers inform the respective TIUs of call-disconnect status, and the TIUs return the satellite channels related to the call back to the subbursts for reassignment to the next call. Periodically, the TIUs report the number of 64-kbit/s channels available to their respective switching centers in the form of a status message. The switching centers use this information during connection establishment. For example, the switching centers may not offer a call to the TIU if sufficient capacity is not available for that call.

The TIUs may occasionally find that their need for channels does not match the actual call arrival rate. Based on cumulative averages and call statistics, a TIU may require more or less of the available capacity. As explained previously, in this basic role a TIU has two means available to alter the inter-TIU capacity: It may reassign subbursts in coordination with all affected earth stations, or it may request additional capacity from the network controller. The decision to change the capacity requirement is based on call-blocking statistics and QOS requirements information collected at the earth station, and therefore occurs infrequently. Reconfiguration of subbursts within a burst, or the use of channels from a global pool in coordination with the NCC, requires BTP changes that affect only a limited set of earth stations.

STEP E. INTERMEDIATE EXCHANGE SIGNALING (Q.763)

When the source switching center receives an S-ACK Q.sat message from the connected earth station, it forwards an IAM to the next switching center to which the destination earth station is connected. In order to carry ISUP messages, the switching centers use the SS7 network, which may bypass the satellite network. The CIC used in this message informs the switching center connected to the destination earth station of the trunk and channels selected for the call. Based on this information, the destination switching center performs outbound seizure to switch the channels and forwards an IAM to the next switching center in the path. The signaling and communications paths are eventually set

up to the remote local switching center, to which the destination user is connected, and the call setup process is completed.

STEP F. LOCAL EXCHANGE/DESTINATION USER SIGNALING (Q.931)

Upon receipt of the IAM, the destination switching center analyzes the called-party number to determine the destination user. It also checks the called party's line condition and performs a number of other checks to verify that the connection is allowable. These checks include compatibility checks and checks associated with supplementary services. The local exchange then generates a Q.931 SETUP message to the destination user. The remainder of the message flow associated with completing call setup is shown in Figure 4. When the calling user receives a Q.931 CONNECT message, an end-to-end call is set up and a communications path is established for information transfer.

The call can be disconnected by either party sending a Q.931 DISCONNECT message to the local switching center. The protocol for disconnecting a call is symmetric, and the same procedures are used in the network irrespective of whether they are initiated by the calling party, the called party, or the network. Upon receipt of a DISCONNECT message from the calling party, the originating switching center immediately initiates release of the switched path by sending a RELEASE ISUP message.

When it receives a RELEASE message, the intermediate switching center sends a Q.SAT RELEASE message to the earth station TIU and forwards a RELEASE ISUP message to the next switching center to which the destination earth station is connected. The TIU sends a channel disconnect message to the correspondent TIU and waits for an acknowledgment. It then acknowledges the release back to the switching center by sending a D-ACK (Q.sat) message.

From the destination switching center, the ISUP RELEASE message reaches the destination local exchange, where it is mapped into a Q.931 DISCONNECT message and forwarded to the destination user. The remainder of the message flow, resulting in complete release, is shown in Figure 4.

BISDN-compatible INTELSAT satellite communications subnetworks

An evolutionary series of architectures can be considered for the integration of BISDN into the INTELSAT system. A set of four architectures, of increasing complexity, is described briefly below, and the major elements of the first two architectures are then discussed in more detail in the subsections that follow.

The first architecture supports BISDN services through the transmission of SDH carriers. SDH defines a worldwide digital hierarchy and network node

TRANSMISSION BIT RATES IN RELATION TO SATELLITE ROUTE SIZES

The lowest SDH level is at 155.52 Mbit/s; however, CCITT has adopted a sub-STM-1 bit rate of 51.84 Mbit/s specifically for radio digital sections (Rec. G.707 and G.708 Annex A). The sub-STM-1 rate is not a standardized SDH multiplex level or an NNI. With the sub-STM-1 frame format derived from the G.708 STM-1 structure, a number of the original SDH overhead functions have been retained for shared/common use with radio systems in a mixed-media SDH network environment.

Because transmission system resources (power, bandwidth, and orbital locations) are limited, efficient satellite network planning and dimensioning are crucial. That is, the transmission bandwidth and bit rate on each link should preferably be matched to the expected level of actual traffic being carried on the route. On major intercontinental thick routes, both 155.52- and 51.84-Mbit/s transmission is expected. On medium routes, 51.84 Mbit/s may suffice. Initial studies are currently under way to define satellite SDH links at even lower bit rates (*e.g.*, 2.4 and 7.0 Mbit/s).

For transport within the INTELSAT SDH subnetwork at the sub-STM-1 rate of 51.84 Mbit/s, the STM-1 signal delivered across the terrestrial NNI must first be converted. If the STM-1 signal is suitably composed of three sub-STM-1 signals, it can easily be demultiplexed and its component sub-STM-1 signals transported separately. However, if the STM-1 signal delivered across the NNI contains a high-bit-rate payload (*e.g.*, 139-Mbit/s high-definition television [HDTV]), then demultiplexing the signal will be prohibitively expensive. Work on the 155-Mbit/s modem is actively under way and anticipates the need for STM-1 signal transmission.

MULTIPOINT TOPOLOGY

To accommodate satellite traffic routes that are much thinner than the sub-STM-1 bit rate, while retaining some of the standard SDH functionalities, further efficiencies could be attained by allowing multideestination/multipoint networking at the sub-STM-1 level and virtual container 3 (vc-3) path layer (*e.g.*, to support 34/45-Mbit/s digital video distribution). vc-3 multipoint networking would also allow distribution of individual vc-2 (6.312-kbit/s) point-to-point path connections.

As presently defined by the CCITT, all SDH section and path overhead functions, bit/byte allocation, and protocols are for point-to-point operation between pairs of functionally equivalent terminating points (*i.e.*, multiplexer section or path terminations). Three categories of backward-maintenance and alarm signals are defined in the SDH (Rec. G.708 and G.782):

- Multiplex section far-end receive failure (MS-FERF)
- VC-3 far-end block error (FEBE) and path FERF
- VC-1/VC-2 FEBE and path FERF.

To extend standardized SDH-based maintenance and alarm signaling (part of O&M) to operate in a multipoint mode, an addressing capability associated with the first two backward indications to multiple correspondents (origins of the failed signals) is necessary.

SDH/PDH INTERWORKING AT THE INTERNATIONAL NETWORK LEVEL

The INTELSAT interconnect network may be required to provide interworking functions between dissimilar national networks, as necessary, to accommodate different implementation plans, technical upgrades, and enhancements in those networks. This will be the case between some countries rapidly converting to SDH technology, and others which continue to use PDH in their digital networks. The flexibility of SDH multiplexing methods, and the use of associated standard multiplexing equipment at the satellite earth station, provides an elegant means of achieving SDH/PDH interworking at the international network level.

CABLE RESTORATION

Cable restoration by satellites could technically be offered with shorter service interruptions if realized with an SDH-based multimedia automatic protection arrangement. Such service must be justified economically, considering its use of satellite resources. The SDH concepts include automatic protection switching facilities for network-level protection over entire SDH multiplex sections, and the use of bit-oriented protocols over multiplex section overhead (MSOH) bytes K1 and K2 (Rec. G. 783). Fixed Satellite Service (FSS)-SDH subnetworks which function only as an SDH regenerator section (at either STM-1 or sub-STM-1 rate) provide transparency to MSOH, and thus to the K1/K2 bytes. Such FSS-SDH subnetworks can thus be part of multimedia (cable-over-satellite) and mixed-media, point-to-point multiplex section protection arrangements, as described in Rec. G.783, Annex A.

NETWORK MANAGEMENT

SDH has an extensive set of features for network management. These include operations, administration, maintenance, and provisioning for SDH multiplex systems; message transport facilities for SDH management subnetworks; and network management communications in the broader telecommunications

management network (TMN) sense (CCITT Rec. M.30). With regard to message transport, SDH data communications channel DCC_R (bytes D1–D3 in the regenerator section overhead [RSOH]) is used to manage SDH network elements within a management subnetwork, whereas SDH DCC_M (bytes D4–D12 in the MSOH) is used for a wide-area, general-purpose communications channel to support TMN, including non-SDH applications. All communications over these DCCs use the embedded communications protocol stack defined in Rec. G.784. Common use of these standard management concepts, principles, and protocols by all systems and subnetworks—including satellite systems such as FSS-SDH subnetworks, and satellite communications multiple-access systems such as TDMA—would facilitate the implementation of integrated network management systems, while providing cost savings through the use of common equipment.

The following aspects of network management are important from a satellite systems perspective:

Commonalty With Terrestrial SDH System. To realize a cost-effective design, the satellite SDH subnetwork should have maximum equipment and management commonalty with the terrestrial SDH system. Nonstandard and/or satellite-specific functions should be implemented in a manner which does not affect system transparency to external SDH functions. Such functions should be implemented in a separate satellite transmission frame complementary overhead (SFCOH).

VC Path Setup and Validation. SDH network management requires the capability to automatically set up and validate VC paths across operator boundaries. The INTELSAT system can be designed to support this capability, considering aspects such as bandwidth management schemes within the satellite subnetwork, path setup protocols, and the allocation of access point identifiers in the subnetwork.

In-Service Path Monitoring. Continuous in-service monitoring of paths is recommended to verify compliance with service commitments. Whenever possible, the satellite subnetwork should perform standard SDH path monitoring functions, supported by the path overhead, using bit-interleaved parity- N techniques.

Automatic Protection/Restoration. CCITT Rec. (G.831) calls for automatic protection/restoration of failed VC paths, to maintain them at a prescribed level of availability. Section-level protection switching in a $1:n$ arrangement within the satellite system is not justified due to nondispersive satellite fading phenomena across the satellite operational band, as well as limited satellite resources.

Remote Maintenance and Supervision. SDH network management should become part of a central network management system based on TMN concepts. The philosophy of centralized network management resembles that of the existing INTELSAT system, which is monitored, controlled, and coordinated by the INTELSAT Operations Center.

ERROR PERFORMANCE MONITORING FACILITIES IN SDH OVERHEAD

The SDH concepts provide a variety of performance monitoring facilities (Rec. 708). From the lowest network layer up, performance monitoring uses the bit interleave parity 8 (BIP-8) code in the SDH RSOH byte B1; BIP-24 code in the SDH MSOH bytes B2 (3x); path BIP-8 code in the VC-3/4 path overhead byte B3; and BIP-2 code in the VC-1/2 path overhead byte. The ability of the satellite FSS-SDH subnetworks to access one or more of these SDH error performance monitoring features depends on the subnetwork architecture, and on the resulting accessibility of the various transport network layers.

Figure 5 gives an overview of the subnetwork to be used in an SDH transport network environment. This subnetwork will be used to provide international interconnections between standard SDH transmission equipment at a select number of public international gateway exchanges (ISCs). Along with the SDH digital transmission technology now being implemented in national networks as the first step toward broadband digital networks, this subnetwork is a precursor to the introduction of BISDN. The terrestrial interfaces at the subnetwork access are in accordance with the NNI standards for SDH defined by the CCITT in Rec. G.707, G.708, and G.709.

The interconnected national SDH transport networks (*e.g.*, international gateways) will conceivably deliver three basic types of traffic payload to the subnetwork: ATM (BISDN); multiplexed 64-kbit/s circuits used for NISDN 64-kbit/s-type circuit-mode-oriented traffic such as 64-kbit/s NISDN and low- and medium-speed data over private network leased circuit groups; and general "new" traffic, such as HDTV and high-speed data over private network leased circuit groups, all encapsulated within standard SDH VCs. All traffic will be received across the NNI within the standard SDH STM- N multiplex format.

The subnetwork provides standardized connectivities to SDH VC paths between national SDH digital transport networks from/to the international gateways. These paths are established on a semipermanent basis by mutual agreement between administrations. SDH international paths can be added, deleted, reconfigured, rerouted, cross-connected, or through-connected at the subnetwork earth station SDH multiplex equipment to meet service demands and operational requirements. Remote configuration control is facilitated by the enhanced network management features of the SDH. The traffic handling capacity of the subnetwork is determined by its total SDH path capacity,

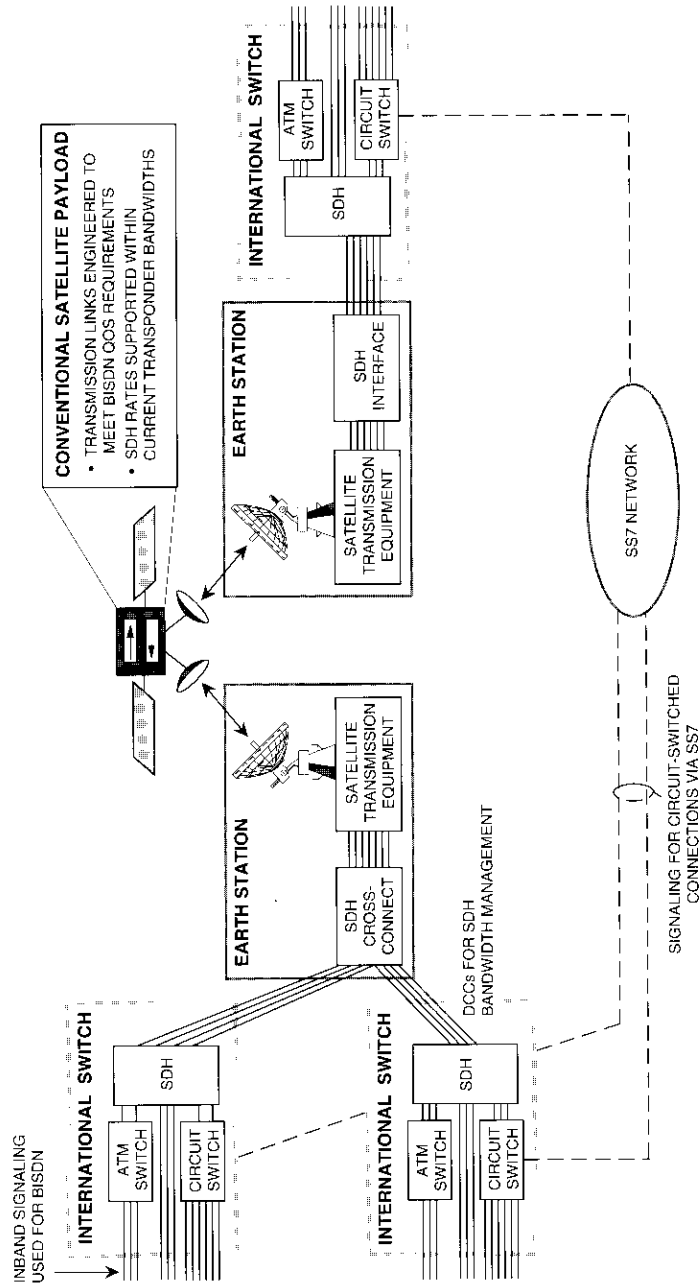


Figure 5. Network Architecture With SDH Cross-Connect at the Earth Stations

which is equal to the maximum incoming and outgoing traffic flow (with no compression).

Digital transport of the SDH VCs within the subnetwork can be in standard SDH STM-1 or sub-STM-1 frame format, or can be based on other non-SDH formats (e.g., within PDH network connections), or a combination of both. Non-SDH transport within the subnetwork is envisaged for SDH/PDH network interconnection and interworking, as well as for thin routes for which the 51.84-Mbit/s sub-STM-1 rate is not justifiable. System-specific operational functions within the subnetwork may require separate transmission over a dedicated SFCOH.

Through standard access to SDH management subnetworks, the subnetwork is amenable to the TMN concepts leading to an integrated network management system, which includes the satellite subnetwork comprising managed network elements.

Earth station virtual path cross-connect

Figure 6 illustrates the subnetwork support for an ATM within an SDH transport network environment. This subnetwork has the added ability to handle BISDN ATM traffic, providing international interconnections between a select number of BISDN international ATM gateway exchanges and ATM transmission network elements (cross-connects). It can also be used to interconnect metropolitan area networks.

The interconnected national BISDNs deliver ATM-type traffic to the subnetwork encapsulated within standard SDH VCs (VC-3 and VC-4). The subnetwork provides standardized connectivities to ATM virtual paths between national ATM networks from, to, or through their international ATM gateways. These paths are established on a semipermanent basis by mutual agreement between administrations. ATM international virtual paths can be added, deleted, reconfigured, rerouted, cross-connected, or through-connected at the subnetwork to meet ATM service demands and operational requirements. Resource efficiency is achieved by taking advantage of the wide statistical variation in ATM traffic flow to concentrate ATM traffic within the earth station ATM path. Capacity gain is achieved by removing unassigned cells.

ATM congestion control indications are provided by the subnetwork as an element of overall ATM network connection admission control. This is accomplished by means of a real-time indication of ATM traffic load to the interconnected exchanges. Under heavy load conditions, when the compressed ATM virtual paths within the subnetwork cannot accommodate new calls at their negotiated QoS, new connections are rerouted or blocked by the ATM gateways to maintain the QoS of existing connections.

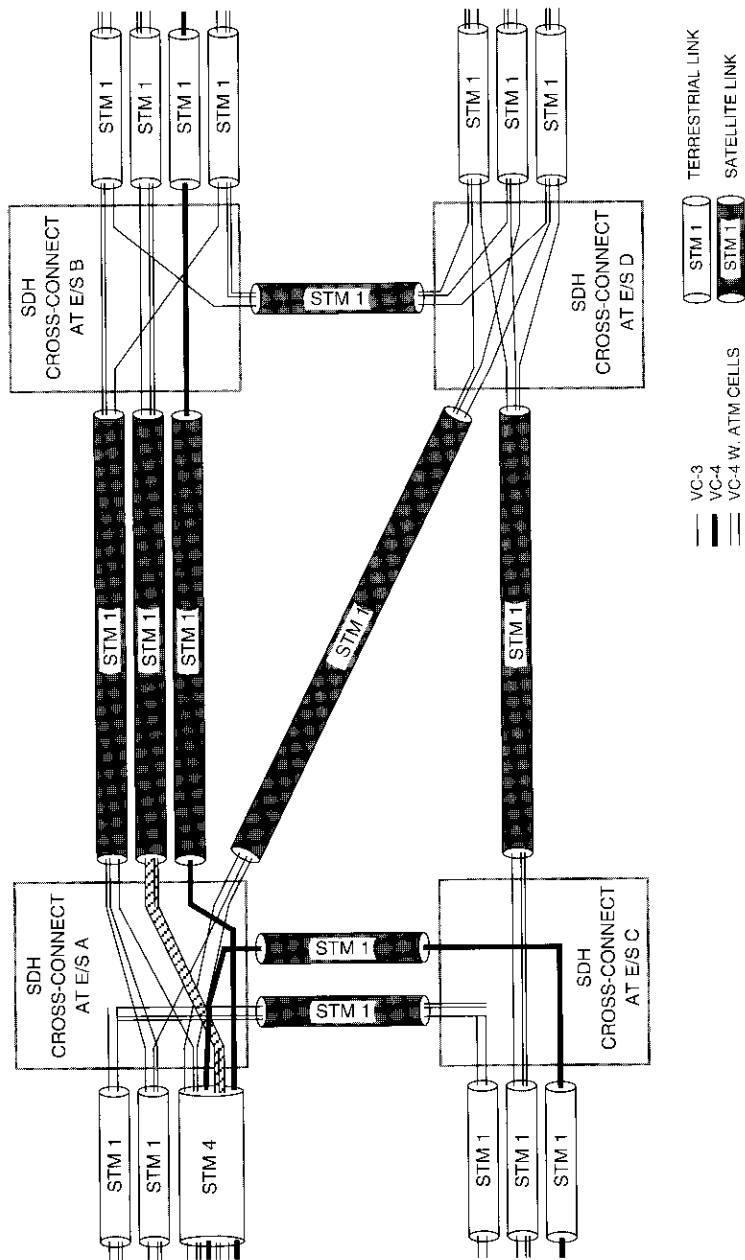


Figure 6. SDH Satellite Network Functional Architecture

At the subnetwork accesses, the STM- N signals are terminated and the ATM virtual paths are removed from the SDH VCs. The signals are cross-connected, regrouped by destination, and compressed into either fewer or smaller satellite virtual paths. Subsequent transport of ATM traffic within the subnetwork is based on either SDH, as shown in Figure 6, or a non-SDH formatted signal. ATM signal formatting for the latter anticipates future migration to a subnetwork with onboard ATM satellite virtual path cross-connect functions.

The potential for future migration of these subnetworks will permit the subnetwork BISDN traffic-handling capability to grow with demand as the number of transponders increases. The functional enhancement is a form of onboard cross-connection to restore inter-spot-beam connectivities associated with the higher number of transponders. Options for connectivity restoration are RF, baseband SDH VCs, and baseband ATM virtual paths (standard and customized formats). For the latter option, to minimize onboard processing of ATM cell header information, a satellite-specific address could be appended in front of groups of ATM cells that have the same beam destination (satellite virtual path concept). Other types of traffic variations that must be accommodated include a change in traffic mix and/or the introduction of new services such as multimedia communications and distributive services. These may require enhanced support of BISDN capabilities by the satellite subnetwork in the form of ground-based ATM call switching and associated network signaling. Signaling capability can be realized either as an integral part of BISDN signaling (with signaling point assignments), or as a "slaved" signaling system controlled by a dedicated external signaling system, similar to the NISDN architecture described earlier.

Conclusions

A series of evolutionary architectures has been presented to show the role that the INTELSAT system can play in future global telecommunications networks comprising NISDN and BISDN. ISDN switching, signaling, and multiplexing can be combined with the capabilities of the INTELSAT system to efficiently support ISDN services.

Acknowledgments

This paper is based on work performed at COMSAT Laboratories in 1990–1991 under the sponsorship of INTELSAT. C. Dhas, F. Faris, P. Samudra, D.-J. Shyy, and L. White made significant contributions to this study. Views reflected herein are those of the authors, and are not necessarily supported by either organization.

Appendix

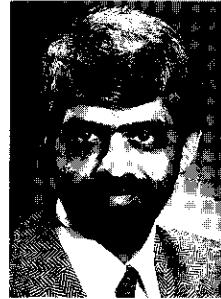
The ISDN Recommendations referred to in this paper can be found in the following volumes of the CCITT *Blue Books* (ITU, Geneva, 1988), or as draft recommendations from the CCITT Study Group XVIII meeting in Matsuyama, Japan, November 26–December 7, 1990.

Volume III

- FASCICLE III.5, "Digital Networks, Digital Sections, and Digital Line Systems," Rec. G.801–G956 (Study Groups XV and XVIII).
- FASCICLE III.7, "Integrated Services Digital Network (ISDN): General Structure and Service Capabilities," Rec. I.110–I.257 (Study Group XVIII).
- FASCICLE III.8, "Integrated Services Digital Network (ISDN): Overall Network Aspects and Functions, ISDN User-Network Interfaces," Rec. I.310–I.470 (Study Group XVIII).
- FASCICLE III.9, "Integrated Services Digital Network (ISDN): Internetwork Interfaces and Maintenance Principles," Rec. I.500–I.600 (Study Group XVIII).

Volume VI

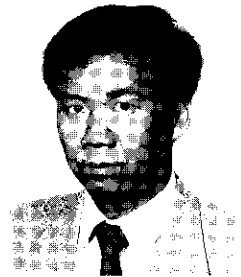
- FASCICLE VI.7, "Specifications of Signaling System No. 7," Rec. Q.700–Q.716, (Study Group XI).
- FASCICLE VI.8, "Specifications of Signaling System No. 7," Rec. Q.721–Q.766 (Study Group XI).
- FASCICLE VI.9, "Specifications of Signaling Systems No. 7," Rec. Q.771–Q.795 (Study Group XI).
- FASCICLE VI.10, "Digital Access Signaling System, Data Link Layer," Rec. Q.920–Q.921 (Study Group XI).
- FASCICLE VI.11, "Digital Access Signaling Systems, Network Layer, User-Network Management," Rec. Q.930–Q.940 (Study Group XI).



Dattakumar M. Chitre received a BSc from the University of Bombay, India; an MA in mathematics from the University of Cambridge, U.K.; and a PhD in physics from the University of Maryland. He is currently an Associate Executive Director of the Network Technology Division at COMSAT Laboratories, where he has been involved in research and development of ISDN, VSAT networks, data communications, and network systems and architectures. He was previously a Principal Scientist in the Network Technology Division.

Dr. Chitre joined COMSAT Laboratories in 1980 and has made major contributions to the analysis and architecture of data communications, ISDN, and BISDN via satellite. In 1990 and 1991, he was program manager on an INTELSAT contract to study satellite communications systems architectures for ISDN and BISDN. He is currently technical manager for a DOD contract to demonstrate ATM via satellite, and program manager for an INTELSAT contract on the analysis and top-level specification of INTELSAT ISDN subnetworks and an SDH-compatible transport network. Dr. Chitre also directs and participates in international and national standards activities for ISDN, BISDN, and data communications as they apply to satellite communications. During 1990–1992, he was Chairman of the Working Group on Protocols and Network Timing Function of the CCIR/CCITT Joint Ad Hoc Group on ISDN/Satellite Matters.

W. Sian Oei received the Engenieur Degree in electrical engineering from the Delft University of Technology, the Netherlands, in 1974. He joined INTELSAT, Washington, D.C., in February 1982, and is currently a Supervising Engineer in the Communications Engineering Section. He has had a number of responsibilities related to implementation of the INTELSAT TDMA system, such as TDMA reference and monitoring station (TRMS) technical evaluation, and the development of specialized test equipment and SSOG procedures. He also was active in developing specifications for digital circuit multiplication equipment (DCME).



Mr. Oei is currently involved in studies on the introduction of efficient ISDN-compatible networks and the new synchronous digital hierarchy (SDH) transmission technology in the INTELSAT system. He has represented INTELSAT in a number of CCITT Study Groups dealing with digital networks, ISDN, data communications, network switching and signaling, and digital transmission systems and equipment. During 1990–1992, he was active in the CCIR/CCITT Joint Ad Hoc Group on ISDN/Satellite Matters, which studied ISDN compatibility issues and other CCITT recommendations dealing with satellite network connection delay.

Index: attitude control, simulation,
communication satellites, models

Design and validation of the ITALSAT AOCS flight simulator

A. RAMOS, R. L. MINCIOTTI, T. HAMPSCH, G. ALLISON,
E. W. HARE, AND J. W. OPIEKUN

(Manuscript received April 16, 1992)

Abstract

A real-time, hardware-in-the-loop simulator of the ITALSAT satellite attitude and orbit control subsystem (AOCS) was developed for the Italian Space Agency. The simulator is called the ITALSAT AOCS Flight Simulator (IAFSIM). The applications, design, and validation of IAFSIM are described, and examples of validation tests are given which cover AOCS modes of operation during the various ITALSAT mission phases. Possible future applications of IAFSIM are also discussed.

Introduction

Spacecraft flight simulators provide a means for training personnel and investigating flight anomalies. Some features of these simulators are independent of the spacecraft system, while others are unique to a particular system. The operation of a simulator can best be described by focusing on one specific version and generalizing to others.

Recently, a real-time, hardware-in-the-loop simulator was developed for the attitude and orbit control subsystem (AOCS) of the ITALSAT spacecraft. This simulator (Figure 1), called the ITALSAT AOCS Flight Simulator (IAFSIM), was developed as part of the ITALSAT program of the Italian Space Agency (ASI), and has been in operation at the ITALSAT Operations Control Center (IOCC) in Fucino, Italy, since April 1990. The ITALSAT program is based on an advanced three-axis-stabilized spacecraft with two 20/30-GHz telecommunications payloads. These payloads include two multibeam

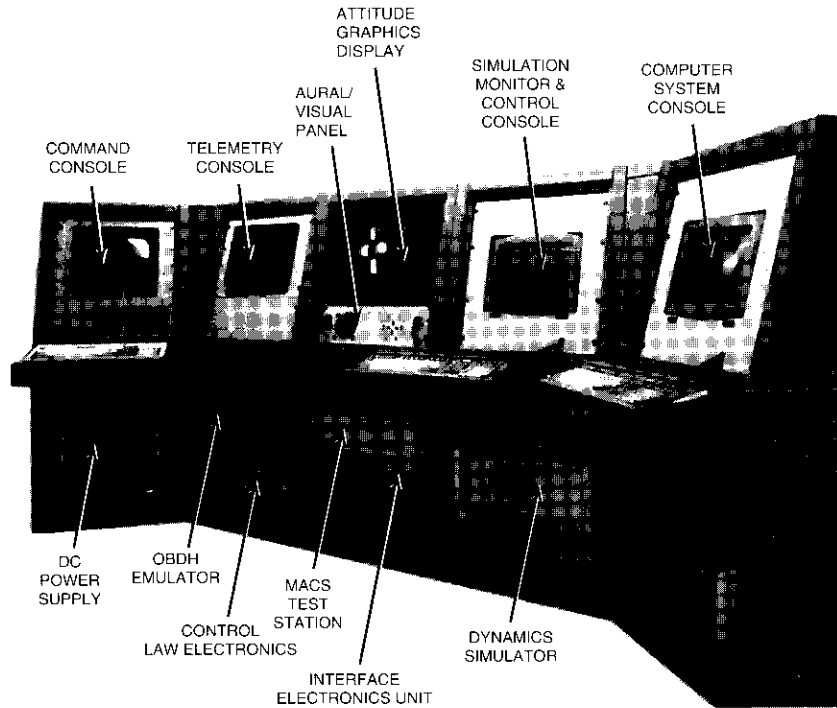


Figure 1. *The ITALSAT AOCS Flight Simulator*

antennas, each with three narrow (0.5°) spot beams. The required antenna pointing accuracy is $\pm 0.03^\circ$. Allowed attitude errors are less than 0.1° for pitch and roll, and 0.3° for yaw. Furthermore, the transfer orbit phase of the mission is carried out with the spacecraft in a variety of three-axis-stabilized orientations. Even though each antenna has an independent RF beacon-based control system, these factors impose stringent demands on the performance of the AOCS and on the ability of ground operations and personnel to respond to any anomalous situations that might arise. IAFSIM was needed to help increase knowledge of the AOCS within the ITALSAT program community, and to assist in validation and use of the IOCC.

A flight simulator had been designed and built for the INTELSAT V program to meet similar objectives [1]. This simulator evolved into a second-generation design that included a three-axis-stabilized Direct Broadcast Satellite (DBS) simulator [2] and a dual spin-stabilized INTELSAT VI simulator, both completed in 1986. The INTELSAT V simulator (which was upgraded in 1987 and

again in 1991) and the INTELSAT VI simulator are currently in operation at the INTELSAT Satellite Control Center in Washington, D.C.

IAFSIM represents a third-generation design. Its significant new features include the capability to support a three-axis-stabilized transfer orbit mission; a dynamics model for the oscillation of liquid propellants; static telemetry for non-AOCS functions to generate the entire telemetry stream; and data communications with the control center through an X.25 packet-switched network, rather than through a simpler non-return-to-zero synchronous line [3]. The human/machine interface was also improved based on lessons learned during development and operation of the previous simulators.

The ITALSAT mission and spacecraft are described first, followed by a discussion of the uses of IAFSIM. System design issues, the simulator design, and simulation software are addressed. Validation issues are then presented, and test results are given. Finally, potential applications for IAFSIM are discussed.

ITALSAT mission and spacecraft

This section provides a brief description of the features of ITALSAT that are relevant to IAFSIM operation. A more detailed description is given in Minciotti *et al.* [4]. The ITALSAT spacecraft is three-axis-stabilized during all phases of its mission, except immediately following separation from the Ariane launch vehicle. Matra built the AOCS as a subcontractor to Alenia Spazio, the ITALSAT spacecraft prime contractor.

Prior to separation, the spacecraft is spun-up to 2.5 rpm and injected into an elliptic transfer orbit with an apogee equal to synchronous altitude. Ground commands put the AOCS into despin and sun acquisition mode, which results in the spacecraft z-axis being pointed toward the sun. This is accomplished by using gyroscopes for rate sensing, coarse analog sun sensors for attitude sensing, and reaction control thrusters for torquing. After sun acquisition, the more accurate modular digital sun sensor replaces the coarse analog sun sensor.

After the sun is acquired, the earth is also acquired with the help of the infrared earth sensor (IRES). These steps are executed so that the spacecraft attitude is fixed in inertial space, thus allowing the drift bias of the gyroscopes to be calibrated and compensated for. In other words, since the spacecraft has zero angular rates relative to inertial space (to within the accuracies of the attitude control system), the gyros should ideally indicate zero rates. Any discrepancies are attributable to drift bias. After the spacecraft is maneuvered into the correct attitude with the aid of the calibrated gyroscopes, the liquid apogee engine (LAE) is fired to raise the orbit perigee. Two more cycles of

earth acquisition/gyro calibration/LAE maneuver/LAE firing (LAEF) are executed to place the spacecraft into synchronous orbit.

After another earth acquisition, the AOCS is commanded into the normal mode. This mode uses the IRES for pitch and roll sensing; a momentum wheel for gyroscopic stiffness in roll and yaw, and for control torque in pitch; and thrusters to limit the increase in the spacecraft's total momentum due to external disturbance torques. Figure 2, which shows the satellite after full deployment of the solar arrays and antennas, defines the body-fixed coordinate frame and indicates the pitch, roll, and yaw attitude angles.

Because of the larger disturbance torque arising from the misalignments and imbalances of the thrusters used during orbit correction maneuvers, the AOCS is switched to the stationkeeping mode, which uses a gyro for yaw sensing, the IRES for pitch and roll sensing, and three-axis thruster control.

The outputs of the attitude sensors are processed by the control law electronics (CLE) to generate signals to the control torquers. The microprocessor-based CLE performs the following functions:

- Requests and receives data from the sensors and torquers.
- Sends control and mode signals to the sensors and torquers.
- Implements the feedback control laws and mode logic.
- Manages the on-off status of the AOCS equipment.
- Decodes telecommands and provides telemetry.
- Manages the fault protection of the AOCS, including the CLE itself.

The CLE employs a multilevel strategy to protect against faults. Since the AOCS is fully redundant, when a fault is detected the system first attempts to maintain earth pointing by switching autonomously from the equipment being used to a set of equipment preselected by the IOCC. If this attempt fails, the spacecraft acquires the sun autonomously, unless spacecraft operators intervene. The IOCC can then diagnose and correct for the fault, reacquire the earth, and finally transfer back to normal mode.

Rationale for a spacecraft simulator

The IAESIM design combines the functions of operator training, control center data processing validation, and engineering evaluation. The simulator can be used to:

- Train spacecraft operators
- Validate control center software and hardware
- Develop and test contingency, as well as normal, procedures

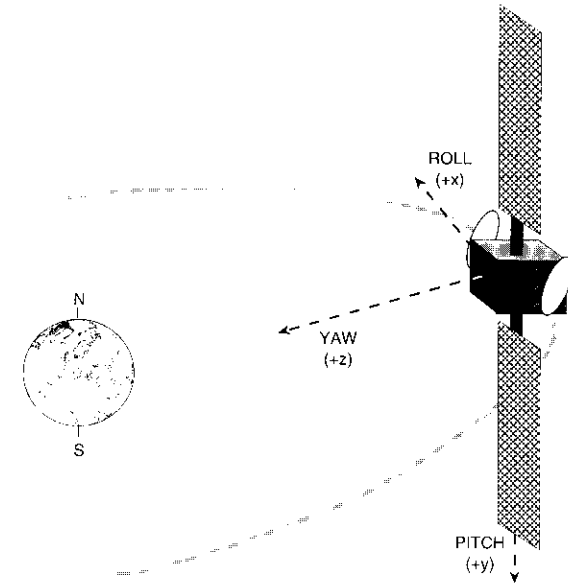


Figure 2. *ITALSAT On-Station*

- Rehearse the ITALSAT mission
- Analyze and optimize AOCS stability and performance
- Diagnose control anomalies or failures
- Test work-around procedures.

In typical spacecraft programs, flight control procedures and strategies are generated through a time-consuming and expensive iterative process which involves many engineers. While it is desirable that this process be completed prior to spacecraft launch, it generally continues for some time following launch (especially of the first spacecraft in a series) because often there is no realistic means of testing the procedures. In principle, the AOCS and the telemetry and command subsystems are fully integrated at the spacecraft level, and thus should be available for development of the flight control procedures. In reality, the spacecraft is not available for extended periods of time for this purpose due to scheduling constraints and the associated cost of preempting an entire spacecraft for such work. Also, the extended use of flight equipment for development purposes carries the risk of damaging or compromising the equipment performance. Finally, the AOCS equipment

typically is not closed around an accurate dynamics model, whereas many flight procedures require closed-loop operation for validation. A simulator like IAFSIM provides the best solution to many of these problems.

IAFSIM offers a means of training spacecraft operators without jeopardizing the operational ITALSAT. Furthermore, operators are trained in the same IOCC environment in which they will perform their tasks. Because the performance characteristics of the actual and simulated spacecraft are very similar, the AOCS knowledge and operational skills gained from training on the simulator can be transferred directly to the operation of ITALSAT.

The features built into IAFSIM, as well as its realistic modeling, make it an effective and efficient tool for fault analysis. Hypotheses regarding the causes of in-orbit failure can be tested rapidly because the simulator's monitoring and control function makes it versatile and easy to use. The high realism achievable by the modeling approach can be illustrated by the following example.

It was discovered that an earth sensor on an orbiting INTELSAT V spacecraft behaved in an unexpected way under certain conditions. The sensor manufacturer had not experienced this behavior during sensor design and testing; however, when the same conditions were set up in the INTELSAT V simulator, the simulated sensor behaved exactly as the one in orbit. Because the modeling was based on the fundamental functions of the sensor's components, the simulator model automatically achieved the high level of realism necessary to account for the unforeseen conditions.

Simulator system design

IAFSIM is a real-time, high-fidelity, operator-interactive system that combines actual spacecraft hardware with software models of the AOCS and its environment. An engineering model of the control law electronics is the single piece of actual spacecraft equipment in the IAFSIM. Everything else related to the AOCS and its environment is modeled in software that runs on a 32-bit minicomputer. This includes software models of the spacecraft dynamics, sensors, actuators, disturbances, telecommand and telemetry functions, and orbital mechanics. The models are customized to accurately represent the specific characteristics and design features of ITALSAT and its AOCS.

Concept of operation

Figure 3 shows the relationships between the elements of IAFSIM and its environment. The simulator can operate in an integrated mode with the IOCC. It accepts telecommands from the control center and sends data back for processing and display by the control center software. To the control center operators, the simulator appears as an actual spacecraft. The simulator can

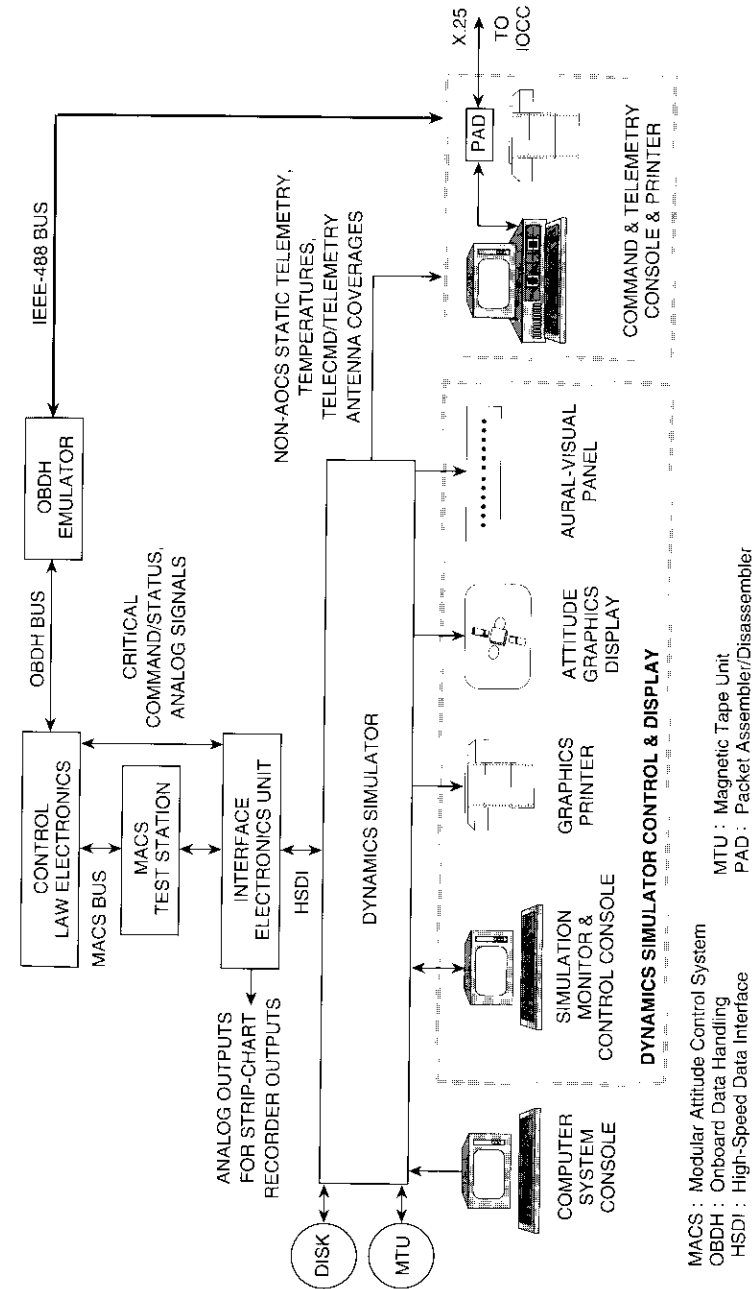


Figure 3. IAFSIM Block Diagram

also operate as a stand-alone system which has the ability to send telecommands and to monitor telemetry in the same formats used in the control center.

The simulated AOCS responds to telecommands and generates dynamic telemetry, both in real time. Static values are assigned to the telemetry associated with other satellite subsystems, such as electrical power, thermal control, and the payload. These values can be changed by the IAFSIM operator at any time. The simulated AOCS telemetry signals, some dynamic but fundamental non-AOCS telemetry such as satellite time, and the static telemetry are combined to create the entire telemetry stream, which is then sent to the control center.

All mathematical and logical models, and all conditions that define the initial state of the simulator, are described by parameters that are accessible directly by the IAFSIM operator as inputs through the simulation monitoring and control software (SIMMON). For example, consider the differential equations of motion for a system comprising a central body and flexible solar arrays, expressed in vector-matrix form as

$$I\dot{\omega} + L_r^T \ddot{q} + \omega \times H = T_{\text{thruster}} + T_{\text{solar}} - \dot{h} \quad (1)$$

and

$$L_r \dot{\omega} + \ddot{q} + D\dot{q} + Eq = 0 \quad (2)$$

where

$$\omega = (\omega_x \quad \omega_y \quad \omega_z)^T = \text{rigid-body rate about the } x, y, \text{ and } z \text{ axes}$$

$$q = (q_{\text{out-of-plane}} \quad q_{\text{in-plane}})^T = \text{flexibility displacement vector with components out of, and within, the plane of the solar array}$$

$$h = \text{control momentum wheel vector}$$

$$L_r = 2 \times 2 \text{ modal participation matrix that couples the body rates with the flexibility displacements}$$

$$D = \begin{bmatrix} 2\xi\omega_{\text{out-of-plane}} & 0 \\ 0 & 2\xi\omega_{\text{in-plane}} \end{bmatrix} = \text{damping matrix expressed in terms of the out-of-plane, } \omega_{\text{out-of-plane}}, \text{ and in-plane, } \omega_{\text{in-plane}}, \text{ flexible-mode natural frequencies and the damping ratio, } \xi$$

$$E = \begin{bmatrix} \omega_{\text{out-of-plane}}^2 & 0 \\ 0 & \omega_{\text{in-plane}}^2 \end{bmatrix} = \text{stiffness matrix.}$$

The system is driven by the thruster and solar torques, $T_{\text{thruster}} + T_{\text{solar}}$ and by the wheel control torque, \dot{h} . Total momentum, H , is given by $I\omega + h + L_r^T \dot{q}$.

The system's response is expressed in terms of the rigid-body rate, ω , and the flexibility displacement vector, q . These time-variable quantities are referred to as the *variables* of the simulation. On the other hand, the moment of inertia matrix (I), the modal participation matrix, and the natural frequencies and damping ratio characterize the system, and are referred to as *parameters*. Overall, IAFSIM has about 1,000 parameters and 1,000 variables. Modeling in terms of parameters allows the simulated characteristics to be tuned to match on-orbit performance, or changed for "what-if" investigations.

The simulator covers the entire range of mission phases, including transfer orbit operation, LAEF, attitude acquisition and reacquisition, normal mode, and stationkeeping mode. A key feature of the simulator is its ability to simulate unit failures. Each AOCS sensor or actuator has credible failures included in its model. For example, the earth sensor output can be clamped to any constant value, the earth presence bit can be made inoperative, or output noise can be increased. These failures can be triggered through SIMMON at any time during a simulation run. Also, since all unit redundancies are modeled, spacecraft operators can be trained not only to detect failures through telemetry, but also to send corrective telecommands.

SIMMON is a menu-driven program that is used to start or stop a simulation run. The initial conditions and parameters are selected from data files which are designed to be created, modified, saved, and restored easily. Data files corresponding to the most important mission phases can be prepared and stored for later use, and files for new cases of interest can be generated readily.

Telemetry displays and strip-chart recorder plots of simulator variables are also available. Telecommands are time-stamped and logged on a printer. Simulation variables can be selected and sampled at a designated rate for storage in computer memory and, if desired, can be plotted or printed following the simulation run. A color monitor displays an image of the spacecraft showing its dynamic attitude, and light-emitting diodes and a speaker provide visual and aural cues when thrusters are fired. These outputs help operators to better understand complex spacecraft motions.

To maximize the simulator's value for training, a clear distinction is made between the functions and console of the spacecraft operator (the trainee) and those of the simulator operator (the instructor). The trainee uses the command and telemetry console (CTC), while the instructor uses the SIMMON console. For example, the instructor triggers simulated failures at the SIMMON console,

which is separate from the CTC that is used to display telemetry and enter telecommands. The simulator is also designed to be operated by one person for purposes other than training, such as anomaly investigation.

System configuration and hardware

At the core of the simulator is an engineering model of the complete CLE. It is built to flight drawings, except that commercial-grade rather than space-quality electronic components are used. Since the CLE is a complex hardware element embodying complex control functions, the use of an actual CLE is the best way to guarantee high fidelity (which cannot be guaranteed by using a software model of the CLE). Although it is not possible to simulate internal failures directly if an actual CLE is used, most can be simulated through their effects on the CLE inputs or outputs. Therefore, for simulators such as IAFSIM, this hardware-in-the-loop approach is preferable.

The CTC is used for telecommand and telemetry input, processing, output, display, and printing. As Figure 3 shows, most CLE inputs and outputs are performed through two bidirectional serial buses: the onboard data handling (OBDH) bus for telemetry and telecommands, and the modular attitude control system (MACS) bus for sensor and actuator signals. Critical telecommands and telemetry are not transmitted over the OBDH bus, but are connected as discrete signals to the CLE. The CLE also accepts analog inputs from the coarse analog sun sensor. The OBDH emulator converts the OBDH bus signals of the CLE to IEEE-488 bus signals, which are processed by the CTC. The CTC (which is based on a personal computer) has a plug-in board for the IEEE-488 bus and a plug-in communications coprocessor board for the several asynchronous serial lines required. One line is an RS-232C port to the packet assembler/disassembler (PAD), which connects the IAFSIM to the IOCC in the integrated mode.

The MACS test station converts the MACS bus signals of the CLE to signals that are processed by the interface electronics unit. This approach—using the OBDH emulator and the MACS test station, which are proven units built by Matra—was selected over other alternatives because it was judged to present the fewest technical risks, at only moderate additional cost.

The interface electronics unit connects the MACS test station with the dynamics simulator through a simple, parallel digital bus called the high-speed data interface (HSDI); provides discrete telecommand, telemetry, and analog signal connections with the CLE; and provides analog output signals suitable for strip-chart recording. This COMSAT-built unit consists of custom-designed electronics assembled in a 19-in. rack. The HSDI board in the dynamics simulator allows direct memory access for input-output transfers, thus minimizing CPU overhead for these operations.

The dynamics simulator is a Gould 32-bit minicomputer designed for real-time applications. It includes a floating-point accelerator board. Outputs to the operator include the color attitude graphics display, the aural-visual display panel with light-emitting diodes and a speaker, and a printer.

The major challenges in the IAFSIM system design were to ensure that the inputs and outputs of the CLE were accurate, that the telemetry and telecommands were modeled accurately, and that the X.25 connection with the IOCC packet-switching network satisfied specifications. These challenges were met through careful study of documentation and accurate design of the IAFSIM hardware and software.

Dynamic simulator software

The dynamics simulator runs the software required to simulate the various elements of the AOCS (except the CLE), drive the attitude graphics display (AGDS), monitor and control the IAFSIM operation (SIMMON), and perform miscellaneous housekeeping functions. Most of this software is written in FORTRAN 77+, which includes extensions for efficient bit-based logic and input-output instructions. The small portion of software used for message processing is written in assembly language.

Software design issues

The major software design challenge was to guarantee accurate simulated AOCS performance in real time. The same strategy used to design previous COMSAT-built simulators was employed for IAFSIM. First, a level of modeling detail appropriate to meet the predefined simulator objectives was selected. Models of the attitude dynamics and kinematics, AOCS sensors and torquers, and orbital mechanics were considered at this point. Next, the timing requirements of the hardware elements were identified. The CLE requests inputs from all the sensors, and generates control outputs to the thruster electronics, every 109 ms. Therefore, the sensors and the thruster electronics models must run at least every 109 ms. Worst-case timing scenarios were hypothesized and examined. These analyses resulted in the requirement that the dynamics and kinematics be calculated at least every 50 ms.

The dominant critical case arose from the fact that the gyro outputs must be available within a small time window after the CLE requests gyro data; otherwise, the CLE declares a fault and may unnecessarily reconfigure itself and the other AOCS components. This design process led to selection of the processing rates for the software modules, as illustrated in Figure 4. Modules are executed periodically, but at various specified time intervals and in a specified order. The basic time interval selected was 50 ms, which is the interval at

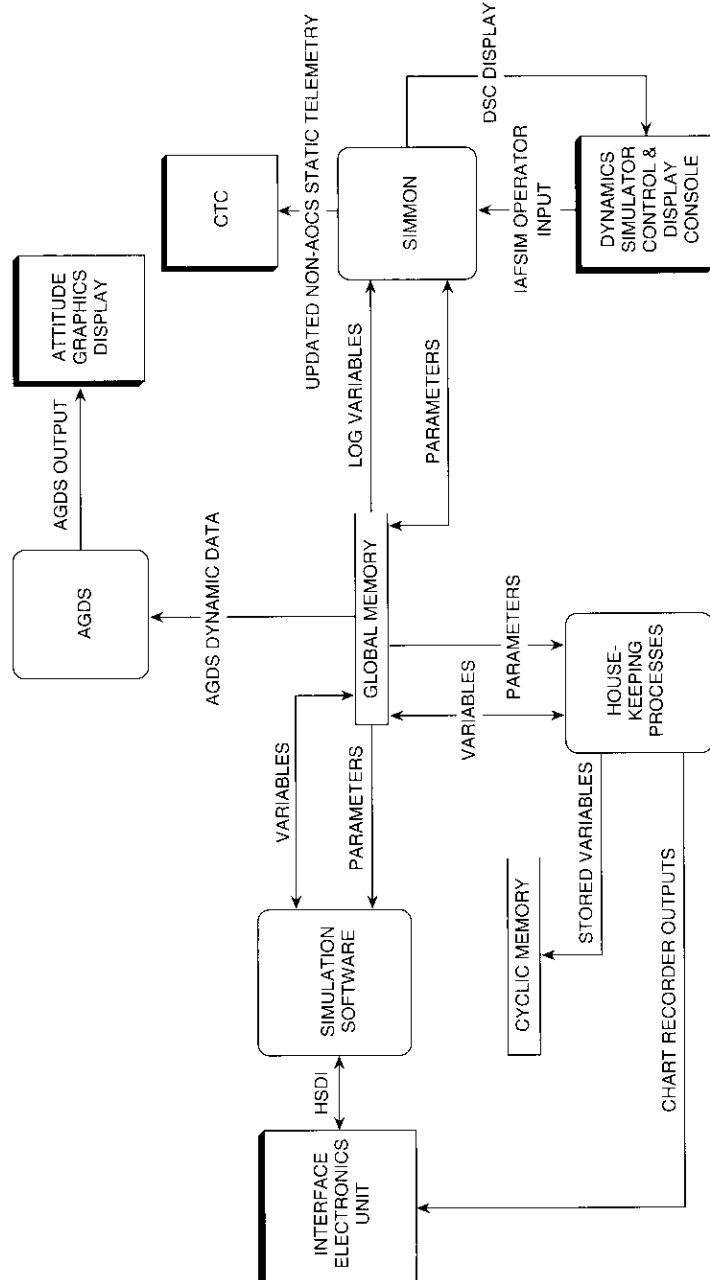


Figure 5. Dynamics Simulator Top-Level Data Flow

orbit phases during which the spacecraft is three-axis-stabilized. The most significant new requirement for the simulation software is to model the dynamics of the liquid in the fuel and oxidizer tanks. At the start of the mission, the liquid mass in the two tanks is about one-half of the total spacecraft mass. Because the propellant dynamics are closely coupled with the dynamics of the rest of the spacecraft during LAEF maneuvers, it is necessary to model the coupled dynamics. The liquid in each tank is modeled as a spherical pendulum which is attached to the spacecraft main body through a two-axis gimbal joint (also known as a "universal" joint). The pendulum masses, lengths, and attachment points, as well as the mass properties of the total spacecraft, are modeled as parameters that change linearly during LAEF. This is the same approach taken by Alenia Spazio, which provided data on the rates of change.

Table 1 shows the different software models and their sources. The major new models are the liquid propellant dynamics, digital sun sensors, input from and output to the CLE, and thruster and latch valve drive electronics. A significant effort was made to accurately model the nonlinear fields of view of the earth and sun sensors, which are unique to ITALSAT. Eclipses (which are of importance to the sun sensors), and sun or moon interference on the earth sensors are also calculated. The fundamental modeling equations and the processing flow are described by Benet *et al.* [2].

To improve the overall software design process and the documentation, it was decided to write new specifications, pseudocode, and code for all modules, even those for existing models.

SIMMON

The SIMMON software gives the IAFSIM operator the means to initialize, run, monitor, and stop simulations. Through SIMMON, the operator can examine and change any part of the global common memory of the simulation, trigger or reset simulated failures, sample and store selected variables, and select variables for strip-chart recording.

SIMMON was derived from the DBS simulator. SIMMON's tree-type menu structure is designed to be flexible and easy to use in the context of real-time flight simulators. Several improvements were made to satisfy the system specifications and to apply lessons learned from work with previous simulators.

The essential changes to SIMMON added the capability to edit static telemetry and incorporated measures to make IAFSIM more forgiving of operator errors. Operator inputs to IAFSIM are checked for physical realizability (*e.g.*, the moment of inertia matrix must be a positive real matrix). In addition, each parameter has maximum and minimum limits associated with it. SIMMON

TABLE 1. SOFTWARE MODELS AND SOURCES

MODEL OR UNIT	SOURCE
<i>Environmental Functions</i>	
Satellite Orbits	Modified for IAFSIM
Sun Position; Moon Position	Reused
Eclipses	New
Rigid-Body Dynamics	Reused
Attitude Kinematics	Reused
Flexible Solar Arrays	Reused
Propellant Liquid Modes	New
Mass Properties	Reused
Plume Disturbance Torque	Modified for IAFSIM
Solar Disturbance Torque	Reused
<i>Satellite Functions</i>	
Scanning Earth Sensor	Modified for IAFSIM
Gyroscope Package	Reused
Digital Sun Sensor	Modified for IAFSIM
Coarse Analog Sun Sensor	Modified for IAFSIM
Momentum Wheels	Reused
Reaction Thrusters	Reused
Propulsion System Latch Valves	New
Liquid Apogee Engine	New
Thruster and Latch Valve Drive Electronics	New
Inputs From, and Outputs to, the CLE	New

blocks any user attempt to change a parameter's value beyond these limits, which were preselected to ensure reasonable behavior of the simulated spacecraft. However, the user is allowed to change the limits without constraint, since such freedom is important, for example, for in-orbit anomaly investigations.

IAFSIM can be placed in either the "alarm mode" or the "hold mode." Certain major variables, such as attitude rates, have been identified to indicate that a simulation run may have crashed. The values of these variables are compared periodically by the housekeeping software (discussed later) against limits whose values are selected through SIMMON. If a major variable exceeds its limits, an alarm message identifying the offending variable is printed on the SIMMON display. In the hold mode, the simulation run is stopped automatically and the simulation variables are frozen for study.

The allowable transitions between the simulator modes are tightly constrained. For example, the simulator cannot be initialized while it is running a simulation; it first must be put into stop mode, which ensures orderly termination of the processing.

Attitude graphics display software

The AGDS program, which has been used in previous simulators, displays a three-dimensional color image of the ITALSAT spacecraft in real time (see Figure 1), updating the image about four times a second. It also displays the values of the most important simulation variables, including simulated time, attitude angles, and attitude rates.

The three-dimensional image that describes the spacecraft is projected onto a plane from a fixed viewpoint (inertial for transfer orbits and earth-centered for synchronous orbits). Images corresponding to the three metamorphoses that ITALSAT undergoes (*i.e.*, solar arrays and antennas stowed, arrays partially deployed, and arrays and antennas fully deployed) were defined to allow IAFSIM to display a representative image on the color monitor.

Housekeeping software

The housekeeping software performs several miscellaneous functions. The major variables discussed above are checked against their limits, and up to 32 of the variables are sampled and stored in a cyclic memory, which allows the operator to process them after a simulation run. Up to eight variables are converted to analog voltages that are suitable to drive a strip-chart recorder. The variable limits, variable choices, and sample rates are selected by the operator through SIMMON.

Simulator validation

The deliverable IAFSIM was governed by a system specification prepared by Telespazio which covered many aspects of the design, including function, performance, operation, interfacing, hardware quality, software quality, safety, and maintainability. All system requirements were verified by test, demonstration, inspection, or analysis. This section focuses on test verification of IAFSIM performance.

Verification test approach

Tests were conducted in a typical sequence—first on the software modules as they were developed, then on integrated software modules, then on the

hardware and software subsystems (dynamics simulator, CTC, *etc.*), and finally on the IAFSIM system. The following examples illustrate the stages of the test approach:

Single Module (e.g., infrared earth sensor)

- Narrow and wide scan modes
- Nonlinear fields of view
- Sensor inaccuracies.

Integrated Modules (e.g., dynamics module integrated with orbital mechanics module). These accuracies were compared with results of analyses.

- Conservation of system momentum accuracy
- Roll-yaw orbital coupling accuracy
- Nutation mode accuracy
- Structural and liquid flexibility modes accuracy
- Pitch rigid-body mode accuracy.

Subsystem (e.g., CTC)

- Telemetry display accuracy
- Proper rate of telemetry display update
- Ability to send AOCs telecommands manually or from a selected computer file
- Accurate receipt of telecommands
- Processing of normal and dwell telemetry.

IAFSIM System

- Tests performed according to the acceptance test plan.

As Table 2 shows, the test plan was organized according to the various AOCs modes. Since IAFSIM performance was to be measured against the AOCs subsystem tests performed by Matra, the telecommands and performance plots for each test were selected from Matra test reports. For each test, the additional tasks of setting up a test scenario, creating a script, and extracting relevant telecommands and attaching specific data to them had to be performed. Each test involved a sequence of 150 to 250 commands. The ability to create command files and execute commands from these files was vital.

An in-plant acceptance test was conducted at COMSAT Laboratories. After the system was installed at Telespazio's IOCC, a preliminary on-site acceptance test that was a subset of the in-plant test (see Table 2) was performed.

TABLE 2. IAFSIM ACCEPTANCE TESTS

TEST NUMBER	TEST	IN-PLANT	PRELIMINARY	FINAL
1	Despin and Sun Acquisition	X	X	
2	Transfer Orbit Sun Acquisition	X		
3	Transfer Orbit Earth Acquisition	X	X	
4	Gyro Calibration	X		
5	Maneuver Mode	X		
6	Liquid Apogee Engine Firing	X	X	X
7	Normal Mode	X	X	X
8	Stationkeeping	X	X	X
9	Geosynchronous Reacquisition	X		X
10	Automatic Reconfiguration	X	X	X

After IAFSIM had been electrically and functionally integrated with the IOCC through the X.25 packet-switching network, a final acceptance test comprising tests 6 through 10 of Table 2 was conducted.

Examples of system test results

The IAFSIM test results were compared with the Matra results in terms of the time response (peak transient values, steady-state values, settling time, *etc.*) of variables such as attitude angles, attitude rates, and wheel currents. Even though the acceptance test plan called for 10 separate tests corresponding to the different modes of operation, the modes were linked so that the tests better represented the mission as it would actually be flown. Two examples of these tests are described below.

LAEF MANEUVER

Figure 6 shows the strip charts of significant variables for a test sequence corresponding to the LAEF maneuver. At the start of the recording ($t = 0$), the AOCs is firing thrusters to maintain the three-axis attitude between limits, with the digital sun sensor for pitch and yaw sensing, and a rate-integrating gyro for roll sensing. Only the variations of the attitude angles about their values at $t = 0$ are relevant to this discussion. When the LAE fires, it accelerates the spacecraft along the positive yaw axis (z -axis of Figure 2). In this condition, the pendulums that model the fuel and oxidizer in the two propellant tanks have equilibrium points along the negative yaw axis.

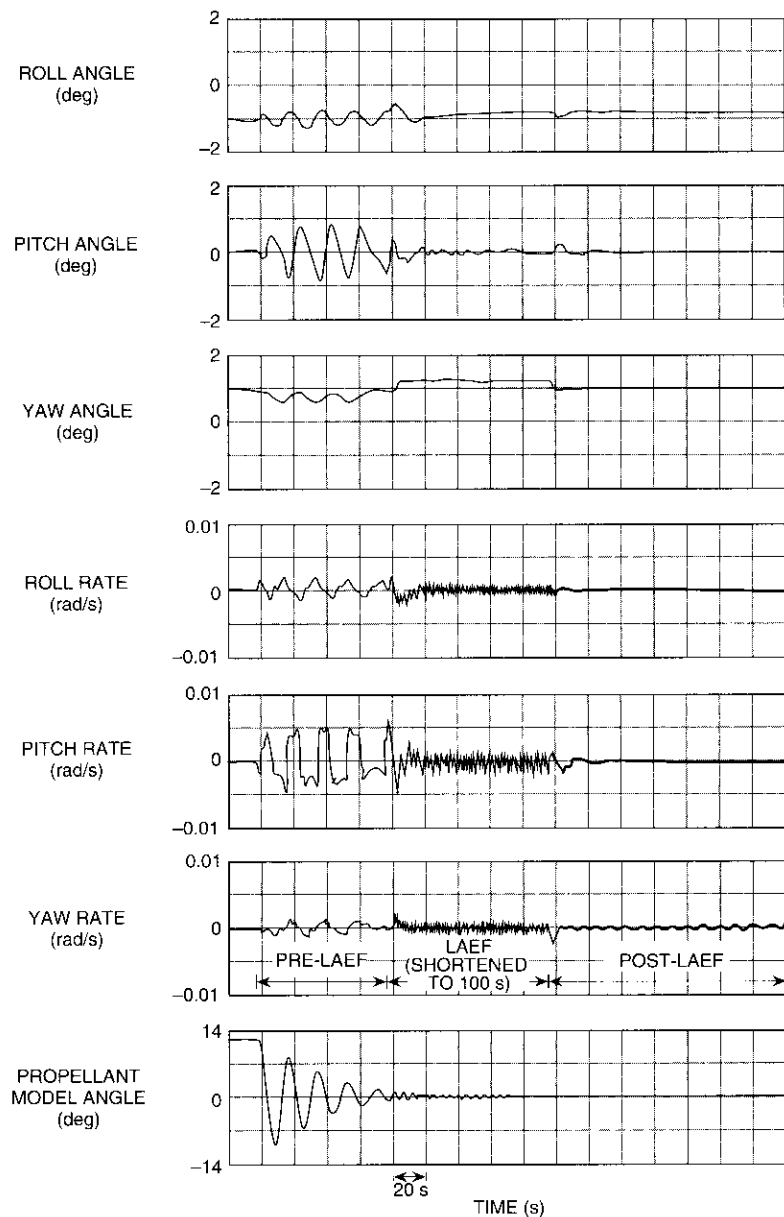


Figure 6. LAEF Maneuver Test

At $t = 0$, the pendulums are essentially stationary at an arbitrary angle of 12° from the equilibrium points. When the spacecraft is assembled, the LAE is aligned to the spacecraft under the assumption that the propellants are at these equilibria. Thus, the disturbance torque due to LAEF is minimized at these positions. With this in mind, at $t = 16$ s, a pre-LAEF maneuver is executed whereby low-thrust control thrusters aligned parallel with the LAE are fired for 80 s to force the propellants to settle closer to their equilibrium points.

Figure 6 shows the damped oscillation of the oxidizer around the roll axis. The other propellant motions are similar. The attitude excursions of up to 0.8° in pitch are as expected, based on Matra test results. At $t = 96$ s, the LAEF maneuver is executed. In the actual ITALSAT mission, two long maneuvers of about 30 minutes each are performed at apogee passages to raise the perigee. For the test, an LAEF maneuver shortened to 100 s is adequate to demonstrate both transient and steady-state performance. After the LAEF, the AOCS settles into behavior similar to that prior to the maneuver.

EARTH ACQUISITION

Figure 7 shows the strip charts for a test sequence of the initial earth acquisition at synchronous altitude. During this entire sequence, the spacecraft is under thruster control for all three axes; however, switching between attitude reference sensors is required. This is a classic acquisition maneuver for communications satellites, whereby the spacecraft's roll axis (x -axis) is pointed toward the sun under thruster control, using the coarse analog sun sensor for pitch and yaw sensing, and a slow roll rate of $0.8^\circ/\text{s}$ (0.014 rad/s) is maintained using a roll gyro as a rate sensor. Since this maneuver is performed near local dawn (if the positive x -axis is pointed at the sun) or local dusk (if the negative x -axis is pointed at the sun), the earth sensor, which is aligned along the positive z -axis, is guaranteed to see the earth in no more than 450 s. At the start of the recording shown ($t = 0$), the AOCS has the roll axis pointed toward the sun and has established the earth search rate. Also, it has been commanded from the control center to execute the earth acquisition autonomously once the earth sensor outputs are proper. At $t = 15$ s, the earth sensor sees the earth and begins to provide a roll output. At this point, the AOCS switches to earth acquisition mode, taking its roll and pitch error information from the earth sensor. As the recording shows, the roll attitude overshoots null by a substantial amount, which is large enough to saturate the earth sensor. Earth capture is completed quickly (within 100 s), mainly because accurate rate information is available from the gyros.

Since the maneuver was started with the roll axis pointed toward the sun, as much as 23.5° of yaw error may exist at this point in the sequence because the

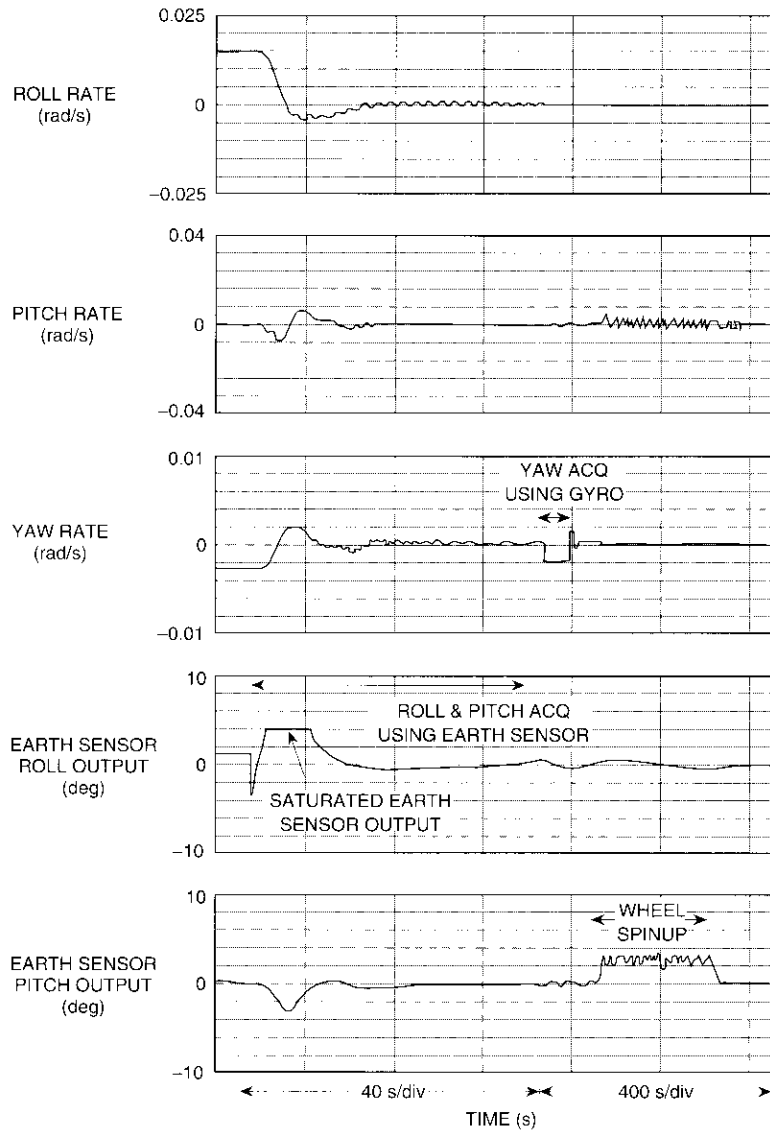


Figure 7. Test of Initial Earth Acquisition at Synchronous Altitude

sun's declination can be as much as 23.5° from the earth's equatorial plane. This error is removed in the next part of the sequence, starting at $t = 150$ s, by applying an open-loop command to the yaw channel until the yaw gyro output has changed by the negative of the original error. Finally, the telecommand to spin up the momentum wheel is sent. It takes 500 s for the wheel to run up to its operating speed. During this time, the wheel exerts a reaction torque about the spacecraft pitch axis, thus requiring thruster firing to maintain pitch control and resulting in a pitch offset of about 3° .

The actual flight sequence described above takes 2 to 3 hours to complete because many checks are made to ensure that all spacecraft subsystems, including the AOCS, are in good working order prior to each step. The sequence shown in Figure 7 was performed expeditiously in about 1,200 s for the purposes of the test because such checks were not required.

Potential applications for IAFSIM

The IAFSIM at the IOCC can be used to develop applications for expert systems and neural networks for control center operations. There is industry-wide interest in using software systems based on these methods to aid in real-time anomaly detection and diagnosis, either to reduce risk to satellites or to lower the cost of operating them. Because of their critical role, these systems must be validated thoroughly before they are used in operations. Since satellites generally perform well and experience few anomalies, there are not sufficient test cases based on flight experience to validate these systems. Furthermore, the systems are required to account for a wide range of anomalies, beyond those that may have been experienced previously. Because of its high fidelity and ability to simulate a variety of failures at any time during a simulation run, IAFSIM is the only practical way to generate extensive test cases for these software systems.

As confidence is gained in using software systems for anomaly detection and diagnosis, these systems can be extended to fault compensation and failure correction. For these applications, it is important that the simulator be well integrated with the systems. IAFSIM can be used to evaluate and practice the recommended corrective procedures, and the systems can use IAFSIM to improve their performance.

Conclusions

IAFSIM was fully integrated with the IOCC in December 1990. The simulator appears to the IOCC as another ITALSAT spacecraft, with its own spacecraft identification. Thus, operators can send commands to it and receive telemetry

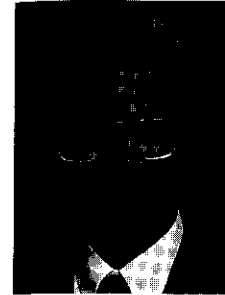
from it, as designed. Simulations lasting as long as 8 days have been run. IAFSIM was initially used to validate the IOCC software and hardware, to train operators, and to develop flight control procedures. It continues to be employed to develop procedures, and has also been used to investigate a few cases of unexpected behavior in flight, as well as to validate a patch to the CLE flight software.

Acknowledgments

The technical contributions of K. Grantham, C. Arvin, J. Talcott, and R. James to this project are gratefully acknowledged. The support of F. Marconicchio of ASI and M. Sasso of Telespazio, who were instrumental in approving the IAFSIM project, and of M. Savage, who energetically championed the project, is also gratefully acknowledged.

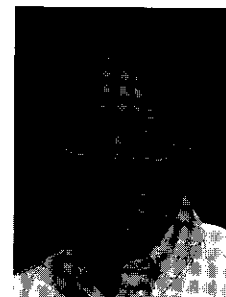
References

- [1] L. Virdee *et al.*, "INTELSAT V Attitude Determination and Control Subsystem Flight Simulator," IFAC Workshop on Simulation and Validation Techniques to Establish Spacecraft Control System Performance, Palo Alto, California, August 1983.
- [2] C. Benet *et al.*, "The COMSAT Attitude and Orbit Control System Flight Simulator," International Telemetering Conference, Las Vegas, Nevada, October 1986, *Proc.*, pp. 37-41.
- [3] W. Stallings, *Data and Computer Communications*, New York: Macmillan, 1985, pp. 70-71, 98, 420-429.
- [4] R. L. Minciotti *et al.*, "The ITALSAT Attitude and Orbit Control Subsystem Flight Simulator (IAFSIM)," International Symposium on Space Dynamics, Toulouse, France, November 1989. Paper No. MECSPA-CNES-89-111.

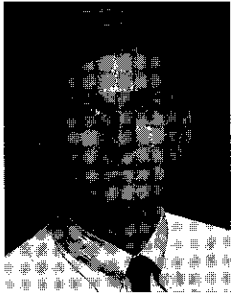


Alberto Ramos received a BSEE (cum laude) from the University of the Philippines in 1958, and an MSEE from Purdue University in 1961. He completed all course work and was admitted to candidacy for a PhD at Northwestern University. Mr. Ramos taught courses in electrical circuits and electronics at the University of the Philippines from 1961 to 1964. In 1967 he joined COMSAT Laboratories, where he had technical and management responsibilities for R&D and spacecraft program support in the fields of attitude and pointing control, and T&C. After leaving COMSAT in 1992, he had a half-year career as a private consultant before joining Orion Satellite Corporation in 1993. He is a member of the IEEE and the American Astronomical Society.

Richard L. Minciotti received a Doctorate degree in aeronautical engineering from the Università degli Studi di Pisa, Italy, in 1989. He subsequently joined Telespazio, Rome, Italy, and was responsible for the in-orbit operation of the AOCS for the ITALSAT and SAX satellites, including simulator procurement and simulation activities. He attended a year-long course in business and finance, and is currently working in the Strategic Planning group at Telespazio.

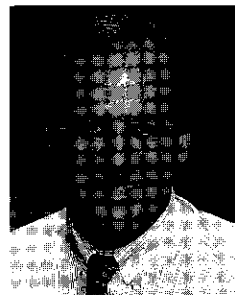
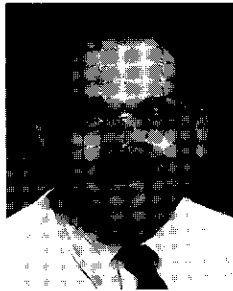


Timothy Hampsch received a BSEE from Tufts University in 1981, and an MS in physics from the University of Maryland in 1986. From 1981 to 1984, he worked on inertial guidance systems and embedded navigation computers at Northrop Corporation. In 1987, he joined COMSAT Laboratories, where he is a Senior Member of the Technical Staff. He has been responsible for the design and development of digital controllers for microwave switch matrix arrays and beam-forming matrix arrays. He has also contributed to the application of parallel processing to real-time satellite flight simulators, and has been involved in designing satellite processors used for attitude control. He is a member of IEEE and Tau Beta Pi.



George Allison received a BS in physics from Old Dominion University, and an MS in applied physics from The Johns Hopkins University. As a member of COMSAT's Communications Products Software Engineering Department, he provides support for the design, integration, and delivery of Inmarsat earth stations. In addition, he was responsible for developing the satellite simulation software for the ITALSAT AOCs Flight Simulator. Prior to joining COMSAT, Mr. Allison worked at The Johns Hopkins Applied Physics Laboratory, where he developed computer modeling of acoustic propagation in the ocean.

Ervan W. Hare has been involved with electronics since 1970, when he began a 4-year term with the U.S. Navy. After completing the Naval Aviation Electronics Course at Memphis Naval Air Station, he was responsible for the electronics systems of the A-6 aircraft. After leaving the service in 1974, he was employed by Fairchild Industries in the F-14 program and performed acceptance testing on the fire control panel. In 1979 he joined COMSAT Telesystems, working with the Echo Canceller program. He is currently an Assistant Staff Member in the Power Systems and Electronics Department of the Satellite and Systems Technologies Division at COMSAT Laboratories. He has been involved in the design and development of the INTELSAT V and VI, and ITALSAT flight simulators, and has gained experience in the areas of beam-forming networks, digital controllers for microwave switch matrices, and spacecraft hardware evaluation and testing.



Jeffrey W. Opiekun received a BS in mathematics from Towson University in 1978, and an MS in computer science from The Johns Hopkins University in 1982. He is currently a Senior Member of the Technical Staff in the System Development Division at COMSAT Laboratories. He has worked on numerous projects, including the ITALSAT AOCs Flight Simulator, the INTELSAT V Attitude Simulator Upgrade, the NASA Advanced Communications Technology Satellite (ACTS) Master Control Station, and communications analysis software for the Universal Modem System for the U.S. Government. From 1980 to 1983 he worked for Computer Sciences Corporation, where he participated in developing software that generated acquisition data for manned and unmanned spacecraft at the Goddard Space Flight Center.

Index: communication satellites, earth stations, in-orbit testing, performance, transponders

The EUTELSAT in-orbit test system

K. D. FULLETT, B. J. KASSTAN, W. D. KELLEY, V. E. RIGINOS,
P-H. SHEN, S. L. TELLER, AND Y. THARAUD

(Manuscript received November 3, 1992)

Abstract

An integrated suite of microwave measurement equipment, computer hardware, and measurement software was designed, fabricated, and installed into a unified test facility for measuring the communications subsystem performance of European Telecommunications Satellite Organization (EUTELSAT) communications satellites. The EUTELSAT in-orbit test (IOT) system software supports UNIX-based multiuser, multi-tasking operation in a networked environment that permits remote access and control of the IOT measurement hardware and includes a scheduler that permits unattended stability measurements. The system's human-machine interface offers point-and-click menu selection and input via a mouse device.

The EUTELSAT IOT facility incorporates a dedicated earth station command and control system computer for earth station status checking and configuration, automatic satellite saturation control hardware, and a radiometer for reading atmospheric attenuation. New tests include a method for quickly measuring the frequency response of a spacecraft channel, as well as procedures for measuring AM-to-PM conversion and AM-to-PM transfer coefficient. In addition, the satellite is used as a far-field calibrated signal source for earth station verification and assistance, which enables EUTELSAT to independently test new or existing earth stations for EIRP, gain-to-noise temperature ratio, transmit polarization isolation, and transmit antenna pattern.

Introduction

Following successful launch of a communications satellite, it is desirable to test the communications subsystem in orbit [1]–[3]. Data measured during in-orbit test (IOT) are compared with prelaunch data to determine whether the

subsystem has successfully survived launch and meets performance specifications. The technical objective of IOT is to measure the communications performance of the satellite under test as completely and accurately as possible. IOT is performed for acceptance testing immediately after launch; to monitor communications subsystem performance throughout the satellite's operational lifetime; and to investigate anomalies [4]. It may also be performed prior to the satellite being sold, or in preparation for carrying new services. These missions determine the basic requirements of the IOT system.

In a laboratory environment, a device under test is near at hand; however, a geostationary satellite is located about 42,000 km from the earth station and the IOT equipment [1],[3], which significantly complicates testing and measurement. For example, one-way signal attenuation from 180 to 215 dB is encountered at the test frequencies, and atmospheric variability along the propagation path must be accounted for. To obtain the desired accuracy and repeatability, precise calibration of the test setup, earth station equipment, and antennas is of paramount importance. On the other hand, the geometry and location of the satellite are ideal for accurately measuring the satellite's far-field antenna patterns, since prelaunch antenna patterns are generally measured on non-ideal ranges. In addition, the satellite serves as a far-field calibrated signal source for earth station verification measurements [5]. By moving the earth station antenna in a predetermined manner while measuring the strength of a test carrier received from the satellite, the pattern of the earth station receive antenna can be accurately measured.

Newer satellites provide more transponders and have greater payload complexity than earlier generations [1],[3],[6]. This trend places increased demands and constraints on the IOT systems built to test them. Because owners desire to place their satellites into revenue-generating operation as soon as possible after launch, the IOT system is expected to perform as quickly as possible, especially during acceptance testing, and to use a minimum of on-board fuel in order to maximize the useful lifetime of the spacecraft [1],[3]. Due to the increased satellite capacity and complexity, the testing process generates large volumes of data that must be maintained and reported. Finally, the pool of spacecraft experts available for performing complex IOTs and evaluating the resulting data is distributed more thinly as the number of satellite networks in service [6] increases.

Although in-orbit measurement is its primary technical objective, the IOT system must also address other requirements such as real-time operation, human/computer interaction, networking, and remote access and control of the measurement hardware. The system must provide a user interface that is easy to use, yet flexible enough to accommodate the various IOT missions. The

capability to execute measurements concurrently and to support a multiuser environment are desirable system features.

IOT technology and techniques have advanced in parallel with communications satellite technology, facilitated by the availability of more powerful, less costly computing hardware and software, as well as newer "smart" instruments that contain their own processors. Major advances were made in IOT from one satellite series to the next for the INTELSTAT III, IV, IV-A, and V satellites, and many of the fundamental IOT measurements performed 20 years ago are still in use today [1]-[4]. The development of the modern, computer-controlled IOT system is traced in References 1, 3, and 6.

IOT measurements are performed by transmitting test signals to the spacecraft and comparing their power, frequency, and phase with the signals retransmitted from the satellite. Fundamental measurements include spacecraft input power flux density (IPFD) and equivalent isotropically radiated power (EIRP), transponder in-band and out-of-band frequency response, gain transfer, group delay, and gain-to-noise temperature ratio, G/T . Over the years, many other measurements have been developed as well [1]-[5].

This paper discusses some of the innovative system features and new IOT measurements implemented in the European Telecommunications Satellite Organization (EUTELSAT) IOT system. For example, the EUTELSAT IOT facility interacts directly with the earth station command and control system (ECCS) computer, incorporates radiometric information, and uses an automatic satellite saturation controller (ASSC) in the earth station. The facility also implements new techniques for rapidly measuring the in-band frequency response of a communications satellite's transponders and for verifying the performance of a second earth station, using the spacecraft as a far-field calibrated signal source. The system's software also incorporates many new features, such as the ability to perform unattended measurements automatically at any scheduled time. The system software runs under the multiuser, multitasking UNIX operating system in a networked environment that permits remote control and access of the IOT measurement equipment and enables it to execute in a multicomputer, distributed processing network.

The user interacts with the IOT system via an X-Window-based graphical display, using a mouse to select items from a menu. Measurements are specified in a "form-fill-in" format, rather than the traditional "remember-and-type" command line interface found on many systems. The effectiveness of such graphically based user interfaces is supported by more than 30 years of research and development (*e.g.*, Reference 7).

IOT system requirements and constraints require that more of the system functionality reside in the software, which must initially address the network,

hardware, and communications environment of a distributed processing system capable of supporting a number of workstations. With development and continuous refinement over the last decade, the Measurement Processing and Control Platform (MPCP) has served as the software foundation for the EUTELSAT IOT system described here. The principal software concepts and innovations underlying implementation of the MPCP are discussed in a companion paper [8].

IOT hardware

The EUTELSAT IOT system consists of a suite of microwave measurement equipment, computer hardware, and measurement software integrated into a unified test facility for measuring the communications subsystem performance of EUTELSAT satellites. The design and operation of this IOT system are discussed in References 4 and 5, and other system features are described in Reference 6. The IOT facility, installed at the Rambouillet earth station near Paris, France, has been used to test the EUTELSAT II spacecraft, F1 through F4.

The major components of the EUTELSAT IOT facility, depicted in Figure 1, are the IOT equipment (IOTE), the earth station equipment, and the dual-polarization transmit/receive antenna. A station radiometer connects to a second antenna. The IOTE comprises microwave measurement system (MMS) hardware and the IOT workstation and peripherals.

The earth station equipment receives uplink signals generated by the IOT hardware, amplifies them, and transmits them to the antenna system. It then receives downlink signals from the spacecraft, amplifies them, and transmits them to the IOTE for measurement. The IOTE supports dual-polarization measurements and accommodates the 14- to 14.5-GHz uplink band and the three downlink bands that fall in the 10.95- to 12.75-GHz frequency range of the EUTELSAT II satellites.

In earlier IOT systems, earth station information was obtained directly from a station operator. The EUTELSAT IOTE interacts with the ECCS computer to monitor and control the earth station equipment. The IOT workstation sends commands via an interconnecting IEEE-488 bus cable to the ECCS computer. For example, the IOT workstation may request uplink power meter readings or the power level and frequency settings on the inject synthesizer. The computer performs the requested operations and returns responses to the IOT workstation.

The ECCS computer, supplied by Direction des Reseaux Exterieurs de FRANCE TELECOM (DTRE), can perform the following measurement-related functions:

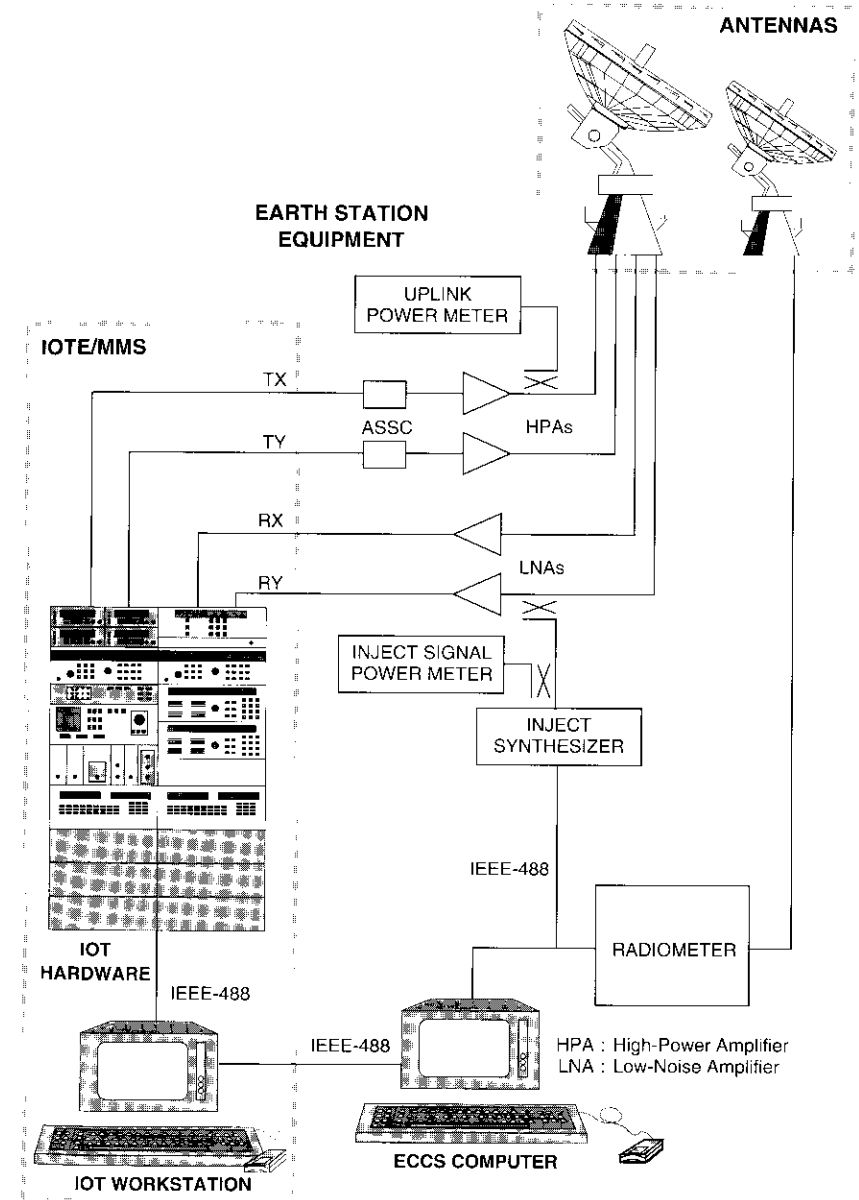


Figure 1. EUTELSAT IOT System Block Diagram

- Control the injected signal power and frequency as commanded by the IOT workstation.
- Control the uplink power level and perform power-leveling as the frequency is varied.
- Control the ASSC equipment to determine the saturation power level.
- Provide a radiometer reading to the IOT workstation on command.
- Read the uplink power meter at the feed and provide the calibrated readings to the IOT workstation.
- Provide the antenna gain and coupler calibration values for any operational uplink or downlink frequency.
- Provide the azimuth and elevation antenna position to the IOT workstation.
- Configure the earth station on command from the IOT workstation.
- Zero and calibrate the uplink and inject signal power meters.

IOT systems must be capable of determining the saturation flux density of the spacecraft. One method that has been used successfully is the amplitude-modulated (AM) nulling technique, described in the IOT system literature (*e.g.*, References 1 and 2). In early IOT systems, AM nulling was applied manually; the EUTELSAT IOT uses the ASSC to perform this function automatically. The ASSC maintains the satellite at saturation, and was designed to meet EUTELSAT specifications [4]. It operates over a large dynamic range of satellite gain.

The ASSC automates the AM nulling technique to determine saturation flux density, as follows. First, an AM carrier is transmitted to the spacecraft. On the downlink, after envelope detection, the AM carrier is phase-locked to the AM source, producing an error voltage proportional to the modulation amplitude, which decreases as saturation is approached. The error voltage is interpreted by the digital processor, which commands the uplink earth station EIRP. As saturation approaches, the EIRP is controlled in 0.05-dB steps. When the error voltage reaches a minimum, saturation has been achieved. Since the ASSC operates as a closed loop, any variation in uplink propagation conditions is counteracted by the detected error voltage, the sign of which governs the relative polarity of the uplink EIRP.

The IOT setup must take into account not only instrumentation, earth station equipment, and antenna uncertainties, but also the RF path between the station and the spacecraft [1],[3]. In the EUTELSAT IOT system, the measurement program obtains atmospheric attenuation data from a radiometer. The radiometric configuration consists of a Cassegrain antenna connected to a noise-injection-type radiometric receiver, and a computer to control operation, pro-

cess the measurement data and perform housekeeping functions [4]. Attenuation calculated at 13 GHz is scaled to other frequencies by the radiometer's computer, using standard frequency-scaling equations. Over the short time period typical of an IOT measurement (a few minutes), the change in atmospheric attenuation is assumed to be negligible.

Figure 2 is a simplified block diagram of the EUTELSAT IOTE MMS hardware configuration. A high-stability, 10-MHz reference signal output by uplink synthesizer 1 (UL Syn 1) is amplified and distributed to the IOT instruments as a common reference signal. The IOT workstation communicates with the instruments via three IEEE-488 buses, and with the ECCS computer via a fourth IEEE-488 bus.

Two test carriers are provided by two RF synthesizers. UL Syn 1 outputs an RF test carrier, as commanded by the IOT workstation. The synthesizer's RF output can be frequency-modulated by an externally supplied modulation signal to disperse the uplink energy, in order to meet the downlink earth surface spectral density specifications of the International Radio Consultative Committee (CCIR) 358-2 during routine operation. Because the synthesizer does not operate over the required uplink frequency range, a 12-times frequency multiplier is employed.

Uplink synthesizer 2 (UL Syn 2) is capable of generating an RF output test signal anywhere in the uplink frequency range. The synthesizer's RF output (in the 14- to 14.5-GHz range) can be amplitude-modulated externally (via the modulator shown in Figure 2) when necessary—for example, when group delay is measured.

An uplink switching/coupling matrix provides flexible uplink configurations and is necessary to support all IOT measurements. The RF output from either synthesizer can be switched and routed to either transmit polarization waveguide, TX or TY. When required, the IOTE can produce two carriers on one of the two polarizations, or a single carrier on each polarization, to support two-tone measurements such as third-order intermodulation, CI_3 .

As shown in Figure 2, the spectrum analyzer (SA) can be switched, via the 8-pole switch, to input the uplink polarization (TX or TY), the received signal (RX or RY, selected by another switch), the IF synthesizer output, or the output from the phase measurement subsystem. Additionally, the spectrum analyzer can be switched to input a sample of either high-power amplifier (HPA) output signal, as well as to receive an input signal from a front panel connector. The video output of the spectrum analyzer can be switched to provide an input to either the network analyzer or the digital voltmeter. The analyzer's IF output can be switched to provide an input to either the modulation analyzer or the frequency counter. The switch configurations for all

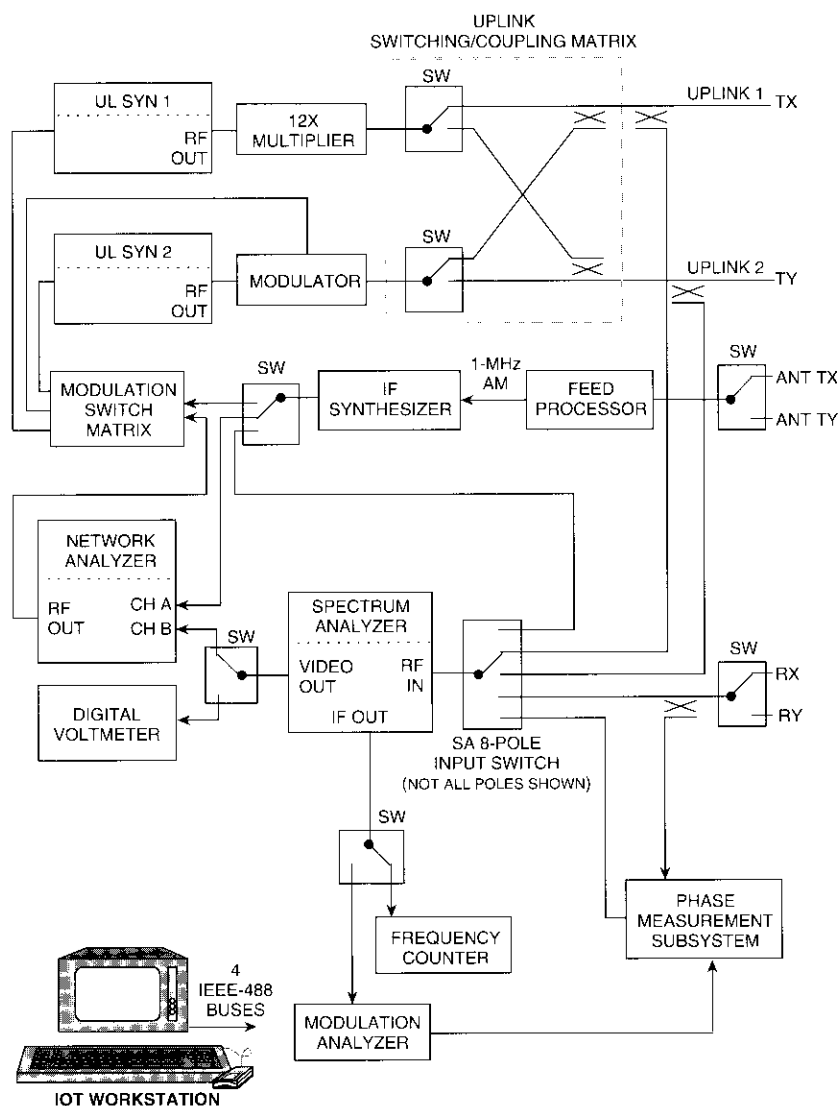


Figure 2. IOTE Microwave Measurement System Block Diagram

measurements are controlled by the IOT workstation via RF switch controllers and IEEE-488 buses.

The feed processor, which is used for measurements such as group delay, performs the following function. When the uplink carrier produced by UL Syn 1 or UL Syn 2 is amplitude-modulated, the modulation is detected by diode detectors located near the antenna feed. Typically, the AM frequency is around 1 MHz. The detected modulation is transmitted to the input of the feed processor, which can be switched to select either of the uplink polarizations (ANT TX or ANT TY in Figure 2). The feed processor amplifies and filters the detected modulation, and supplies it to the IF synthesizer as a reference. The synthesizer's 1-MHz, frequency-adjusted output is fed into the network analyzer, which measures its phase relationship with respect to the Doppler-shifted 1-MHz modulation on the carrier received by the spacecraft.

The phase measurement subsystem is used to perform phase noise measurements on the received RF signal, such as AM-PM conversion, AM-PM transfer coefficient, and spurious modulation. It consists of a down-converter, a phase reference synthesizer, and a dedicated low-frequency spectrum analyzer.

An important innovation of the EUTELSAT IOT system is its ability to perform unattended stability measurements. While measurements are normally performed with operator interaction, some can be executed in a non-interactive mode if directed by the user via the X Window interface. The EUTELSAT IOT system allows the user to specify measurements to execute at any scheduled time and at specified intervals throughout a specified duration.

The ability to schedule measurements and to have them execute periodically provides the basis for performing stability measurements, which track various quantities as a function of time. For example, the EIRP measurement can be scheduled to run every hour over a 24-hr period to determine EIRP variation. Stability measurements can be performed for spacecraft EIRP, spacecraft IPFD, in-band and out-of-band transponder frequency response, spacecraft G/T , beacon EIRP, and beacon frequency.

The IOT system scheduler launches measurements at the scheduled time and allocates resources to a measurement that has requested them. It also manages scheduling conflicts between two or more measurements on a first-come, first-served basis. When a measurement completes execution, it returns resources such as the spectrum analyzer and other measurement instruments to the scheduler, which makes them available to the next scheduled measurement. The operation of the IOT scheduler, and its interaction with the measurement user interface program and the actual measurement program (which are

separate programs that can execute on different workstations and at different times), are described in the companion paper [8].

The IOTE is controlled by a 32-bit, reduced instruction set computing (RISC)-based engineering workstation with 16 Mbytes of memory and a 600-Mbyte hard disk for program and data storage. The workstation executes IOT system and measurement software to perform IOT measurements and to process, store, and retrieve measurement data. The software runs under a licensed version of the UNIX System V operating system. The IOT workstation controls the microwave measurement hardware and communicates with the ECCS computer across an IEEE-488 bus. It also communicates with the user via an X-Window-based, graphical user interface with keyboard and mouse input. The workstation supports connection to an IEEE 802.3 local area network (LAN). Its peripherals include a 19-in., high-resolution, color bit-mapped display; a multipen plotter; a printer; a cathode-ray tube (CRT) terminal; and a 9,600-bit/s modem for remote access and control. The IOT software is described in detail in Reference 8.

Standard IOT measurements

Most satellite communications payload parameters, such as antenna patterns, EIRP, and receive G/T , can be derived from fundamental measurements of microwave power and frequency [3]. During the past 20 years, the evolution of IOT measurement techniques has been governed by the increasing complexity of communications payloads and the requirement to place the spacecraft into operational service as quickly as possible while minimizing consumption of onboard fuel. Continuous refinement of measurement techniques has permitted more parameters to be measured with a higher level of confidence. This has resulted in an expanding amount of data from the increased number of transponders and connectivity configurations [1],[3].

For each IOT measurement, all uncertainties must be identified and accounted for in an error budget. The total root-sum-square (RSS) uncertainty resulting from all error sources is computed for each measurement. As discussed in Reference 9, uncertainties can arise from the spacecraft (antenna pointing, platform stability, and repeatability of switching), atmospheric loss and variability, the earth station (antenna calibration and pointing, up and downlink coupler calibration), and measurement instrumentation. Numerical uncertainties due to digital processing of raw measurement data within the workstation must be considered for some measurements, such as the "Fastswep" measurement described later.

The human operator is another potential source of measurement error (*e.g.*, improper use of instrumentation, lack of skill, and improper measurement

technique). Human interface engineering can detect and prevent (or minimize) operator errors, as discussed in References 6 and 8.

To enhance measurement accuracy, the measurements of absolute quantities necessary for an IOT have been reduced to microwave power, frequency, and phase [1]; all other measurements are relative to, or can be derived from, these values. For the uplink, transmit power is measured directly by a directional coupler that provides power from the uplink waveguide to a power meter.

The EUTELSAT IOT system performs a large number of measurements that can be grouped according to the basic quantity measured: power, frequency, or phase.

Power measurements

The fundamental power measurement performed by an IOT system is the accurate measurement of spacecraft EIRP. Many other measurements are derived from the EIRP, including the point-to-point transponder frequency response and gain transfer measurements.

For measuring downlink signals, an injected carrier technique has proved to be the best approach and continues to be used in IOT systems [1]–[3]. A locally generated carrier (the inject signal) is offset slightly in frequency from the carrier received from the satellite, and is injected via a directional coupler into the waveguide between the receive antenna feed and the low-noise amplifier (LNA), as shown in Figure 1. After amplification by the LNA (and additional amplifiers, if necessary), both the received and injected signals are displayed on the spectrum analyzer and measured. The difference is used by the EIRP program to adaptively adjust the injected signal power to within about 1 dB of the received signal. The final difference is then measured by the spectrum analyzer, and the power level of the final injected carrier is measured precisely by a power meter. Based on this knowledge of the injected signal level and its difference from the received signal level, the level of the received signal (even if noisy) can be determined to within a few tenths of a decibel. This adaptive technique ensures a wider dynamic range, while reducing logarithmic amplifier errors within the spectrum analyzer. The injected carrier technique permits accurate measurement of received continuous-wave (CW) carriers and is unaffected by any change in the gain of the receive chain. The calibration effort can thus be restricted to a few passive microwave components, such as the inject coupler [1].

The spacecraft EIRP is computed from the measured injected signal power meter reading, the level difference measured by the spectrum analyzer, the inject signal coupler value, the downlink antenna gain at the frequency of

interest, the downlink path loss, and the downlink atmospheric loss. Spacecraft EIRP measurement using the injected signal technique is well established and has been described in earlier IOT literature (*e.g.*, References 1 and 2.)

The EUTELSAT IOT system performs the following power measurements and monitoring functions:

- EIRP (downlink only, with no uplink test signal from the IOT station)
- Combined spacecraft IPFD and spacecraft EIRP
- Amplitude linearity (gain transfer) and intermodulation (CI_3)
- G/T and G/T stability
- Point-to-point frequency response (in-band, in-band stability, out-of-band, and out-of-band stability)
- Fast sweep frequency response
- Overall cross-polarization isolation
- Receive and transmit cross-polarization
- Antenna pattern
- Gain adjustment
- Spurious output
- Beacon measurements (EIRP, EIRP stability, cross-polarization isolation)
- Communications system monitoring (CSM)
- Payload monitoring (IPFD/EIRP, linear gain, gain transfer, local oscillator frequency)
- Earth station verification and assistance (ESVA).

The Fast sweep and ESVA measurements are new with the EUTELSAT IOT system, and are described later in this paper.

Frequency measurements

Frequency measurements are the second category of fundamental measurements performed by an IOT system. The EUTELSAT IOT system can measure frequency conversion error and stability, beacon frequency and beacon frequency stability, and routine spacecraft payload monitoring (RSPM) frequency conversion error. Since the uplink frequency and nominal spacecraft local oscillator frequency are known, the spectrum analyzer (Figure 2) can be tuned to the nominal downlink frequency, where it performs peak and zero-span measurements. The frequency of the analyzer's IF output is measured precisely by the counter. The measured received signal frequency offset from the

center frequency of the analyzer IF is used in conjunction with the analyzer's tuned microwave frequency to fine-tune the analyzer to the frequency of the received signal. This technique is employed in all IOTE measurements to ensure that the spectrum analyzer is tuned precisely to the received signal frequency, so that power measurements are performed accurately.

For some measurements in which the precise frequency is the objective, the IOTE can correct for the Doppler shift caused by non-zero radial velocity between the spacecraft and the earth station. For example, in measuring the spacecraft local oscillator frequency, the IOT user interface permits the user to specify that Doppler correction be performed. The measurement then computes the Doppler-effect frequency contribution, based on the velocity, and corrects the received frequency.

Phase noise measurements

The EUTELSAT IOT phase measurement subsystem, shown in Figure 2, measures the AM-PM conversion coefficient, K_p ; AM-PM transfer coefficient, K_t ; and spurious modulation. The AM-PM conversion and transfer coefficient measurements are new, and are described in the next section.

New measurements

Among the system features mentioned above are several new measurements implemented in the EUTELSAT IOT system: Fast sweep frequency response, AM-PM conversion coefficient, AM-PM transfer coefficient, and several ESVA measurements (EIRP, G/T , transmit polarization isolation, and transmit antenna pattern).

Fast sweep frequency response measurement

Measurement of a spacecraft channel's frequency response is a fundamental IOT system requirement. The standard technique measures the response point-to-point throughout the band of interest. Because of the larger number of channels on board the latest generation of communications satellites, such as EUTELSAT II, measuring the frequency response of all channels requires substantial testing time. Since this activity deprives the satellite owner of revenue, there is continual pressure on IOT systems designers to shorten the time required for IOT.

A new technique called Fast sweep has been developed which measures frequency response by continuously sweeping the desired spacecraft channel, while simultaneously measuring the received downlink signal on the spectrum

analyzer. The synthesizer generating the swept uplink signal sweeps much slower than—and is not synchronized to—the spectrum analyzer measuring the received downlink signal. Raw measurement data are captured digitally by the spectrum analyzer and read into the computer for numerical post-processing and to determine the frequency response. Because most of the measurement processing is performed in the computer, standard equipment such as the HP-8673E synthesizer and HP-8566B spectrum analyzer can be used to obtain the raw data. No special equipment is required to synchronize the sweeps of the two instruments.

It is instructive to examine the traditional IOT point-to-point measurement technique in terms of the time it requires. The technique consists of a combination of EIRP and IPFD measurements repeated over a set of predetermined discrete frequencies across the bandwidth of interest. The frequency response of a transponder is determined by measuring downlink power relative to a band-center measurement in either the linear or saturated region of the traveling wave tube amplifier (TWTA) frequency band of the transponder under test, with the uplink power kept constant as the frequency is varied. Measurement at saturation gives the frequency response of all filters after the output TWTA, while measurement in the linear region gives the overall frequency response.

Initially, the system is tuned to the channel center frequency and the IPFD is measured at saturation, as described in References 1 and 2. The uplink power is then reduced to an operator-specified backoff level, and the system is tuned to the lowest frequency to be measured. The IPFD is measured at each frequency and used in conjunction with the EIRP measurement to calculate the transponder gain, thus compensating for uplink power variations due to changes in uplink frequency. The frequency is then stepped to the next discrete frequency, and the gain is again calculated. This process is repeated until the transponder gain has been measured at all frequencies in the desired band. Measurements of EIRP and IPFD employ radiometric data to account for atmospheric attenuation.

The point-to-point frequency response measurement uses the injected signal technique, described earlier and in References 1 and 2. A limitation of this approach is the measurement time required. For each frequency point, the uplink synthesizer is tuned and the spectrum analyzer waits approximately 240 ms for the downlink signal. The analyzer is tuned to the received signal and measures it. The inject synthesizer is then tuned by the FCCS computer. The spectrum analyzer is retuned to the inject signal and measures it. At least one adjustment of the inject synthesizer power level is necessary to bring the received and injected signal levels to within 1 dB of each other. Each adjust-

ment is commanded through the FCCS. Finally, the inject power meter is read. These operations typically require a few seconds per frequency point, with the majority of time being associated with ECCS communications and reading the power meter. Thus, measuring a 40-MHz channel in 1-MHz steps requires about 8 minutes.

By comparison, FastSweep measures the frequency response of a spacecraft channel in a much shorter time, but with some reduction in accuracy and dynamic range. The accuracy of FastSweep, with earth station correction, is 0.27-dB RSS uncertainty, as compared with 0.17-dB RSS uncertainty for point-to-point measurement performed in the linear region of the TWTA.

Typically, FastSweep measures the response of a 40-MHz channel in approximately 8 s, and an 80-MHz channel in approximately 10 s, plus a display time of about 1 s. The dynamic range of the measurement is approximately 50 dB, exclusive of limitations within the earth station. By comparison, the stepped point-to-point measurement has a dynamic range in excess of 80 dB; however, the measurement time is considerably longer. The FastSweep measurement configuration is depicted in Figure 3.

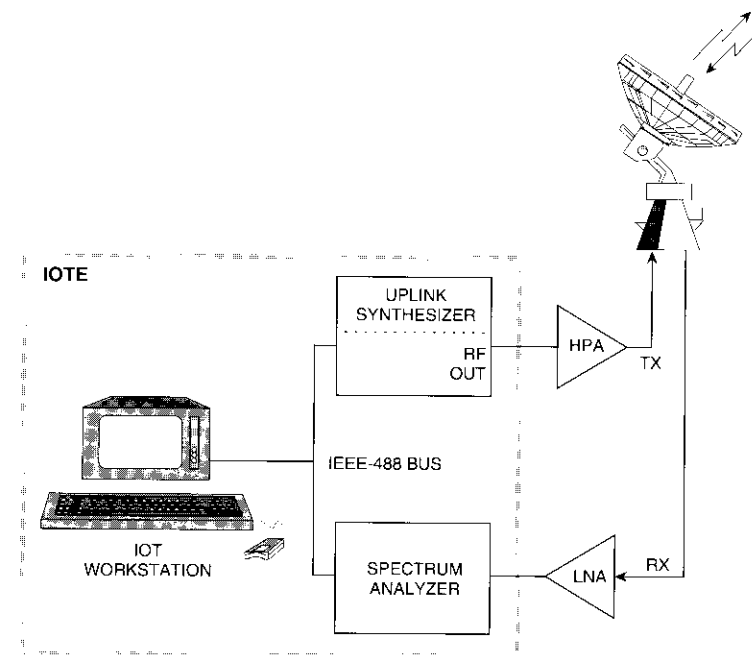


Figure 3. *FastSweep Measurement Configuration*

Fastsweep generates a frequency response that is relative in both frequency and power to band center. The major factors contributing to uncertainty in the Fastsweep method within the filter passband are the gain slope in the uplink, the ability to rapidly level the uplink power over the measurement bandwidth, the downlink gain slope, and the spectrum analyzer gain slope over any 80-MHz bandwidth.

If requested by the operator during measurement specification, the earth station noise contribution can be taken into account by pointing the earth station antenna to the sky and performing a Fastsweep when no downlink signal is present. Several Fastsweep calibration measurements may be performed and averaged to lessen the effect of noise variation. The resultant noise-only Fastsweep, which includes the nonlinearities of the earth station receive chain, is stored in an earth station calibration file and can be used to correct the Fastsweep measurements of spacecraft transponders. Calibration measurements are performed for each receive polarization across each of the three EUTELSAT II downlink receive bands.

Fastsweep is performed in two phases: sweeping of the uplink by the uplink synthesizer, and measurement of the received downlink by the spectrum analyzer. This is followed by numerical post-processing to extract the frequency response from the raw data. When the measurement phase begins, the synthesizer generates a frequency sweep over the desired uplink band, the amplitude of which is leveled by the leveling loop controlled by the ECCS computer. For each sweep, the synthesizer outputs a sequence of discrete, rather than continuous, frequencies. The synthesizer dwells at each frequency for the minimum time that allows several measurements (*i.e.*, spectrum analyzer sweeps) of the received signal by the spectrum analyzer, as illustrated in Figure 4.

While the synthesizer is sweeping the uplink, the spectrum analyzer continuously sweeps the received signal, asynchronously with respect to the synthesizer sweeps, using the max-hold measurement mode. The resolution bandwidth is chosen to optimize sweep speed vs the measurement signal-to-noise ratio, S/N . Smaller bandwidths require a much longer sweep time, while larger bandwidths degrade the available carrier-to-noise power density ratio, C/N_0 . Typically, a 100-kHz-resolution bandwidth is used.

After a sufficient number of analyzer sweeps, the measurement phase terminates and the data processing phase commences. The measurement program reads the stored trace from the spectrum analyzer, which contains N frequency-vs-amplitude data points (f_i, A_i), where $i = 1, \dots, N$. For the HP-8566B spectrum analyzer used in the EUTELSAT IOTE, $N = 1,001$. The amplitude value, A_i , for each data point is the peak power that was measured at

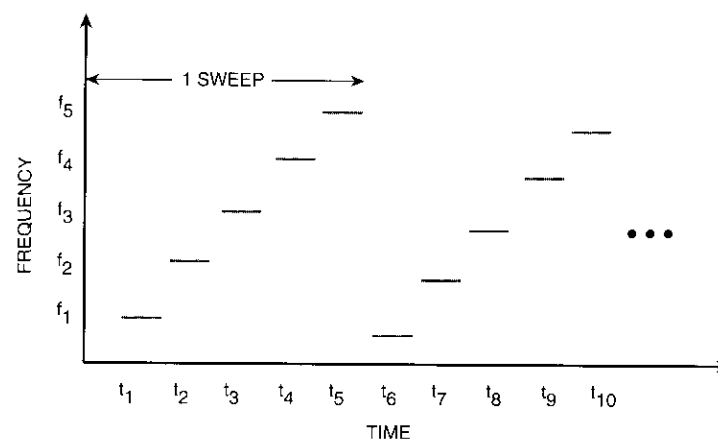


Figure 4. Synthesizer Output vs Time

frequency f_i during the entire measurement phase. The array of measured data points read from the analyzer is time-sequenced, such that the i th frequency, f_i , always occurs earlier than the $(i + 1)$ frequency, f_{i+1} . The trace read from the spectrum analyzer resembles the one shown in Figure 5.

As can be seen in the figure, the trace contains peaks and valleys. Peaks are actual measurements of the downlink signal, while valleys are signal dropouts that occur during the frequency step transitions of the synthesizer and the retraces of the synthesizer sweep. The dropouts are signal fades, which are measurement artifacts that occur because the spectrum analyzer and synthesizer sweeps are not synchronized. The spectrum analyzer measures noise peaks, rather than the actual signal, during synthesizer switching transitions to new frequencies.

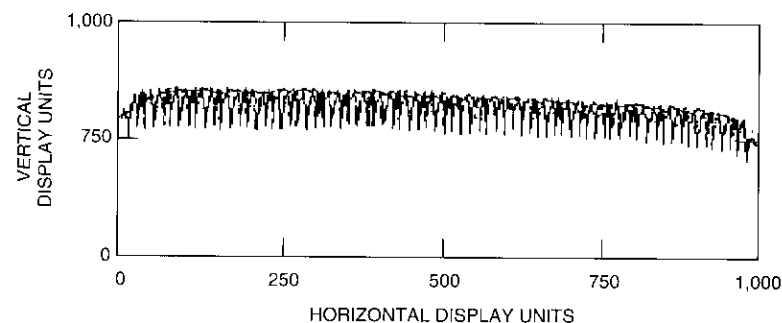


Figure 5. Fastsweep Spectrum Analyzer Trace Output

The desired response can be obtained by extracting the envelope of the trace data. This is accomplished by numerically post-processing the data, as follows. The analyzer trace depicted in Figure 5 can be viewed as a time-sequenced "signal" with low-frequency components (*i.e.*, the envelope that is the desired response) and high-frequency components (the signal dropouts). The envelope can then be extracted by applying a numerical low-pass filter to the "signal." The filter consists of a fast Fourier transform (FFT) operation on the data set, followed by removal of high-frequency points, followed by a second FFT. A peak detection is then performed on the filtered data to obtain the envelope.

Although the numerically implemented low-pass filter algorithm removes the systematic high-frequency perturbations contained in the measured data set, random noise in the correlated samples is not removed. To minimize the noise, multiple Fastsweps are performed and averaged. Figure 6 is a typical plot output of a Fastswep.

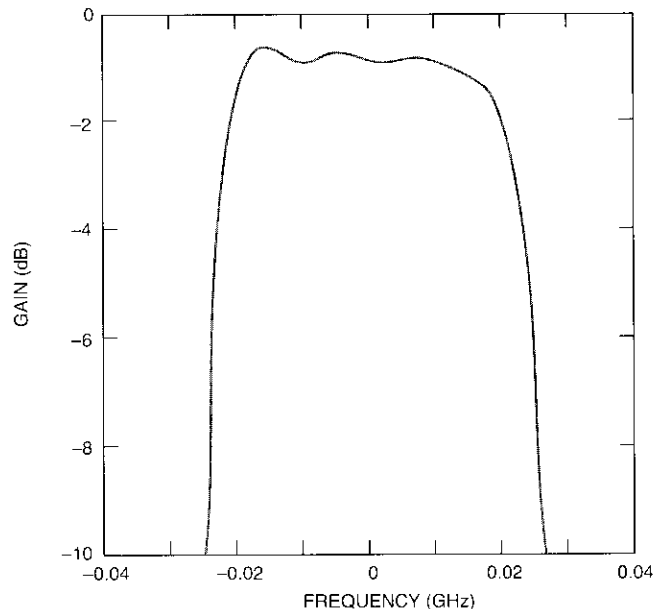


Figure 6. *Fastswep Measurement Plot Output*

AM-PM conversion and phase shift

The AM-PM conversion measurement determines that the AM-PM conversion coefficient, K_p , for each transponder is within the limits specified for drive levels to the TWTA, from 20-dB input backoff to saturation. The total phase shift is calculated by integrating the conversion coefficient phase for comparison with the satellite specification.

In this measurement, the IOTE transmits an amplitude-modulated carrier with a low modulation index at an uplink power level corresponding to 20-dB input backoff of the TWTA. The power level is then stepped up to TWTA saturation in 1-dB steps. For each uplink power level, the corresponding downlink signal is phase-demodulated by the modulation analyzer and the phase measurement subsystem. Using a test translator, the above sequence can be repeated for the earth station loop in order to measure the phase modulation of the earth station receive chain for inclusion in the AM-PM conversion coefficient computation. The coefficient, K_p , is then plotted against the TWTA input backoff.

The measurement sequence proceeds as follows. First, a calibration procedure (described below) is performed and the synthesizer is amplitude-modulated via the external PIN modulator (see Figures 2 and 7 for the hardware configuration). The power level of the modulated carrier is then adjusted to the user-specified backoff level. The demodulated tone, output by the modulation analyzer (HP-8901A), is measured using the low-frequency spectrum analyzer (SA), and data are gathered to perform the K_p computations.

The AM-PM conversion measurement employs the phase measurement subsystem of Figure 2, which consists of an HP-11729C carrier noise test set, a low-frequency HP-3582A spectrum analyzer, and an HP-8662B RF synthesizer [10]. The subsystem configuration is depicted in Figure 7.

The instrumentation used to perform the measurement depends on the modulation frequency of the carrier, as shown in the figure. If the modulation frequency is less than or equal to 20 kHz, the modulation analyzer and low-frequency spectrum analyzer are used. If the modulation frequency is greater than 20 kHz, the HP-11729C carrier noise test set may be used.

The K_p calibration procedure is performed as follows. A single CW test carrier is transmitted to the spacecraft to verify test signal levels and the spacecraft local oscillator frequency. The IF synthesizer outputs a calibration signal into the FM port of the uplink synthesizer via the modulation input matrix switch. The modulation voltage is selected to generate a low-deviation FM signal having a nominal phase modulation of 5° peak-to-peak, which

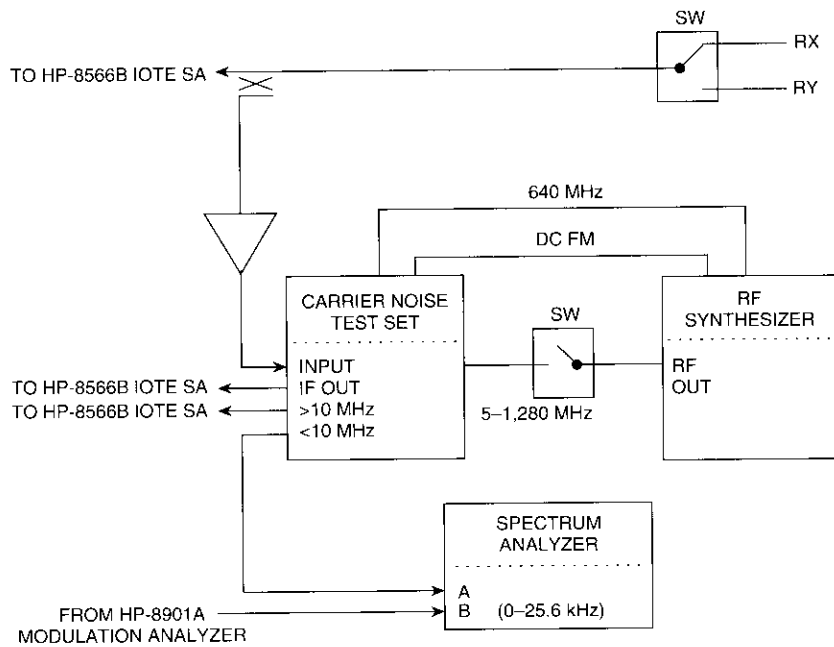


Figure 7. Phase Measurement Subsystem

serves to calibrate the receive chain phase measurement. The spectrum analyzer is then switched to the test uplink path to verify the modulation index. The carrier-to-sideband ratio is measured, adjusted if necessary, and stored. Next, the measurement system, consisting of the spectrum analyzer, modulation analyzer, and low-frequency spectrum analyzer, is connected to the uplink signal. The level of the demodulated tone at the modulation frequency is measured to establish a reference level for the phase deviation (which is about 5° peak-to-peak) and used as a calibration. The uplink signal and FM calibration modulation are turned off, completing the calibration procedure.

The calibration power level (in dBm) measured during the calibration sequence is converted to a voltage, as is the power measured at the baseband spectrum analyzer for each measurement point. The phase is then computed and used as a basis for calculating K_p from the following formulas:

$$V_c = 10^{P_c/20} \quad (\text{V}) \quad (1)$$

$$V_m = 10^{P_m/20} \quad (\text{V}) \quad (2)$$

$$\varphi = \beta \left(\frac{V_m}{V_c} \right) \quad (\text{rad}) \quad (3)$$

$$K_p = \frac{\varphi}{M} \quad (\text{deg/dB}) \quad (4)$$

where

V_c = equivalent voltage of calibration power (V)

P_c = measured calibration power (dBm)

V_m = equivalent voltage of measured power (V)

P_m = measured phase modulation power level (dBm)

φ = computed peak-to-peak phase (deg)

β = peak-to-peak phase during FM calibration (deg)

K_p = AM-PM conversion coefficient (deg/dB)

M = measured AM modulation (dB).

Figure 8 shows a typical plot output of a K_p measurement.

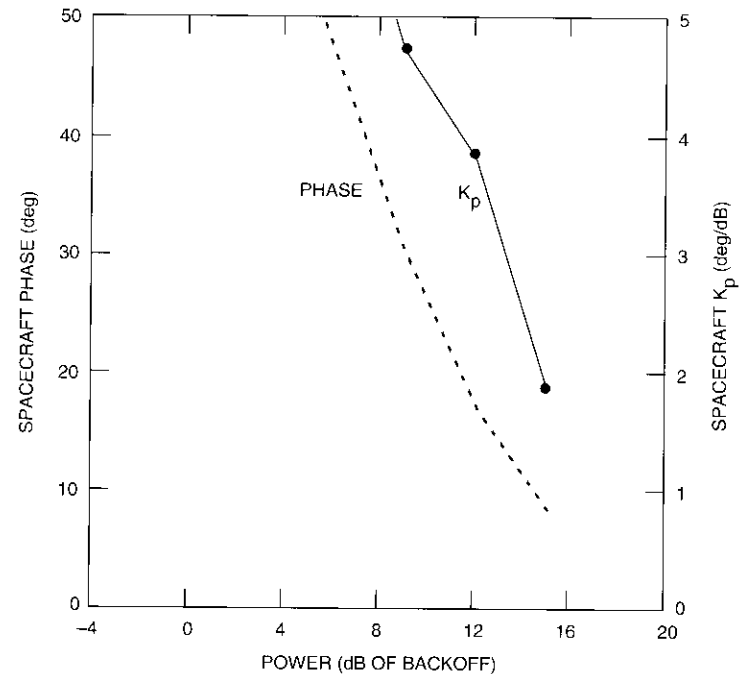


Figure 8. AM-PM Conversion Coefficient Plot Output

AM-PM transfer coefficient

The AM-PM transfer coefficient, K_T , measurement determines the amount of phase modulation imposed on an unmodulated carrier (called the "target") by an amplitude-modulated carrier (called the "source"), which is offset in frequency from the target. The IOT earth station transmits the source and target carriers simultaneously via the two independent uplink chains. After reception of the resulting downlink signal at the IOT station, both carriers are down-converted, and the target signal is passed to the modulation analyzer and phase measurement subsystem to measure its phase modulation. The AM-PM transfer coefficient, K_T , is then computed based on the ratio of the measured phase modulation of the target to the depth of the source AM.

The instrumentation used to perform the measurement depends on the modulation frequency of the source carrier, as shown in Figure 7. If the modulation frequency is less than or equal to 20 kHz, the modulation analyzer and low-frequency spectrum analyzer are used. If the modulation frequency is greater than 20 kHz, the noise test set may be employed.

For the K_T measurement, the phase demodulator is initially calibrated with a 5° peak-to-peak phase-demodulated carrier, exactly as for the K_p measurement. The source carrier from the synthesizer is then amplitude-modulated via the external PIN modulator. The power levels of the modulated source and unmodulated target carriers are adjusted so that the sum of the two is equal to the operator-specified backoff level, and then transmitted to the spacecraft. The demodulated tone output by the modulation analyzer is measured, and data are gathered for the K_T computations.

The calibration power level (in dBm) measured during the calibration sequence is converted to a voltage, as is the power measured at the spectrum analyzer for each measurement point. The phase is then computed as in the K_p measurement. Figure 9 shows a typical plot output for the AM-PM transfer coefficient measurement.

Earth station verification measurements

A new class of measurements, developed jointly by COMSAT Laboratories and EUTELSAT, uses the orbiting satellite as a calibrated signal source for performing independent ESVA measurements on a second earth station. The EUTELSAT IOT facility is located in one earth station—referred to as the earth reference station (ERS)—which performs the measurements. The second earth station is the station under test (SUT). Both stations must be able to access the satellite simultaneously. The operators at the stations coordinate their activities via telephone.

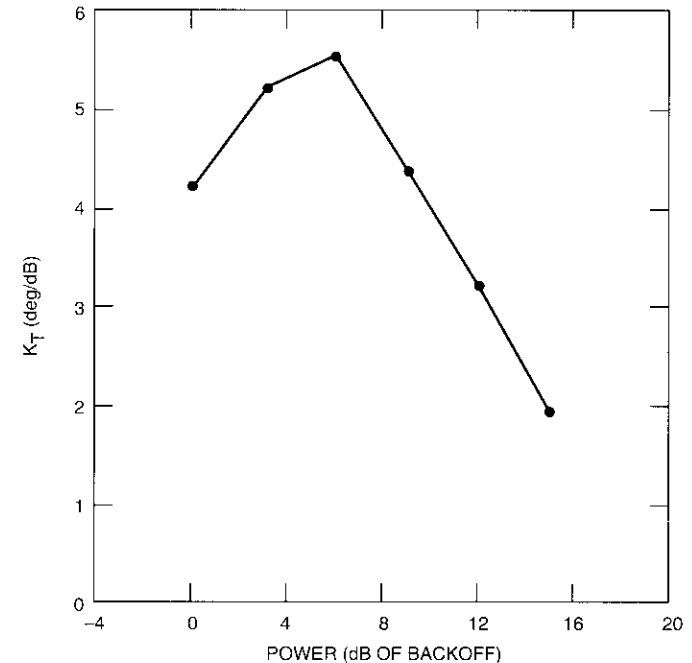


Figure 9. AM-PM Transfer Coefficient Plot Output

Four ESVA measurements have been developed and tested with an actual SUT: EIRP, G/T , transmit cross-polarization isolation, and SUT transmit antenna sidelobe pattern. References 4 and 5 contain additional information on ESVA measurement.

Because the ERS and SUT are generally off-axis relative to the spacecraft receive and transmit antennas, the spacecraft gain for the ERS and SUT signals is adjusted for the off-axis loss to the stations. The off-axis loss values are operator inputs to the measurements.

EARTH STATION EIRP MEASUREMENT

The objective of the earth station EIRP test is to verify the transmit capabilities of the SUT in terms of its accuracy and adjustment range. The basic principle of this test is that, since the ERS and SUT both transmit signals through the spacecraft at the same time and at nearly equal levels, the accuracy of the ERS measurement system will be transferred directly to the measurement of the SUT parameters. Figure 10 depicts the ESVA EIRP measurement configuration and the quantities involved.

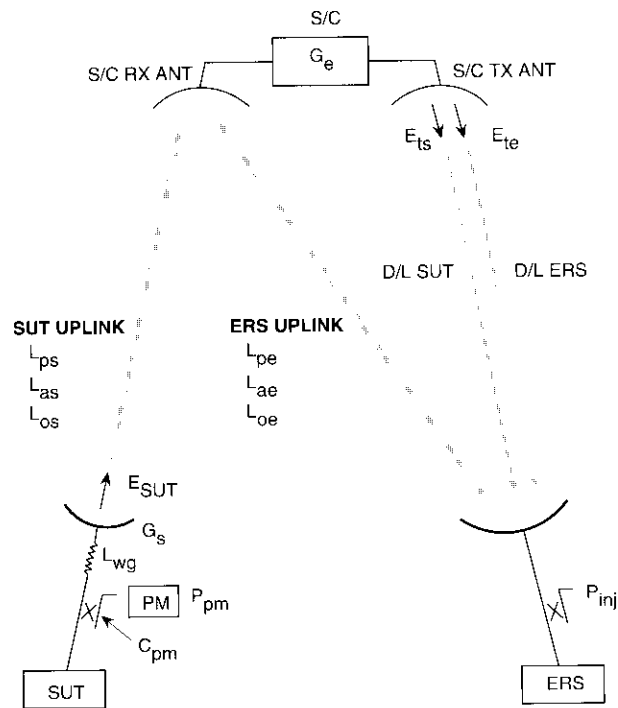


Figure 10. ESVA EIRP Measurement Configuration

The EIRP measurement is performed as follows. First, the operator is asked to ensure that the SUT is not transmitting. The operator then enters the following parameters via the measurement's user interface window:

- SUT uplink path loss (dB)
- SUT uplink atmospheric loss (dB)
- SUT transmit coupler calibration (dB)
- SUT transmit antenna waveguide loss (dB)
- SUT uplink off-axis loss (dB)
- ERS power range (dB)
- ERS power step (dB)
- ERS frequency offset from the SUT uplink (MHz)
- ERS EIRP (dBW)
- ERS uplink off-axis loss (dB)

- Maximum power balance delta between SUT and ERS (dB)
- Search bandwidth (MHz)

Next, the ERS uplink and downlink chains are configured for the measurement. The ERS transmits a signal and measures the local oscillator frequency of the spacecraft transponder being used. The ERS signal is then turned off, and the ERS operator is requested to instruct the SUT to begin transmitting. The frequency of the SUT downlink signal is measured by the ERS, which then transmits at a frequency that is offset from the SUT uplink frequency, at the power level specified by the operator. Both stations are now transmitting simultaneously to the spacecraft. The power level at which the ERS transmits takes into account the atmospheric attenuation at the ERS. The ERS and SUT uplink signals are "power-balanced" at the spacecraft's transmit antenna, as described below. The IOTE then measures the SUT station's transmit EIRP for each power level across the operator-specified range. Given the SUT antenna input power supplied to the ERS operator by the SUT operator, the SUT transmit antenna gain is calculated.

The ERS measures SUT power over a range of power levels specified by the operator input parameters. The input parameters are the power range (in dB), the power step size (in dB), and the initial level of the ERS transmit EIRP (in dBW) during the measurement setup phase. The measurement procedure is repeated for a typical 15-dB adjustment range of the SUT transmit EIRP level. The ERS EIRP power level (also an operator input) is used instead of the normal spacecraft saturation level as the backoff reference level.

For each power level in the sweep, the following steps are performed. The SUT operator is requested by the ERS operator to perform a power balance at the spacecraft's transmit antenna. When power balance is complete, the SUT operator provides the SUT uplink power meter reading to the ERS operator, who enters the value into the measurement. Power balance is achieved when the difference between the spacecraft's transmit EIRP due to the ERS uplink signal (E_{te} in Figure 10) and the spacecraft's transmit EIRP due to the SUT uplink signal (E_{ts} in Figure 10) is less than an operator-specified delta (typically 1 dB). The ERS then measures the spacecraft transmit EIRPs due to the SUT and ERS uplink signals. The ERS confirms the power balance at this point and computes the SUT earth station transmit EIRP.

The SUT's transmitted EIRP can be determined from the following quantities: the spacecraft transmit EIRP due to the SUT uplink signal, the spacecraft gain for the ERS uplink signal, the off-axis losses for the ERS and SUT, and the SUT's uplink path and atmospheric losses. The IOTE measures the spacecraft transmit EIRP due to the SUT signal. The SUT transmit EIRP is then calculated as follows:

$$E_{SUT} = E_{ts} - G_c + (L_{os} - L_{oe}) + L_{ps} + L_{as} \quad (5)$$

where

- E_{SUT} = SUT transmit EIRP (dBW)
- E_{ts} = spacecraft transmit EIRP due to the SUT uplink signal (dBW)
- G_c = spacecraft gain for the ERS uplink signal (dB)
- L_{os} = off-axis loss to the SUT (dB)
- L_{oe} = off-axis loss to the ERS (dB)
- L_{ps} = SUT uplink path loss (dB)
- L_{as} = SUT uplink atmospheric loss (dB).

Once the transmitted EIRP is determined, the antenna gain of the SUT can also be computed. With the SUT operator providing the waveguide loss of the SUT transmit antenna, the power meter reading of the SUT uplink carrier (in dBm), and the power meter coupler calibration, the antenna gain is computed according to

$$G_s = E_{SUT} + L_{wg} - P_{pm} - C_{pm} + 30 \quad (6)$$

where

- G_s = gain of the SUT transmit antenna (dB)
- L_{wg} = waveguide loss of the SUT transmit antenna (dB)
- P_{pm} = SUT uplink power meter reading (dBm)
- C_{pm} = SUT uplink power meter coupler calibration (dB).

The accuracy of this earth station antenna gain measurement at the ERS is comparable to that of the basic EUTELSAT IOTE EIRP measurement, with an expected small loss in accuracy due to dependence on the assumed values for the SUT parameters. Figure 11 shows a typical earth station EIRP plot output.

Earth station G/T measurement

The ESVA G/T test measures the G/T of the SUT, using the satellite as a calibrated signal source in the far field of the SUT antenna. Figure 12 depicts the G/T measurement configuration and the quantities involved.

The test derives the G/T of the SUT directly from two power measurements made with the SUT configured so that the output of the station down-converter is connected to an IF bandpass filter that has a calibrated noise bandwidth. The ERS sets its uplink power to the backoff level specified by the operator via the measurement's user interface. This backoff is referenced to the ERS maximum uplink EIRP specified by the operator (not to the spacecraft saturation level). The ERS transmits at this level.

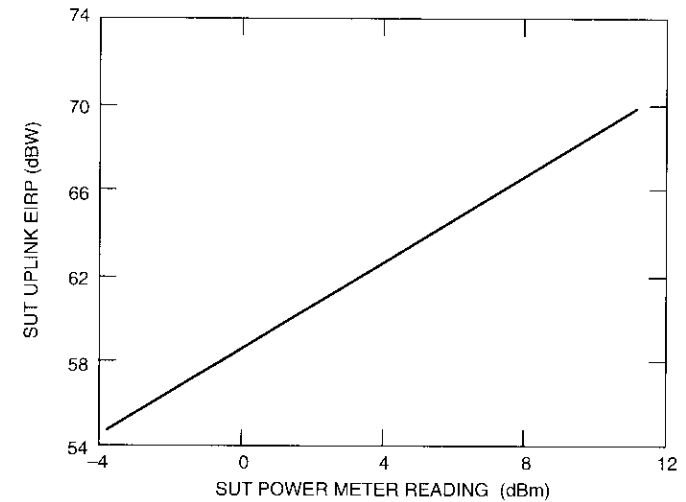


Figure 11. Earth Station EIRP Measurement Output

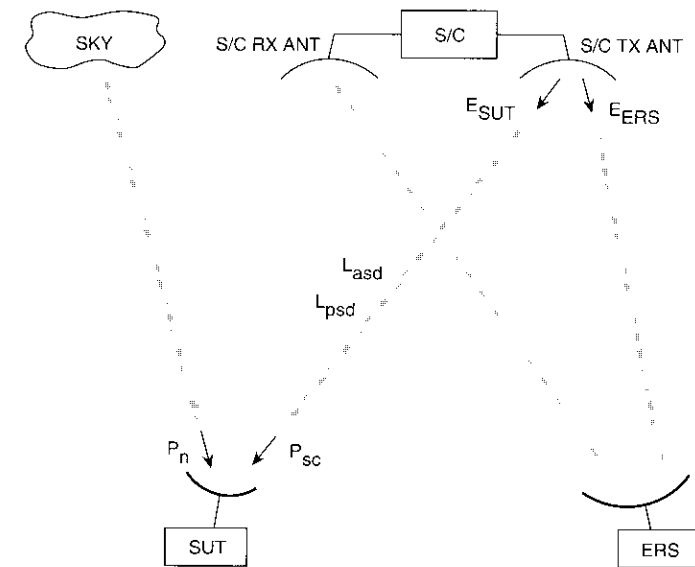


Figure 12. ESVA G/T Measurement

The SUT antenna is pointed toward the satellite, and the power, P_{sc} , at the filter output is measured. The SUT antenna is then pointed toward the sky, away from the satellite, and the noise power, P_n , at the filter output is measured. G/T is computed using P_{sc} and P_n .

The ERS uplink and downlink are configured for each channel being measured, and the local oscillator frequency of the spacecraft is measured, if it is different from that of the last channel. The uplink at the ERS is then set to the operator-specified backoff level from the specified maximum uplink power, and the IPFD and EIRP are measured. Next, the ERS operator enters the off-axis losses, as well as the downlink atmospheric and path losses, as seen from the SUT and provided by the SUT operator. The SUT operator is directed to measure the received power at the SUT, and then to move the SUT antenna away from the spacecraft and measure the noise received from the sky. The IOTE determines the spacecraft's transmit EIRP as seen at the SUT by calculating the spacecraft's transmit EIRP as seen at the ERS. The SUT G/T is computed as follows:

$$G/T_s = -228.6 + BW_s + L_{psd} + L_{asd} - E_{SUT} + 10 \times \log P_3 - CF \quad (7)$$

where

G/T_s = measured SUT G/T (dB/K)

-228.6 = dB equivalent of Boltzmann's constant

BW_s = SUT filter bandwidth (dB-Hz)

L_{psd} = SUT downlink path losses (dB)

L_{asd} = SUT downlink atmospheric loss (dB)

E_{SUT} = spacecraft EIRP seen by SUT (dBW)

$P_3 = (P_2/P_1 - 1)$

where

$$P_1 = 10^{(P_n/10)}$$

$$P_2 = 10^{(P_{sc}/10)}$$

CF = operator-entered correction factor (dB).

ESVA transmit polarization isolation measurement

This test measures the transmit polarization isolation of the SUT. In the EUTELSAT IOT, the test can be performed in both the X and the Y polarizations at various SUT antenna pointing angles. Figure 13 illustrates the ESVA transmit cross-polarization isolation measurement configuration and the quantities involved.

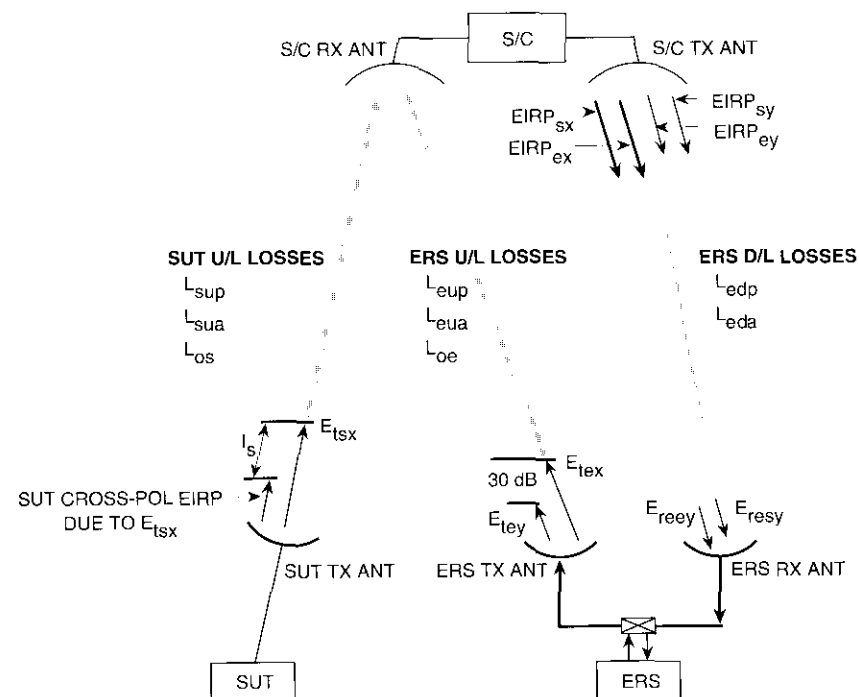


Figure 13. ESVA Transmit Cross-Polarization Isolation Measurement

When the SUT transmits a carrier in one polarization, a small amount of the carrier's power spills over, or leaks, into the opposite polarization transmit path due to imperfect isolation between the two paths. This leakage power is also transmitted in the opposite polarization. The SUT transmit cross-polarization isolation, I_s , between the two transmission paths measures the degree of isolation.

The measurement uses two spacecraft transponders: one designated as the copolarization (copol) transponder, and the other as the cross-polarization (cross-pol) transponder. First, the ERS operator configures the measurement by entering various parameters into the measurement's user interface window, and establishes communication with the SUT operator, who supplies SUT parameter values for entry via the user interface window. During the measurement, the ERS operator is prompted via dialog windows to provide input and perform various actions. The ERS operator is then requested to turn on the copol transponder and turn off the cross-pol transponder. The ERS configures

its uplink and downlink chains for the spacecraft channel being used and transmits an uplink carrier in the copol transponder at the center frequency of the channel. The downlink signal is received at the ERS, and the spacecraft's local oscillator frequency is measured. The SUT operator is then instructed to transmit at the same frequency and polarization as the ERS uplink carrier. The ERS stops transmitting, and the frequency of the SUT transmission is measured at the ERS. The ERS is retuned to a frequency that is offset from the SUT uplink frequency, and then transmits at a backoff level relative to the maximum earth station uplink transmit EIRP allowed by the measurement program.

An interactive power balance procedure is now performed, as in the ESVA EIRP measurement. The balancing procedure ensures that the spacecraft transmit EIRP due to the ERS uplink carrier ($EIRP_{oc}$ in Figure 13) and the spacecraft transmit EIRP due to the SUT uplink carrier ($EIRP_{sx}$) differ by less than an operator-specified amount. The SUT copol transmit EIRP is designated as E_{tsx} , where the subscripts indicate transmission (t) by the SUT (s) in the arbitrarily chosen X polarization (x). Uplink and downlink parameters (path and atmospheric losses) are measured for both the ERS and SUT uplink and downlink carriers.

Next, the SUT operator is requested to turn off the SUT uplink carrier. The copol transponder is turned off, and the cross-pol transponder is turned on. The ERS then transmits a cross-pol carrier (*i.e.*, a carrier on the opposite polarization, E_{tey}) at the same frequency used in the copol measurement procedure above, but 30 dB down from the level transmitted by the ERS during the copol measurement (E_{tcx}) just performed.

At this time, a series of measurements are performed. The SUT operator is requested to transmit again in the copolarization at the level of E_{tsx} , as before. Some of the power from the SUT transmission of a copol uplink carrier leaks into the transmission path of the opposite polarization and is also transmitted by the SUT as a small cross-pol carrier. This undesirable carrier causes a corresponding spacecraft EIRP ($EIRP_{sy}$) to be transmitted. The ERS cross-pol uplink carrier, E_{tey} , causes a new level of spacecraft transmit EIRP, $EIRP_{cy}$. The uplink and downlink parameters for the ERS and SUT signals are measured for use in the cross-pol measurement.

The ERS operator is prompted for the SUT power meter reading, the SUT antenna azimuth or elevation, and the contour value of the SUT antenna gain. Based on the copol and cross-pol measurements just performed, the SUT antenna transmit isolation is computed (in dB) as follows:

$$I_s = E_{tsx} - (E_{resy} - E_{reey}) - E_{tey} - (L_{sup} - L_{cup}) - (L_{sua} - L_{eua}) + (L_{os} - L_{oe}) \quad (8)$$

where

- I_s = SUT transmit cross-pol isolation (dB)
- E_{tsx} = SUT transmit copol EIRP (dBW)
- E_{resy} = computed equivalent spacecraft EIRP at the ERS receive antenna due to the SUT transmit cross-pol carrier (dBW)
- E_{reey} = computed equivalent spacecraft EIRP at the ERS receive antenna due to the ERS transmit cross-pol carrier (dBW)
- E_{tey} = earth station EIRP transmitted by the ERS in the cross-pol carrier (dBW)
- L_{sup} = SUT uplink path loss (dB)
- L_{cup} = ERS uplink path loss (dB)
- L_{sua} = SUT uplink atmospheric loss (dB)
- L_{eua} = ERS uplink atmospheric loss (dB)
- L_{os} = off-axis loss to the SUT (dB)
- L_{oe} = off-axis loss to the ERS (dB).

Because the SUT and ERS downlink frequencies are very close (typically 2 MHz apart at 12-GHz carrier frequencies), the measurement assumes that the difference in downlink losses for the ERS and SUT signals is negligible for the downlink path and atmospheric losses.

ESVA transmit sidelobe pattern measurement

This test, which measures the transmit sidelobe levels of the SUT transmit antenna, is performed to ensure that the SUT meets EUTELSAT specifications. Figure 14 depicts the ESVA transmit sidelobe measurement configuration and the quantities involved.

First, the SUT transmits in the linear region of the spacecraft TWTA gain transfer characteristic. It then slews the SUT antenna in azimuth or elevation, and the ERS measures the downlink power. Next, the SUT antenna is offset by 1° and the uplink power is increased by 15 dB. The SUT antenna is then steered away from beam center while the ERS measures the downlink power. This procedure is repeated for both sides of the SUT antenna beam. The ERS EIRP power level (an operator input) is used, instead of the spacecraft saturation level, as the backoff reference level. The measurements for each side of the SUT antenna beam are then combined in an interactive data analysis and manipulation software package and plotted to show the SUT antenna pattern.

A gain transfer measurement is performed, using the injected signal technique, and saved for later use in computing spacecraft transmit EIRP. The SUT

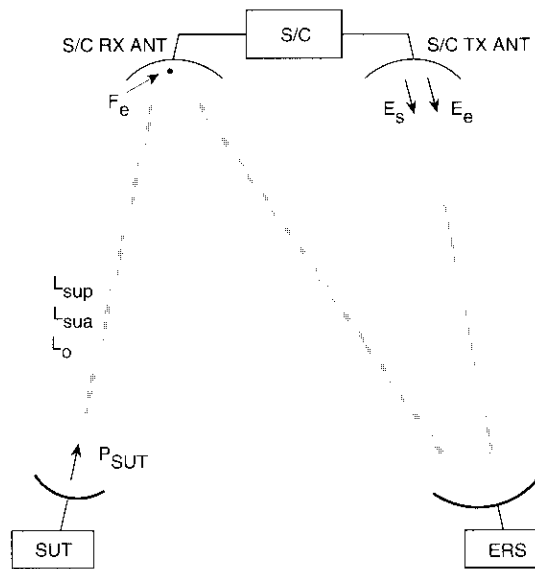


Figure 14. ESVA Transmit Sidelobe Measurement

is directed to turn off its transmitter during this measurement. The SUT then turns on its transmitter and transmits a carrier to the spacecraft, and the carrier's downlink frequency is measured by the ERS. The ERS transmits an uplink carrier at a frequency that is offset from the SUT uplink. The SUT and ERS signals are power-balanced, as in the ESVA EIRP measurement, and the ERS turns off its uplink signal.

The SUT is then directed to slew its antenna at a user-specified rate, and the measurement is initiated by the ERS operator via a dialog window and continues until stopped by the operator. For each SUT transmit EIRP measurement, the measurement program computes the antenna slew angle in real time, based on the initial angle, start time, and slew rate inputs supplied by the operator, and the time elapsed since the start.

The spacecraft EIRP due to the SUT uplink carrier is expressed in terms of the EIRP caused by the ERS uplink carrier and the levels measured on the spectrum analyzer for both downlink carriers, as follows:

$$E_s = E_e + (S_s - S_e) \quad (\text{dBW}) \quad (9)$$

where

$$E_s = \text{spacecraft transmit EIRP due to SUT carrier (dBW)}$$

- E_e = spacecraft transmit EIRP due to ERS carrier (dBW)
- S_s = received SUT signal measured on spectrum analyzer (dBm)
- S_e = received ERS signal measured on spectrum analyzer (dBm).

The spacecraft transmit EIRP due to the SUT carrier can be obtained by measuring only three quantities: E_e , S_s , and S_e . The value for E_e and the associated signal level measured on the spectrum analyzer, S_e , are arbitrarily chosen as the first point in the gain transfer measurement performed earlier. The above relationship assumes the following:

- The ERS gain transfer measurement is performed using the injected signal technique.
- The ERS is not transmitting during measurement under slewing conditions.
- The SUT downlink carrier is at the same frequency and polarization as the gain transfer measurement.
- The injected signal power level is the same in both measurements.
- There is negligible change in the ERS distance to the spacecraft between the gain transfer measurement and the ERS EIRP measurement a few minutes later.
- Because the gain transfer and EIRP measurements are performed a few minutes apart, the downlink path loss, downlink atmospheric loss, ERS receive antenna gain, and inject signal coupler value are assumed to be constant during the measurement.
- The SUT antenna slews over the desired range in a few minutes. If the slew rate is a typical 0.02°/s, the SUT requires 5 minutes to slew 6°.

Since E_e and S_e were measured and stored during the gain transfer test, the spacecraft EIRP due to the SUT uplink carrier can be determined by measuring the received signal level on the spectrum analyzer while the SUT antenna is slewing in real time. The spectrum analyzer is set to a reference vertical scale level and left on that scale setting during the slew measurement. The measurement then makes successive and rapid readings of the voltage measured by the digital voltmeter and converts them to equivalent power in dBm. The above relationship [equation (9)] is used to compute the spacecraft transmit EIRP due to the SUT uplink carrier in real time and "on the fly," while the SUT antenna is slewing. Thus, it is not necessary to perform actual injected-signal EIRP measurements for the SUT signal. The relationship has been verified empirically with measurement data.

The spacecraft EIRP due to the SUT uplink carrier is converted to an equivalent spacecraft IPFD by linear interpolation from the gain transfer table stored previously. The gain transfer table gives the relationship of spacecraft IPFD to spacecraft transmit EIRP for the measured transponder. Since the data in the gain transfer table were measured with an uplink carrier from the ERS and not the SUT, the interpolated input flux for the SUT carrier must be corrected to compensate for the difference of the off-axis losses between the spacecraft and the respective earth stations.

The equivalent IPFD of the SUT carrier at the spacecraft receive antenna is converted to an equivalent EIRP, which can then be related to the SUT uplink EIRP. The SUT uplink and atmospheric losses are supplied by the SUT operator to the ERS operator, who enters these parameters into the measurement. The SUT transmit EIRP is then computed according to the following relationship:

$$P_{\text{SUT}} = F_e + L_o + 10 \log \frac{(c/f_s)^2}{4\pi} + L_{\text{sup}} + L_{\text{sua}} \quad (\text{dBW}) \quad (10)$$

where

- P_{SUT} = SUT uplink EIRP (dBW)
- F_e = input flux to the spacecraft that would have to be transmitted by the ERS to cause the same level of spacecraft transmit EIRP due to the SUT uplink signal (dBW/m²)
- L_o = difference between the ERS off-axis loss and the SUT off-axis loss (dB)
- c = velocity of light (m/s)
- f_s = SUT uplink frequency (Hz)
- L_{sup} = SUT uplink path loss (dB)
- L_{sua} = SUT uplink atmospheric loss (dB).

The SUT uplink antenna gain is determined relative to the measurement starting point gain by computing the delta between the reference starting point SUT uplink EIRP value and the measured uplink EIRP, and subtracting the deltas from the reference gain level.

For each SUT uplink EIRP measurement, the IOTE computes the slew angle based on the initial angle, start time, slew rate, and elapsed time. The initial SUT angle, the SUT antenna slew rate, and the SUT starting slew time are supplied by the SUT operator to the ERS operator, who inputs them into the measurement. Finally, the procedure measures the elapsed time since the start of the measurement. Figure 15 shows typical data for a single-sided earth station transmit sidelobe measurement.

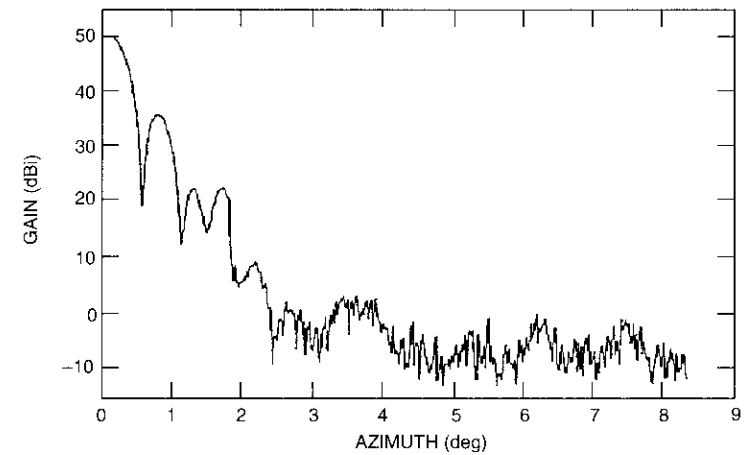


Figure 15. Earth Station Transmit Sidelobe Measurement

Conclusions

The continuing trend toward higher-capacity, more complex communications satellites, such as the EUTELSAT II series, places greater demands and constraints on the IOT systems built to test them. Because of the larger number of transponders and configurations to be tested and the expanded repertoire of tests to be performed, a modern IOT system must acquire and analyze an increasing volume of test data. This situation tends to lengthen the testing time required, which conflicts with the owner's desire that the satellite be placed into operational, revenue-generating service as soon as possible after launch.

A UNIX workstation-based, highly automated IOT system installed at the EUTELSAT earth station in Rambouillet, France, includes several innovative features and measurements. The X-Window-based graphical user interface provides operational flexibility and is easier to use than older, command-line interfaces. The system's scheduler permits unattended stability measurements to be performed at specified intervals by sharing equipment and earth station resources among IOT measurements. A new technique called Fast sweep reduces the time needed to measure a spacecraft channel's frequency response from several minutes to a few seconds, using an asynchronous swept-frequency measurement technique and post-measurement digital processing. The use of the spacecraft as a calibrated far-field signal source enables EUTELSAT to independently measure and evaluate the performance characteristics of a second earth station.

The EUTELSAT IOT system was developed to support EUTELSAT's testing of its second-generation satellites, and has been used for the IOT of the EUTELSAT II F1, F2, F3, and F4 spacecraft.

Acknowledgments

The authors would like to acknowledge the following individuals. C. Mahle of COMSAT Laboratories has been a constant source of help and encouragement. His past and current contributions to this work are major. S. Bangara, currently with INTELSAT, played a key role in defining the system requirements for the EUTELSAT IOTE, and R. Issler of DTRE made significant contributions to the IOTE-ECCS interface implementation and testing. The DTRE staff at the Rambouillet earth station are acknowledged for their assistance and support during the system installation, testing, and deployment of the EUTELSAT IOTE.

The earth station (excluding the IOTE/MMS) was made available to EUTELSAT by DTRE, the overseas arm of the French Post, Telephone, and Telegraph Administration (PTT). The ECCS computer and its station control and status software are supplied to EUTELSAT by DTRE.

References

- [1] I. Dostis *et al.*, "In-Orbit Testing of Communications Satellites," *COMSAT Technical Review*, Vol. 7, No. 1, Spring 1977, pp. 197-226.
- [2] A. F. Standing, *Measurement Techniques for In-Orbit Testing of Satellites*. Computer Science Press, New York: W. H. Freeman, 1990.
- [3] C. E. Mahle, "In-Orbit Testing of Commercial Communications Satellites," 23rd General Assembly of the International Union of Radio Science (URSI), Prague, Czechoslovakia, August-September 1990.
- [4] Y. Tharaud, B. Kasstan, and P. Barthmann, "IOT System for the EUTELSAT II Satellites," IEEE Global Satellite Communications Symposium, Nanjing, China, May 1991, *Proc.*, pp. 168-177.
- [5] Y. Tharaud and V. Riginos, "EUTELSAT's Facilities for Measurement of Earth Stations and In-Orbit Satellite Payloads," 23rd General Assembly of the International Union of Radio Science (URSI), Prague, Czechoslovakia, August-September 1990.
- [6] V. Riginos, P. Shen, and S. Bangara, "In-Orbit Testing of Communications Satellites: The State of the Art," IEEE Global Satellite Communications Symposium, Nanjing, China, May 1991, *Proc.*, pp. 150-159.
- [7] S. K. Card, T. P. Moran, and A. Newell, *The Psychology of Human-Computer Interaction*, Hillsdale, NJ: Lawrence Erlbaum, 1983.

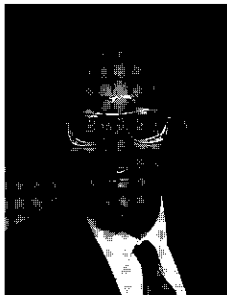
- [8] K. D. Fullett *et al.*, "Microwave Measurement Software System," *COMSAT Technical Review*, Vol. 23, No. 1, Spring 1993, pp. 101-137 (this issue).
- [9] K. D. Fullett and V. E. Riginos, "Error Analysis of In-Orbit Measurements on Communications Satellites," 23rd General Assembly of the International Union of Radio Science (URSI), Prague, Czechoslovakia, August-September 1990.
- [10] Hewlett-Packard, "Phase Noise Characterization of Microwave Oscillators," HP Product Note No. 11729B-1.



Kenneth D. Fullett received a BSEE and MSEE from the University of Illinois, Urbana-Champaign, in 1979 and 1981, respectively. He joined COMSAT Laboratories in 1981 as a member of the Transponders Department of the Microwave Technology Division and participated in all aspects (including both microwave hardware and computer software system design) of many IOT systems, including those for INTELSAT, MCI, and EUTELSAT. His work also involved software development for COMPACT Software, and he was a project manager for the RF Terminal Supervisory System of the NASA/ACTS earth station. Mr. Fullett is currently engaged in high-energy physics research in the Anti-Proton Source Department of the Accelerator Division of Fermi National Accelerator Laboratory, Batavia, Illinois.

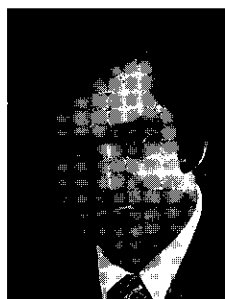
Bernard J. Kasstan received an Honours degree in physics and electronics from Newcastle-upon-Tyne Polytechnic, U. K., in 1981; and a Masters degree in telecommunications from the University of Essex in 1982. He subsequently conducted research on tropospheric propagation on earth-to-satellite paths. He joined EUTELSAT in 1984, and was responsible for the verification of new earth stations in the EUTELSAT space segment. In 1987, he moved to IOT activities, including payload subsystem performance evaluation, investigations of payload anomalies in orbit, and supervision of IOT installation at the host stations. In conjunction with the System Verification Test Section, Mr. Kasstan has developed new IOT techniques that have been discussed in numerous published papers.



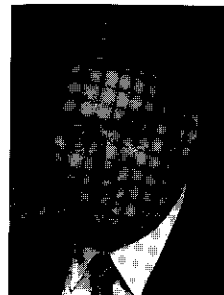


Walter D. Kelley, Jr., earned a BS in electrical engineering at the Catholic University of America, Washington, D.C., in 1974; and an MBA at Marymount University, Arlington, VA, in 1983. In 1991, he joined the Transponders Department of the Satellite and Systems Technologies Division at COMSAT Laboratories as a Member of the Technical Staff. At COMSAT, he has participated in development of the IOT system for Hughes Communications' DirecTv™, an IOT system for EUTELSAT, and the NASA/ACTS ground station control and status subsystem.

Vasilis E. Riginos received a BE, MEng, and PhD in electrophysics from the Stevens Institute of Technology, Hoboken, NJ, in 1964, 1970, and 1973, respectively. He is currently Manager of the Transponders Department of the Satellite and Systems Technologies Division at COMSAT Laboratories, where he is responsible for directing research and development on communications system performance as applied to satellite transponders. He also supervises research and development in advanced microwave circuits such as high-power amplifiers, regenerative receivers, filters, and multiplexers. Dr. Riginos participated in the evaluation of the Inmarsat program, and has been project manager for the GTE ATEF IOT system, the INTELSAT Maritime Communications Subsystem IOT station, the EUTELSAT IOT system, and the Hughes DirecTv™ IOT system. He is a member of Sigma Xi, AAAS, IEEE, and the American Physical Society.

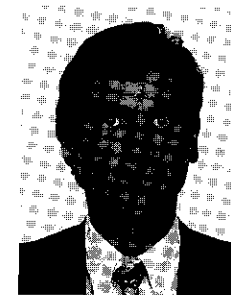


Pei-Hong Shen received a BS and MS in genetics, and an MS in computer science, from Washington State University in 1983, 1984, and 1986, respectively. From 1978 to 1981, she studied biology and genetics while attending Fudan University in Shanghai, Peoples Republic of China. Ms. Shen is currently a Senior Member of the Technical Staff in the Transponders Department of the Satellite and Systems Technologies Division at COMSAT Laboratories, where she is primarily responsible for design and development of software for communications satellite applications. Since joining COMSAT in 1987, she has been involved in the design and development of the following systems: NASA/ACTS, EUTELSAT IOT, and Hughes' DirecTv™ IOT. She is a member of the IEEE Computer Society.



Steven L. Teller received an AS and AA from Harper College in 1979; and a BA in information and computer sciences from Hood College in 1991. He is currently a Member of the Technical Staff in the Transponders Department of the Satellite and Systems Technologies Division at COMSAT Laboratories. Since joining COMSAT, he has been involved in various aspects of the IOT of communications satellites, including the NASA/ACTS RF terminal supervisor, and IOT for EUTELSAT, MCI, INTELSAT, GTE, and the Hughes DirecTv™ system. He has been responsible for software vs manual measurement verification during system development, in-plant testing, and on-site testing. He was also involved in prototyping and testing various new measurement schemes, and was a major contributor to final system installation testing.

Yves Tharaud received an MSc in electronics, electrotechnology, and automatics from the University of Bordeaux, France, in 1974; and the title of Engineer from the Ecole Nationale Supérieure d'Electronique et de Radioélectricité de Bordeaux in 1975. He joined EUTELSAT in 1981 and participated in the definition and implementation of new facilities dedicated to IOT, earth station verification and assistance (ESVA), and payload traffic monitoring for the EUTELSAT II satellites. He served as manager of the System Verification Test Section in the Operations Department, where he supervised activities related to satellite payload IOT and ESVA. Mr. Tharaud cooperated with the European Space Agency in similar activities on the ECS satellites and participated in the payload IOT and various other experiments on the OTS satellite as a member of the CNET in FRANCE TELECOM.



Microwave measurement system software

K. D. FULLETT, W. D. KELLEY, V. E. RIGINOS, P-H. SHEN,
AND S. L. TELLER

(Manuscript received December 9, 1992)

Abstract

To facilitate efficient, cost-effective development of in-orbit test (IOT) measurements and turnkey systems, microwave measurement system (MMS) software built on an engineered platform of reusable software services and facilities has been developed over the past several years and deployed in operational systems. The Measurement Processing and Control Platform (MPCP) provides modular software components that have been developed and tested for measurement scheduling, interprocess communications, and resource and system information sharing. Its code libraries support graphically based user interfaces, instrument control, instrument bus management, and error detection and reporting; and its data processing subsystems support database management, report generation, and interactive data analysis.

Operating in a network environment under a UNIX System V operating system, this multiuser, multitasking MMS software supports both local and wide-area networking, including remote access and control of the IOT measurement equipment. It executes in a distributed processing system architecture spanning a number of dissimilar workstations. With interprocess/intermachine communications provided by the MPCP mail system, the separate user interface and measurement programs can execute on different machines at different times, for improved operational flexibility.

This paper describes the design and implementation of the MMS software. The concepts and methods presented are also applicable to other measurement-oriented systems (such as those used for communications system monitoring), where escalating software costs must be controlled.

Introduction

Computer-controlled in-orbit test (IOT) systems integrate microwave measurement equipment, computer hardware, and measurement software into a unified test facility for measuring the communications subsystem performance of an orbiting satellite. To assess performance, the IOT system conducts a variety of microwave frequency measurements. These include the measurement of spacecraft input power flux density (IPFD) and equivalent isotropically radiated power (EIRP); transponder frequency response; gain transfer; group delay; gain-to-noise temperature ratio, G/T ; and others [1],[2].

The development of modern IOT systems is traced by Shen *et al.* [3]. As noted in that paper, IOT is performed for acceptance testing immediately following launch; to monitor communications subsystem performance throughout the satellite's operational lifetime; and to investigate anomalies. The specific missions determine the IOT system's basic requirements. The fact that newer satellites contain more transponders and have increased payload complexity compared to earlier generations places greater demands and constraints on the IOT systems built to test them. Because the satellite owner desires to place the satellite into revenue-generating operational service as soon as possible after launch, the IOT system is constrained to accomplish its task as quickly as possible, especially during acceptance testing. Increased satellite capacity and complexity have also resulted in greater volumes of test data, which must be maintained and reported. Finally, the pool of spacecraft experts available for performing complex IOTs and evaluating the data is distributed more thinly as the number of satellite networks in service increases.

In addition to its primary mission of performing IOT measurements, the modern computer-controlled IOT system must address such system requirements as real-time and network operation, human-machine interaction, and remote access and control of the measurement hardware. The system must provide a user interface that is easy to use, yet flexible enough to accommodate the various IOT missions. The capability to execute measurements concurrently and to support a multiuser environment are desirable system features.

These requirements and constraints place greater responsibility for IOT system functionality on the software, which must address the network, hardware, and communications environment of a distributed processing system spanning a number of workstations. As a result, the IOT software, with its volume, sophistication, complexity, and difficulty of development and control, has come to dominate both overall system cost and scheduling. The development of custom software is time-consuming and costly, and requires highly skilled personnel. Methods and techniques are continually being sought to make the

IOT software production process more efficient. By contrast, the cost and scheduling aspects of hardware implementation for IOT and similar measurement systems are generally well-understood and well-controlled.

This paper discusses the principal software concepts underlying development of the Measurement Processing and Control Platform (MPCP), which served as the foundation for design and implementation of the microwave measurement system (MMS) software. Specific applications for computer-controlled IOT measurements and turnkey systems are addressed. A companion paper [4] describes the implementation of the MPCP software in a specific IOT system.

The principles underlying a robust, software-engineered platform such as MPCP are also applicable to the software implementation of similar measurement-oriented, computer-controlled systems, such as communications monitoring systems. Like computer-controlled IOT systems, these systems require escalating amounts of software for which costs, scheduling, and quality must be controlled.

Software development methodology

IOT systems are uniquely designed to test specific satellite characteristics and networks; however, many IOT measurement subtasks are the same from one IOT system to the next. Such commonality of function underlies much of the MMS design.

Because IOT systems are unique and custom-built, the software implementation of computer-controlled IOT systems is not standardized, nor is there a standard IOT software architecture. Riginos *et al.* [5] contrasts two approaches to designing such software. In one approach, measurements are implemented one at a time in a self-contained manner. Each measurement performs all required functions, including instrument control, user interface, and data processing tasks such as database management, printing, and plotting. As new measurements are required, an existing measurement is copied and modified to meet the specific requirements. While this self-contained approach has certain attributes, such as moderate levels of developmental effort for succeeding measurements, its use for large-scale systems software development also contributes to problems in terms of life cycle maintenance, quality, capability, flexibility, and extensibility.

Early implementations of computer-controlled IOT systems employed the self-contained measurement methodology. After several such systems had been implemented, it was realized that 80 to 90 percent of the measurement tasks—such as managing the user interface, controlling and managing the

instruments, managing data and files, reporting and logging errors, plotting and printing output data—were common to all IOT measurements. This realization formed the basis for a fundamentally different strategy of building IOT systems and measurements.

This alternative approach, based on a software-engineered platform of reusable software components, was the one selected for developing the MPCP and MMS described here. Although the initial design and development effort is substantial, the engineered platform implementation results in improved software characteristics in terms of life cycle (reusability, maintainability, expandability, portability, and evolution), quality (methodology, robustness, consistency, and flexibility), and capability (remote control, networking, concurrent measurements, distributed systems, and user-driven changes).

Well-conceived and well-implemented reusable software components can significantly decrease the scheduling and performance risks associated with large-scale software development. With MPCP components as a base, new IOT systems and measurements can be implemented in a cost-effective and timely manner.

The MPCP operating system

The MPCP is a special-purpose operating system that provides an integrated platform of facilities, subsystems, and services to the measurement application program. These include interprocess/intermachine mail communications, measurement scheduling and resource management, a system-wide shared-data depository called the datapool, standardized file management, database management, alarm management, and printing and plotting. Object code libraries are provided for instrument control, IEEE-488 bus control, uniform error handling, user interface support facilities, and other utility functions that can be linked with applications such as IOT measurements.

The MPCP operating system is implemented via the UNIX System V operating system, enhanced with Berkeley sockets for communication and IEEE-488 bus control functions for measurement equipment interfacing. Because MPCP is implemented in the C and C++ languages, it executes with high run-time efficiency and is highly portable to other machines.

The basic concept is to design and implement task-specific modules that can be independently tested, refined, and expanded. Although the modules are functionally specialized, a major design goal is generality within the problem domain of the specific function. Over a period of several years, MPCP was developed as a platform of IOT system and measurement code building blocks that could be reused between measurements and across systems. The use of pre-tested modules substantially reduces the development time, cost, and per-

formance risk of unproven software. Because of the functional similarity of IOT systems and measurements, the code reuse percentage for MPCP is quite high.

MPCP design goals

MPCP implementation follows generally accepted software engineering principles, practices, and open system standards. These are briefly described below, with emphasis on why certain design choices were made, rather than on how the software is specifically implemented.

Because customers require remote access and control of an IOT system, an important design goal was to support a networked, distributed-processing hardware environment. The MPCP executes in such an environment. A typical IOT system architecture is shown in Figure 1.

Another principal design goal was to separate functional tasks into dedicated processes that could execute in distributed-processing, networked environments. A "process" is a program that is being executed in the host machine. Each process performs a specialized task with well-defined external interfaces. For example, an IOT measurement inputs parameters from the user, manages the hardware during data acquisition, saves the data in a database, and prints or plots the measured data. The overall measurement is implemented as two separate processes: one that interfaces with the user, and another that manages the measurement equipment and performs the actual measurement. The IOT system's scheduler, datapool, and earth station management facilities are implemented as self-contained dedicated "daemon" processes (*i.e.*, processes executing continuously in the background of the UNIX operating system). The printing and plotting tasks are similarly managed. Problems are generally contained within a specific process, and task-specific programs can be modified and recompiled when necessary, with little or no impact on the interfaces.

With separately executing processes, interprocess communication is required. This capability is provided by the MPCP mail subsystem, which client processes can access via calls to a library of mail functions. The mechanisms used by the mail subsystem are completely transparent to clients. To support a distributed processing (multiple-host) execution environment, the mail subsystem facilitates intermachine interprocess communications in which processes can execute on different host workstations and computers connected via a transmission control protocol/internet protocol (TCP/IP) network. Figure 2 depicts such an arrangement, with each box representing a separate workstation or computer.

Following another software principle, the MPCP is structured in a top-down hierarchy which permits the software to be partitioned according to function, and distinguishes between high-level and low-level functions. An

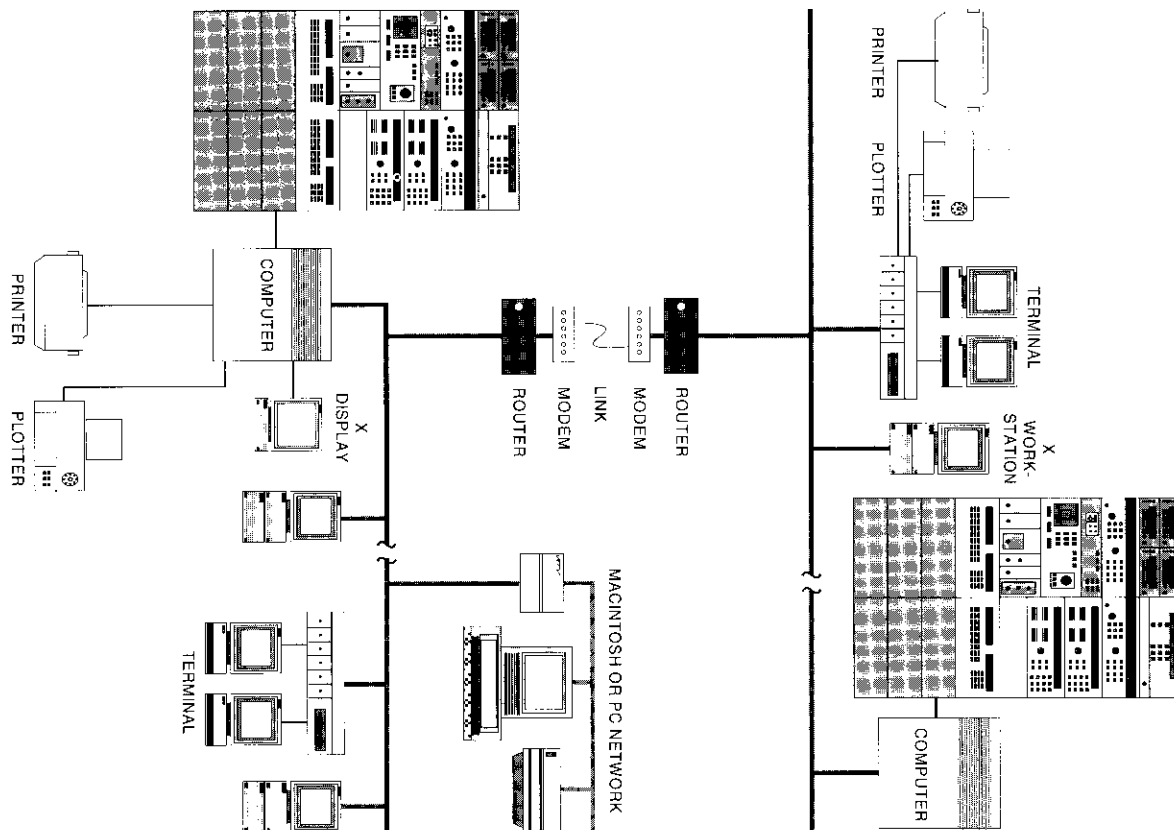
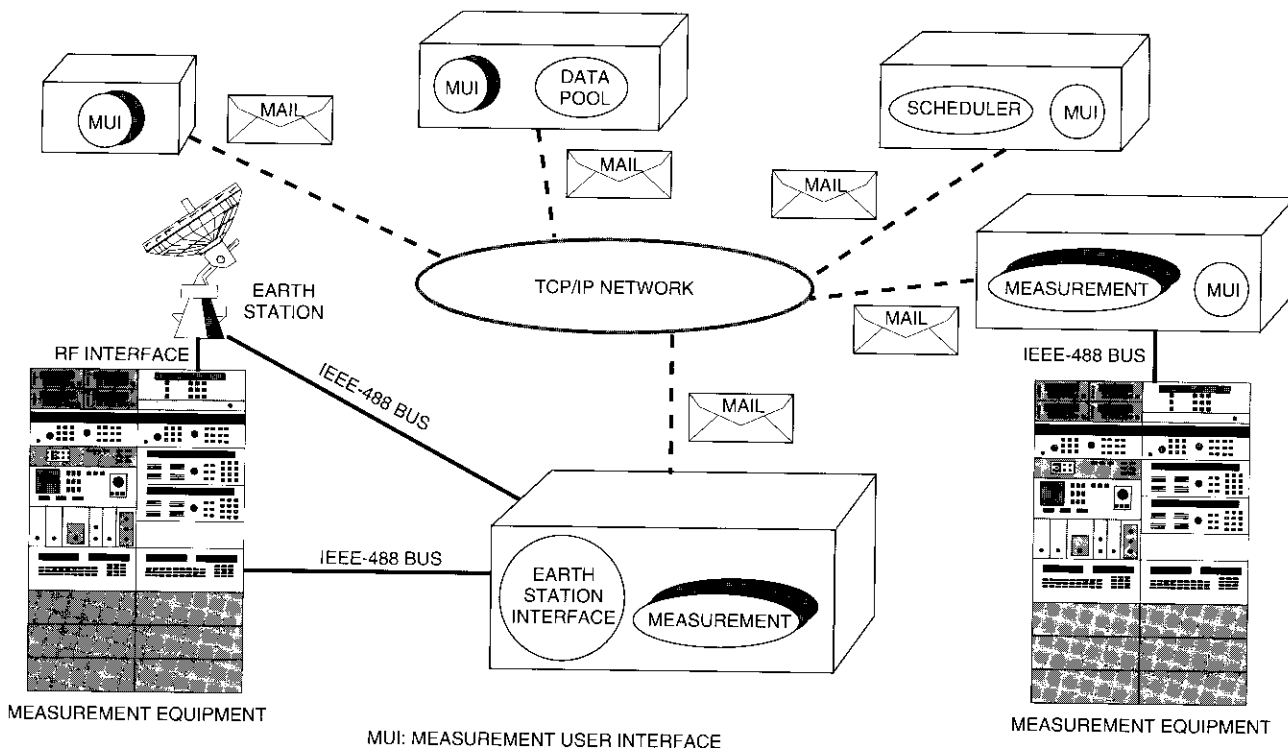


Figure 1. Networked System Architecture



MUI: MEASUREMENT USER INTERFACE

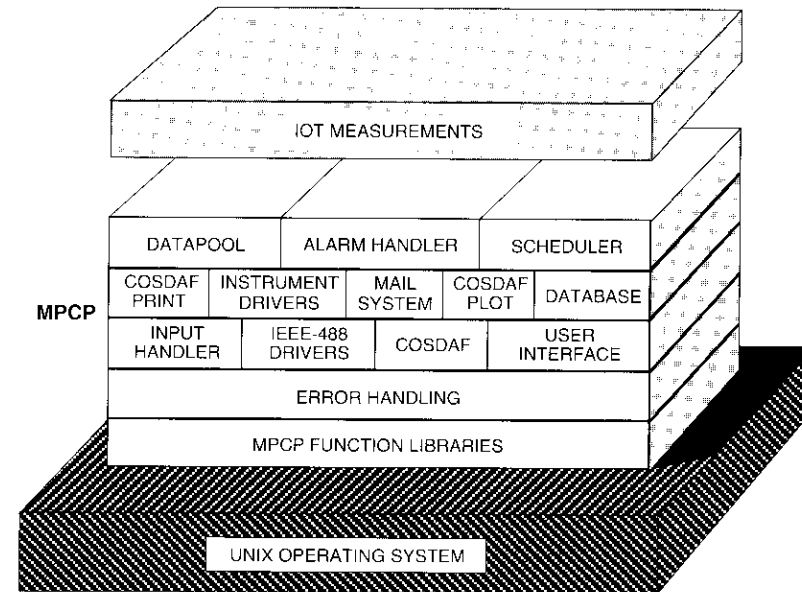
Figure 2. Distributed Processing Execution Environment

IOT measurement program, for example, is a high-level task. With proper code structuring, the software developer who implements a high-level measurement program need only be concerned with orchestrating the logical sequence of activities necessary to perform the measurement, and not with the details of lower-level functions. While the measurement may be required to access instruments, the details of instrument management are left to the driver that controls each instrument. Similarly, while the instrument driver exerts control via messages sent across the IEEE-488 bus that connects the instrument to the computer, the developer of the instrument driver need not be concerned with the details of managing the bus. Instead, the developer has available an IEEE-488 library of bus management functions. MPCP services such as the scheduler and datapool are conceptually at a level below that of the IOT measurement, but above lower-level functions such as the 488 library. At any level, the software developer has available the building blocks of lower-level MPCP facilities, and can access them through well-defined interfaces. Figure 3 illustrates the general nature of this hierarchical implementation of MPCP.

An important objective in building computer-controlled IOT systems is to maintain data integrity by preventing corruption [5]. "Defensive code" is used to detect error conditions and trap them before they propagate through to corrupt the measurement data. Each module performs extensive error checking of its inputs, as well as on the results of its own processing. Error-trapping is performed by all levels of code. When errors are detected at any level, they are managed consistently by calls to an error handling library, which underlies all upper levels of code, as depicted in Figure 3. Error detection and reporting throughout the code allows effective tracing of both programming errors and operational errors (*e.g.*, a disconnected instrument). Error handling techniques are discussed later in this paper.

The MPCP Function Libraries also extend under all upper levels of code. These libraries are used to segregate low-level functions from higher levels, and are generally accessible by any program, although access to functions is usually through the hierarchy of code modules.

As in hardware system design, a large software system such as an IOT or measurement system is more easily managed by decomposing it into smaller functional components, which are then treated as individual subsystems. Subsystems are self-standing software projects which encompass a group of similar and related functions that can be specified and implemented individually. Changes in one subsystem are generally localized and do not usually affect other subsystems. Decomposition of a large software project promotes modular system design, with the result that the project is easier to design, implement, and enhance.



COSDAF: COMSAT Data File Format

Figure 3. MPCP Operating System

To achieve the design goals of maximum code reusability and system implementation flexibility, the concept of data-driven design is employed throughout the MMS. Whenever possible, the data that programs use are separated into static ASCII text files that are human-readable and easily edited. The program's behavior can be altered by simply editing the data file, rather than changing the program code that processes it. This results in programs that are easier to develop, test, and maintain, and that have the flexibility to accommodate varying requirements from one IOT system to the next.

The user interface is designed for ease of use and flexibility, and also has the ability to check for erroneous user input (as far as practicable). The interface is implemented separately from the measurement program, and is called the measurement-user interface (MUI). The user interacts with the MUI via an X Window to specify IOT measurement parameters and scheduling information. The MUI display format is controlled by input data files, which are easily modified by simple editing of ASCII-encoded text files, without the need for program code changes. The user is notified if out-of-range data values are entered. To reduce keying, the MUI is initially displayed with default values preloaded in all fields and parameters.

Because each task is specialized, the module's developer focuses on the specific problem at hand and optimizes the code for that task. With well-defined, constant interfaces, modules can be modified or improved without affecting other modules. New modules, such as new instrument drivers, can readily be added to the system, often by using an existing driver as a template and modifying it as necessary.

Systems applications

Two systems are described which demonstrate the code reusability of the MPCP software building blocks. Although these systems differ substantially in mission and requirements, the MPCP platform provided the software foundation upon which the application-specific code was built.

In the first example, an IOT system using MPCP building blocks was designed, implemented, and deployed for the European Telecommunications Satellite Organization (EUTELSAT) [1],[2]. This system has performed the IOT of four EUTELSAT II spacecraft, and continues to monitor their performance.

In the second example, MPCP components were used to implement RF terminal supervisory equipment for a National Aeronautics and Space Administration (NASA) ground station for the Advanced Communications Technology Satellite (ACTS) program. In this system, a network of three engineering workstations, supporting three simultaneous operators, performs supervisory, status, and control functions for terminal and ground station RF equipment.

Communications and network environment

The IOT system architecture supports local and wide-area networking (LAN/WAN), as well as several communications protocols, network structures, and transmission media. The system's transport/network layer implements TCP/IP to guarantee end-to-end data delivery and integrity between communicating devices on networks that support this protocol. The LAN's physical layer implements the IEEE 802.3 (CSMA/CD Ethernet) protocol on coaxial cable operating at 10 Mbit/s. The LAN connects to workstations, displays, terminal servers, peripherals, communications equipment, and other PC-based LANs, as shown in Figure 1. The system supports WAN across leased lines, public switched telephone networks, and public data networks at rates ranging from 2.4 to 19.2 kbit/s, with link-limited transmission speed. Standard serial communications via RS-232 protocols and modem-connected data links are also supported. As illustrated in Figure 1, a complement of microwave measure-

ment equipment is connected to the IOT system workstation at the host earth station via the IEEE-488 digital instrumentation standard bus.

This networked system architecture provides for equipment and resource sharing, operational flexibility, performance enhancement, incremental redundancy, and vendor and hardware independence. System resources such as measurement hardware, plotters, printers, and communications facilities are shared among IOT measurements and users. Incremental expansion of computing, storage, display, and communications devices, as well as additional peripherals, are readily accommodated. Additional workstations can be connected to the network for load-sharing, and processes can execute on different machines for operational flexibility and improved performance.

An important consideration when implementing a network-oriented system is the ability to support interprocess and intermachine communications. The X Window protocol supports communications in a network of dissimilar but X-compatible workstations. When processes reside on the same machine, Berkeley sockets support interprocess communications. The MPCP mail subsystem also uses Berkeley sockets to implement a higher-level mechanism for interprocess communications that extends across machine boundaries.

MPCP mail interprocess communications

The MPCP mail subsystem provides clients with high-level, reliable, and easy-to-program facilities for interprocess, intermachine, and internetwork communications. The subsystem does the following:

- Provides interprocess communications (using TCP/IP) for different processes operating on separate workstations across the network.
- Provides "atomic" transmission (data treated as an indivisible unit) of large data structures.
- Provides the sender with verification of transmission.
- Implements a client-server model.
- Notifies clients if a connection is lost to a server process.

The MPCP mail subsystem supports the first three features in a fashion similar to its main paradigm: the postal system. A client process mails data to another process at a given address. The various data items to be mailed are enclosed in an "envelope," which is received and/or delivered at the same time. Like the postal mail system, the mail subsystem handles all delivery details. Atomic transmission ensures that input/output transactions, once started, are completed without interruption. When the addressee receives an envelope,

the sender is provided with a "return receipt" (acknowledgment) verifying successful transmission.

The MPCP mail subsystem software implements the last two features based on a second paradigm: an open telephone line between a client and a server. Using the mail subsystem, a client (*i.e.*, a process that requires some service) establishes an open line with a server (the process providing the service, such as the scheduler or datapool). Once the line is established, mail can be exchanged between client and server. If the server process terminates or there are problems in the network, the line is disconnected. The client process detects the disconnection and reports an error condition. Any number of clients can be supported in the network. For example, all MUI processes are served by the scheduler. There can be any number of servers of different kinds in the network, but there is only one server of a particular kind, such as the MPCP scheduler.

Process-to-process mail communications are supported when processes execute on different machines connected to the network. This feature permits a distributed processing system implementation in which there may be more than one machine with multiple clients and servers hosted on different machines, as depicted in Figure 4. In the figure, S1, S2, S3, and S4 represent different kinds of server processes, such as the scheduler, datapool, alarm manager, and earth station interface manager. The lines connecting clients to servers are mail connections, which are supported across serial data links.

The MPCP scheduler

The MPCP scheduler is a server process that provides scheduling and resource allocation across the network. The scheduler executes in the UNIX system background as an independent daemon process and accepts requests for jobs and resources from other processes. Scheduling is non-preemptive and is provided on a first-come, first-served basis. Jobs are run based on the requested time and the availability of resources. The scheduler exchanges messages with its clients via the mail subsystem, and receives requests from MUI processes to schedule a measurement process at a specified time. The scheduler manages the sharing of resources, handles global remote/local control of instrumentation, and provides the means for a user to determine the status of a job that is running in the background.

Measurements can be scheduled by the user to run at any time of day, on any day. They can also be scheduled to run repetitively for a user-specified duration at a user-specified interval. Multiple measurements can be scheduled for execution at any time. The scheduler also supplies the link necessary to

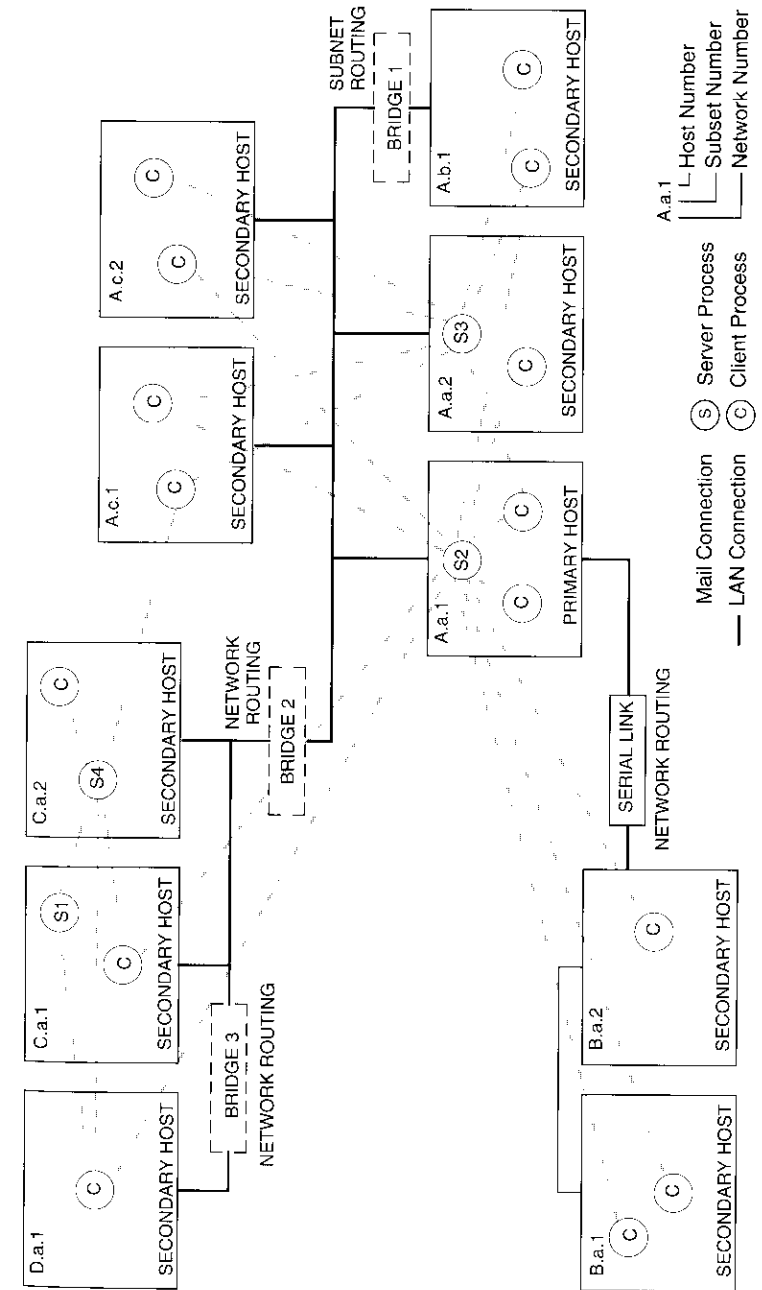


Figure 4. MPCP Distributed Processing Mail System

communicate scheduling information between the MUI and the measurement processes.

When the time arrives to execute the requested measurement, the scheduler verifies the availability of the required resources and initiates the measurement process in the appropriate workstation. When the measurement process begins, it requests from the scheduler (via mail) the needed resources. The scheduler determines that a mail connection has been established with the measurement process, and that the process is actually executing. It then grants the requested resources and locks them for the duration of the measurement, or until the mail connection between the scheduler and the measurement process is broken. By ensuring that the process is actually running before resources are committed, the scheduler prevents a potential lockup situation. If the scheduler were to begin a measurement process and immediately allocate and lock the resources, the measurement could fail to start for some reason, or fail to establish a mail connection, and the resources would be unavailable for other uses.

If the resources required for a scheduled measurement are unavailable, execution of the measurement is deferred until they become available. Since scheduling conflicts are resolved on a first-come, first-served basis, a particular measurement may have to wait its turn in a job queue. A planned expansion of the scheduler will provide for the prioritization of measurements.

An example will illustrate the scheduler's operation and interaction with measurement processes. A system comprising three workstations, with one spectrum analyzer and two power meters connected to workstation 3, is assumed. MUI programs in workstations 1 and 2 have each requested that an EIRP measurement be performed at 10:00 a.m. the next morning. In addition, workstation 2 has requested a power measurement at the same time. EIRP measurements require both a spectrum analyzer and a power meter, while power measurements require only a single power meter.

At 10:00 a.m. the following morning, the scheduler ascertains that both power meters and the spectrum analyzer are available, and grants the request from workstation 1 (which was received first) by executing an EIRP measurement and locking power meter 1 and the spectrum analyzer. As a result, the EIRP measurement request from workstation 2 cannot be granted at this time, since only power meter 2 is available. Since the power measurement also requested by workstation 2 requires a single power meter, the scheduler initiates the power measurement process, establishes a mail connection with that process, and locks power meter 2. When the first EIRP measurement terminates and both the spectrum analyzer and power meter 1 become available, the scheduler executes the EIRP measurement requested by the MUI process running on workstation 2, establishes an open mail connection with the EIRP

measurement process, and locks power meter 1 and the spectrum analyzer for the duration of that measurement. When the measurement process terminates (normally or abnormally), the scheduler releases the resources, which are then available for the next request.

The scheduler determines when to start a particular measurement, based on the system clock and the scheduling information provided by the MUI when the measurement was specified. The UNIX operating system could start jobs at the scheduled time, if that were the extent of the requirement. However, the scheduler performs two additional, essential functions. First, it begins a job at the scheduled time *with the user-specified arguments*, which can vary in number and value with each running of a measurement.

The second, more fundamental function of the scheduler is to manage the sharing of one set of microwave measurement and earth station equipment resources. These resources include microwave test equipment (such as the spectrum analyzer and power meters), earth station equipment (such as uplink and downlink chains, the antenna, automatic saturation control units, and radiometers), files, mail connections, and memory. Each resource is identified by name (resource ID) and the maximum number of users. Resources may also belong to resource groups, in which case the group is given a single name, such as "Uplink 1," which would include the entire chain of earth station equipment forming an uplink. The scheduler can allocate both individual resources and resource groups to jobs. Resource sharing is cooperative, not enforced or preemptive.

The scheduler also manages the state of resources when they are not controlled by a measurement process. For example, it makes certain that instrumentation used by a job is placed into a quiescent state when a job is complete. This ensures that jobs cancelled abortively do not leave instrument resources in an undesirable or unknown state. Since the scheduler controls all system resources, it is responsible for handling user requests to place instrumentation into its local state when it is not being used by an executing process. Such requests from measurement processes are handled via the MPCP mail subsystem.

The MPCP datapool

The MPCP datapool server is a memory-resident data area that functions as a depository for information to be shared system-wide. All IOT system processes can access the datapool, which will accommodate arbitrary data. The datapool implements a client-server model in which clients such as MUI processes update entries in the datapool and/or request the most up-to-date information from the datapool, via the mail subsystem.

Maintaining data integrity within the datapool and preventing "racing" conditions are critical design issues. A racing condition can arise as follows. Suppose process A reads the current value for datum 1 in the datapool and, based on that information, updates datum 2 in the datapool. Process B has previously read datum 2, prior to its update by process A, and, based on this information, updates datum 1. Process A assumes that the datum 1 value it read is valid and up-to-date, when in fact datum 1 was subsequently updated by process B. Thus, process A continues execution with data that are not current. Similarly, process B assumes that the datum 2 value it read is valid and up-to-date, when in fact datum 2 was subsequently updated by process A. At this point, a racing condition has been created in the datapool, and neither process has up-to-date data. This situation is avoided by implementing the datapool as described below.

The datapool is not merely a passive receptacle and reporter of data, because it can notify clients of changes to datapool entries. A client can register with the datapool a list of entries of interest. Whenever the status of a list entry changes (*e.g.*, it is changed in value or deleted, or the process that owns the entry terminates), the client is notified by the datapool and provided with the current value for the data item. A client may request and receive the current value of any item in the datapool at any time, and thus is assured of having the most up-to-date values for items of interest.

As shown in Figure 5, client processes do not access the datapool directly. When they need to add, modify, or remove data, clients access the datapool via a library of datapool functions. These functions then transmit the request to the datapool process, which accesses the data area on behalf of the clients. Only the datapool process can access entries in the data area itself, to prevent potential corruption of the datapool by client processes and to maintain datapool integrity. A data-locking mechanism is applied to guarantee that only one data update can occur at any given time.

System-wide standard messages are used to transmit information to and from the datapool. A typical datapool process operation involves two types of message transmission: the client's request message received by the datapool process, and the acknowledgment returned with the requested data to the client. All communications between the datapool and its clients (Figure 5) are via the MPCP mail subsystem, which is transparent to clients. Datapool functions are available to the client to request data creation, deletion, modification, retrieval, and the addition or deletion of the client process from the notification list. These functions assemble mail messages, send mail to the datapool process via the mail subsystem, and inform the calling program whether or not the operation was successful. The datapool library implementation hides both the

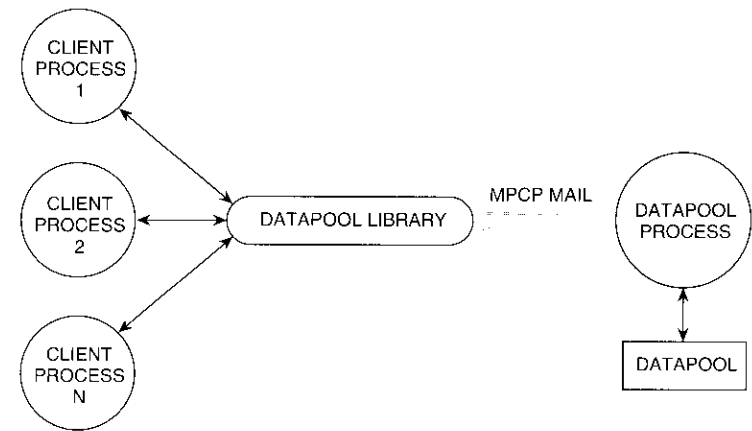


Figure 5. MPCP Datapool and Clients

type of interprocess communications media and the fact that messages are used.

The datapool also supports the operation of the MUIs. When an MUI is opened by a user, it establishes a mail connection with the datapool. Assume, for example, that client process 1 in Figure 5 is an MUI in which the user has specified spacecraft 1, and client process 2 is another MUI in which spacecraft 2 is specified. If a third MUI is opened, it may want to know toward which spacecraft the earth station is currently pointing, or if another process changes the current spacecraft in the datapool. The datapool maintains such system-level information and can notify a requesting client process of the current status and configuration for both the spacecraft and the earth station.

IOT measurement implementation

IOT measurements are the core of computer-controlled IOT systems. An IOT system is composed of numerous IOT measurement programs, their corresponding MUIs, and system control and data processing functions. This section discusses the concepts and principles underlying the implementation of measurements. Overall software organization, data-driven design, user interface implementation, error handling, and data processing features are described.

Since measurement data are a primary concern in an IOT system, data integrity is essential. Because the measurement is often fully automated, the measurement code must be able to detect and report errors, which can arise

from many sources, including real-world anomalies. For example, a measurement may require the use of a piece of test equipment that has been turned off or disconnected. The code then issues an error message, and the user may correct the problem (e.g., reconnect the instrument) and request that the measurement continue, or cancel the measurement.

Measurement architecture

The ideal IOT is one in which the overall measurement is implemented as two separate programs: the MUI, and the measurement itself. A model of the IOT measurement architecture is shown in Figure 6.

Communication between the MUI and the measurement processes is facilitated by the MCP mail subsystem, the scheduler, and the datapool server. The mail subsystem provides interprocess communications between the MUI and the scheduler, and between the scheduler and the measurement program or other peer client processes. Properly designed interfaces between communicating processes are essential for coordinating the various activities associated with the overall measurement.

The scheduler allocates system resources, including earth station resources, and maintains their availability status. The MUI sends a job request message via the mail system to the scheduler and communicates the name of the measurement program, the name of a file containing a list of measurement arguments (called the "argsfile"), and scheduling information. Before starting a job that invokes a measurement program, the scheduler determines the availability of required resources by accessing a file that lists the resources required by each measurement. If the resources are currently unavailable, the scheduler places the job in a job-wait queue and reschedules it.

If the resources are available, the scheduler starts the measurement via a command to the UNIX operating system. If UNIX initiation is successful, the program becomes an executing process. The measurement process performs an initialization and establishes a mail session connection to the scheduler. It then accesses the resources file and sends the scheduler a message indicating that the process is initialized and running, and requesting access to system resources such as the spectrum analyzer, an uplink path in the earth station, and an uplink synthesizer. If available, the resources are allocated as requested.

By structuring the overall measurement in this manner, MUI and measurement programs can be designed, implemented, tested, and maintained independently and in parallel. This supports modularity and encapsulation of the respective programs. Team personnel with complementary skills can work on different tasks, making optimum use of their software capabilities and

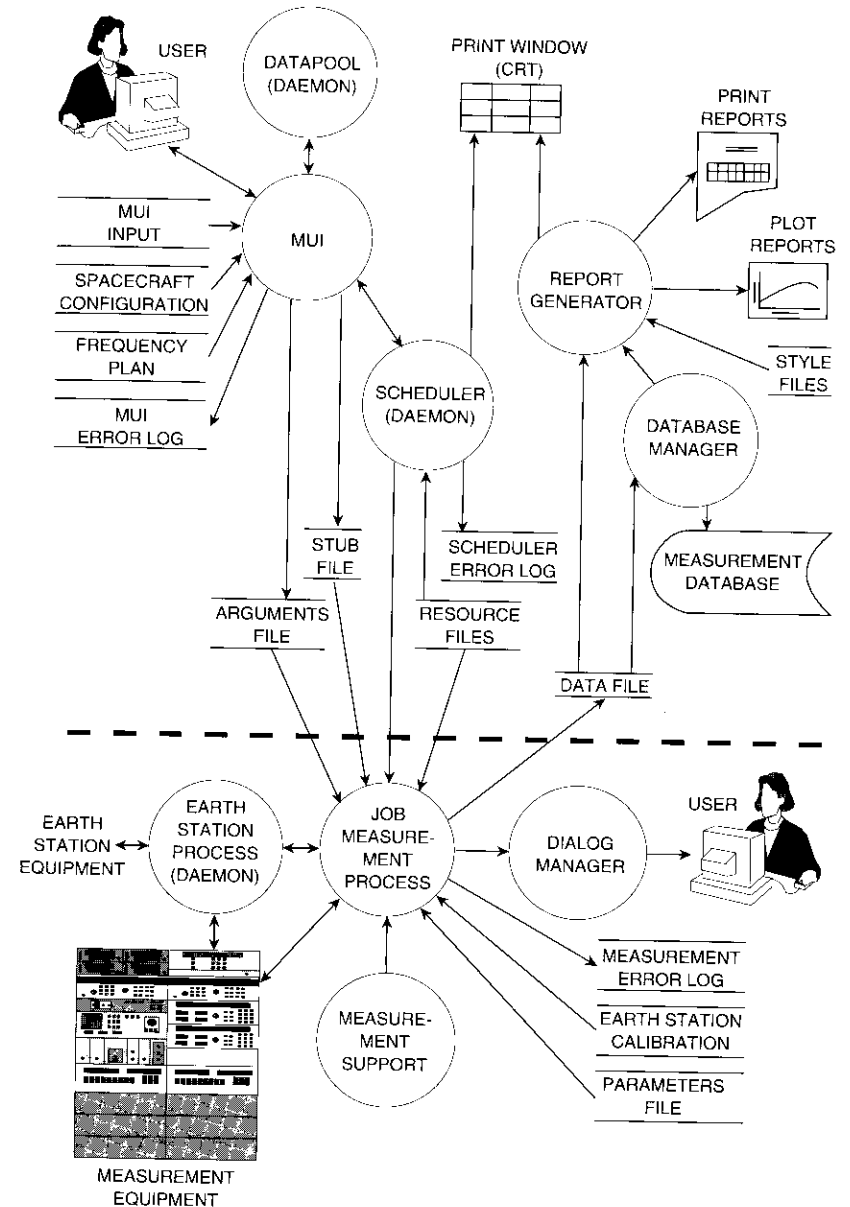


Figure 6. IOT Measurement Model

experience. Each program developer uses the most appropriate programming paradigm. For example, since the user interacts with the MUI via a mouse and keyboard, the MUI must respond to unpredictable events (*e.g.*, a mouse click or the pressing of a key) and is therefore implemented using an event-oriented programming paradigm. The measurement program, on the other hand, interacts with the microwave measurement and earth station equipment in a predictable manner, and thus is implemented in an algorithmic, procedure-oriented programming paradigm (although it can be interrupted by unexpected behavior when an instrument issues a service request interrupt on the IEEE-488 bus).

Data-driven implementation

The MMS software is implemented by using text files and avoiding hard-coding wherever possible. As shown in Figure 6, text files are used to exchange information between processes, as a complement to interprocess mail communications. The following files are used, and will be discussed in context: MUI input, measurement argument, stub, resource, spacecraft configuration, earth station calibration data, measurement parameter, and print and plot style. Since these files are structured during the system design phase, they can be constructed to hold any information desired, and can be customized to meet customer requirements. Thus, the files provide flexibility and adaptability to the measurement system design.

Both the file management procedures and storage format are standardized within the MMS software. File operations such as open, read, write, and close are performed via calls to an MPCP library. Files are formatted in a standard COMSAT Data File Format (COSDAF) and stored as ASCII-coded text. COSDAF files can be viewed, edited, and imported into other application programs.

System behavior can be altered by editing the files, which minimizes the need to recompile the program when changes are required. For example, the appearance of an MUI window on the display is controlled by an MUI input file. The number of MUI controls, their position, and type (*e.g.*, pushbuttons, edit fields, and pop-up menu selections) are easily changed by editing this file.

Although MMS files are easily edited, they are static in the sense that they generally remain unchanged for a particular sequence of IOT measurements. In fact, once constructed, they seldom change, although they can be modified when necessary. The spacecraft configuration file, for example, includes information regarding spacecraft characteristics, channel characteristics such as center frequency and bandwidth, transmit and receive beams, transponder gain settings, and orbital parameters. Another file, the frequency plan, identifies channels and/or carrier slots, their center frequencies and bandwidths, power threshold levels for alarms, expected signal modulation, and other frequency-

related information. Other files, such as the earth station calibration file, store calibration information such as antenna gain vs frequency and coupler value vs frequency.

The measurement process reads particular files when required. The use of common files by different measurement processes guarantees uniformity of information. Also, since the user does not have to constantly reenter the same information through the keyboard, user input errors and fatigue are reduced.

User interface design

Effective operation of a measurement system is highly dependent on the design, behavior, flexibility, ease of use, and consistency of the user interface. More than 30 years of human-machine interface research (References 6 and 7, for example) have indicated that the most effective technique is a graphically based interface that allows a user to indicate a desired action by "pointing and clicking" in windows on the display by using a mouse device. The keyboard is used to enter parameter values and data. This technique is in contrast to the older command-line-based interface that requires the user to accurately remember and type in esoteric command codes. Graphically based interfaces are now common on many computer systems, such as the popular Apple Macintosh [8] and desktop computers running Microsoft Windows. The X Window-based MUI enables the IOT system user to specify measurement parameters. It contains edit fields, pushbuttons, toggle buttons, and radio buttons. Buttons are actuated by pointing and clicking with the mouse. A typical MUI is shown in Figure 7.

MUIs and other windows meet the following IOT system operational requirements:

- Permit the user to easily, quickly, and intuitively set up IOT measurements.
- Enable the user to search through the measurement database to retrieve files meeting user-specified criteria.
- Enable the user to process high volumes of measurement data into plots and printouts.
- Inform the user of input range and type errors.
- Inform the system operator of errors encountered during measurements and other activities.
- Require minimal training, so new users can gain proficiency rapidly.
- Preserve operational flexibility for nonroutine activities, such as anomaly investigations.

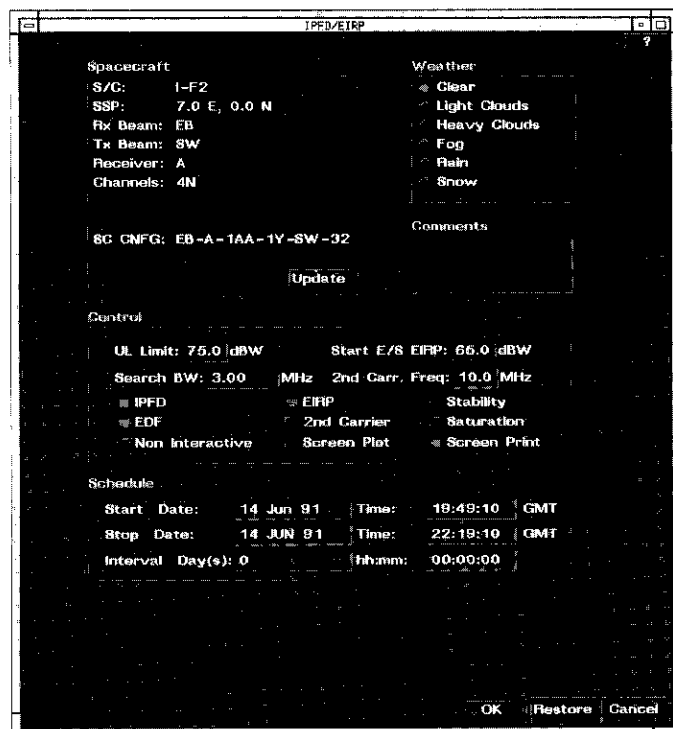


Figure 7. FLUX/EIRP Measurement User Interface Window

Some IOT measurements can be run automatically, without the presence of an operator, while others are interactive and require operator inputs throughout the measurement. Some measurements can be run in either mode (selectable by the user as the "Non Interactive" option shown in Figure 7), which can be toggled on or off by clicking the mouse.

Implementation of an effective user interface requires careful thought and considerable effort. All MUIs and other windows are implemented using Open Software Foundation's OSF/Motif toolkit and style guidelines [7]. MUIs are implemented to be consistent in behavior and similar in appearance. Buttons and controls that perform the same function from one MUI to another are positioned in the same location, so that the user who has learned one MUI has a familiar model to follow. When opened, MUIs are displayed with default parameter values and control settings, and have a "form-fill-in"/menu-selection presentation format. The default values are read from an ASCII file, which is

easily modified. If an input is invalid (e.g., an out-of-range value is typed in), the user is immediately notified of the error and prompted for another input.

Often, several input parameters are coupled in a dependency relationship to preserve maximum operational flexibility. If a user specifies a parameter that is coupled to others, the related parameter or parameters will also be changed automatically. For example, the user may be required to specify a bandwidth, a step size, and the number of steps to be performed by a measurement. These parameters may be coupled such that specifying the number of steps and step size automatically determines the bandwidth parameter as their product.

MUI-measurement process interface

Once the user has configured the measurement via the MUI, the specified parameters and controls are communicated to the measurement process via a command-line interface similar to the standard UNIX system command interface. In normal operation, the user initiates a particular measurement by filling in the appropriate MUI and scheduling the measurement. The MUI is displayed on a workstation or X-Terminal. The user then presses the OK button on the MUI (see Figure 7), and the MUI communicates this information to the measurement process via the scheduler. At the scheduled time, the scheduler checks to see if the required resources are available, starts the measurement process, establishes a mail connection to the process, and allocates the requested resources.

To preserve maximum system flexibility, measurement programs can be run without an MUI workstation or X-Terminal by using a standard character-based ASCII terminal. A user can run an IOT measurement at the host earth station from a remote site, such as the user's home, by using a personal or portable computer and modem. For example, during an anomaly investigation, it may be desirable to alter the normal flow of system operation or to make a particular series of measurements not implemented by the IOT system MUIs. This flexibility is achieved as described below.

Following UNIX conventions, an IOT measurement program can be invoked from a connected terminal by typing the name of the executable program and optional arguments as follows:

```
meas_name [-opt <opt_arg> ...]
```

where `meas_name` is the name of the measurement program, `-opt` specifies an option, and `<opt_arg>` specifies an argument to an option. For example, the command line to invoke the IPFD/EIRP measurement with options set for a 3-MHz search bandwidth and saturation is

```
flux_eirp -Search_bw 3.0 -Saturation
```

The IPFD/EIRP measurement program is invoked and instructed to set the search bandwidth on the spectrum analyzer to 3.0 MHz and perform the measurement at saturation. The arguments available to each IOT measurement are customized for that particular measurement. Any control available in the MUI can be entered as a command-line argument.

A measurement typically requires numerous controls and parameter settings. Normally, the MUI handles all controls; however, the number of controls can present a problem for manual entry via a command line. Since the command is transitory, whenever a measurement is repeated (perhaps with different options), the measurement command and its arguments must be reentered—a tedious and error-prone process. One solution is to place measurement arguments into an arguments file. Once constructed, this file is permanent, regardless of the options stored. The argsfile can be configured with a set of default options.

To accommodate the use of the argsfile, the measurement program extends the conventional UNIX command-line invocation with one additional argument `-args <argsfile>`. The `-args` option instructs the measurement process to obtain its command-line arguments from the file named in the parameter, `<argsfile>`. If an argsfile has been created for the IPFD/EIRP measurement, the measurement program can be invoked from the UNIX command line as follows:

```
flux_eirp -args my_args
```

where the file `my_args` contains the arguments `-Search_bw 3.0` and `-Saturation`. Once again, a data-driven design approach is used to preserve maximum operational flexibility and adaptability.

The ability of the measurement program to receive its arguments from an argsfile provides the necessary interface between the MUI and the measurement program. When the MUI window (e.g., Figure 7) is opened, the parameters are displayed with default settings which the user is free to alter to accommodate a specific measurement configuration. When the measurement specification is complete, the user presses OK. The MUI program then creates an argsfile containing the specified arguments and parameters for use by the measurement process (as depicted in Figure 6). Use of the argsfile minimizes the number of entries required from the user, since most of the defaults are unchanged.

Measurement program implementation

The measurement program focuses on the measurement task itself. For example, although the measurement process (a program in execution) outputs a data file of results, it is not responsible for storing, displaying, printing, or plotting the data. These tasks are managed by other processes. Similarly, the measurement program is decoupled from the particular spacecraft upon which

it will perform the measurement, and spacecraft information is communicated from the MUI program via the argsfile.

Measurement programs are implemented in a modular manner using object-oriented design and implementation techniques [9]. This results in a high degree of encapsulation. Using the class terminology of object-oriented programming, a generic "Measurement" class is implemented with attributes (such as data declarations, data structures, and methods) that are common to all IOT measurements. Measurement-class methods include performing initialization and establishing a mail session with the scheduler, opening files, checking arguments passed via the argsfile for validity, configuring uplink and downlink equipment, performing up- and downlink measurements, storing the final output data, pausing the measurement, and cancelling the measurement when requested by the user. Since these common tasks comprise the bulk of the measurement, it is appropriate to aggregate them into a generic class.

Measurement programs are coded in C++, a language designed to support object-oriented programming and the construction of classes of objects with inheritance relationships. Figure 8 illustrates the class structuring and inheritance relationships of some of the IOT measurements. The implementation of measurement programs as classes of objects allows the developer to "leverage" code using inheritance, as explained below. This enhances reliability because each software element is tested thoroughly every time it is leveraged and reused. As a result, greater emphasis can be placed on measurement technique, rather than measurement mechanics.

Inheritance enables the measurement developer to leverage code as follows. Using the inheritance properties of C++ [10], an EIRP measurement is implemented as a subclass (or derived class) of the generic Measurement class. The EIRP measurement inherits all of the data structures and methods of the "parent" Measurement class, and implements additional structures and methods as well.

The gain transfer, in-band frequency response, and spurious output measurements are subclasses derived from the EIRP class. Gain transfer is an EIRP measurement performed at different uplink power levels of a test signal; frequency response is an EIRP measurement performed at different frequencies in a spacecraft transponder channel; and spurious output is an EIRP measurement performed on a specific spurious signal received from the communications satellite. These measurements inherit the data structures and methods from the parent EIRP class, as well as from the "grandparent" Measurement class, with additional structures and methods implemented to accommodate measurement-specific requirements. Thus, the developer of the gain transfer measurement can focus on issues unique to that particular measurement, while reusing or

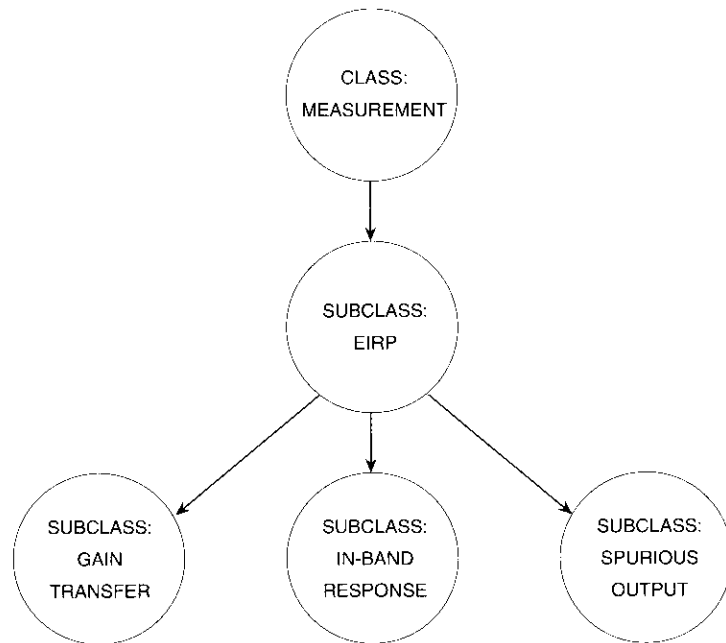


Figure 8. IOT Measurement Class Structure

“leveraging” the previously tested code for the EIRP and Measurement classes from which it is derived. This repeated testing improves overall software reliability.

Class-structured, object-oriented implementation of measurement procedures enhances code flexibility and adaptability. For example, the gain transfer measurement program can be modified without affecting other measurement programs, such as in-band frequency response. On the other hand, global changes can be made by modifying and recompiling the generic Measurement class. Its derived classes inherit the modifications upon recompilation.

An IOT measurement is constructed as a hierarchy of modularized code layers. The main program is linked with various libraries to create the executable program. These libraries include application-level libraries (*e.g.*, Measurement and EIRP class libraries); MPCP libraries (*e.g.*, measurement support, instrument drivers, IEEE-488 bus management, mathematical, and utility functions, and error management); and UNIX system libraries (*e.g.*, device input/output). The typical layered code organization of the in-band frequency response measurement program is illustrated in Figure 9.

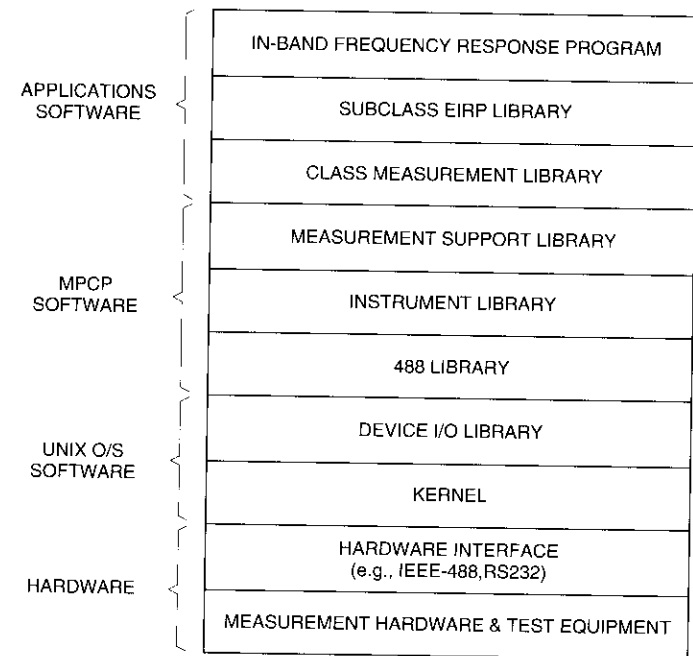


Figure 9. Layered Measurement Program Code

The main program makes a sequence of calls to functions in the EIRP and Measurement class libraries. These, in turn, call functions in the MPCP measurement support library, which perform tasks required by all measurements, such as initializing hardware, creating and opening files required by the measurement program, and performing housekeeping and cleanup activities.

Instruments are accessed by measurement support library functions via drivers in an instrument library. Instrument drivers perform high-level operations such as initializing the instrument, changing its settings, and reading the measured results. Each driver contains functions for its particular instrument. Drivers have been implemented for:

- Spectrum analyzers
- RF and waveform synthesizers
- Network analyzers
- Modulation analyzers
- Noise analyzers

- Frequency counters
- Power meters
- Voltmeters
- RF switch controllers
- Data acquisition units.

The driver provides a simple interface with the software developer using the instrument. Because data integrity is a principal concern, the driver is capable of detecting and reporting errors that may arise from interactions with the instrument, and handles the instrument's software control capabilities. This enables the developer to focus on instrument usage, rather than on the detailed mechanics of communicating with the instrument.

Instrument drivers communicate with instruments via the IEEE-488 bus by using the MPCP 488 library, which provides high-level bus management function calls to the driver. The library performs atomic I/O with a given instrument, so that an I/O transaction, once started, cannot be interrupted. This allows the same instrument to be shared by multiple processes.

The 488 library also performs such functions as sending an Interface Clear signal to all instruments, writing a command string to an instrument, reading a response string from an instrument, addressing an instrument to talk or listen, retrieving the bus and address of an instrument when multiple buses are present, and performing a serial poll of an instrument to obtain its status byte. These functions are generally called by the instrument drivers, but can also be called by other programs for communication with other IEEE-488-compatible devices such as computers or special-purpose hardware. The 488 library frees its user from bus management details.

Functions in the 488 library call low-level, primitive functions supplied with the UNIX operating system device I/O library. These primitives interact with the UNIX kernel (which directly controls the IEEE-488 bus) through an interface card. A cable connects the workstation's interface card with the instruments, which are daisy-chained onto the IEEE-488 bus through cables.

An instrument may be used in the shared mode in which it is checked out from the scheduler, or may be managed completely by a device process. In the shared mode, the instrument (if available) is checked out from the scheduler as described previously. The measurement is not allowed to run if any of the required instrumentation or other resources are unavailable. In the second case, the instrument is fully managed by a device process. All requests are issued to the instrument in the form of messages to the device process, which then communicates with the particular device or instrument. The device is not always a measurement instrument, but may be another computer that controls and communicates with such earth station equipment as the uplink power

meter, radiometer, or antenna control unit. In general, the shared mode is employed for instruments that are used occasionally by some measurements, while the device process is employed for instruments used by all measurements (e.g., to communicate with a separate earth station control computer).

Other MPCP libraries, including utility libraries, a mathematics library, and the error handling library, are also linked to the measurement program. Several utility libraries provide useful functions required by IOT measurements or by other libraries, such as calculating EIRP, flux density, path loss, spacecraft gain, spreading factor, and slant range. The math library contains numerous mathematical functions routinely required in IOT and other measurement systems, such as numerical integration and linear regression analysis. The error handling library, which is used universally by all components of the software system, is described below.

Measurement programs execute as processes to perform actual measurements. In object-oriented terminology, a measurement process is an "instantiation" of the measurement; that is, it is an instance of a measurement program executing with parameters specified by the user.

A measurement process accesses several files, as illustrated in Figure 6. When the user specifies and schedules a measurement in an MUI window, the MUI process creates an argsfile and a stubfile. The stubfile contains annotations for the specific measurement (e.g., the spacecraft selected, earth station name, weather conditions, comments, and the date and time) which do not affect the measurement itself. The measurement process obtains arguments from the argsfile and opens the stubfile, to which it appends measurement data. The process reads the resource file for the resources it requires, and the earth station calibration file for earth station antenna and coupler calibration data. The process may also access a parameters file for measurement-specific parameters.

Also, during measurement execution, the measurement process configures and controls the microwave measurement equipment for data acquisition, and communicates with the scheduler. It interacts with the earth station daemon process to obtain relevant information, and issues dialog windows to the user via a dialog manager process. Real-time measurement data are displayed on the workstation monitor as the measurement progresses (as depicted in Figure 6), along with the status of the measurement. The final measurement data file is stored in the database, printed, and plotted.

Error subsystem design

Error detection and management are critical considerations in the design and implementation of a computer-controlled IOT system or similar

measurement-oriented system. The MMS software is implemented to detect as many errors as possible, in order to prevent data corruption.

Two broad categories of errors can be manifested. Operational errors occur when the measurement process detects some condition or circumstance coded in the program to be an error. For example, an operational error occurs when an instrument required by a measurement cannot be initialized because it is powered-off or disconnected from the computer, or a printer is off-line or out of paper. If an operational error cannot be corrected, the measurement process must be aborted. Other errors are manifested as programming errors. It is important to detect both types of errors in a timely fashion and to obtain as much information as possible concerning the circumstances that gave rise to the error, to assist in diagnosis and correction.

The MPCP error library contains functions for assembling logging, and displaying error messages. When an error is detected, the specific function name and line number at which the error occurred are recorded.

Each layer of code is implemented to detect and report errors occurring at that level. Because of the layered software architecture, error reporting is stacked into a composite error message, as shown in Figure 10. When an error is detected, an IOT measurement program at the highest code level [e.g., f1()] places a message into a stack. Each lower layer of code [f2(), f3(), and f4()] then places its own message onto the stack, so that the composite error message depicts the full path from the application program, down through successive layers, to the lowest-level function [f4()] in which the error was detected. Figure 11 depicts a sample of a composite error message. The complete error diagnostic, showing the full path through the various layers of code, provides a context and clues for those tasked with troubleshooting and correcting the error. Error files can be printed in hardcopy form for later examination and analysis.

Measurement output files and data processing subsystems

If an IOT measurement process executes successfully to completion, it produces a measurement data file. These files are formatted as standard COSDAF files, and, because they are ASCII-encoded, can be viewed, edited, and imported into other applications, such as word processing or graphics software. Once data files have been produced, they can be processed by other MPCP subsystems for database entry, printing, and plotting. Permanent measurement data files are stored in a database.

The MPCP Database Management subsystem stores, searches, and retrieves files for display, printing, and plotting, as depicted in Figure 6. The subsystem

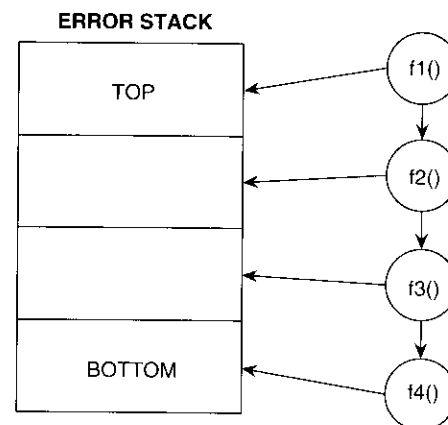


Figure 10. Error-Reporting Stack Mechanism

```

Mon May 17 14:11:34 1993 /proj/eutel/bin/flxerp
flxerp measurement cannot measure flux/eirp for channel 4.
meas_init_hdwr(): Unable to initialize hardware.
ms_init_hdwr(): hp3488a_new failed.
_hp3488a_init(): ZZ401 switch unit - slot #1 unavailable.
_hp3488a_get_slot(): ZZ401 switch unit - cannot communicate with switch control unit.
_hpib_io_dcderr(): HP-IB timeout, receive data ZZ401 9 /dev/hpib/1.
System call hpib_io(): Connection timed out (errno is 238).

[ Try Again ] [ Cancel ]

```

Figure 11. Composite Error Message Format

consists of a formal database containing a summary of the information associated with every measurement that has been stored (called the "index"), and a set of separate measurement data files containing the raw and processed results from each measurement (called "files"). The index is used to quickly locate data files of interest, just as a card catalog is used in a library. Once a particular data file has been located, it may be plotted, printed, or post-processed in some fashion.

The MPCP Plotting Services subsystem plots measurement data both during and after the measurement. The subsystem supports measurement systems in which many different types of data plots, to either soft output (e.g., CRT displays) or hardcopy devices, are necessary for real-time measurements and post-measurement data analysis, as depicted in Figure 6. Plot formatting is specified by a style file that can easily be edited to change the appearance of the plot, without changing either the measurement data or the plotting program. Figure 12 illustrates specifications that can be accommodated in the plot style file.

The MPCP Printing Services subsystem prints measurement data, supports systems output, and formats data in much the same way as the plotting subsystem. Printouts are generated automatically at the conclusion of a measurement process, or at user request.

The MPCP Interactive Plotting subsystem significantly extends the post-measurement data analysis and manipulation capability of the measurement system beyond that supplied by MPCP Plotting Services, and provides a general-purpose capability to prepare finished, report-quality plots and graphs. It can plot any pair of columns of data in a COSDAF file. This is significant because, although the measurement data file contains a table with many columns of data, the MPCP Plotting Services subsystem normally plots only two columns (or three columns: Y1 and Y2 vs X). The Interactive Plotting subsystem also supports graphs with two y axes (Y1 and Y2 vs X). The data on a plot can be manipulated and edited in the following ways:

- Points can be cut and pasted.
- Scales, axes, and labels can be changed.
- Graphs or points can be annotated and/or marked.
- The plot can be zoomed in or out.
- New data points can be added via the keyboard and/or from existing files.
- Data from one or more files can be plotted on the same graph as data from another file.

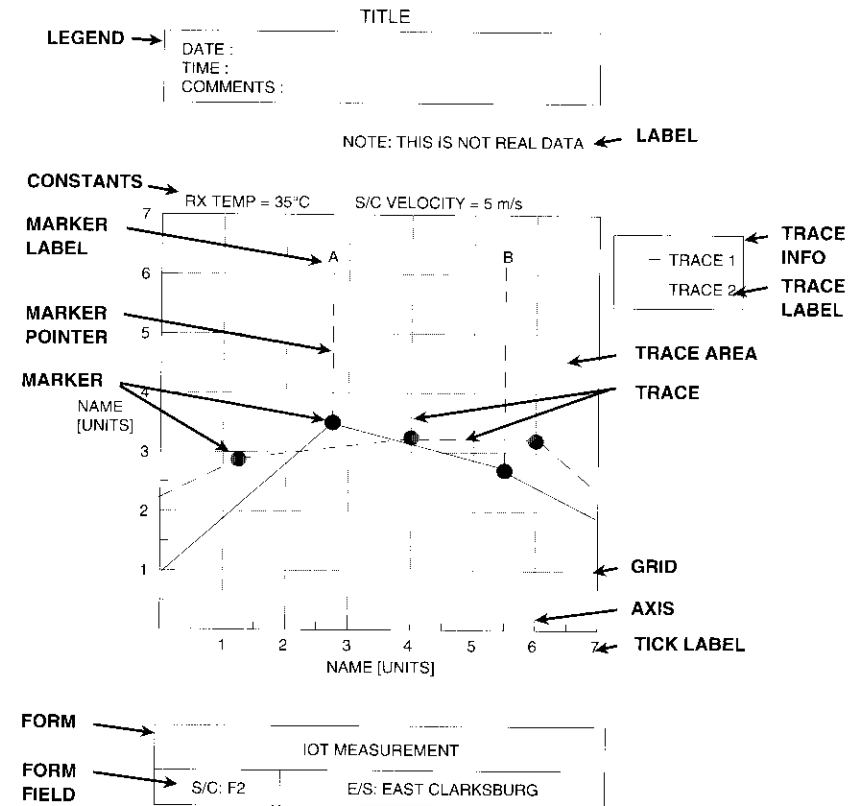


Figure 12. MPCP Plotting Specifications

Various data transformations are also supported. Two or more traces can be merged, algebraically added, or algebraically subtracted. For example, a calibration file can be subtracted from a measurement file, or two measurement traces can be subtracted from one another, leaving the residual differences. Finished plots can be stored and later retrieved.

Conclusions

The concept of building MMS software on an engineered platform of reusable facilities and services has been presented. Contemporary software engineering principles and practices—such as design-for-reusability; modularity and encapsulation of task-specific functions; object-oriented methodology and

implementation; hierarchical layering of code; linkable object code libraries; and processing subsystems—were used to develop and deploy robust, flexible, adaptable MMS software.

The desire for code reusability directed development of the MPCP, a special-purpose operating system that significantly reduces the time and expense involved in developing and implementing a cost-effective MMS. The field-tested MPCP software enables the limited number of expert software developers available to focus on the application's design and implementation, rather than on the software infrastructure required to support modern IOT and other microwave measurement and control systems.

Supported by the MPCP interprocess/intermachine mail communications subsystem, scheduler, and datapool, the IOT measurement architecture physically and logically partitions the overall task into separate user interface and measurement program entities, each optimized to perform a specific task. The network system architecture enables the user interface program and measurement program to execute on different machines and at different times of day—providing the system with a high degree of operational flexibility, including remote access and control of the IOT measurement equipment.

The concepts and methods applied in this study to the complex task of building automated IOT systems in a dynamic environment are also applicable to similar measurement-oriented systems, such as those used for communications systems monitoring.

References

- [1] Y. Tharaud, B. Kasstan, and P. Barthmann, "IOT System for the EUTELSAT II Satellites," Global Satellite Communications Symposium, Nanjing, China, May 1991, *Proc.*, pp. 168–177.
- [2] Y. Tharaud and V. Riginos, "EUTELSAT's Facilities for Measurement of Earth Stations and In-Orbit Satellite Payloads," 23rd General Assembly of the International Union of Radio Science (URSI), Prague, Czechoslovakia, August–September 1990.
- [3] P.-H. Shen, V. Riginos, and S. Bangara, "In-Orbit Testing of Communications Satellites: The State of the Art," Global Satellite Communications Symposium, Nanjing, China, May 1991, *Proc.*, pp. 150–159.
- [4] K. D. Fullett *et al.*, "The EUTELSAT In-Orbit Test System," *COMSAT Technical Review*, Vol. 23, No. 1, Spring 1993, pp. 61–99 (this issue).
- [5] V. Riginos *et al.*, "In-Orbit Test and Monitoring Systems Architecture," AIAA 14th International Communications Satellite Systems Conference, Washington, DC, March 1992, *Proc.*, pp. 951–961.

- [6] S. K. Card, T. P. Moran, and A. Newell, *The Psychology of Human-Computer Interaction*, Hillsdale, NJ: Lawrence Erlbaum, 1983.
- [7] *OSF/Motif Style Guide*, Rev. 1.1, Open Software Foundation, Englewood Cliffs, NJ: Prentice-Hall, 1991.
- [8] *Apple Human Interface Guidelines: The Apple Desktop Interface*, Apple Computer, Inc., Cupertino, CA, 1987.
- [9] G. Booch, *Object Oriented Design With Applications*, Redwood City, CA: Benjamin-Cummings, 1991.
- [10] B. Stroustrup, *The C++ Programming Language*, Reading, MA: Addison-Wesley, 1986.

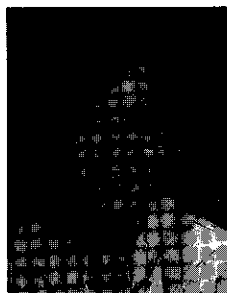


Kenneth D. Fullett received a BSEE and MSEE from the University of Illinois, Urbana-Champaign, in 1979 and 1981, respectively. He joined COMSAT Laboratories in 1981 as a member of the Transponders Department of the Microwave Technology Division and participated in all aspects (including both microwave hardware and computer software system design) of many IOT systems, including those for INTELSAT, MCI, and EUTELSAT. His work also involved software development for COMPACT Software, and he was a project manager for the RF Terminal Supervisory System of the NASA/ACTS earth station. Mr. Fullett is currently engaged in high-energy physics research in the Anti-Proton Source Department of the Accelerator Division of Fermi National Accelerator Laboratory, Batavia, Illinois.

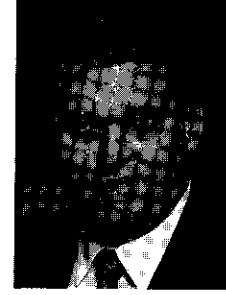


Walter D. Kelley, Jr., earned a BS in electrical engineering at the Catholic University of America, Washington, D.C., in 1974; and an MBA at Marymount University, Arlington, VA, in 1983. In 1991, he joined the Transponders Department of the Satellite and Systems Technologies Division at COMSAT Laboratories as a Member of the Technical Staff. At COMSAT, he has participated in development of the IOT system for Hughes Communications' DirecTv™, an IOT system for EUTELSAT, and the NASA/ACTS ground station control and status subsystem.

Vasilis E. Riginos received a BE, MEng, and PhD in electrophysics from the Stevens Institute of Technology, Hoboken, NJ, in 1964, 1970, and 1973, respectively. He is currently Manager of the Transponders Department of the Satellite and Systems Technologies Division at COMSAT Laboratories, where he is responsible for directing research and development on communications system performance as applied to satellite transponders. He also supervises research and development in advanced microwave circuits such as high-power amplifiers, regenerative receivers, filters, and multiplexers. Dr. Riginos participated in the evaluation of the Inmarsat program, and has been project manager for the GTE ATEF IOT system, the INTELSAT Maritime Communications Subsystem IOT station, the EUTELSAT IOT system, and the Hughes DirecTv™ IOT system. He is a member of Sigma Xi, AAAS, IEEE, and the American Physical Society.



Pei-Hong Shen received a BS and MS in genetics, and an MS in computer science, from Washington State University in 1983, 1984, and 1986, respectively. From 1978 to 1981, she studied biology and genetics while attending Fudan University in Shanghai, Peoples Republic of China. Ms. Shen is currently a Senior Member of the Technical Staff in the Transponders Department of the Satellite and Systems Technologies Division at COMSAT Laboratories, where she is primarily responsible for design and development of software for communications satellite applications. Since joining COMSAT in 1987, she has been involved in the design and development of the following systems: NASA/ACTS, EUTELSAT IOT, and Hughes' DirecTv™ IOT. She is a member of the IEEE Computer Society.



Steven L. Teller received an AS and AA from Harper College in 1979; and a BA in information and computer sciences from Hood College in 1991. He is currently a Member of the Technical Staff in the Transponders Department of the Satellite and Systems Technologies Division at COMSAT Laboratories. Since joining COMSAT, he has been involved in various aspects of the IOT of communications satellites, including the NASA/ACTS RF terminal supervisor, and IOT for EUTELSAT, MCI, INTELSAT, GTE, and the Hughes DirecTv™ system. He has been responsible for software vs manual measurement verification during system development, in-plant testing, and on-site testing. He was also involved in prototyping and testing various new measurement schemes, and was a major contributor to final system installation testing.

CTR Note

Geostationary communications satellite log for year-end 1992

L. W. KEMP AND D. C. MAY

(Manuscript received August 11, 1993)

The following tables list in-orbit geostationary communications satellites and planned networks for which advance publications had been submitted to the International Telecommunication Union (ITU) Radio Regulations Board (formerly the International Frequency Registration Board [IFRB]) as of year-end 1992. They are intended to provide a summary index of key parameters for existing and proposed satellites, as well as a reference guide to their corresponding ITU filings.

For the purpose of this compilation, geostationary satellites are defined as satellites having an orbit period approximately equivalent to one sidereal day and an apogee and perigee of roughly the same height. Satellites with a north-south inclination greater than 5° have been excluded from consideration. Communications satellites are defined as networks operating in the frequency bands assigned to the fixed, mobile, or broadcasting satellite services.

Table 1 (see p. 141) lists in-orbit satellites in order by their current orbital location, as published in the National Aeronautics and Space Administration (NASA) situation reports and other public sources. In each instance, the most recent available data were used, and in some cases the current orbital location shown in this table is different than the location actually occupied in December 1992. For comparison, the orbital location registered with the ITU is shown in the adjoining column and, where possible, orbit eccentricity and north-south inclination are also provided as a further indication of station-keeping status.

The remaining data in Table 1, including network designation, registering country or organization, frequency bands, and service type, are derived from the relevant special sections of the Radio Regulations Board weekly circulars. For satellites not yet launched, a subset of this information is provided in Table 2 (see p. 170).

Louis W. Kemp is a Systems Planner with the Engineering and Operations Department of COMSAT World Systems.

Douglas C. May is a Senior Advisor with the INTELSAT Policy and Representation Department of COMSAT World Systems.

Sources

1. L. W. Kemp, "Geostationary Satellite Log for Year-End 1989," *COMSAT Technical Review*, Vol. 20, No. 1, Spring 1990, pp. 105-215.
2. "List of Geostationary and Non-Geostationary Space Stations (List A/List B)," International Frequency Registration Board, International Telecommunication Union, Geneva, December 1992.
3. "Quarterly Publication of the Space Network List," Radiocommunication Bureau, International Telecommunication Union, Geneva, June 1993.
4. "Satellite Situation Report," National Aeronautics and Space Administration, Goddard Space Flight Center, Project Operations Branch, Vol. 33, No. 1, March 1993.
5. "Geosynchronous Satellite Report," National Aeronautics and Space Administration, Goddard Space Flight Center, Project Operations Branch, January 1993.
6. "Table of Artificial Satellites Launched in 1992," *Telecommunication Journal*, Vol. 60-VI, International Telecommunication Union, Geneva, 1993.
7. "Table of Artificial Satellites Launched in 1991," *Telecommunication Journal*, Vol. 59-IX, International Telecommunication Union, Geneva, 1992.
8. "Table of Artificial Satellites Launched in 1990," *Telecommunication Journal*, Vol. 58-VI, International Telecommunication Union, Geneva, 1991.

TABLE 1. IN-ORBIT GEOSTATIONARY COMMUNICATIONS SATELLITES FOR YEAR-END 1992

SUBSAT. LONGITUDE CURRENT REGISTERED (°)	ORBIT ECCEN. & INCL. (°)	LAUNCH DATE & INTL. CATALOG NO.	SAT. NAME & ITU DESIGNATION	ITU REGISTERING COUNTRY	FREQUENCY UP/DOWN LINK (GHz)	SERVICE TYPE	ITU SPECIAL SECTION	
							ADVANCED	COORDINATION
0.9 E	359.0 E (1.0 W)	30 Aug 1990 1990-079-A 20776	SKYNET 4C SKYNET-4A	UK	0.290-0.315/ 0.245-0.270 7.975-8.110/ 7.250-7.285 8.145-8.230/ 7.420-7.505 8.255-8.315/ 7.530-7.590 8.340-8.400/ 7.615-7.675 43.500-45.500/ 7.615-7.675	FSS MSS	SPA-AA/313/1466 SPA-AA/336/1478	AR11/C/182/1611
1.0 E	—	04 Aug 1984 1984-081-A 15158	EUTELSAT 1 F2 ECS 2	FRANCE Eutelsat	Not registered at this location			
3.0 E	3.0 E	11 Mar 1988 1988-018-B 18952	TELECOM 1C TELECOM-1C	FRANCE	2.029-2.033/ 2.203-2.208 5.925-6.425/ 3.700-4.200 7.980-8.045/ 7.255-7.460 14.000-14.250/ 12.500-12.750	FSS	AR11/A/29/1539	AR11/C/115/1589 AR11/C/131/1584 AR11/C/157/1598
5.1 E	5.0 E	02 Apr 1989 1989-027-A 19919	TELE-X TELE-X	SWEDEN Swedish Space Corp.	2.027-2.035/ 17.300-17.314 14.085-14.250/ 17.908-17.935 18.062-18.098/ 12.100-12.500	FSS BSS	AR11/A/27/1535	AR11/C/733/1674
6.9 E	7.0 E	09 Jul 1992 1992-041-B 22028	EUTELSAT 2 F4 EUTELSAT 2-7E	FRANCE Eutelsat	2.084-2.091/ 2.264-2.271 1.626-1.660/ 1.530-1.590	FSS MSS	AR11/A/305/1732	AR11/C/1205/1809 AR11/C/1736/1942

TABLE 1. IN-ORBIT GEOSTATIONARY COMMUNICATIONS SATELLITES FOR YEAR-END 1992 (CONT'D)

SUBSAT. CURRENT (°)	LONGITUDE REGISTRD (°)	ORBIT ECCEN. & INCL. (°)	LAUNCH DATE & INT'L CATALOG NO.	SAT. NAME & ITU DESIGNATION	ITU REGISTERING COUNTRY	FREQUENCY UP/DOWN- LINK (GHz)	SERVICE TYPE	ITU SPECIAL SECTION	
								ADVANCED	COORDINATION
7.2 E	7.0 E	0.000356 0.04	16 Sep 1987 1987-078-B 18351	EUTELSAT 1 F4 ECS 4 EUTELSAT 1-3	FRANCE Eutelsat	14.000-14.500/ 10.950-11.200 or 11.450-11.700 or 12.500-12.750	FSS	AR11/A/59/1578	AR11/C/446/1644 AR11/C/1079/1789
8.4 E	—	0.000261 4.38	08 May 1985 1985-035-B 15678	TELECOM 1B	FRANCE	Not registered at this location			
9.9 E	10.0 E	0.000725 0.04	15 Jan 1991 1991-003-B 21056	EUTELSAT 2 F2 EUTELSAT 2-10E	FRANCE Eutelsat	2.084-2.091/ 2.264-2.271 1.626-1.660/ 1.530-1.590 14.000-14.500/ 10.950-11.200 or 11.450-11.700 or 12.500-12.750	FSS MSS	AR11/A/349/1766	AR11/C/1206/1809 AR11/C/1738/1942
12.2 E	12.0 E	0.000451 2.19	20 Oct 1988 1988-095-A 19596	RADUGA 22 STATIONAR-27	USSR	5.725-6.275/ 3.400-3.950	FSS	AR11/A/392/1799	AR11/C/1593/1888
13.0 E	13.0 E	0.001387 0.07	30 Aug 1990 1990-079-B 20777	EUTELSAT 2 F1 EUTELSAT 2-13E	FRANCE Eutelsat	2.084-2.091/ 2.264-2.271 1.626-1.660/ 1.530-1.590 14.000-14.500/ 10.950-11.200 or 11.450-11.700 or 12.500-12.750	FSS MSS	AR11/A/306/1732	AR11/C/1207/1809 AR11/C/1740/1942
13.4 E	13.2 E	0.007234 0.08	15 Jan 1991 1991-003-A 21055	ITALSAT 1 ITALSAT	ITALY	27.500-30.000/ 18.100-20.200	FSS	AR11/A/151/1633	AR11/C/772/1679 AR11/C/827/1697
14.4 E	15.0 E	0.002635 0.93	14 Feb 1991 1991-010-F 21129	COSMOS 2133 STATIONAR-23	USSR	5.725-6.275/ 3.400-3.950	FSS	AR11/A/318/1740	AR11/C/1195/1804
16.1 E	16.0 E	0.002441 0.09	07 Dec 1991 1991-083-1 21803	EUTELSAT 2 F3 EUTELSAT 2-16E	FRANCE Eutelsat	2.084-2.091/ 2.264-2.271 1.626-1.660/ 1.530-1.590 14.000-14.500/ 10.950-11.200 or 11.450-11.700 or 12.500-12.750	FSS MSS	AR11/A/478/1861 AR11/A/479/1861	AR11/C/1677/1922 AR11/C/1742/1942
16.9 E	—	0.003488 2.87	31 Mar 1988 1988-028-A 19017	GORIZONT 15	USSR	Not registered at this location			
19.2 E	19.2 E	0.001165 0.07	11 Dec 1988 1988-109-B 19688	ASTRA 1A GDL-6	LUXEMBOURG Societe Europeene des Satellites	14.250-14.500/ 10.700-10.950 or 11.200-11.450	FSS	AR11/A/94/1594	AR11/C/614/1657 AR11/C/1283/1827
19.3 E	19.2 E	0.000373 0.02	02 Mar 1991 1991-015-A 21139	ASTRA 1B GDL-7	LUXEMBOURG Societe Europeene des Satellites	14.000-14.250/ 10.950-11.200 or 11.450-11.700	FSS	AR11/A/472/1860	AR11/C/1663/1972
19.9 E	—	0.000578 4.92	04 Feb 1983 1983-006-A 13782	CS-2A SAKURA 2A	JAPAN	Not registered at this location			
21.6 E	21.5 E	0.000486 0.03	21 Jul 1988 1988-063-B 19331	EUTELSAT 1 F5 ECS-5 EUTELSAT 1-5	FRANCE Eutelsat	0.149/ 0.137 14.000-14.500/ 10.950-11.700 or 12.500-12.583	FSS	AR11/A/520/1893	AR11/C/1291/2039
23.5 E	23.5 E	0.000152 0.04	12 Oct 1992 1992-066-A 22175	DFS KOPERNICUS 3 DFS-1	GERMANY	2.025-2.110/ 2.200-2.290 14.000-14.500/	FSS	AR11/A/40/1556	AR11/C/695/1670

TABLE I. IN-ORBIT GEOSTATIONARY COMMUNICATIONS SATELLITES FOR YEAR-END 1992 (CONT'D)

SUBSAT. CURRENT	LONGITUDE REGISTRD	ORBIT ECCEN. & INCL. (°)	LAUNCH DATE & INT'L CATALOG NO.	SAT. NAME & ITU DESIGNATION	ITU REGISTERING COUNTRY	FREQUENCY UP/DOWN- LINK (GHz)	SERVICE TYPE	ITU SPECIAL SECTION	
								ADVANCED	COORDINATION
						11.450-11.700 or 12.500-12.750 29.500-30.000/ 19.700-20.200			
25.5 E	—	0.000285 2.95	18 Jun 1983 1983-058-A 14128	EUTELSAT 1 F1 ECS 1	FRANCE Eutelsat	Not registered at this location			
28.6 E	28.5 E	0.000581 0.02	24 Jul 1990 1990-063-B 20706	DFS KOPERNICUS 2 DFS-2	GERMANY	2.025-2.110/ 2.200-2.290 14.000-14.500/ 11.450-11.700 or 12.500-12.750 29.700-30.000/ 19.700-20.200	FSS	AR11/A/41/1556	AR11/C/698/1670
30.8 E	31.0E	0.002312 0.07	26 Feb 1992 1992-010-B 21894	ARABSAT 1C ARABSAT 1-C	SAUDI ARABIA Arabsat	5.909-6.422/ 3.710-4.197 or 2.560-2.634	FSS BSS	AR11/A/345/1764	AR11/C/1366/1854 AR11/C/2124/2025
33.5 E	33.5 E	0.001473 0.02	05 Jun 1989 1989-041-B 20041	DFS KOPERNICUS 1 DFS-5	GERMANY	2.027-2.029/ 2.201-2.203 14.000-14.500 or 13.150-13.250/ 11.350-11.700 or 12.500-12.750 29.500-30.000/ 19.700-20.200	FSS	AR11/A/465/1840	AR11/C/2025/2002
34.4 E	35.0 E	0.000107 4.25	25 Oct 1986 1986-082-A 17046	RADUGA 19 STATIONAR-2	USSR	5.725-6.275/ 3.400-3.950	FSS	SPA-AA/76/1179	SPA-AJ/26/1251
34.6 E	35.0 E	0.000059 0.69	19 Dec 1991 1991-087-A 21821	RADUGA 28 STATIONAR-2	USSR	5.725-6.275/ 3.400-3.950	FSS	SPA-AA/76/1179	SPA-AJ/26/1251
35.2 E	—	0.000941 4.08	23 Jan 1984 1984-005-A 14659	BS-2A YURI 2A	JAPAN	Not registered at this location			
39.8 E	40.0 E	0.000059 0.35	23 Nov 1990 1990-102-A 20953	GORIZONT 22 STATIONAR-24 LOUTCH-7	USSR	5.725-6.275/ 3.400-3.950 14.000-14.500/ 10.950-11.200 or 11.450-11.700	FSS	SPA-AA/1271/1425 AR11/A/270/1707	AR11/C/878/1737 AR11/C/1122/1793
40.7 E	40.0 E	0.003173 2.85	01 Aug 1988 1988-066-D 19347	COSMOS 1961 STATIONAR-24 LOUTCH-7	USSR	5.725-6.275/ 3.400-3.950 14.000.14.500/ 10.950-11.200 or 11.450-11.700	FSS	SPA-AA/1271/1425 AR11/A/270/1707	AR11/C/878/1737 AR11/C/1122/1793
44.3 E	45.0 E	0.000071 1.16	15 Dec 1989 1989-098-A 20367	RADUGA 24 STATIONAR-9 STATIONAR-9A	USSR	5.725-6.275/ 3.400-3.950	FSS	SPA-AA/96/1197 AR11/A/402/1803	SPA-AJ/51/1276 AR11/C/1632/1919 AR11/C/2203/2040
45.0 E	45.0 E	0.002030 1.18	15 Dec 1989 1989-098-D 20370	RADUGA 24 R STATIONAR-9 STATIONAR-9A	USSR	5.725-6.275/ 3.400-3.950	FSS	SPA-AA/96/1197 AR11/A/402/1803	SPA-AJ/51/1276 AR11/C/1632/1919 AR11/C/2203/2040
45.4 E	45.0 E	0.001774 1.84	14 Apr 1989 1989-030-D 19931	RADUGA 23 R STATIONAR-9 STATIONAR-9A	USSR	5.725-6.275/ 3.400-3.950	FSS	SPA-AA/96/1197 AR11/A/402/1803	SPA-AJ/51/1276 AR11/C/1632/1919 AR11/C/2203/2040
47.9 E	49.0 E	0.000296 4.50	10 Jun 1986 1986-044-A 16769	GORIZONT 12 STATIONAR-24	USSR	5.725-6.275/ 3.400-3.950	FSS	AR11/A/411/1806	AR11/C/1753/1948
48.4 E	49.0 E	0.000107 0.24	27 Dec 1990 1990-116-A 21038	RADUGA 1-2 STATIONAR-24	USSR	5.725-6.275/ 3.400-3.950	FSS	AR11/A/411/1806	AR11/C/1753/1948
51.9 E	—	0.000388 4.22	05 Aug 1983 1983-081-A 14248	CS-2 SAKURA 2B	JAPAN	Not registered at this location			
52.7 E	53.0 E	0.000330 2.37	26 Jan 1989 1989-004-A 19765	GORIZONT 17 STATIONAR-5 LOUTCH-2	USSR	5.725-6.225/ 3.400-3.900 14.007-14.439/ 10.939-11.711	FSS	SPA-AA/93/1197 SPA-AA/150/1271	AR11/C/1114/1793 AR11/C/1191/1804

TABLE I. IN-ORBIT GEOSTATIONARY COMMUNICATIONS SATELLITES FOR YEAR-END 1992 (CONT'D)

SUBSAT CURRENT	LONGITUDE REGISTRD (°)	ORBIT ECCEN. & INCL. (°)	LAUNCH DATE & INT'L CATALOG NO.	SAT. NAME & ITU DESIGNATION	ITU REGISTERING COUNTRY	FREQUENCY UP/DOWN- LINK (GHz)	SERVICE TYPE	ITU SPECIAL SECTION	
								ADVANCED	COORDINATION
52.7 E	53.0 E	0.000111 1.08	27 Nov 1992 1992-082-A 22245	GORIZONT 27 STATIONAR-5 LOUTCH-2	USSR Intersputnik	5.725 - 6.225/ 3.400 - 3.900 14.007-14.439/ 10.939-11.711	FSS	SPA-AA/93/1197 SPA-AA/150/1271	AR11/C/1114/1793 AR11/C/1191/1804
53.0 E	53.0 E	0.000427 0.54	11 Dec 1988 1988-109-A 19687	SKYNET 4B SKYNET-4C	UK	0.290-0.315/ 0.245-0.270 7.975-8.110/ 7.250-7.285 8.145-8.230/ 7.420-7.505 8.225-8.315/ 7.530-7.590 8.340-8.400/ 7.615-7.675 43.500-45.500/ 7.615-7.675	MSS FSS	AR11/A/84/1588	AR11/C/867/1737 AR11/C/871/1737
54.0 E	53.0 E	0.000424 3.48	26 Nov 1987 1987-096-A 18575	COSMOS 1897 STATIONAR-5 LOUTCH-2	USSR Intersputnik	5.725-6.225/ 3.400-3.900 14.007-14.439/ 10.939-11.711	FSS	SPA-AA/93/1197 SPA-AA/150/1271	AR11/C/1114/1793 AR11/C/1191/1804
55.2 E	—	0.000842 0.99	18 Jun 1985 1985-048-C 15825	ARABSAT 1B	SAUDI ARABIA	Not registered at this location			
56.9 E	57.0 E	0.005188 2.49	19 Oct 1983 1983-105-A 14421	INTELSAT 5 F7 INTELSAT 5- INDOC3	USA Intelsat	5.925-6.425/ 3.700-4.200 14.000-14.500/ 10.950-11.700	FSS	SPA-AA/262/1423	SPA-AJ/374/1511
58.4 E	—	0.000960 2.80	21 Jul 1988 1988-063-A 19330	INSAT 1C	INDIA	Not registered at this location			
58.7 E	—	0.000580 1.45	26 Aug 1982 1982-082-A 13431	ANIK D1	CANADA	Not registered at this location			
59.7 E	—	0.001378 4.14	18 Nov 1986 1986-090-A 17083	GORIZONT 13	USSR	Not registered at this location			
60.8 E	60.0 E	0.007495 0.04	23 Jun 1990 1990-056-A 20667	INTELSAT 6 F4 INTELSAT 6 60E	USA Intelsat	5.850-6.425/ 3.625-4.200 14.000-14.500/ 10.950-11.700	FSS	AR11/A/71/1584	AR11/C/626/1658 AR11/C/1624/1905
62.9 E	63.0 E	0.000237 0.01	27 Oct 1989 1989-087-A 20315	INTELSAT 6 F2 INTELSAT 6 63E	USA Intelsat	5.850-6.425/ 3.625-4.200 14.000-14.500/ 10.950-11.700	FSS	AR11/A/366/1782	AR11/C/1269/1819
64.4 E	64.5 E	0.000593 1.82	30 Oct 1990 1990-093-A 20918	INMARSAT 2 F1 INMARSAT 2 IOR 1	UK Inmarsat	1.626-1.649/ 1.530-1.548 6.170-6.180/ 3.945-3.955 6.425-6.443/ 3.600-3.623	MSS	AR11/A/178/1644	AR11/C/1840/1968
65.9 E	66.0 E	0.000344 2.79	28 Sep 1982 1982-097-A 13595	INTELSAT 5 F5 INTELSAT 5- INDOC4	USA Intelsat	5.925-6.425/ 3.700-4.200 14.000-14.500/ 10.950-11.700	FSS	SPA-AA/253/1149	SPA-AJ/375/1511
69.2 E	70.0 E	0.002653 2.86	26 Apr 1988 1988-034-D 19076	COSMOS 1940 STATIONAR-20	USSR	5.725-6.275/ 3.400-3.950	FSS	AR11/A/316/1740	AR11/C/1193/1804
69.3 E	70.0 E	0.000142 1.00	15 Feb 1990 1990-016-A 20499	RADUGA 25 STATIONAR-20	USSR	5.725-6.275/ 3.400-3.950	FSS	AR11/A/316/1740	AR11/C/1193/1804
70.2 E	70.0 E	0.000285 1.62	21 Jun 1989 1989-048-A 20083	RADUGA 1-1 STATIONAR-20	USSR	5.725-6.275/ 3.400-3.950	FSS	AR11/A/316/1740	AR11/C/1193/1804
71.7 E	72.0 E	0.000593 2.66	10 Jan 1990 1990-002-B 20410	LEASAT 5 FLSATCOM - INDOC	USA	0.240-0.322/ 0.240-0.322 0.335-0.400/ 0.335-0.400 7.970-8.010/ 7.255-7.265	MSS FSS	AR11/A/475/1860	—

TABLE I. IN-ORBIT GEOSTATIONARY COMMUNICATIONS SATELLITES FOR YEAR-END 1992 (CONT'D)

SUBSAT. CURRENT	LONGITUDE		ORBIT ECCEN. & INCL. (°)	LAUNCH DATE & INT'L CATALOG NO.	SAT. NAME & ITU DESIGNATION	ITU REGISTERING COUNTRY	FREQUENCY UP/DOWN- LINK (GHz)	SERVICE TYPE	ITU SPECIAL SECTION	
	REGISTERD (°)	(°)							ADVANCED	COORDINATION
72.9 E	—		0.001728 2.27	20 Oct 1988 1988-095-F 19777	RADUGA 22 R	USSR	Not registered at this location			
73.1 E	—		0.002533 2.87	26 Apr 1988 1988-034-A 19073	COSMOS 1940	USSR	Not registered at this location			
74.0 E	74.0 E		0.000414 0.06	09 Jul 1992 1992-041-A 22027	INSAT 2A INSAT-2C	INDIA	5.850-6.410/ 3.705-4.185 6.735-6.975/ 4.510-4.750	FSS	AR11/A/262/1702	AR11/C/1083/1789
79.6 E	80.0 E		0.000071 0.63	18 Jul 1990 1990-061-A 20693	COSMOS 2085 STATSIONAR-13 LOUTCH-8	USSR Intersputnik	5.725-6.275/ 3.400-3.950 14.000-14.500/ 10.950-11.200 or 11.450-11.700	FSS	SPA-AA/276/1425 AR11/A/271/1707	SPA-AJ/305/1469 AR11/C/598/1655 AR11/C/1124/1793
79.9 E	80.0 E		0.000285 2.44	01 Aug 1988 1988-066-A 19344	COSMOS 1961 GEIZER POTOK-2	USSR Intersputnik	5.725-6.275/ 3.400-3.950 14.000-14.500/ 10.950-11.200 or 11.450-11.700	FSS	SPA-AA/276/1425 AR11/A/271/1707	SPA-AJ/305/1469 AR11/C/598/1655 AR11/C/1124/1793
80.2 E	80.0 E		0.000107 0.55	23 Oct 1991 1991-074-A 21759	GORIZONT 24 STATSIONAR-13 LOUTCH-8	USSR Intersputnik	5.725-6.275/ 3.400-3.950 14.000-14.500/ 10.950-11.200 or 11.450-11.700	FSS	SPA-AA/276/1425 AR11/A/271/1707	SPA-AJ/305/1469 AR11/C/598/1655 AR11/C/1124/1793
83.1 E	83.0 E		0.000949 0.11	12 Jun 1990 1990-051-A 20643	INSAT 1D INSAT-1D	INDIA	5.850-6.425/ 3.700-4.200	FSS	AR11/A/126/1617	AR11/C/860/1735
85.2 E	85.0 E		0.002146 0.91	02 Apr 1992 1992-017-D 21925	GORIZONT 25 STATSIONAR-3	USSR	5.725-6.225/ 3.400-3.900	FSS	SPA-AA/77/1179	SPA-AJ/27/1251

85.3 E	85.0 E		0.001751 3.38	10 Dec 1987 1987-100-D 18634	RADUGA 21 R/B STATSIONAR-3	USSR	5.725-6.225/ 3.400-3.900	FSS	SPA-AA/77/1179	SPA-AJ/27/1251
85.5 E	85.0 E		0.000107 0.31	20 Dec 1990 1990-112-A 21016	RADUGA 26 STATSIONAR-3	USSR	5.725-6.225/ 3.400-3.900	FSS	SPA-AA/77/1179	SPA-AJ/27/1251
87.6 E	87.5 E		0.000462 0.02	07 Mar 1988 1988-014-A 18922	PRC 22 CHINASAT-1 DFH-3-0C	CHINA	5.925-6.425/ 3.700-4.200	FSS	AR11/A/470/1850	AR11/C/1959/1983
90.1 E	90.0 E		0.000154 0.39	03 Nov 1990 1990-094-A 20923	GORIZONT 21 STATSIONAR-6 LOUTCH-3	USSR	5.725-6.275/ 3.400-3.900 14.000-14.500/ 10.950-11.200 or 11.450-11.700	FSS	SPA-AA/108/1210 SPA-AA/151/1261	SPA-AJ/30/1251 AR11/C/1116/1793 SPA-AJ/86/1318
91.4 E	91.5 E		0.000554 4.61	23 May 1981 1981-050-A 12474	INTELSAT 5 F1 INTELSAT5A 91.5E	USA Intelsat	5.925-6.425/ 3.700-4.200 14.000-14.500/ 10.950-11.700	FSS	AR11/A/84/2038	—
93.4 E	93.5 E		0.000581 2.94	31 Aug 1983 1983-089-B 14318	INSAT 1B INSAT-1C	INDIA	5.850-6.425/ 3.700-4.200	FSS	AR11/A/191/1673	AR11/C/851/1708
96.4 E	96.5 E		0.000237 1.42	28 Sep 1989 1989-081-A 20263	GORIZONT 19 STATSIONAR-14 LOUTCH-9	USSR	5.725-6.275/ 3.400-3.950 14.000-14.500/ 10.950-11.200 or 11.450-11.700	FSS	SPA-AA/272/1425 AR11/A/272/1707	SPA-AJ/306/1469 AR11/C/1181/1802 AR11/C/1050/1779
98.1 E	98.0 E		0.000119 0.03	04 Feb 1990 1990-011-A 20473	PRC 26 CHINASAT-3	CHINA	6.025-6.425/ 3.800-4.200	FSS	AR11/A/257/1703	AR11/C/1039/1778
98.9 E	99.0 E		0.000273 2.86	27 Dec 1987 1987-109-A 18715	EKRAN STATSIONAR-T2	USSR	5.976-6.024/ 0.730-0.778	FSS BSS	SPA2-3-AA/10/1426	SPA2-3-AJ/7/1469
99.0 E	99.0 E		0.000154 2.16	10 Dec 1988 1988-108-A 19683	EKRAN 19 STATSIONAR-T2	USSR	5.976-6.024/ 0.730-0.778	FSS BSS	SPA2-3-AA/10/1426	SPA2-3-AJ/7/1469

TABLE 1. IN-ORBIT GEOSTATIONARY COMMUNICATIONS SATELLITES FOR YEAR-END 1992 (CONT'D)

SUBSAT. CURRENT (°)	LONGITUDE REGISTERD (°)	ORBIT ECCEN. & INCL. (°)	LAUNCH DATE & INT'L CATALOG NO.	SAT. NAME & ITU DESIGNATION	ITU REGISTERING COUNTRY	FREQUENCY UP/DOWN-LINK (GHz)	SERVICE TYPE	ITU SPECIAL SECTION	
								ADVANCED	COORDINATION
99.7 E	99.0 E	0.000522 1.45	30 Oct 1992 1992-074-A 22210	EKRAN 20 STATIONAR-T2	USSR	5.976-6.024/ 0.730-0.778	FSS BSS	SPA2-3-AA/10/1426	SPA2-3-AJ/7/1469
102.6 E	103.0 E	0.000273 3.88	01 Feb 1986 1986-010-A 16526	PRC 18 STW-2	CHINA	6.225-6.425/ 4.000-4.200	FSS	AR11/A/245/1695	AR11/C/1023/1777
102.6 E	103.0 E	0.000273 0.90	02 Apr 1992 1992-017-A 21922	GORIZONT 25 STATIONAR-21 LOUTCH-5	USSR	5.725-6.275/ 3.400-3.950 14.000-14.500/ 10.950-11.200 or 11.450-11.700	FSS	AR11/A/243/1694 AR11/A/244/1694	AR11/C/905/1748 AR11/C/966/1766
105.5 E	105.5 E	0.000012 0.07	07 Apr 1990 1990-030-A 20558	ASIASAT 1 ASIASAT-1	UK Asia Satellite Telecommuni- cations	5.925-6.425/ 3.700-4.200	FSS	AR11/A/493/1877	AR11/C/1614/1899
107.4 E	—	0.000852 0.30	13 Sep 1991 1991-064-B 21703	COSMOS 2155	USSR	Not registered at this location			
108.0 E	108.0 E	0.000012 0.01	13 Apr 1990 1990-034-A 20570	PALAPA B2R PALAPA-B1	INDONESIA	5.850-6.425/ 3.625-4.200	FSS	SPA-AA/197/1319	SPA-AJ/185/1397
108.6 E	—	0.002754 1.65	21 Jun 1989 1989-048-D 20086	RADUGA 1-1R	USSR	Not registered at this location			
109.7 E	—	0.003177 0.56	18 Jul 1990 1990-061-D 20696	COSMOS 2085	USSR	Not registered at this location			
109.8 E	110.0 E	0.000320 0.01	28 Aug 1990 1990-077-A 20771	BS 3A BS-3	JAPAN	14.000-14.500/ 11.702-11.711 or 12.500-12.750	FSS	AR11/A/334/1750	AR11/C/1424/1864
109.9 E	110.0 E	0.000308 0.01	25 Aug 1991 1991-060-A 21668	BS 3B BS-3	JAPAN	2.025-2.110/ 2.200-2.290 14.000-14.500/ 11.702-11.711 or 12.500-12.750 2.025-2.110/ 2.200-2.290	FSS	AR11/A/334/1750	AR11/C/1424/1864
110.6 E	110.5 E	0.000095 0.02	22 Dec 1988 1988-111-A 19710	PRC 25 CHINASAT-2	CHINA	6.025-6.425/ 3.800-4.200	FSS	AR11/A/256/1702	AR11/C/1034/1778
111.9 E	—	0.000189 0.97	16 Jan 1982 1982-004-A 13035	GE SATCOM 4	USA GE American Communications	Not registered at this location			
112.8 E	113.0 E	0.000036 0.02	20 Mar 1987 1987-029-A 17706	PALAPA B2P PALAPA-B2	INDONESIA	5.850-6.425/ 3.625-4.200	FSS	SPA-AA/198/1319	SPA-AJ/187/1397
117.2 E	—	0.001258 1.69	08 Feb 1985 1985-015-A 15560	ARABSAT 1A	SAUDI ARABIA	Not registered at this location			
117.4 E	—	0.000391 3.14	29 Aug 1985 1985-076-D 15995	LEASAT 4 SYNCOM 4-4	USA	Not registered at this location			
117.7 E	118.0 E	0.000047 0.06	14 May 1992 1992-027-A 21964	PALAPA B4 PALAPA-B3	INDONESIA	5.927-6.423/ 3.702-4.198	FSS	AR11/A/157/1637	AR11/C/654/1666
118.9 E	—	0.001614 2.08	10 Dec 1988 1988-108-D 19686	EKRAN 19R/B	USSR	Not registered at this location			
125.1 E	—	0.001473 0.61	20 Jun 1990 1990-054-D 20662	GORIZONT 20	USSR	Not registered at this location			
126.2 E	—	0.001909 2.01	12 Feb 1986 1986-016-A 16597	BS 2B	JAPAN	Not registered at this location			

TABLE 1. IN-ORBIT GEOSTATIONARY COMMUNICATIONS SATELLITES FOR YEAR-END 1992 (CONT'D)

SUBSAT. CURRENT	LONGITUDE REGISTERED	ORBIT ECCEN. & INCL. (°)	LAUNCH DATE & INT'L CATALOG NO.	SAT. NAME & ITU DESIGNATION	ITU REGISTERING COUNTRY	FREQUENCY UP/DOWN- LINK (GHz)	SERVICE TYPE	ITU SPECIAL SECTION		
								ADVANCED	COORDINATION	
127.1 E	128.0 E	0.003185 1.08	27 Dec 1989 1989-101-G 21648	COSMOS 2054 STATIONAR-15	USSR	5.725-6.275/ 3.400-3.950	FSS	SPA-AA/273/1425	SPA-AJ/307/1469	
127.2 E	128.0 E	0.001138 4.06	18 Nov 1986 1986-090-D 17125	GORIZONT 13 STATIONAR-15	USSR	5.725-6.275/ 3.400-3.950	FSS	SPA-AA/273/1425	SPA-AJ/307/1469	
128.3 E	128.0 E	0.000130 0.42	28 Feb 1991 1991-014-A 21132	RADUGA 27 STATIONAR-15	USSR	5.725-6.275/ 3.400-3.950	FSS	SPA-AA/273/1425	SPA-AJ/307/1469	
130.8 E	—	0.000166 4.47	10 Aug 1979 1979-072-A 11484	WESTAR 3	USA	Not registered at this location				
132.0 E	132.0 E	0.000071 0.01	19 Feb 1988 1988-012-A 18877	CS 3A SAKURA 3A CS-3A	JAPAN	2.096-2.097/ 2.276-2.277 5.955-6.395/ 3.730-4.170 27.525-29.045/ 17.725-19.245	FSS	AR11/A/212/1680	AR11/C/1128/1794	
134.1 E	134.0 E	0.000107 2.33	19 Jun 1983 1983-059-C 14134	PALAPA B1 PALAPA PACIFIC-1	INDONESIA	5.925-6.425/ 3.700-4.200	FSS	AR11/A/811/2025	—	
136.0 E	136.0 E	0.000083 0.04	16 Sep 1988 1988-086-A 19508	CS 3B SAKURA 3B CS-3B	JAPAN	2.096-2.097/ 2.276-2.277 5.955-6.395/ 3.730-4.170 27.525-29.045/ 17.725-19.245	FSS	AR11/A/212/1680	AR11/C/1128/1794	
139.9 E	140.0 E	0.000130 1.53	05 Jul 1989 1989-052-A 20107	GORIZONT 18 STATIONAR-7 LOUTCH-4	USSR	5.735-6.268/ 3.412-3.943 14.007-14.493/ 10.957-11.683	FSS	SPA-AA/94/1197 SPA-AA/152/1261	AR11/C/1118/1793 SPA-AJ/87/1318 SPA-AJ/31/1251	
141.3 E	140.0 E	0.000130 0.21	22 Nov 1991 1991-079-D 21792	COSMOS 2172 STATIONAR-7 LOUTCH-4	USSR	5.735-6.268/ 3.412-3.943 14.007-14.493/ 10.957-11.683	FSS	SPA-AA/94-1197 SPA-AA/152/1261	AR11/C/1118/1793 SPA-AJ/87/1318 SPA-AJ/31/1251	
145.8 E	—	0.002445 3.66	06 May 1988 1988-036-E 19094	EKRAN 18 R/B	USSR	Not registered at this location				
146.3 E	—	0.003443 1.94	04 Aug 1984 1984-081-B 15159	TELECOM 1A	FRANCE	Not registered at this location				
150.0 E	150.0 E	0.000119 0.07	06 Mar 1989 1989-020-A 19874	JCSAT 1 JCSAT-1	JAPAN Japan Satellite Communications	14.000-14.500/ 12.250-12.750	FSS	AR11/A/253/1700	AR11/C/946/1763	
150.4 E	150.0 E	0.000427 1.28	27 Aug 1987 1987-070-A 18316	ETS 5 ETS-5	JAPAN	1.642-1.650/ 1.540-1.548 2.100/ 2.280-2.281 5.948-6.396/ 5.104-5.241	MSS	AR11/A/217/1685	AR11/C/920/1754 AR11/C/923/1754	
151.3 E	—	0.006308 2.77	27 Dec 1987 1987-109-D 18718	EKRAN R/B	USSR	Not registered at this location				
154.0 E	154.0 E	0.000142 0.01	01 Jan 1990 1990-001-B 20402	JCSAT 2 JCSAT-2	JAPAN Japan Satellite Communications	14.000-14.500/ 12.250-12.750	FSS	AR11/A/254/1700	AR11/C/953/1763	
155.6 E	—	0.001565 0.69	19 Dec 1991 1991-087-D 21824	RADUGA 28R	USSR	Not registered at this location				
156.0 E	156.0 E	0.000166 0.06	28 Nov 1985 1985-109-C 16275	AUSSAT 2 AUSSAT-A 156E AUSSAT-A 156 PAC	AUSTRALIA Optus Communications	14.195-14.240/ 12.450-12.500 14.320-14.360/ 12.575-12.620 14.450-14.500/ 12.700-12.750	FSS	SPA-AA/300/1456 AR11/A/607/1922	AR11/C/305/1624 AR11/C/2018/2000	

TABLE 1. IN-ORBIT GEOSTATIONARY COMMUNICATIONS SATELLITES FOR YEAR-END 1992 (CONT'D)

SUBSAT. CURRENT	LONGITUDE REGISTRD	ORBIT ECCEN. & INCL. (°)	LAUNCH DATE & INT'L CATALOG NO.	SAT. NAME & ITU DESIGNATION	ITU REGISTERING COUNTRY	FREQUENCY UP/DOWN- LINK (GHz)	SERVICE TYPE	ITU SPECIAL SECTION	
								ADVANCED	COORDINATION
160.0 E	160.0 E	0.000119 0.01	27 Aug 1985 1985-076-B 15993	AUSSAT 1 AUSSAT-A 160E AUSSAT-A 160 PAC	AUSTRALIA Optus Communications	14.195-14.240/ 12.450-12.500 14.320-14.360/ 12.575-12.620 14.450-14.500/ 12.700-12.750	FSS	SPA-AA/299/1456 AR11/A/606/1922	AR11/C/296/1624 AR11/C/2019/2000
160.2 E	160.0 E	0.000356 0.11	13 Aug 1992 1992-054-A 22087	OPTUS B1 AUSSAT B1 AUSSAT B1-MOB AUSSAT B1-N2 AUSSAT-B 160E MXL	AUSTRALIA Optus Communications	14.000-14.500/ 12.200-12.750 1.646-1.660/ 1.545-1.559	FSS MSS	AR11/A/355/1772 AR11/A/379/1796 AR11/A/360/1779 AR11/A/785/2009	AR11/C/2041/2005 AR11/C/654/1666 AR11/C/1807/1963 AR11/C/2209/2040
161.9 E	162.0 E	0.000391 0.04	26 Feb 1992 1992-010-A 21893	SUPERBIRD B1 SUPERBIRD-B	JAPAN Space Communications Corp.	7.925-8.025/ 7.295-7.375 14.002-14.398/ 12.352-12.748 27.575-29.115/ 17.775-19.315	FSS MSS	AR11/A/341/1762	AR11/C/1307/1836
161.9 E	—	0.001507 0.70	09 Jun 1982 1982-058-A 13269	WESTAR 5	USA	Not registered at this location			
164.0 E	164.0 E	0.000083 0.02	16 Sep 1987 1987-078-A 18350	AUSSAT K3 AUSSAT-A 164E AUSSAT-A 164E PAC	AUSTRALIA Optus Communications	14.000-14.500/ 12.250-12.750	FSS	SPA-AA/301/1456 AR11/A/215/1684	AR11/C/314/1624 AR11/C/1008/1773
173.0 E	—	0.003788 4.97	04 Apr 1986 1986-027-F 16676	COSMOS 1738	USSR	Not registered at this location			
174.0 E	174.0 E	0.000344 0.40	22 Mar 1985 1985-025-A 15629	INTELSAT 5A-10 INTELSAT5A PAC1	USA Intelsat	5.925-6.425/ 3.700-4.200 14.000-14.500/ 10.950-11.700	FSS	AR11/A/65/1580	AR11/C/660/1668 AR11/C/1642/1917
177.0 E	177.0 E	0.000356 0.04	30 Jun 1985 1985-055-A 15873	INTELSAT 5A-11 INTELSAT5A PAC2	USA Intelsat	5.925-6.425/ 3.700-4.200 14.000-14.500/ 10.950-11.700	FSS	AR11/A/66/1580	AR11/C/678/1668 AR11/C/1643/1917
178.3 E	178.0 E	0.000368 2.06	16 Dec 1991 1991-084-B 21814	INMARSAT 2 F3 INMARSAT POR-2	UK Inmarsat	1.626-1.649/ 1.530-1.548 6.170-6.180/ 3.945-3.955 6.425-6.443/ 3.600-3.623	MSS	AR11/A/545/1904	AR11/C/1764/1953
180.0 E (180.0 W)	180.0 E (180.0 W)	0.000320 1.46	05 Mar 1984 1984-023-A 14786	INTELSAT 5A-8 INTELSAT5 PAC3 INTELSAT MCS PAC A	USA Intelsat	1.626-1.649/ 1.530-1.548 5.925-6.425/ 3.700-4.200 14.000-14.500/ 10.950-11.700	MSS FSS	SPA-AA/255/1419 SPA-AA/332/1476	AR11/C/682/1668 AR11/C/692/1669 AR11/C/859/1735
182.2 E (177.8)	183.0 E (177.0 W)	0.000012 3.99	31 Aug 1984 1984-093-C 15236	LEASAT 2 SYNCOM 4-2 FLTSATCOM-A W PAC	USA	0.240-0.322/ 0.240-0.322 0.335-0.400/ 0.335-0.400 7.979-8.010/ 7.255-7.265	MSS FSS	AR11/A/335/1762	AR11/C/1862/1968 AR11/C/1869/1968
182.4 E (177.6 W)	—	0.001890 0.37	23 Nov 1990 1990-102-D 21046	GORIZONT 22	USSR	Not registered at this location			
183.0 E (177.0 W)	183.0 E (177.0 W)	0.000344 3.35	15 Dec 1981 1981-119-A 12994	INTELSAT 5 F3 INTELSAT5 183E	USA Intelsat	5.925-6.425/ 3.700-4.200 14.000-14.500/ 10.950-11.700	FSS	SPA-AA/254/1419	AR11/C/1813/1964
183.9 E (176.1 W)	—	0.002877 0.21	20 Dec 1990 1990-112-D 21019	RADUGA 26R	USSR	Not registered at this location			
185.6 E (174.4 W)	186.0 E (174.0 W)	0.007206 0.03	02 Aug 1991 1991-054-B 21639	TDRS F5 R/B TDRS 174W USASAT-14E	USA Columbia Communications	2.034-2.037/ 2.208-2.213 14.287-15.537/ 13.075-14.375 5.925-6.425/ 3.700-4.200	FSS	AR11/A/502/1883 AR11/A/421/1815	AR11/C/1710/1936

TABLE I. IN-ORBIT GEOSTATIONARY COMMUNICATIONS SATELLITES FOR YEAR-END 1992 (CONT'D)

SUBSAT. CURRENT	LONGITUDE REGISTERED (°)	ORBIT ECCEN. & INCL. (°)	LAUNCH DATE & INT'L CATALOG NO.	SAT. NAME & ITU DESIGNATION	ITU REGISTERING COUNTRY	FREQUENCY UP/DOWN- LINK (GHz)	SERVICE TYPE	ITU SPECIAL SECTION	
								ADVANCED	COORDINATION
189.5 E (170.5 W)	190.0 E (170.0 W)	0.00261 3.18	10 Dec 1987 1987-100-A 18631	RADUGA 21 STATSIONAR-10 STATSIONAR-10A	USSR	5.725-6.025/ 3.400-3.700	FSS	SPA-AA/97/1197	SPA-AJ/52/1276
192.2 E (167.8 W)	—	0.001241 2.33	N/A 1992-074-D 22213	EKRAN 20R	USSR	Not registered at this location			
192.6 E (167.4 W)	—	0.001125 1.09	N/A 1992-082-D 22248	GORIZONT 27R	USSR	Not registered at this location			
197.4 E (162.6 W)	—	0.002724 0.44	28 Feb 1991 1991-014-D 21135	RADUGA 27R	USSR	Not registered at this location			
198.1 E (161.9 W)	—	0.002174 4.24	04 Sep 1987 1987-073-D 18331	EKRAN 16 R/B	USSR	Not registered at this location			
205.2 E (154.8 W)	205.0 E (155.0 W)	0.001984 2.39	18 Aug 1988 1988-071-D 19400	GORIZONT 16 STATSIONAR-26	USSR	5.725-6.275/ 3.400-3.950	FSS	AR11/A/385/1797	AR11/C/1313/1836
207.3 E (152.7 W)	205.0 E (155.0 W)	0.000401 3.73	28 Oct 1987 1987-091-A 18443	COSMOS 1894 STATSIONAR-26	USSR	5.725-6.275/ 3.400-3.950	FSS	AR11/A/385/1797	AR11/C/1313/1836
220.9 E (139.1 W)	221.0 E (139.0 W)	0.000059 0.03	29 May 1991 1991-037-A 21392	AURORA 2 SATCOM-C5 USASAT-221	USA Alascom	5.925-6.425/ 3.700-4.200	FSS	AR11/A/844/2041	
221.7 E (138.3 W)	—	0.002937 4.31	19 Mar 1987 1987-028-A 17611	RADUGA 20	USSR	Not registered at this location			

222.9 E (137.1 W)	223.0 E (137.0 W)	0.000296 0.02	20 Nov 1990 1990-100-A 20945	SATCOM C1 USASAT-22G	USA GE American Communications	5.925-6.425/ 3.700-4.200	FSS	AR11/A/690/1971	AR11/C/2007/1993
224.9 E (135.1 W)	225.0 E (135.0 W)	0.000071 0.07	31 Aug 1992 1992-057-A 22096	SATCOM C4 USASAT-21A	USA GE American Communications	5.925-6.425/ 3.700-4.200	FSS	AR11/A/483/1864	AR11/C/2005/1993
227.1 E (132.9 W)	227.0 E (133.0 W)	0.000130 0.03	28 Jun 1983 1983-065-A 14158	GALAXY 1 USASAT-11D	USA Hughes Communications	5.925-6.425/ 3.700-4.200	FSS	AR11/A/120/1615	AR11/C/821/1696
227.1 E (132.9 W)	—	0.001065 1.14	27 Dec 1989 1989-101-D 20394	COSMOS 2054	USSR	Not registered at this location			
229.1 E (130.9 W)	229.0 E (131.0 W)	0.000273 0.07	11 Apr 1983 1983-030-A 13984	GE SATCOM 6 US SATCOM 3-R	USA GE American Communications	5.925-6.425/ 3.700-4.200	FSS	SPA-AA/329/1476	AR11/C/347/1625
229.3 E (130.7 W)	229.0 E (131.0 W)	0.000373 0.09	10 Sep 1992 1992-060-B 22117	SATCOM C3 USASAT 22H	USA GE American Communications	5.925-6.425/ 3.700-4.200	FSS	AR11/A/1600/1920	AR11/C/2009/1993
229.9 E (130.1 W)	230.0 E (130.0 W)	0.000178 2.45	30 Oct 1982 1982-106-B 13637	DSCS 3 F1 USGCSS PH2E	USA	7.900-8.400/ 7.250-7.750	FSS MSS	AR11/A/404/1805	—
230.5 E (129.5 W)	—	0.000451 4.46	04 Sep 1987 1987-073-A 18328	EKRAN 16	USSR	Not registered at this location			
232.0 E (128.0 W)	232.0 E (128.0 W)	0.000178 0.01	27 Aug 1985 1985-076-C 15994	ASC 1 ASC-1	USA GTE Spacenet	5.925-6.425/ 3.700-4.200 14.000-14.500/ 11.700-12.200	FSS	AR11/A/202/1676	AR11/C/1066/1784
234.5 E (125.5 W)	—	0.001212 3.57	21 Nov 1987 1987-095-A 18570	TV SAT 1	GERMANY	Not registered at this location			
235.0 E (125.0 W)	235.0 E (125.0 W)	0.000059 0.04	28 Mar 1986 1986-026-A 16649	GSTAR 2 USASAT-23E	USA GTE Spacenet	14.000-14.500/ 11.700-12.200	FSS	AR11/A/576/1912	AR11/C/1772/1953

TABLE I. IN-ORBIT GEOSTATIONARY COMMUNICATIONS SATELLITES FOR YEAR-END 1992 (CONT'D)

SUBSAT. CURRENT (°)	LONGITUDE REGISTRD (°)	ORBIT ECCEN. & INCL. (°)	LAUNCH DATE & INT'L CATALOG NO.	SAT. NAME & ITU DESIGNATION	ITU REGISTERING COUNTRY	FREQUENCY UP/DOWN- LINK (GHz)	SERVICE TYPE	ITU SPECIAL SECTION	
								ADVANCED	COORDINATION
235.1 E (124.9 W)	235.0 E (125.0 W)	0.000036 0.09	14 Mar 1992 1992-013-A 21906	GALAXY 5 USASAT-22B	USA Hughes Communications	5.925-6.425/ 3.700-4.200	FSS	AR11/A/537/1903	AR11/C/1780/1954
237.1 E (122.9 W)	234.0 E (126.0 W)	0.000071 0.04	19 Jun 1985 1985-048-D 15826	TELSTAR 303 TELSTAR 3D USASAT-20A	USA AT&T	5.925-6.425/ 3.700-4.200	FSS	AR11/A/304/1730	AR11/C/968/1769
237.1 E (122.9 W)	238.0 E (122.0 W)	0.000119 0.02	08 Sep 1988 1988-081-B 19484	SBS 5 USASAT-10A	USA Hughes Communications	14.000-14.500/ 11.700-12.200	FSS	AR11/A/105/1609	AR11/C/883/1741
240.0 E (120.0 W)	240.0 E (120.0 W)	0.000012 0.03	23 May 1984 1984-049-A 14985	SPACENET 1 SPACENET-1	USA GTE Spacenet	5.925-6.425/ 3.700-4.200 14.000-14.500/ 11.700-12.200	FSS	AR11/A/10/1525	AR11/C/833/1699
241.2 E (118.8 W)	—	0.001394 0.35	02 Jul 1991 1991-046-D 21536	GORIZONT 23	USSR	Not registered at this location			
243.3 E (116.7 W)	243.2 E (116.8 W)	0.000130 0.02	27 Nov 1985 1985-109-B 16274	MORELOS B MORELOS 2 ILHUICAHUA-2	MEXICO	5.925-6.425/ 3.700-4.200 14.000-14.500/ 11.700-12.200	FSS	AR11/A/30/1540	AR11/C/387/1628
245.1 E (114.9 W)	245.1 E (114.9 W)	0.000166 1.21	12 Nov 1982 1982-110-C 13652	ANIK C3 TELESAT C-3 ANIK C-1	CANADA Telesat Canada	14.000-14.500/ 11.700-12.200	FSS	SPA-AA/357/1500	AR11/C/569/1649 AR11/C/1617/1904
246.4 E (113.6 W)	246.5 E (113.5)	0.000154 0.01	07 Jun 1985 1985-048-B 15824	MORELOS A MORELOS 1 ILHUICAHUA-1	MEXICO	5.925-6.425/ 3.700-4.200 14.000-14.500/ 11.700-12.200	FSS	AR11/A/28/1539	AR11/C/386/1628
248.9 E (111.1 W)	248.9 E (111.1 W)	0.000273 0.07	26 Sep 1991 1991-067-A 21726	ANIK E1 TELESAT E-B ANIK E-A	CANADA Telesat Canada	5.922-6.425/ 3.698-4.200 14.000-14.500/ 11.700-12.200	FSS	AR11/A/323/1744	AR11/C/1293/1832
249.0 E (111.0 W)	—	0.003620 1.49	02 Aug 1991 1991-054-D 21641	TDRS F5 R/B	USA	Not registered at this location			
250.8 E (109.2 W)	250.0 E (110.0 W)	0.000130 1.14	18 Jun 1983 1983-059-B 14133	ANIK C2 TELESAT C-1 ANIK C-2	CANADA Telesat Canada	14.000-14.500/ 11.700-12.200	FSS	SPA-AA/137/1252	AR11/C/829/1698
250.8 E (109.2 W)	250.0 E (110.0 W)	0.000225 0.02	13 Apr 1985 1985-028-B 15642	ANIK C1 TELESAT C-1 ANIK C-2	CANADA Telesat Canada	14.000-14.500/ 11.700-12.200	FSS	SPA-AA/137/1252	AR11/C/829/1698
252.7 E (107.3 W)	252.7 E (107.3 W)	0.000202 0.04	04 Apr 1991 1991-026-A 21222	ANIK E2 TELESAT E-A ANIK E-A	CANADA Telesat Canada	5.922-6.425/ 3.698-4.200 14.000-14.500/ 11.700-12.200	FSS	AR11/A/322/1744	AR11/C/1291/1832
254.6 E (105.4 W)	—	0.000308 1.56	28 Oct 1982 1982-105-A 13631	GE SATCOM 5	USA	Not registered at this location			
254.7 E (105.3 W)	255.0 E (105.0 W)	0.000083 3.26	13 Apr 1985 1985-028-C 15643	LEASAT 3 SYNCOM 4-3 FLTSATCOM-A EAST PAC	USA	0.240-0.322/ 0.240-0.322 0.355-0.400/ 0.355-0.400 7.979-8.010/ 7.255-7.265	MSS FSS	AR11/A/93/1605	AR11/C/1855/1968
254.9 E (105.1 W)	255.0 E (105.0 W)	0.000083 0.02	20 Nov 1990 1990-100-B 20946	GSTAR 4 GSTAR-2	USA GTE Spacenet	14.000-14.500/ 11.700-12.200	FSS	AR11/A/14/1525	AR11/C/1075/1789
255.2 E (104.8 W)	—	0.003063 4.39	25 Oct 1986 1986-082-F 17065	RADUGA 19 R/B	USSR	Not registered at this location			
256.1 E (103.9 W)	—	0.001519 4.84	04 Apr 1986 1986-027-A 16667	COSMOS 1738	USSR	Not registered at this location			
256.7 E (103.3 W)	—	0.001095 4.63	10 Jun 1986 1986-044-F 16797	GORIZONT 12	USSR	Not registered at this location			

TABLE I. IN-ORBIT GEOSTATIONARY COMMUNICATIONS SATELLITES FOR YEAR-END 1992 (CONT'D)

SUBSAT. CURRENT (°)	LONGITUDE REGISTERED (°)	ORBIT ECCEN. & INCL. (°)	LAUNCH DATE & INT'L CATALOG NO.	SAT. NAME & ITU DESIGNATION	ITU REGISTERING COUNTRY	FREQUENCY UP/DOWN- LINK (GHz)	SERVICE TYPE	ITU SPECIAL SECTION	
								ADVANCED	COORDINATION
257.0 E (103.0 W)	257.0 E (103.0 W)	0.000119 0.05	08 May 1985 1985-035-A 15677	GSTAR 1 GSTAR-1	USA GTE Spacenet	14.000-14.500/ 11.700-12.200	FSS	AR11/A/15/1525	AR11/C/1073/1784
259.0 E (101.0 W)	259.0 E (101.0 W)	0.000225 0.01	13 Apr 1991 1991-028-A 21227	SPACENET 4 (formerly ASC-2) USASAT-7D	USA GTE Spacenet	5.925-6.425/ 3.700-4.200 14.000-14.500/ 11.700-12.200	FSS	AR11/A/12/1525	AR11/C/1842/1968
259.1 E (100.9 W)	—	0.001747 3.08	26 Nov 1987 1987-096-D 18578	COSMOS 1897	USSR	Not registered at this location			
259.1 E (100.9 W)	—	0.000095 1.69	20 Nov 1981 1981-114-A 12967	GE SATCOM 3R	USA	Not registered at this location			
260.6 E (99.4 W)	260.0 E (100.0 W)	0.001447 0.42	05 Dec 1986 1986-096-A 17181	USA 20 FLTSATCOM EPAC FLTSATCOM -B EAST PAC	USA	43.500-45.500/ 20.200-21.200 0.240-0.329/ 0.240-0.329 0.335-0.400/ 0.335-0.400 7.975-8.025/ 7.255-7.265	MSS	AR11/A/50/1561 SPA-AA/85/1186	—
260.9 E (99.1 W)	261.0 E (99.0 W)	0.000154 0.06	12 Oct 1990 1990-091-A 20872	SBS 6 USASAT-6B	USA Hughes Communications	14.000-14.500/ 11.700-12.200	FSS	SPA-AA/124/1235	SPA-AJ/61/1280
261.0 E (99.0 W)	261.0 E (99.0 W)	0.000213 0.05	12 Oct 1990 1990-091-B 20873	GALAXY 6 WESTAR 6-S	USA Hughes Communications	5.925-6.425/ 3.700-4.200	FSS	AR11/A/299/1722	AR11/C/962/1765
261.8 E (98.2 W)	—	0.003726 0.36	03 Nov 1990 1990-094-D 20926	GORIZONT 21	USSR	Not registered at this location			
263.0 E (97.0 W)	263.0 E (97.0 W)	0.000213 4.36	24 Sep 1981 1981-096-A 12855	SBS 2 USASAT-6A	USA Comsat	14.000-14.500/ 11.700-12.200	FSS	AR11/A/34/1553	AR11/C/325/1624
264.0 E (96.0 W)	263.0 E (97.0 W)	0.000166 0.03	28 Jul 1983 1983-077-A 14234	TELSTAR 301 TELSTAR-3A	USA AT&T	5.925-6.425/ 3.700-4.200	FSS	AR11/A/8/1524	AR11/C/879/1738
264.9 E (95.1 W)	265.0 E (95.0 W)	0.000213 1.16	11 Nov 1982 1982-110-B 13651	SBS 3 USASAT-6C	USA Comsat	14.000-14.500/ 11.700-12.200	FSS	AR11/A/35/1553	AR11/C/331/1624
266.5 E (93.5 W)	266.5 E (93.5 W)	0.000166 0.03	21 Sep 1984 1984-101-A 15308	GALAXY 3 USASAT-12B	USA Hughes Communications	5.925-6.425/ 3.700-4.200	FSS	AR11/A/122/1615	AR11/C/824/1697
266.9 E (93.1 W)	267.0 E (93.0 W)	0.000273 4.56	08 Sep 1988 1988-081-A 19483	GSTAR 3 USASAT-16A	USA GTE Spacenet	14.000-14.500/ 11.700-12.200	FSS	AR11/A/222/1687	AR11/C/998/1772
268.9 E (91.1 W)	269.0 E (91.0 W)	0.000130 0.02	31 Aug 1984 1984-093-B 15235	SBS 4 USASAT-9A	USA Hughes Communications	14.000-14.500/ 11.700-12.200	FSS	AR11/A/101/1609	AR11/C/818/1696
268.9 E (91.1 W)	269.0 E (91.0 W)	0.000242 0.08	28 Oct 1992 1992-072-A 22205	GALAXY 7H USASAT-9A WESTAR-3	USA Hughes Communications	14.000-14.500/ 11.700-12.200 5.927-6.403/ 3.702-4.178	FSS	AR11/A/101/1609 SPA-AA/37/1152	AR11/C/818/1696 SPA-AJ/197/1406
273.0 E (87.0 W)	273.0 E (86.0 W)	0.000107 0.02	11 Mar 1988 1988-018-A 18951	SPACENET 3R SPACENET-3	USA GTE Spacenet	5.925-6.425/ 3.700-4.200 14.000-14.500/ 11.700-12.200	FSS	AR11/A/13/1525	AR11/C/834/1699
275.0 E (85.0 W)	275.0 E (85.0 W)	0.000166 0.02	12 Jan 1986 1986-003-B 16482	GE SATCOM KU-1 USASAT-9C	USA GE American Communications	14.000-14.500/ 11.700-12.200	FSS	AR11/A/103/1609	AR11/C/1052/1780
275.1 E (84.9 W)	274.0 E (86.0 W)	0.000273 0.01	01 Sep 1984 1984-093-D 15237	TELSTAR 302 TELSTAR 3C USASAT-3C	USA AT&T	5.925-6.425/ 3.700-4.200	FSS	AR11/A/9/1524	AR11/C/1084/1790
275.4 E (84.6 W)	—	0.003883 0.98	15 Feb 1990 1990-016-D 20502	RADUGA 25 R	USSR	Not registered at this location			

TABLE I. IN-ORBIT GEOSTATIONARY COMMUNICATIONS SATELLITES FOR YEAR-END 1992 (CONT'D)

SUBSAT. CURRENT (°)	LONGITUDE REGISTRD (°)	ORBIT ECCEN. & INCL. (°)	LAUNCH DATE & INTL. CATALOG NO.	SAT. NAME & ITU DESIGNATION	ITU REGISTERING COUNTRY	FREQUENCY UP/DOWN LINK (GHz)	SERVICE TYPE	ITU SPECIAL SECTION	
								ADVANCED	COORDINATION
278.0 E (82.0 W)	—	0.000154 0.07	09 Nov 1984 1984-113-B 15383	ANIK D2	CANADA	Not registered at this location			
279.0 E (81.0 W)	279.0 E (81.0 W)	0.000178 0.01	28 Nov 1985 1985-109-D 16276	GE SATCOM KU-2 USASAT-9D	USA GE American Communications	14.000-14.500/ 11.700-12.200	FSS	AR11/A/104/1609	AR11/C/1053/1780
279.4 E (80.6 W)	—	0.000130 1.06	26 Feb 1982 1982-014-A 13069	WESTAR 4	USA	Not registered at this location			
285.9 E (74.1 W)	286.0 E (74.0 W)	0.000142 0.01	22 Sep 1983 1983-098-A 14365	GALAXY 2 USASAT-7A	USA Hughes Communications	5.925-6.425/ 3.400-4.200	FSS	SPA-AA/312/1465	AR11/C/812/1689
287.9 E (72.1 W)	288.0 E (72.0 W)	0.000285 0.02	08 Sep 1983 1983-094-A 14328	GE SATCOM 2R USASAT-8B	USA GE American Communications	5.925-6.425/ 3.700-4.200	FSS	AR11/A/37/1553	AR11/C/221/1617
290.0 E (70.0 W)	290.0 E (70.0 W)	0.000178 0.07	28 Mar 1986 1986-026-B 16650	BRASILSAT 2 SBTS A1	BRAZIL	5.925-6.425/ 3.700-4.200	FSS	AR11/A/16/1526	AR11/C/94/1576
290.7 E (69.3 W)	—	0.012118 2.96	31 Mar 1988 1988-028-D 19020	GORIZONT 15	USSR	Not registered at this location			
291.0 E (69.0 W)	291.0 E (69.0 W)	0.000320 0.01	10 Nov 1984 1984-114-A 15385	SPACENET 2 USASAT-7C	USA GTE Spacenet	5.925-6.425/ 3.700-4.200 14.000-14.500/ 11.700-12.200	FSS	AR11/A/11/1525	AR11/C/835/1699
294.7 E (65.3 W)	—	0.001315 1.19	10 Sep 1992 1992-059-D 22115	COSMOS 2209	USSR	Not registered at this location			
295.0 E (65.0 W)	295.0 E (65.0 W)	0.000320 0.05	08 Feb 1985 1985-015-B 15561	BRASILSAT 1 SBTS A2	BRAZIL	5.925-6.425/ 3.700-4.200	FSS	AR11/A/17/1526	AR11/C/99/1576
297.5 E (62.5 W)	—	0.000055 0.27	13 Sep 1991 1991-064-A 21702	COSMOS 2155	USSR	Not registered at this location			
305.7 E (54.3 W)	306.0 E (54.0 W)	0.000769 2.26	15 Apr 1992 1992-021-B 21940	INMARSAT 2 F4 INMARSAT 2 AOR- WEST-2	UK Inmarsat	1.626-1.649/ 1.530-1.548 6.170-6.180/ 3.945-3.955 6.425-6.443/ 3.600-3.623	MSS	AR11/A/775/2006	—
306.8 E (53.2 W)	—	0.001351 3.79	06 May 1988 1988-036-A 19090	EKRAN 18	USSR	Not registered at this location			
307.0 E (53.0 W)	307.0 E (53.0 W)	0.000142 0.04	17 May 1988 1988-040-A 19121	INTELSAT 5A F13 INTELSAT5A CONT1	USA Intelsat	5.925-6.425/ 3.700-4.200 14.000-14.500/ 10.950-11.700 or 11.700-11.950 or 12.500-12.750	FSS	AR11/A/115/1609 AR11/A/128/1617	AR11/C/674/1667 AR11/C/1640/1917 AR11/C/704/1673
310.1 E (49.9 W)	310.0 E (50.0 W)	0.000296 1.78	19 May 1983 1983-047-A 14077	INTELSAT 5 F6 INTELSAT5 CONT2 INTELSAT MCS ATL A	USA Intelsat	1.626-1.649/ 1.530-1.548 5.925-6.425/ 3.700-4.200 14.000-14.500/ 10.950-11.700	MSS FSS	AR11/A/75/1586 SPA-AA/212/1348	AR11/C/592/1652 AR11/C/1948/1980
310.3 E (49.7 W)	—	0.003149 1.23	14 Jul 1992 1992-043-D 22044	GORIZONT 26	USSR	Not registered at this location			
313.3 E (46.7 W)	—	0.003514 0.20	27 Dec 1990 1990-116-D 21041	RADUGA 1-2R	USSR	Not registered at this location			
314.9 E (45.1 W)	315.0 E (45.0 W)	0.000130 0.04	15 Jun 1988 1988-051-C 19217	PANAMSAT 1 PAS 1 USASAT-13I USASAT-13F	USA Pan American Satellite	14.000-14.500/ 10.950-11.200 or 11.700-12.200 or 12.500-12.750	FSS	AR11/A/199/1675 AR11/A/154/1635	AR11/C/866/1736 AR11/C/755/1676 AR11/C/1423/1864

TABLE 1. IN-ORBIT GEOSTATIONARY COMMUNICATIONS SATELLITES FOR YEAR-END 1992 (CONT'D)

SUBSAT. CURRENT (°)	LONGITUDE REGISTRD (°)	ORBIT ECCEN. & INCL. (°)	LAUNCH DATE & INT'L CATALOG NO.	SAT. NAME & ITU DESIGNATION	ITU REGISTERING COUNTRY	FREQUENCY UP/DOWN- LINK (GHz)	SERVICE TYPE	ITU SPECIAL SECTION	
								ADVANCED	COORDINATION
						5.925-6.425/ 3.700-4.200			
318.2 E (41.8 W)	—	0.002708 4.23	19 Mar 1987 1987-028-D 17705	RADUGA 20 R/B	USSR	Not registered at this location			
319.0 E (41.0 W)	319.0 E (41.0 W)	0.000296 0.06	13 Mar 1989 1989-021-B 19883	TDRS FH TDRS D TDRS EAST USASAT-14A	USA Columbia Communications	2.034-2.037/ 2.208-2.213 14.287-15.537/ 13.075-14.375 5.925-6.425/ 3.700-4.200	FSS	SPA-AA/231/1381 AR11/A/158/1637	AR11/C/46/1588 AR11/C/1183/1802
325.5 E (34.5 W)	325.5 E (34.5 W)	0.000035 0.17	14 Mar 1990 1990-021-A 20523	INTELSAT 6 F3 INTELSAT6 325.5E	USA Intelsat	5.850-6.425/ 3.625-4.200 14.000-14.500/ 10.950-11.700	FSS	AR11/A/288/1711	AR11/C/1272/1821
325.9 E (34.1 W)	325.0 E (35.0 W)	0.000130 1.81	01 Jan 1990 1990-001-A 20401	SKYNET 4A SKYNET-4D	UK	0.290-0.315/ 0.245-0.270 7.975-8.110/ 7.250-7.285 8.145-8.230/ 7.420-7.505 8.255-8.315/ 7.530-7.590 8.340-8.400/ 7.615-7.675 43.500-45.500/ 7.615-7.675	MSS FSS	AR11/A/708/1978	AR11/C/2050/2005
328.2 E (31.8 W)	—	0.002740 3.30	28 Oct 1987 1987-091-D 18446	COSMOS 1894	USSR	Not registered at this location			
328.6 E (31.4 W)	329.0 E (31.0 W)	0.000389 3.34	05 Mar 1982 1982-017-A 13083	INTELSAT 5 F4 INTELSAT5 ATL6	USA Intelsat	5.925-6.425/ 3.700-4.200 14.000-14.500/ 10.950-11.700	FSS	AR11/A/118/1611	AR11/C/683/1668
328.6 E (31.4 W)	—	0.000248 1.80	05 Jun 1989 1989-041-A 20040	SUPERBIRD A	JAPAN	Not registered at this location			
328.9 E (31.1 W)	329.0 E (31.0 W)	0.000083 0.07	27 Aug 1989 1989-067-A 20193	MARCOPOLO 1 BSB-1 UNISAT-1	UK British Sky Broadcasting	17.371-17.705/ 11.771-12.105 14.000-14.005/ 12.490 or 14.490-14.495/ 12.500	BSS	AR11/A/23/1532	AR11/C/173/1605 AR11/C/181/1611 AR11/C/731/1674 AR11/C/1209/1815
329.1 E (30.1 W)	—	0.000154 1.34	14 Nov 1984 1984-115-A 15391	NATO 3	BELGIUM	Not registered at this location			
330.0 E (30.0 W)	330.0 E (30.0 W)	0.00190 0.05	10 Sep 1992 1992-060-A 22116	HISPASAT 1A HISPASAT-1	SPAIN	7.900-8.025/ 7.250-7.375 14.000-14.500/ 11.700-12.200 or 12.500-12.750 2.025-2.110/ 2.200-2.290	FSS MSS	AR11/A/487/1871	AR11/C/1746/1943
332.5 E (27.5 W)	332.5 E (27.5 W)	0.000083 0.01	29 Oct 1991 1991-075-A 21765	INTELSAT 6 F1 INTELSAT6 332.5E	USA Intelsat	5.850-6.425/ 3.625-4.200 14.000-14.500/ 10.950-11.700	FSS	AR11/A/70/1584	AR11/C/628/1658 AR11/C/1625/1905
335.4 E (24.6 W)	335.0 E (25.0 W)	0.000107 0.01	14 Aug 1991 1991-055-A 21653	INTELSAT 6 F5 INTELSAT6 335.5E	USA Intelsat	5.850-6.425/ 3.625-4.200 14.000-14.500/ 10.950-11.700	FSS	AR11/A/69/1584	AR11/C/627/1658 AR11/C/1626/1905
335.4 E (24.6 W)	335.0 E (25.0 W)	0.000544 1.18	10 Sep 1992 1992-059-A 22112	COSMOS 2209 STATSIONAR-8	USSR	5.736-5.918/ 3.413-3.595	FSS	SPA-AA/95/1197	SPA-AJ/50/1276
335.6 E (24.4 W)	335.0 E (25.0 W)	0.000224 2.19	14 Apr 1989 1989-030-A 19928	RADUGA 23 STATSIONAR-8	USSR	5.736-5.918/ 3.413-3.595	FSS	SPA-AA/95/1197	SPA-AJ/50/1276

TABLE I. IN-ORBIT GEOSTATIONARY COMMUNICATIONS SATELLITES FOR YEAR-END 1992 (CONT'D)

SUBSAT. CURRENT (°)	LONGITUDE REGISTRD (°)	ORBIT ECCEN. & INCL. (°)	LAUNCH DATE & INT'L CATALOG NO.	SAT. NAME & ITU DESIGNATION	ITU REGISTERING COUNTRY	FREQUENCY UP/DOWN- LINK (GHz)	SERVICE TYPE	ITU SPECIAL SECTION	
								ADVANCED	COORDINATION
337.2 E (22.8 W)	337.5 E (22.5 W)	0.000379 3.01	25 Sep 1989 1989-077-A 20253	USA 46 FLTSATCOM ATL FLTSATCOM-B EAST ATL	USA	0.240-0.329/ 0.240-0.329 0.335-0.400/ 0.335-0.400 7.975-8.025/ 7.255-7.265 43.500-45.500/ 20.200-21.200	MSS FSS	SPA-AA/84/1186 AR11/A/48/1561	SPA-AJ/163/1382
338.5 E (21.5 W)	338.5 (21.5 W)	0.000083 0.06	10 Jun 1992 1992-032-A 21989	INTELSAT K INTELSATK 338.5E	USA Intelsat	14.000-14.500/ 11.450-11.950 or 12.500-12.750	FSS	AR11/A/614/1923	AR11/C/1876/1971
338.7 E (21.3 W)	338.5 E (21.5 W)	0.000379 3.71	06 Dec 1980 1980-098-A 12089	INTELSAT 5 F2 INTELSAT ATL5	USA Intelsat	5.925-6.425/ 3.400-4.200 14.000-14.500/ 10.950-11.700	FSS	SPA-AA/252/1419	SPA-AJ/378/1511
340.8 E (19.2 W)	341.0 E (19.0 W)	0.000509 0.05	08 Aug 1989 1989-062-A 20168	TV SAT 2 TV-SAT 2	GERMANY	17.716-18.051/ 11.700-12.500 2.027/ 2.202	BSS	AR11/A/350/1767	AR11/C/1768/1953
340.9 E (19.1 W)	341.0 E (19.0 W)	0.000130 0.57	12 Jul 1989 1989-053-A 20122	OLYMPUS 1 L-SAT	FRANCE ESA	28.050-28.650/ 17.100-17.850 18.900-19.500/ 12.000-12.750	BSS FSS	SPA-AA/308/1463 SPA-AA/337/1479 AR11/A/32/1544 AR11/A/88/1590	AR11/C/6/1554 AR11/C/174/1605 AR11/C/232/1619 AR11/C/782/1682
341.1 E (18.9 W)	341.0 E (19.0 W)	0.000332 0.05	24 Jul 1990 1990-063-A 20705	TDF 2 TDF-2	FRANCE	2.036/ 2.212 17.300-17.700/ 11.700-12.100	BSS	AR11/A/216/1684	AR11/C/1346/1839
341.2 E (18.8 W)	341.0 E (19.0 W)	0.000213 0.02	28 Oct 1988 1988-098-A 19621	TDF 1 TDF-1	FRANCE	2.036/ 2.212 17.300-17.700/ 11.700-12.100	BSS	RR/042/2/1521 AR11/A/57/1570	AR11/C/107/1578 AR11/C/124/1592 AR11/C/142/1597 AR11/C/703/1670 AR11/C/741/1674

341.9 E (18.1 W)	342.0 E (18.0 W)	0.000308 0.02	27 Jan 1989 1989-006-A 19772	INTELSAT 5A F15 INTELSAT5A 342E INTELSAT IBS 342E	USA Intelsat	5.925-6.425/ 3.700-4.200 14.000-14.500/ 10.950-11.700 or 11.700-11.950 or 12.500-12.750	FSS	AR11/A/64/1580 AR11/A/131/1617	AR11/C/1639/1917 AR11/C/705/1673
342.2 E (17.8 W)	342.0 E (18.0 W)	0.000012 3.13	08 Jan 1991 1991-001-A 21047	NATO 4A SATCOM PHASE-3	BELGIUM NATO	7.975-8.165/ 7.250-7.270 and 7.340-7.440	FSS	SPA-AA/144/1257	—
343.6 E (16.4 W)	344.0 E (16.0 W)	0.000237 1.09	27 Dec 1989 1989-101-A 20391	COSMOS 2054	USSR WSDRN	14.500-14.740/ 10.700-10.940 or 11.200-11.440 or 13.410-13.990 14.760-15.340/ 13.400-13.640	FSS	SPA-AA/341/1484	AR11/C/67/1570
344.5 E (15.5 W)	344.5 E (15.5 W)	0.000473 2.24	08 Mar 1991 1991-018-A 21149	INMARSAT 2 F2 INMARSAT2 AOR- EAST	UK Inmarsat	1.626-1.649/ 1.530-1.548 6.170-6.180/ 3.945-3.955 6.425-6.443/ 3.600-3.623	MSS	AR11/A/153/1634	AR11/C/1840/1968
345.1 E (14.9 W)	334.0 E (26.0 W)	0.000367 3.39	10 Nov 1984 1984-114-B 15386	MARECS B2 MARECS ATL1	FRANCE ESA	0.149/ 0.137 1.638-1.645/ 1.537-1.542 6.416-6.425/ 4.188-4.200	MSS	SPA-AA/221/1353	SPA-AJ/244/1432
346.1 E (13.9 W)	346.0 E (14.0 W)	0.000332 0.68	20 Jun 1990 1990-054-A 20659	GORIZONT 20 STATSIONAR-4 LOUTCH-1	USSR Intersputnik	5.725-6.275/ 3.400-3.950 14.000-14.500/ 10.950-11.200 or 11.450-11.700	FSS	SPA-AA/92/1197 SPA-AA/157/1262	AR11/C/765/1677 AR11/C/875/1737 AR11/C/1112/1793 AR11/C/1203/1809 AR11/C/1630/1910 AR11/C/1814/1964 SPA-AJ/84/1318 AR11/C/887/1743 AR11/C/1189/1804 AR11/C/1197/1809

TABLE I. IN-ORBIT GEOSTATIONARY COMMUNICATIONS SATELLITES FOR YEAR-END 1992 (CONT'D)

SUBSAT. CURRENT	LONGITUDE REGISTERD	ORBIT ECCEN. & INCL. (°)	LAUNCH DATE & INT'L CATALOG NO.	SAT. NAME & ITU DESIGNATION	ITU REGISTERING COUNTRY	FREQUENCY UP/DOWN- LINK (GHz)	SERVICE TYPE	ITU SPECIAL SECTION	
								ADVANCED	COORDINATION
346.3 E (13.7 W)	346.0 E (14.0 W)	0.000225 0.56	22 Nov 1991 1991-079-A 21789	COSMOS 2172 STATIONAR-4 LOUTCH-1	USSR Intersputnik	5.725-6.275/ 3.400-3.950 14.000-14.500/ 10.950-11.200 or 11.450-11.700	FSS	SPA-AA/92/1197 SPA-AA/157/1262	AR11/C/765/1677 AR11/C/875/1737 AR11/C/1112/1793 AR11/C/1203/1809 AR11/C/1630/1910 AR11/C/1814/1964 SPA-AJ/84/1318 AR11/C/887/1743 AR11/C/1189/1804 AR11/C/1197/1809
346.4 E (13.6 W)	346.5 E (13.5 W)	0.000581 3.24	01 Oct 1987 1987-084-A 18384	COSMOS 1888 GEIZER POTOK-1	USSR Sokol America	4.400-4.500/ or 4.630-4.680/ 3.950-4.000	FSS	SPA-AA/344/1485	AR11/C/18/1557
346.6 E (13.4 W)	346.0 E (14.0 W)	0.000248 0.59	23 Oct 1991 1991-074-D 21762	GORIZONT 24 STATIONAR-4 LOUTCH-1	USSR Intersputnik	5.725-6.275/ 3.400-3.950 14.000-14.500/ 10.950-11.200 or 11.450-11.700	FSS	SPA-AA/92/1197 SPA-AA/157/1262	AR11/C/765/1677 AR11/C/875/1737 AR11/C/1112/1793 AR11/C/1203/1809 AR11/C/1630/1910 AR11/C/1814/1964 SPA-AJ/84/1318 AR11/C/887/1743 AR11/C/1189/1804 AR11/C/1197/1809
348.5 E (11.5 W)	349.0 E (11.0 W)	0.002959 1.43	05 Jul 1989 1989-052-D 20110	GORIZONT 18 STATIONAR-11 LOUTCH-6	USSR	5.725-6.268/ 3.400-3.943 14.007-14.439/ 10.939-11.711	FSS	SPA-AA/270/1425 AR11/A/269/1707	AR11/C/1120/1793 AR11/C/1201/1809
349.5 E (10.5 W)	349.0 E (11.0 W)	0.000439 1.19	14 Jul 1992 1992-043-A 22041	GORIZONT 26 STATIONAR-11 LOUTCH-6	USSR	5.725-6.268/ 3.400-3.943 14.007-14.439/ 10.939-11.711	FSS	SPA-AA/270/1425 AR11/A/269/1707	AR11/C/1120/1793 AR11/C/1201/1809
349.9 E (10.1 W)	349.0 E (11.0 W)	0.000109 2.43	18 Aug 1988 1988-071-A 19397	GORIZONT 16 STATIONAR-11 LOUTCH-6	USSR	5.725-6.268/ 3.400-3.943 14.007-14.439/ 10.939-11.711	FSS	SPA-AA/270/1425 AR11/A/269/1707	AR11/C/1120/1793 AR11/C/1201/1809
352.0 E (8.0 W)	352.0 E (8.0 W)	0.000344 0.01	16 Dec 1991 1991-084-A 21813	TELECOM 2A TELECOM-2A	FRANCE	2.029-2.032/ 2.203-2.207 5.925-6.425/ 3.700-4.200 7.900-8.400/ 7.250-7.750 14.000-14.250/ 12.500-12.750	FSS MSS	AR11/A/324/1745	AR11/C/1097/1792 AR11/C/1162/1795 AR11/C/1325/1839
355.0 E (5.0 W)	355.0 E (5.0 W)	0.000367 0.01	15 Apr 1992 1992-021-A 21939	TELECOM 2B TELECOM-2B	FRANCE	2.029-2.032/ 2.203-2.207 5.925-6.425/ 3.700-4.200 7.900-8.400/ 7.250-7.750 14.000-14.250/ 12.500-12.750	FSS MSS	AR11/A/325/1745	AR11/C/1100/1792 AR11/C/1164/1795 AR11/C/1328/1839
355.8 E (4.2 W)	—	0.002048 3.19	01 Oct 1987 1987-084-D 18387	COSMOS 1888	USSR	Not registered at this location			
359.1 E (0.9 W)	359.0 E (1.0 W)	0.000332 0.03	29 Sep 1985 1985-087-A 16101	INTELSAT 5A-12 INTELSAT5A CONT4	USA Intelsat	5.925-6.425/ 3.700-4.200 14.000-14.500/ 10.950-11.700	FSS	AR11/A/117/1609	AR11/C/677/1668
359.2 E (0.8 W)	359.2 E (0.8 W)	0.000178 0.06	18 Aug 1990 1990-074-A 20762	THOR BIFROST	NORWAY	17.371-17.705/ 11.771-12.105 14.000-14.005/ or 14.490-14.495/ 12.490-12.500	BSS	AR11/A/894/2069	—

TABLE 2. PLANNED GEOSTATIONARY COMMUNICATIONS SATELLITES FOR YEAR-END 1992

SUBSATELLITE REGISTERED LONGITUDE (°)	PLANNED IN-USE DATE	PERIOD OF VALIDITY (yrs)	SATELLITE DESIGNATION	ITU REGISTERING COUNTRY	FREQUENCY UP/DOWNLINK (GHz)		SERVICE TYPE	ITU SPECIAL SECTION	
								ADVANCED	COORDINATION
1.0 E	31 DEC 1992	20	RADUGA STATIONAR-22	USSR	5.7-5.9/	3.4-3.7	FSS	AR11/A/410/1806	AR11/C/1752/1948
1.0 E	1 JUN 1992	20	TOR-15	USSR	42.5-43.5/ 43.5-45.5/	18.2-20.2 20.2-21.2	FSS MSS	AR11/A/372/1790	AR11/C/1418/1862
1.0 E	1 JUN 1992	20	VOLNA-21	USSR	0.27-0.28/ 0.33-0.40/	0.24-0.29 0.31-0.32	MSS	AR11/A/375/1793	AR11/C/1581/1887
1.5 E	30 DEC 1994	—	AMOS 1-A	ISRAEL	14.0-14.5/ or	10.9-11.2 11.4-11.7	FSS	AR11/A/803/2019	—
3.0 E	30 SEP 1991	10	TELECOM 2C TELECOM-2C	FRANCE	2.0 / 5.9-6.4/ 7.9-8.0/	2.2 3.7-4.2 7.2-7.4	FSS	AR11/A/326/1745	AR11/C/1103/1792 AR11/C/1166/1795 AR11/C/1331/1839
4.0 E	1 JUN 1991	20	MILSTAR-13	USA	0.29-0.32/ 43.5-45.5/ 1.8 /	0.24-0.27 20.2-21.2 2.2	MSS	AR11/A/454/1837	AR11/C/1549/1885 AR11/C/1658/1761
5.0 E	1 JUN 1992	20	TOR-19	USSR	42.5-43.5/ 43.5-45.5/	18.2-20.2 20.2-21.2	FSS MSS	AR11/A/390/1798	AR11/C/1492/1878
6.0 E	1 JAN 1994	20	SKYNET-4G	UK	43.5-45.5/	20.2-21.2	FSS MSS	AR11/A/692/1972	—
7.0 E	31 DEC 1987	10	F-SAT 1	FRANCE	2.0-2.1/ 5.9-6.4/ 29.5-30.0/	2.2-2.3 3.7-4.1 19.7-20.1	FSS	AR11/A/79/1587	AR11/C/564/1649
8.0 E	30 AUG 1990	20	RADUGA STATIONAR-18	USSR	5.7-6.3/	3.4-3.9	FSS	AR11/A/220/1686	AR11/C/911/1749
8.0 E	1 JUN 1992	20	TOR-8	USSR	42.5-43.5/ 43.5-45.5/	18.2-20.2 20.2-21.2	FSS MSS	AR11/A/285/1710	AR11/C/1361/1851
8.0 E	15 OCT 1990	20	VOLNA-15	USSR	.27-.28/ .34-.40/ 1.6 /	.24-.29 .31-.32 1.5	MSS	AR11/A/241/1693	AR11/C/983/1769
10.0 E	31 DEC 1988	10	APEX	FRANCE	2.0 / 5.9-6.4/ 29.5-30.0/	2.2 3.7-4.2 19.7-20.1	FSS	AR11/A/62/1578	AR11/C/388/1628 AR11/C/479/1648 AR11/C/582/1651
12.0 E	1 JUN 1992	20	TOR-18	USSR	42.5-43.5/ 43.5-45.5/	18.2-20.2 20.2-21.2	FSS MSS	AR11/A/389/1798	AR11/C/1479/1877
12.0 E	1 JUN 1992	20	VOLNA-27	USSR	.27-.28/ .33-.39/	.24-.29 .31-.32	MSS	AR11/A/378/1793	AR11/C/1590/1887
15.0 E	30 APR 1992	10	ZENON-B	FRANCE	2.0 / 1.6-1.7/ 6.4-6.5/	2.2 1.5-1.6 3.6-3.7	FSS MSS	AR11/A/364/1781	—
15.0 E	31 JUL 1987	10	AMOS 1 AMS-1	ISRAEL	5.9-6.4/	3.7-4.2	FSS	AR11/A/39/1554	AR11/C/816/1695
15.0 E	31 JUL 1987	10	AMOS 2 AMS-2	ISRAEL	5.9-6.4/ 14.0-14.5/ or	3.7-4.2 10.9-11.2 11.4-11.7	FSS	AR11/A/39/1554	AR11/C/817/1695
15.0 E	31 DEC 1990	20	TOR-12	USSR	42.5-43.5/ 43.5-45.5/	18.2-20.2 20.2-21.2	FSS MSS	AR11/A/309/1736	AR11/C/1444/1872
15.0 E	1 JUN 1992	20	VOLNA-23	USSR	.27-.28/ .33-.39/	.24-.29 .31-.32	MSS	AR11/A/376/1793	AR11/C/1584/1887
16.0 E	5 JAN 1994	8	SICRAL-1A	ITALY	.33-.40/ 7.9-8.4/ 14.0-14.2/ 43.5-45.5/	.23-.32 7.2-7.7 12.2-12.7 20.2-21.2	FSS MSS	AR11/A/44/1557	AR11/C/1678/1924 AR11/C/1682/1924 AR11/C/1687/1924 AR11/C/1728/1993 AR11/C/2013/1998
17.0 E	30 APR 1992	20	SABS-1	SAUDI ARABIA	14.0-14.5/	11.7-12.5	BSS FSS	AR11/A/353/1768	—
17.0 E	17 APR 1993	20	SABS 1-2	SAUDI ARABIA	14.0-14.5/	11.7-12.5	BSS	AR11/A/125/1616	AR11/C/1212/1815

TABLE 2. PLANNED GEOSTATIONARY COMMUNICATIONS SATELLITES FOR YEAR-END 1992 (CONT'D)

SUBSATELLITE REGISTERED LONGITUDE (°)	PLANNED IN-USE DATE	PERIOD OF VALIDITY (yrs)	SATELLITE DESIGNATION	ITU REGISTERING COUNTRY	FREQUENCY UP/DOWNLINK (GHz)		SERVICE TYPE	ITU SPECIAL SECTION	
								ADVANCED	COORDINATION
19.0 E	1 JUN 1994	20	ARABSAT 2A ARABSAT 2-A	SAUDI ARABIA Arabsat	5.9-6.4/	3.7-4.2	FSS	AR11/A/679/1963	AR11/C/2128/2029
19.0 E	30 APR 1992	10	ZENON-C	FRANCE	2.0 / 1.6-1.7/ 6.4-6.5/	2.2 1.5-1.6 3.6-3.7	FSS MSS	AR11/A/365/1781	—
19.0 E	1 MAR 1993	20	TOR-26	USSR	42.5-43.5/ 43.5-45.5/	18.2-20.2 20.2-21.2	FSS MSS	AR11/A/459/1839	—
19.0 E	1 FEB 1991	20	MILSTAR-9	USA	29-32/ 43.5-45.5/ 1.8 /	24-27 20.2-21.2 2.2	MSS	AR11/A/450/1837	AR11/C/1533/1885 AR11/C/1654/1919
20.0 E	1 JAN 1998	20	INMARSAT4 GSO-1D	UK Inmarsat	1.6 / 6.4-6.6/	2.5 3.6-3.8	FSS MSS	AR11/A/824/2032	—
20.0 E	1 JAN 1998	20	INMARSAT4 GSO-2D	UK Inmarsat	1.9 / 6.4-6.7/	2.2 3.6-3.9	FSS MSS	AR11/A/831/2032	—
21.0 E	30 APR 1993	20	BABYLONSAT-3	IRAQ	14.0-14.5/ or	10.9-11.2 11.4-11.7	FSS	AR11/A/441/1832	—
21.5 E	30 NOV 1993	20	EUTELSAT 2 F6 EUTELSAT 2-21.5E	FRANCE Eutelsat	2.0 / 1.6-1.7/ 14.0-14.5/ or or	2.3 1.5-1.6 10.9-11.2 11.4-11.7 12.5-12.7	FSS MSS	AR11/A/654/1957 AR11/A/686/1969	AR11/C/1967/1987 AR11/C/1968/1987
22.0 E	2 JAN 1994	8	SICRAL-1B	ITALY	33-40/ 7.9-8.4/ 14.0-14.2/ 43.5-45.5/	23-32 7.2-7.7 12.2-12.7 20.2-21.2	FSS MSS	AR11/A/45/1557	AR11/C/1680/1924 AR11/C/1684/1924 AR11/C/1687/1924 AR11/C/1732/1993
23.0 E	1 AUG 1990	20	RADUGA STATSIONAR-19	USSR	5.7-6.3/	3.4-3.9	FSS	AR11/A/221/1686	AR11/C/916/1752

23.0 E	1 AUG 1990	20	TOR-7	USSR	42.5-43.5/ 43.5-45.5/	18.2-20.2 20.2-21.2	FSS MSS	AR11/A/284/1710	AR11/C/1356/1851
23.0 E	15 OCT 1990	20	VOLNA-17	USSR	1.6 / 27-28/ 34-40/	1.5 24-29 31-32	MSS	AR11/A/242/1693	AR11/C/986/1769
26.0 E	20 MAY 1996	20	ARABSAT 2B ARABSAT 2-B	SAUDI ARABIA Arabsat	5.9-6.4/ 14.0-14.5/ or	3.7-4.2 10.9-11.2 11.4-11.5	FSS	AR11/A/680/1963	AR11/C/2131/2029
26.0 E	15 SEP 1992	20	DFS-6	GERMANY	2.0 / 14.0-14.5/ or 29.0-30.0/	2.2 11.4-11.7 12.5-12.7 19.7-20.2	FSS	AR11/A/547/1906	AR11/C/2112/2020
26.0 E	30 APR 1991	20	ZOHREH 2 ZOHREH-2	IRAN	14.0-14.5/ or	10.9-11.2 11.4-11.7	FSS	AR11/A/297/1719	AR11/C/1235/1818
26.0 E	1 JUN 1995	20	TURKSAT-K1	TURKEY	14.0-14.5/ or	10.9-11.2 11.4-11.7	FSS	AR11/A/797/2014	—
27.0 E	1 JUN 1992	20	TOR-20	USSR	42.5-43.5/ 43.5-45.5/	18.2-20.2 20.2-21.2	FSS MSS	AR11/A/391/1798	AR11/C/1484/1877
28.0 E	30 NOV 1992	20	FLTSATCOM-C INDOC1	USA	29-32/ 1.8 / 7.9-8.0/ 43.5-45.5/	24-27 2.2 7.2-7.3 20.2-21.2	FSS MSS	AR11/A/702/1973	—
28.5 E	1 JUN 1995	10	KEPLER 1	GERMANY	2.0 / 14.0-14.5/ or	2.2 11.4-11.7 12.5-12.7	FSS	AR11/A/496/1880	—
29.0 E	15 FEB 1995	—	STRATSAT-1	SAUDI ARABIA	7.9-8.4/	7.2-7.7	FSS MSS	AR11/A/835/2033	—
30.0 E	30 APR 1993	20	BABYLONSAT-1	IRAQ	14.0-14.5/ or	10.9-11.2 11.4-11.7	FSS	AR11/A/439/1832	—
30.0 E	1 MAR 1991	20	MILSTAR-10	USA	29-32/ 1.8 / 43.5-45.5/	24-27 2.2 20.2-21.2	MSS	AR11/A/451/1837	AR11/C/1537/1885 AR11/C/1655/1761

TABLE 2. PLANNED GEOSTATIONARY COMMUNICATIONS SATELLITES FOR YEAR-END 1992 (CONT'D)

SUBSATELLITE REGISTERED LONGITUDE (°)	PLANNED IN-USE DATE	PERIOD OF VALIDITY (yrs)	SATELLITE DESIGNATION	ITU REGISTERING COUNTRY	FREQUENCY UP/DOWNLINK (GHz)		SERVICE TYPE	ITU SPECIAL SECTION	
								ADVANCED	COORDINATION
31.0 E	30 NOV 1993	20	EUTELSAT 2-31E	FRANCE Eutelsat	2.0 / 1.6-1.7/ 14.0-14.5/ or 11.4-11.7 or 12.5-12.7	2.3 1.5-1.6 10.9-11.2	FSS MSS	AR11/A/655/1951 AR11/A/687/1969	AR11/C/1970/1987 AR11/C/1971/1987
31.0 E	1 NOV 1992	20	TURKSAT 2 TURKSAT-1B	TURKEY	14.0-14.5/ or 12.5-12.7	10.9-11.2 11.4-11.7	FSS	AR11/A/610/1923	AR11/C/1900/1979
32.0 E	1 JUL 1994	15	VIDEOSAT-4	FRANCE	2.0 / 14.0-14.2/	2.2 12.5-12.7	FSS	AR11/A/572/1911	AR11/C/1950/1980
32.0 E	31 JUL 1992	20	TOR-21	USSR	42.5-43.5/ 43.5-45.5/	18.2-20.2 20.2-21.2	FSS MSS	AR11/A/416/1815	AR11/C/1568/1886
33.0 E	30 NOV 1993	20	EUTELSAT 2-33E	FRANCE Eutelsat	2.0 / 1.6-1.7/ 14.0-14.5/ or 11.4-11.7 or 12.5-12.7	2.3 1.5-1.6 10.9-11.2	FSS MSS	AR11/A/656/1957 AR11/A/688/1969	AR11/C/1973/1987 AR11/C/1974/1987
34.0 E	30 APR 1991	20	ZOHREH 1 ZOHREH-1	IRAN	14.0-14.5/ or 11.4-11.7	10.9-11.2 11.4-11.7	FSS	AR11/A/296/1719	AR11/C/1224/1818
34.0 E	30 JUN 1988	20	STATSIONAR-D3	USSR	6.4-6.7/	4.5-4.8	FSS	AR11/A/195/1675	AR11/C/1170/1796
35.0 E	1 AUG 1990	20	TOR-2	USSR	42.5-43.5/ 43.5-45.5/	18.2-20.2 20.2-21.2	FSS	AR11/A/279/1710	AR11/C/1299/1832
35.0 E	31 OCT 1991	20	VOLNA-11	USSR	.27-.28/ .34-.40/ 1.6 /	.24-.29 .31-.32 1.5	MSS	AR11/A/150/1631	AR11/C/977/1769
36.0 E	28 FEB 1994	20	EUTELSAT 2 F5 EUTELSAT 2-36E	FRANCE Eutelsat	2.0 / 1.6-1.7/ 14.0-14.5/	2.3 1.5-1.6 10.9-11.2	FSS MSS	AR11/A/307/1732	AR11/C/1208/1809 AR11/C/1744/1942
37.5 E	5 JUN 1996	20	SEYSAT-2	SEYCHELLES	5.9-6.4/ 14.0-14.2/	3.7-4.2 10.9-11.2	FSS	AR11/A/642/1947	—
38.0 E	31 DEC 1991	15	PAKSAT-1	PAKISTAN	14.0-14.5/ 14.5-14.8/	11.2-11.7 11.7-12.2	BSS FSS	AR11/A/90/1592	AR11/C/1367/1858
39.0 E	30 DEC 1996	—	AMOS 1-C	ISRAEL	14.0-14.5/ or 11.4-11.7	10.9-11.2 11.4-11.7	FSS	AR11/A/805/2019	—
40.0 E	31 DEC 1993	20	EXPRESS 4 EXPRESS-4	USSR Informkosmos	5.7-6.5/ 14.0-14.5/ or 11.4-11.7	3.4-4.2 10.9-11.2	FSS	AR11/A/760/2003	—
40.0 E	31 JUL 1992	20	TOR-22	USSR	42.5-43.5/ 43.5-45.5/	18.2-20.2 20.2-21.2	FSS MSS	AR11/A/417/1815	AR11/C/1563/1886
40.0 E	1 AUG 1992	—	VOLNA-40E	USSR	1.6 / 6.1 /	1.5 3.8	FSS MSS	AR11/A/816/2029	—
41.0 E	15 FEB 1995	—	STRATSAT-2	SAUDI ARABIA	7.9-8.4/	7.2-7.7	FSS	AR11/A/836/2033	—
41.0 E	30 JUL 1992	20	ZOHREH-4	IRAN	14.0-14.5/ or 11.4-11.7	10.9-11.2 11.4-11.7	FSS	AR11/A/394/1800	—
41.0 E	31 DEC 1992	15	PAKSAT-2	PAKISTAN	14.0-14.5/ 14.5-14.8/	11.2-11.7 11.7-12.2	BSS FSS	AR11/A/91/1692	—
42.0 E	1 NOV 1992	12	TURKSAT 1 TURKSAT-1A	TURKEY	14.0-14.5/ or 11.4-11.7 or 12.5-12.7	10.9-11.2 11.4-11.7 12.5-12.7	FSS	AR11/A/609/1923	AR11/C/1897/1979
42.5 E	5 JUN 1995	20	SEYSAT-1	SEYCHELLES	5.9-6.4/ 14.0-14.2/	3.7-4.2 10.9-11.2	FSS	AR11/A/641/1947	—
43.0 E	1 JAN 1994	20	EUROPE*STAR-2	GERMANY	12.5 / 14.0-14.5/ or 12.5-12.7	12.5 11.4-11.7 12.5-12.7	FSS	AR11/A/746/2000	—
45.0 E	30 SEP 1993	20	EUROPE*STAR-1	GERMANY	14.0-14.5/ or 12.5-12.7	11.4-11.7 12.5-12.7	FSS	AR11/A/715/1986	—

TABLE 2. PLANNED GEOSTATIONARY COMMUNICATIONS SATELLITES FOR YEAR-END 1992 (CONT'D)

SUBSATELLITE REGISTERED LONGITUDE (°)	PLANNED IN-USE DATE	PERIOD OF VALIDITY (YRS)	SATELLITE DESIGNATION	ITU REGISTERING COUNTRY	FREQUENCY UP/DOWNLINK (GHz)		SERVICE TYPE	ITU SPECIAL SECTION	
								ADVANCED	COORDINATION
45.0 E	1 NOV 1993	20	MELITASAT-1A	MALTA	14.0-14.5/ or 12.5-12.7	10.9-11.2 11.4-11.7	FSS	AR11/A/770/2004	—
45.0 E	30 JUN 1988	20	STATSIONAR-D4	USSR	6.4-6.7/	4.5-4.8	FSS	AR11/A/196/1675	AR11/C/1171/1796
45.0 E	1 AUG 1990	20	TOR-3	USSR	42.5-43.5/ 43.5-45.5/	18.2-20.2 20.2-21.2	FSS MSS	AR11/A/280/1710	AR11/C/1336/1839
45.0 E	1 DEC 1990	20	VOLNA-3M	USSR	1.6 /	1.5	MSS	AR11/A/249/1697	AR11/C/1398/1861
45.5 E	1 NOV 1993	20	MELITASAT-1B	MALTA	14.0-14.5/ or 12.5-12.7	10.9-11.2 11.4-11.7	FSS	AR11/A/771/2004	—
46.0 E	1 JUN 1995	20	TURKSAT-2	TURKEY	14.0-14.5/ or	10.9-11.2 11.4-11.7	FSS	AR11/A/798/2014	—
47.0 E	1 APR 1996	15	EDRSS-EC	FRANCE ESA	2.0-2.1/ 27.5-30.0/	2.2-2.3 18.1-20.2	FSS	AR11/A/630/1935	—
47.0 E	30 APR 1991	20	ZOHREH-3	IRAN	14.0-14.5/ or	10.9-11.2 11.4-11.7	FSS	AR11/A/298/1719	AR11/C/1246/1818
47.5 E	1 JUN 1994	20	EUROPE-STAR-3	GERMANY	12.5 / 14.0-14.5/ or	12.5 11.4-11.7 12.5-12.7	FSS	AR11/A/747/2000	—
49.0 E	1 JUN 1992	20	TOR-16	USSR	42.5-43.5/ 43.5-45.5/	18.2-20.2 20.2-21.2	FSS MSS	AR11/A/373/1790	AR11/C/1454/1872
49.0 E	1 JUN 1992	20	VOLNA-25	USSR	.27-.28/ 34-.40/	24-.29 .31-.32	MSS	AR11/A/377/1793	AR11/C/1587/1887
50.0 E	1 NOV 1992	12	TURKSAT-1C	TURKEY	14.0-14.5/ or 12.5-12.7	10.9-11.2 11.4-11.7	FSS	AR11/A/611/1923	AR11/C/1903/1979

51.0 E	30 APR 1993	20	BABYLONSAT-2	IRAQ	14.0-14.5/ or	10.9-11.2 11.4-11.7	FSS	AR11/A/440/1832	—
53.0 E	1 JAN 1994	20	SKYNET-4H	UK	43.5-45.5/	20.2-21.2	FSS MSS	AR11/A/693/1972	—
53.0 E	31 DEC 1996	20	EXPRESS-5	USSR	5.7-6.5/ 14.0-14.5/ or	3.4-4.2 10.9-11.2 11.4-11.7	FSS	AR11/A/761/2003	—
53.0 E	1 SEP 1990	15	MORE-53	USSR	1.6 / 6.0-6.1/	1.5 3.7-3.8	FSS MSS	AR11/A/185/1662	AR11/C/1088/1791
53.0 E	31 JUL 1992	20	TOR-23	USSR	42.5-43.5/ 43.5-45.5/	18.2-20.2 20.2-21.2	FSS MSS	AR11/A/418/1815	AR11/C/1573/1886
55.0 E	1 SEP 1990	20	MILSTAR-4	USA	.29-.32/ 1.8 / 43.5-45.5/	.24-.27 2.2 20.2-21.2	MSS	AR11/A/445/1837	AR11/C/1513/1885
56.0 E	19 DEC 1998	15	USGCSS PH4 INDOC1	USA	43.5-45.5/ 1.8 /	20.2-21.2 2.2	FSS MSS	AR11/A/553/1907	AR11/C/1938/1980 AR11/C/1842/1980
57.0 E	30 JUN 1993	10	USGCSS PH3 INDOC2 USGCSS PH3B INDOC2	USA	1.8 / 7.9-8.4/	2.2 7.2-7.7	FSS MSS	AR11/A/490/1875 AR11/A/719/1986	—
57.0 E	1 MAR 1996	20	INTELSAT 7 F8 INTELSAT 7 57E	USA Intelsat	5.9-6.4/ 14.0-14.5/ or or or	3.4-4.2 10.9-11.2 11.4-11.7 11.7-11.9 12.5-12.7	FSS	AR11/A/587/1918	AR11/C/1877/1974
58.0 E	31 DEC 1990	20	TOR-13	USSR	42.5-43.5/ 43.5-45.5/	18.2-20.2 20.2-21.2	FSS MSS	AR11/A/310/1736	AR11/C/1413/1862
59.0 E	1 APR 1996	15	EDRSS-E	FRANCE ESA	2.0-2.1/ 27.5-30.0/	2.2-2.3 18.1-20.2	FSS	AR11/A/631/1935	—
60.0 E	31 MAR 1996	15	USGCSS PH3 INDOC USGCSS PH3B INDOC	USA	1.8 / 7.9-8.4/	2.2 7.2-7.7	FSS MSS	AR11/A/267/1706 AR11/A/670/1960	AR11/C/413/1829 AR11/C/1219/1816 AR11/C/1223/1816

TABLE 2. PLANNED GEOSTATIONARY COMMUNICATIONS SATELLITES FOR YEAR-END 1992 (CONT'D)

SUBSATELLITE REGISTERED LONGITUDE (°)	PLANNED IN-USE DATE	PERIOD OF VALIDITY (yrs)	SATELLITE DESIGNATION	ITU REGISTERING COUNTRY	FREQUENCY UP/DOWNLINK (GHz)		SERVICE TYPE	ITU SPECIAL SECTION	
								ADVANCED	COORDINATION
60.0 E	31 DEC 1998	15	USGCSS PH1 INDOC2	USA	43.5-45.5/ 1.8 /	20.2-21.2 2.2	FSS MSS	AR11/A/554/1907	AR11/C/1943/1980 AR11/C/1947/1980
62.0 E	31 JUL 1992	20	TOR-24	USSR	42.5-43.5/ 43.5-45.5/	18.2-20.2 20.2-21.2	FSS MSS	AR11/A/419/1815	AR11/C/1595/1890
64.0 E	31 NOV 1994	20	INMARSAT3 IOR-1	UK Inmarsat	1.6/ 6.2 / 6.4 /	1.5 3.9 3.6	FSS MSS	AR11/A/598/1920	AR11/C/1991/1989
64.0 E	1 JAN 1998	20	INMARSAT4 GSO-1E	UK Inmarsat	1.6 / 6.4-6.6/	2.5 3.6-3.8	FSS MSS	AR11/A/825/2032	—
64.0 E	1 JAN 1998	20	INMARSAT4 GSO-2E	UK Inmarsat	1.9 / 6.4-6.7/	2.2 3.6-3.9	FSS MSS	AR11/A/832/2032	—
65.0 E	1 JUN 1994	20	INMARSAT3 IOR-2	UK Inmarsat	1.6-1.7/ 6.2 / 6.4 /	1.5-1.6 3.9 3.6	FSS MSS	AR11/A/791/2011	AR11/C/2224/2043
65.0 E	31 JUL 1992	20	TOR-25	USSR	42.5-43.5/ 43.5-45.5/	18.2-20.2 20.2-21.2	FSS MSS	AR11/A/420/1815	AR11/C/1600/1890
66.0 E	1 AUG 1993	20	INTELSAT 7 F4 INTELSAT7 66E	USA Intelsat	5.9-6.4/ 14.0-14.5/ or or or	3.4-4.2 10.9-11.2 11.4-11.7 11.7-11.9 12.5-12.7	FSS	AR11/A/580/1918	AR11/C/1880/1974
68.0 E	1 AUG 1993	20	PANAMSAT 6 PAS-6 USASAT-14I	USA Pan American Satellite	5.9-6.4/ 14.0-14.5/ or	3.7-4.2 11.4-11.7 12.2-12.7	FSS	AR11/A/748/2000	—
69.0 E	31 DEC 1990	20	TOR-14	USSR	42.5-43.5/ 43.5-45.5/	18.2-20.2 20.2-21.2	FSS MSS	AR11/A/311/1736	AR11/C/1449/1872
70.0 E	3 FEB 1994	—	TONGASAT-H70	TONGA Friendly Islands Satellite	14.0-14.5/ 5.9-6.4/	10.9-11.2 3.7-4.2	FSS	AR11/A/851/2050	—
70.0 E	1 JUN 1992	20	TOR-17	USSR	42.5-43.5/ 43.5-45.5/	18.2-20.2 20.2-21.2	FSS MSS	AR11/A/371/1790	AR11/C/1474/1877
70.0 E	1 JUN 1992	20	VOLNA-19	USSR	.27-.28/ .34-.40/	.24-.29 .31-.32	MSS	AR11/A/374/1793	AR11/C/1578/1887
70.0 E	1 NOV 1991	10	UNICOM 2 USASAT-13N	USA Unicom Satellite	14.0-14.5/ or	11.2-11.7 12.5-12.7	FSS	AR11/A/344/1763	AR11/C/1438/1871
72.0 E	30 NOV 1992	20	FLTSATCOM-C INDOC2	USA	.29-.32/ 7.9-8.0/ 1.8 / 43.5-45.5/	.24-.27 7.2-7.3 2.2 20.2-21.2	FSS MSS	AR11/A/703/1973	—
72.0 E	1 AUG 1993	20	PANAMSAT-7 PAS-7 USASAT-14J	USA Pan American Satellite	5.9-6.4/ 14.0-14.5/ or	2.7-4.2 11.4-11.7 12.2-12.7	FSS	AR11/A/749/2000	—
73.5 E	15 FEB 1995	—	STRATSAT-3	SAUDI ARABIA	7.9-8.4/	7.2-7.7	FSS MSS	AR11/A/837/2033	—
73.5 E	1 NOV 1992	12	TURKSAT-1D	TURKEY	14.0-14.5/ or or	10.9-11.2 11.4-11.7 12.5-12.7	FSS	AR11/A/612/1923	—
74.0 E	30 JAN 1994	20	INSAT 2KC	INDIA	14.0-14.5/ or	10.9-11.2 11.4-11.7	FSS	AR11/A/741/1997	—
75.0 E	30 NOV 1992	20	FLTSATCOM-C INDOC3	USA	.29-.32/ 7.9-8.0/ 1.8 / 43.5-45.5/	.24-.27 7.2-7.3 2.2 20.2-21.2	FSS	AR11/A/704/1973	—
77.0 E	17 OCT 1989	20	CSSRD-2	USSR	14.6 / or 15.0 /	11.2 12.6 13.5	FSS	AR11/A/188/1672	—

TABLE 2. PLANNED GEOSTATIONARY COMMUNICATIONS SATELLITES FOR YEAR-END 1992 (CONT'D)

SUBSATELLITE REGISTERED LONGITUDE (°)	PLANNED IN-USE DATE	PERIOD OF VALIDITY (yrs)	SATELLITE DESIGNATION	ITU REGISTERING COUNTRY	FREQUENCY UP/DOWNLINK (GHz)		SERVICE TYPE	ITU SPECIAL SECTION	
								ADVANCED	COORDINATION
77.5 E	1 APR 1993	20	ASIASAT 2 ASIASAT-D ASIASAT-DK1	UK Asia Satellite Telecom	5.8-6.7/ 14.0-14.5/ or or	3.4-4.2 10.9-11.2 11.4-11.7 12.2-12.7	FSS	AR11/A/617/1929 AR11/A/782/2007	AR11/C/1896/1978 AR11/C/2235/2049
78.5 E	1 JAN 1994	15	THAICOM 2 THAICOM-A2	THAILAND Shinawatra Computer	5.9-6.4/ 14.0-14.5/ or or	3.7-4.2 10.9-11.2 11.4-11.7 12.2-12.7	FSS	AR11/A/727/1988	AR11/C/2186/2036
80.0 E	31 DEC 1994	20	EXPRESS-6	USSR	5.7-6.5/ 14.0-14.5/ or	3.4-4.2 10.9-11.2 11.4-11.7	FSS	AR11/A/762/2003	—
81.5 E	1 MAR 1994	10	FOTON-2	USSR	6.5-6.6/	4.6-4.7	FSS	AR11/A/236/1692	AR11/C/1015/1776
81.5E	30 JAN 1995	20	INSAT-2KA	INDIA	14.0-14.5/ or	10.9-11.2 11.4-11.7	FSS	AR11/A/739/1997	—
83.0 E	31 JAN 1990	20	INSAT 2C INSAT-2A	INDIA	5.8-6.4/ 6.7-7.0/	3.7-4.2 4.5-4.7	FSS	AR11/A/260/1702	AR11/C/1081/1789
83.3 E	1 NOV 1995	20	TONGASAT AP-KU-4	TONGA Friendly Islands Satellite	14.0-14.5/ or	11.7-12.2 12.2-12.7	FSS	AR11/A/673/1960	AR11/C/2004/1990
85.0 E	30 JUN 1988	20	STATIONAR-D5	USSR	6.4-6.7/	4.5-4.8	FSS	AR11/A/197/1675	AR11/C/1172/1796
85.0 E	1 AUG 1990	20	TOR-4	USSR	42.5-43.5/ 43.5-45.5/	18.2-20.2 20.2-21.2	FSS MSS	AR11/A/281/1710	AR11/C/1341/1839
85.0 E	1 DEC 1990	20	VOLNA-5M	USSR	1.6 /	1.5	MSS	AR11/A/250/1697 AR11/A/470/1850	AR11/C/1400/1861
90.0 E	31 DEC 1994	20	EXPRESS-7	USSR	5.7-6.5/ 14.0-14.5/ or	3.4-4.2 10.9-11.2 11.4-11.7	FSS	AR11/A/763/2003	—
90.0 E	1 SEP 1990	15	MORE-90	USSR	1.6 / 6.0-6.1/	1.5 3.7-3.8	FSS MSS	AR11/A/184/1662	AR11/C/1090/1791
90.0 E	1 OCT 1990	20	MILSTAR-5	USA	0.29-0.32/ 1.8 / 43.5-45.5/	0.24-0.27 2.2 20.2-21.2	MSS	AR11/A/446/1837	AR11/C/1517/1885 AR11/C/1650/1919
91.5 E	1 APR 1994	—	MEASAT-1	MALAYSIA	5.9-6.7/ 14.0-14.5/ or or	3.4-4.2 10.9-11.2 11.4-11.7 12.2-12.7	FSS	AR11/A/839/2034	—
91.5 E	1 APR 1994	—	INTELSAT 7 91.5E	USA Intelsat	5.9-6.4/ 14.0-14.5/ or or or	3.4-4.2 10.9-11.2 11.4-11.7 11.7-11.9 12.5-12.7	FSS	AR11/A/860/2054	—
93.5 E	20 JAN 1996	20	INSAT 2KB INSAT-2KB	INDIA	14.0-14.5/ or	10.9-11.2 11.4-11.7	FSS	AR11/A/740/1997	—
93.5 E	31 MAR 1990	20	INSAT 2B INSAT-2B	INDIA	5.9-6.4/ 6.7-7.0/	3.7-4.2 4.5-4.7	FSS	AR11/A/261/1702	AR11/C/1082/1789
95.0 E	1 APR 1994	—	MEASAT-3	MALAYSIA	5.9-6.7/ 14.0-14.5/ or or	3.4-4.2 10.9-11.2 11.4-11.7 12.2-12.7	FSS	AR11/A/854/2053	—
95.0 E	1 JUN 1986	20	CSDRN	USSR	14.6 / 15.0 /	10.8 or 11.3 13.5 or 13.7	FSS	SPA-AA/342/1484	AR11/C/69/1570
95.0 E	1 APR 1994	—	INTELSAT 7 95E	USA Intelsat	5.9-6.4/ 14.0-14.5/ or or or	3.4-4.2 10.9-11.2 11.4-11.7 11.7-11.9 12.2-12.7	FSS	AR11/A/861/2054	—
96.5 E	31 DEC 1995	20	EXPRESS-8	USSR	5.7-6.5/ 14.0-14.5/ or	3.4-4.2 10.9-11.2 11.4-11.7	FSS	AR11/A/764/2003	—

TABLE 2. PLANNED GEOSTATIONARY COMMUNICATIONS SATELLITES FOR YEAR-END 1992 (CONT'D)

SUBSATELLITE REGISTERED LONGITUDE (°)	PLANNED IN-USE DATE	PERIOD OF VALIDITY (yrs)	SATELLITE DESIGNATION	ITU REGISTERING COUNTRY	FREQUENCY UP/DOWNLINK (GHz)		SERVICE TYPE	ITU SPECIAL SECTION	
								ADVANCED	COORDINATION
99.0 E	31 DEC 1996	20	EXPRESS-13	USSR	5.7-6.5/ 14.0-14.5/ or	3.4-4.2 10.9-11.2 11.4-11.7	FSS	AR11/A/769/2003	—
100.5 E	1 APR 1993	20	ASIASAT E ASIASAT-EK1	UK Asia Satellite Telecom	5.8-6.7/ 14.0-14.5/ or	3.4-4.2 10.9-11.2 11.4-11.7 12.2-12.7	FSS	AR11/A/750/2001 AR11/A/783/2007	AR11/C/2110/2017 AR11/C/2236/2049
101.0 E	1 JAN 1994	15	THAISAT A1 THAICOM-A1 THAICOM-1	THAILAND Shinawatra Computer	5.9-6.4/ 14.0-14.5/ or	3.7-4.2 10.9-11.2 11.4-11.7 12.2-12.7	FSS	AR11/A/710/1979	AR11/C/2184/2036 AR11/C/2195/2039
101.5 E	15 MAR 1993	20	CHINASAT-11	CHINA	14.0-14.5/	11.4-11.7	FSS	AR11/A/777/2007	—
103.0 E	15 JUN 1992	10	DFH-3-0B	CHINA	5.9-6.4/	3.7-4.2	FSS	AR11/A/469/1850	AR11/C/1955/1983
103.0 E	31 DEC 1995	20	EXPRESS-9	USSR	5.7-6.5/ 14.0-14.5/ or	3.4-4.2 10.9-11.2 11.4-11.7	FSS	AR11/A/765/2003	—
103.0 E	1 AUG 1992	—	VOLNA-103E	USSR	1.6 / 6.0 /	1.5 3.7	FSS MSS	AR11/A/817/2029	—
105.5 E	15 MAR 1994	20	CHINASAT-12	CHINA	14.0-14.5/	11.4-11.7	FSS	AR11/A/778/2007	—
105.5 E	1 APR 1993	20	ASIASAT-CK ASIASAT-CK1	UK	5.8-6.7/ 14.0-14.5/ or	3.4-3.7 10.9-11.2 11.4-11.7 12.2-12.5	FSS	AR11/A/713/1981 AR11/A/781/2007	AR11/C/2037/2004 AR11/C/2234/2049
110.0 E	1 JAN 1998	20	INMARSAT4 GSO-1F	UK Inmarsat	1.6 / 6.4-6.6/	2.5 3.6-3.8	FSS MSS	AR11/A/826/2032	—
110.0 E	1 JAN 1998	20	INMARSAT4 GSO-2F	UK Inmarsat	1.9 / 6.4-6.7/	2.2 3.6-3.9	FSS MSS	AR11/A/833/2032	—
110.0 E	1 MAR 1997	—	JMCS-2	JAPAN	7.9-8.0/	7.3-7.4	FSS MSS	AR11/A/800/2015	—
110.0 E	1 AUG 1996	20	N-SAT-110	JAPAN NTT	14.0-14.5/	12.2-12.7	FSS	AR11/A/753/2001	AR11/C/2121/2023
113.0 E	1 OCT 1995	15	KOREASAT 2 KOREASAT-2	KOREA	14.0-14.5/	12.2-12.7	FSS	AR11/A/707/1975	AR11/C/2086/2010
115.5 E	31 DEC 1992	20	DFH-3-0D	CHINA	5.9-6.4/	3.7-4.2	FSS	AR11/A/535/1900	—
116.0 E	1 APR 1993	20	ASIASAT-BK ASIASAT-BK1	UK	5.8-5.9/ 6.4-6.7/ 14.0-14.5/	3.4-3.7 3.4-3.7 12.2-12.7	FSS	AR11/A/712/1981 AR11/A/780/2007	AR11/C/2036/2004 AR11/C/2233/2049
116.0 E	1 APR 1995	15	KOREASAT 1 KOREASAT-1	KOREA	14.0-14.5/	12.2-12.7	FSS	AR11/A/706/1975	AR11/C/2085/2010
120.0 E	1 JAN 1995	12	SAJAC 2 SJC-2	JAPAN Satellite Japan	14.0-14.5/	12.2-12.7	FSS	AR11/A/745/1999	AR11/C/2088/2012
120.0 E	1 JAN 1994	20	THAISAT A3 THAICOM-3 THAICOM-A3	THAILAND Shinawatra Computer	5.9-6.4/ 14.0-14.5/ or	3.7-4.2 10.9-11.2 11.4-11.7 12.2-12.7	FSS	AR11/A/728/1988	AR11/C/2188/2036 AR11/C/2197/2039
121.0 E	31 DEC 1995	20	DFH-3-0E	CHINA	5.9-6.4/	3.7-4.2	FSS	AR11/A/730/1992	—
122.0 E	1 APR 1993	20	ASIASAT-AK ASIASAT-AK1	UK	5.8-5.9/ 6.4-6.7/ 14.0-14.5/ or	3.4-3.7 3.4-3.7 10.9-11.2 11.4-11.7 12.2-12.7	FSS	AR11/A/711/1981 AR11/A/779/2007	AR11/C/2035/2004 AR11/C/2232/2049
124.0 E	31 DEC 1988	13	SCS-1B	JAPAN	27.5-29.0/ 14.0-14.2/	17.7-19.2 12.5-12.7	FSS	AR11/A/274/1854 AR11/A/274/1708	AR11/C/1387/1860
124.0 E	1 JUL 1994	12	SAJAC 1 SJC-1	JAPAN Satellite Japan	14.0-14.5/	12.2-12.7	FSS	AR11/A/744/1999	AR11/C/2087/2012
125.0 E	15 DEC 1991	10	DFH-3-0A	CHINA	5.9-6.4/	3.7-4.2	FSS	AR11/A/468/1850	AR11/C/1951/1983
128.0 E	1 MAR 1994	20	N-STAR A N-SAT-128	JAPAN NTT	14.0-14.5/	12.2-12.7	FSS	AR11/A/754/2001	AR11/C/2122/2023

SCS SATELLITE	PLANNED	IN-USE	PERIOD OF	REGISTRATION	COUNTRY	FREQUENCY (UP/DOWN) (GHz)	SERVICE	ADVANCED	COORDINATION
REGISTRATION	DATE	DATE	VALIDITY (yrs)	SATELLITE	DESIGNATION		TYPE	CTR SPECIAL SECTION	
128 0 E	30 JUN 1988	30 JUN 1988	20	STATIONAR-D6	USSR	6.4-6.7 /	FSS	AR11/A/198/1675	AR11/C/1173/1796
128 0 E	1 AUG 1990	1 AUG 1990	20	TOR-6	USSR	42.5-43.5 /	FSS	AR11/A/283/1710	AR11/C/1315/1838
128 0 E	1 DEC 1990	1 DEC 1990	20	VOLNA-9M	USSR	1.6 /	MSS	AR11/A/251/1697	AR11/C/1402/1861
130 0 E	15 DEC 1992	15 DEC 1992	10	CHINASAT-4	CHINA	6.0-6.4 /	FSS	AR11/A/733/1996	—
130 0 E	1 NOV 1992	1 NOV 1992	20	TONGASAT AP-1	TONGA	5.9-6.4 /	FSS	AR11/A/512/1893	AR11/C/1720/1941
130 0 E	1 NOV 1993	1 NOV 1993	20	TONGASAT C/KU-1	TONGA	5.9-6.4 /	FSS	AR11/A/646/1957	AR11/C/1963/1984
130 0 E	1 AUG 1990	1 AUG 1990	20	TOR-10	USSR	42.5-43.5 /	FSS	AR11/A/290/1711	AR11/C/1320/1838
132 0 E	1 FEB 1994	1 FEB 1994	20	N-STAR B	JAPAN	2.6 /	FSS	AR11/A/751/2001	AR11/C/2115/2021
132 0 E	1 DEC 1990	1 DEC 1990	20	MILSTAR-7	USA	29-.32 /	MSS	AR11/A/448/1837	AR11/C/1525/1885
133 0 E	1 MAY 1992	1 MAY 1992	10	PALAPA PACIFIC 1	INDONESIA	5.9-6.4 /	FSS	AR11/A/811/2025	—
134 0 E	1 NOV 1992	1 NOV 1992	20	TONGASAT AP-2	TONGA	5.9-6.4 /	FSS	AR11/A/513/1893	AR11/C/1721/1941
134 0 E	1 NOV 1993	1 NOV 1993	20	TONGASAT C/KU-2	TONGA	5.9-6.4 /	FSS	AR11/A/647/1957	AR11/C/1964/1984
136 0 E	1 AUG 1995	1 AUG 1995	20	N-STAR-B	JAPAN	2.6 /	FSS	AR11/A/752/2001	AR11/C/2118/2021
138 0 E	1 NOV 1992	1 NOV 1992	20	TONGASAT AP-3	TONGA	5.9-6.4 /	FSS	AR11/A/514/1893	AR11/C/1722/1941
138 0 E	1 NOV 1994	1 NOV 1994	20	TONGASAT C/KU-3	TONGA	5.9-6.4 /	FSS	AR11/A/648/1957	AR11/C/1965/1984
139 0 E	1 JAN 1994	1 JAN 1994	10	PALAPA PACIFIC 2	INDONESIA	5.9-6.4 /	FSS	AR11/A/812/2025	—
140 0 E	31 DEC 1996	31 DEC 1996	20	EXPRESS-10	USSR	5.7-6.5 /	FSS	AR11/A/766/2003	—
140 0 E	1 SEP 1990	1 SEP 1990	15	MORE-140	USSR	1.6 /	FSS	AR11/A/186/1662	AR11/C/1092/1791
142 0 E	1 JAN 1995	1 JAN 1995	20	THAISAT-A4	THAILAND	5.9-6.4 /	FSS	AR11/A/729/1988	—
142.5 E	1 NOV 1992	1 NOV 1992	20	TONGASAT AP-4	TONGA	5.9-6.4 /	FSS	AR11/A/515/1893	AR11/C/1723/1941
142.5 E	29 JUN 1996	29 JUN 1996	20	TONGASAT C/KU-4	TONGA	5.9-6.4 /	FSS	AR11/A/649/1957	AR11/C/1966/1984
144 0 E	1 AUG 1995	1 AUG 1995	15	PALAPA PACIFIC 3	INDONESIA	5.9-6.4 /	FSS	AR11/A/813/2025	—

TABLE 2. PLANNED GEOSTATIONARY COMMUNICATIONS SATELLITES FOR YEAR-END 1992 (CONT'D)

TABLE 2. PLANNED GEOSTATIONARY COMMUNICATIONS SATELLITES FOR YEAR-END 1992 (CONT'D)

SUBSATELLITE REGISTERED LONGITUDE (°)	PLANNED IN-USE DATE	PERIOD OF VALIDITY (yrs)	SATELLITE DESIGNATION	ITU REGISTERING COUNTRY	FREQUENCY UP/DOWNLINK (GHz)		SERVICE TYPE	ITU SPECIAL SECTION	
								ADVANCED	COORDINATION
145.0 E	31 DEC 1996	20	EXPRESS-11	USSR	5.7-6.5/ 14.0-14.5/ or 11.4-11.7	3.4-4.2 10.9-11.2	FSS	AR11/A/767/2003	—
145.0 E	31 DEC 1992	20	STATSIONAR-16 LOUTCH-10	USSR	6.0-6.2/ 14.0-14.5/ or 11.4-11.7	3.6-3.9 10.9-11.2	FSS	AR11/A/76/1586 AR11/A/677/1960	AR11/C/849/1707 AR11/C/1126/1793 AR11/C/2198/2040
146.0 E	1 OCT 1996	—	JMCS-1	JAPAN	7.9-8.0/	7.3-7.4	FSS	AR11/A/799/2015	—
146.0 E	1 MAR 1994	20	N-SAT-146	JAPAN NTT	14.0-14.5/	12.2-12.7	FSS	AR11/A/755/2001	AR11/C/2123/2023
148.0 E	1 APR 1994	—	MEASAT-2	MALAYSIA	5.9-6.7/ 14.0-14.5/ or 11.4-11.7 or 12.2-12.7	3.4-4.2 10.9-11.2	FSS	AR11/A/853/2053	—
150.0 E	1 AUG 1991	20	MILSTAR-15	USA	.29-.32/ 1.8 / 43.5-45.5/	.24-.27 2.2 20.2-21.2	MSS	AR11/A/456/1837	AR11/C/1557/1885 AR11/C/1660/1919
152.0 E	1 APR 1991	20	MILSTAR-11	USA	.29-.32/ 1.8 / 43.5-45.5/	.24-.27 2.2 20.2-21.2	MSS	AR11/A/452/1837	AR11/C/1541/1885 AR11/C/1656/1919
154.0 E	1 AUG 1992	20	ETS-6-FS ETS-6-I ETS-6-IS ETS-6-MSS	JAPAN	2.0-2.1/ 2.6 / 5.9-6.7/ 27.5-31.0/ 32.0-33.0/ 42.5-43.5/	2.2-2.3 2.5 3.4-4.2 17.7-21.2 22.5-23.5 37.5-39.5	FSS MSS	AR11/A/508/1889 AR11/A/505/1888 AR11/A/507/1888 AR11/A/506/1888	AR11/C/2165/2036 AR11/C/1747/2011 AR11/C/2101/2012 AR11/C/1751/1948
154.0 E	1 AUG 1993	20	ETS-6-FSM ETS-6-ISM	JAPAN	25.2-27.0/	22.5-23.5	FSS	AR11/A/732/1996 AR11/A/731/1993	AR11/C/2177/2036 AR11/C/2183/2036
155.0 E	19 DEC 1998	15	USGCSS PH4 W PAC-1	USA	43.5-45.5/	20.2-21.2	FSS MSS	AR11/A/552/1907	AR11/C/1820/1965 AR11/C/1935/1980
156.0 E	1 APR 1993	15	OPTUS B2 AUSSAT B2 AUSSAT B2 MC AUSSAT B2-MOB AUSSAT B2-NZ AUSSAT B2-S AUSSAT-B 156E MXL	AUSTRALIA Optus Communications	14.0-14.5/ 1.6 /	12.2-12.7 1.5	BSS FSS MSS	AR11/A/361/1779 AR11/A/356/1772 AR11/A/380/1796 AR11/A/435/1828 AR11/A/495/1878 AR11/A/784/2009	AR11/C/1810/1963 AR11/C/1800/1962 AR11/C/2044/2005 AR11/C/1804/1963 AR11/C/1802/1962 AR11/C/2206/2040
158.0 E	1 APR 1989	13	SUPERBIRD-A	JAPAN	27.5-29.1/ 14.0-14.4/ 7.9-8.0/	17.7-19.3 12.3-12.7 7.2-7.3	FSS	AR11/A/340/1762	AR11/C/1303/1836
164.0 E	1 JUL 1996	15	AUSSAT-B 164E AUSSAT-B 164E MOB AUSSAT-B 164E MXL	AUSTRALIA	14.0-14.5/ 1.6 /	12.2-12.7 1.5	FSS MSS	AR11/A/659/1957 AR11/A/660/1957 AR11/A/786/2009	AR11/C/2149/2033 AR11/C/2047/2005 AR11/C/2212/2040
166.0 E	1 JUN 1993	20	USASAT-14H	USA	5.9-6.4/ 14.0-14.5/ or 12.2-12.7	3.7-4.2 11.7-12.2	FSS	AR11/A/737/1997	—
167.0 E	17 OCT 1989	20	VSSRD-2	USSR	14.6/ or 15.0/	11.2 12.6 13.5	FSS	AR11/A/187/1672	—
167.5 E	30 JUN 1991	20	PACSTAR A-1 PACSTAR-1	PAPUA NEW GUINEA	1.6 / 14.0-14.5/ 6.5-7.0/	1.5 12.2-12.7 3.7-4.2	FSS MSS	AR11/A/200/1676 AR11/A/331/1749	AR11/C/1179/1801 AR11/C/1432/1866
168.0 E	1 JUN 1993	20	PANAMSAT 4 PAS-4 USASAT-14G	USA Pan American Satellite	5.9-6.4/ 14.0-14.5/ or 12.2-12.7	3.7-4.2 11.7-12.2	FSS	AR11/A/736/1997	—
170.0 E	3 MAR 1996	10	UNICOM 1 USASAT-13M	USA Unicom Satellite	14.0-14.5/ or 12.5-12.7	11.7-12.2 12.5-12.7	FSS	AR11/A/343/1763	AR11/C/1436/1871
170.7 E	3 FEB 1994	20	TONGASAT C-1 TONGASAT C-1-R	TONGA Friendly Islands Satellite	5.9-6.4/	3.7-4.2	FSS	AR11/A/430/1828	AR11/C/1717/1940
172.0 E	30 NOV 1992	20	FLTSATCOM-C WEST PAC1	USA	1.8 / .29-.32/ 7.9-8.0/ 43.5-45.5/	2.2 .24-.27 7.2-7.3 20.2-21.2	FSS MSS	AR11/A/699/1973	—

TABLE 2. PLANNED GEOSTATIONARY COMMUNICATIONS SATELLITES FOR YEAR-END 1992 (CONT'D)

SUBSATELLITE REGISTERED LONGITUDE (°)	PLANNED IN-USE DATE	PERIOD OF VALIDITY (yrs)	SATELLITE DESIGNATION	ITU REGISTERING COUNTRY	FREQUENCY UP/DOWNLINK (GHz)	SERVICE TYPE	ITU SPECIAL SECTION		
							ADVANCED	COORDINATION	
172.0 E	30 SEP 1994	12	PACIFICOM 1 <i>USASAT-14K</i>	USA TRW	5.9-6.4/ 14.0-14.5/	3.7-4.2 12.0-12.7	FSS	AR11/A/814/2027	—
174.0 E	1 NOV 1992	20	INTELSAT 7 F1 <i>INTELSAT7 174E</i>	USA Intelsat	5.9-6.4/ 14.0-14.5/ or or or	3.7-4.2 10.9-11.2 11.4-11.7 11.7-11.9 12.5-12.7	FSS	AR11/A/509/1889	AR11/C/1754/1949
174.0 E	1 JAN 1996	20	INTELSAT 8 F1 <i>INTELSAT FOS 174E</i>	USA Intelsat	5.8-6.4/ 14.0-14.5/ or or or	3.6-4.2 10.9-12.5 11.4-11.7 11.7-11.9 12.5-12.7	FSS	AR11/A/864/2054	—
175.0 E	31 MAR 1996	15	<i>USGCSS PH3 W PAC</i> <i>USGCSS PH3B W PAC</i>	USA	1.8 / 7.9-8.4/	2.2 7.2-7.7	FSS MSS	AR11/A/266/1706 AR11/A/669/1960	AR11/C/1216/1816 AR11/C/1222/1817 AR11/C/1257/1818
175.0 E	30 NOV 1996	15	<i>USGCSS PH4 WPAC-3</i>	USA	43.5-45.5/ 1.8 /	20.2-21.2 2.2	FSS MSS	AR11/A/726/1986	—
177.0 E	1 APR 1993	20	INTELSAT 7 F3 <i>INTELSAT7 177E</i>	USA Intelsat	5.9-6.4/ 14.0-14.5/ or or or	3.7-4.2 10.9-11.2 11.4-11.7 11.7-11.9 12.5-12.7	FSS	AR11/A/510/1889	AR11/C/1755/1949
177.0 E	1 JAN 1996	20	INTELSAT 8 F2 <i>INTELSAT FOS 177E</i>	USA Intelsat	5.8-6.4/ 14.0-14.5/ or or or	3.6-4.2 10.9-11.2 11.4-11.7 11.7-11.9 12.5-12.7	FSS	AR11/A/865/2054	—
177.5 E	1 JUL 1991	20	<i>MILSTAR-14</i>	USA	29-.32/ 1.8 / 43.5-45.5/	24-.27 2.2 20.2-21.2	MSS	AR11/A/455/1837	AR11/C/1553/1885 AR11/C/1659/1919
178.0 E	1 APR 1996	20	<i>INMARSAT3 POR-2</i>	UK Inmarsat	1.6 / 6.2 / 6.4 /	1.5 3.9 3.6	FSS MSS	AR11/A/790/2011	AR11/C/2228/2043
179.0 E	31 MAR 1995	20	<i>INMARSAT3 POR-1</i>	UK Inmarsat	1.6 / 6.2 / 6.4 /	1.5 3.9 3.6	FSS MSS	AR11/A/599/1637	AR11/C/1996/1989
179.0 E	1 JAN 1998	20	<i>INMARSAT4 GSO-1G</i>	UK Inmarsat	1.6 / 6.4-6.6/	2.5 3.6-3.8	FSS MSS	AR11/A/827/2032	—
179.0 E	1 JAN 1998	20	<i>INMARSAT4 GSO-2G</i>	UK Inmarsat	1.9 / 6.4-6.7/	2.2 3.6-3.9	FSS MSS	AR11/A/834/2032	—
180.0 E	30 NOV 1996	15	<i>USGCSS PH3</i> <i>W PAC-2</i> <i>USGCSS PH3B</i> <i>W PAC-2</i>	USA	1.8 / 7.9-8.4/	2.2 7.2-7.7	FSS MSS	AR11/A/408/1806 AR11/A/718/1986	—
180.0 E	20 NOV 1996	15	<i>USGCSS PH4</i> <i>W PAC-2</i>	USA	43.5-45.5/ 1.8 /	20.2-21.2 2.2	FSS MSS	AR11/A/725/1986	—
180.0 E	15 AUG 1994	20	INTELSAT 7 F1 <i>INTELSAT7 180E</i>	USA Intelsat	5.9-6.4/ 14.0-14.5/ or or or	3.7-4.2 10.9-11.2 11.4-11.7 11.7-11.9 12.5-12.7	FSS	AR11/A/511/1889	AR11/C/1756/1949
182.0 E (178.0 W)	1 JUL 1990	10	<i>USASAT-13K</i>	USA	5.9-6.4/	3.7-4.2	FSS	AR11/A/264/1703	AR11/C/945/1763
183.0 E (177.0 W)	30 NOV 1992	20	<i>FLTSATCOM-C</i> <i>W PAC2</i>	USA	.29-.32/ 1.8 / 7.9-8.0/ 43.5-45.5/	.24-.27 2.2 7.2-7.3 20.2-21.2	FSS MSS	AR11/A/700/1973	—
183.0 E (177.0 W)	1 JUN 1996	20	<i>INTELSAT7 183E</i>	USA Intelsat	5.9-6.4/ 14.0-14.5/ or or or	3.7-4.2 10.9-11.2 11.4-11.7 11.7-11.9 12.5-12.7	FSS	AR11/A/663/1957	AR11/C/2003/1990
185.0 E (175.0 W)	30 JUN 1991	20	<i>PACSTAR A-2</i> <i>PACSTAR-2</i>	PAPUA NEW GUINEA	6.4-7.0/ 14.0-14.5/	3.6-4.2 11.7-12.7	FSS MSS	AR11/A/201/1676 AR11/A/332/1749	AR11/C/1180/1801 AR11/C/1434/1866

TABLE 2. PLANNED GEOSTATIONARY COMMUNICATIONS SATELLITES FOR YEAR-END 1992 (CONT'D)

SUBSATELLITE REGISTERED LONGITUDE (°)	PLANNED IN-USE DATE	PERIOD OF VALIDITY (yrs)	SATELLITE DESIGNATION	ITU REGISTERING COUNTRY	FREQUENCY UP/DOWNLINK (GHz)		SERVICE TYPE	ITU SPECIAL SECTION	
								ADVANCED	COORDINATION
190.0 E (170.0 W)	30 JUN 1988	20	STATSIONAR-D2	USSR	6.4-6.7/	4.5-4.8	FSS	AR11/A/194/1675	AR11/C/1169/1796
190.0 E (170.0 W)	1 AUG 1990	20	TOR-5	USSR	42.5-43.5/ 43.5-45.5/	18.2-20.2 20.2-21.2	FSS MSS	AR11/A/282/1710	AR11/C/1351/1851
192.0 E (168.0 W)	1 JUN 1990	10	FOTON-3	USSR	6.5-6.6/	4.6-4.7	FSS	AR11/A/237/1692	—
195.0 E (165.0 W)	1 SEP 1991	10	USASAT-13L CCC-1	USA Columbia Communications	14.0-14.5/ or	10.7-11.2 11.7-12.2	FSS	AR11/A/354/1770	—
200.0 E (160.0 W)	1 MAY 1993	—	MARAFON-4	USSR	1.6-1.7/ 5.7-6.4/	1.5-1.6 3.4-4.1	FSS MSS	AR11/A/840/2035	—
205.0 E (155.0 W)	31 DEC 1996	20	EXPRESS-12	USSR	5.7-6.5/ 14.0-14.5/ or	3.4-4.2 10.9-11.2 11.4-11.7	FSS	AR11/A/768/2003	—
212.0 E (148.0 W)	1 MAY 1991	20	MILSTAR-12	USA	.29-.32/ 1.8 / 43.5-45.5/	.24-.27 2.2 20.2-21.2	MSS	AR11/A/453/1837	AR11/C/1545/1885 AR11/C/1657/1919
214.0 E (146.0 W)	JUN 1985	10	AMIGO-2	MEXICO	17.3-18.1/	12.2-12.7	BSS FSS	RES33/A/2/1560	—
214.0 E (146.0 W)	15 NOV 1990	10	USASAT-20C	USA	5.9-6.4/	3.7-4.2	FSS	AR11/A/259/1702	AR11/C/970/1769
215.0 E (145.0 W)	1 DEC 1990	20	VOLNA-21M	USSR	1.6 /	1.5	MSS	AR11/A/252/1697	AR11/C/1404/1861
215.0 E (145.0 W)	30 NOV 1992	20	FLTSATCOM-C W PAC3	USA	.29-.32/ 1.8 / 7.9-8.0/ 43.5-45.5/	.24-.27 2.2 7.2-7.3 20.2-21.2	FSS MSS	AR11/A/701/1973	—

216.0 E (144.0 W)	30 JUN 1990	10	USASAT-20B	USA	5.9-6.4/	3.7-4.2	FSS	AR11/A/258/1702	—
220.0 E (140.0 W)	31 DEC 1989	10	USASAT-17C	USA	5.9-6.4/	3.7-4.2	FSS	AR11/A/228/1687	AR11/C/933/1761
221.0 E (139.0 W)	10 SEP 1990	15	AMSC 3 ACS-3	USA American Mobile Satellite	1.6 /	1.5	MSS	AR11/A/303/1723	AR11/C/1110/1792
221.0 E (139.0 W)	1 JUL 1997	—	MCS-3	USA	1.6 /	1.5	MSS	AR11/A/881/2058	—
222.0 E (138.0 W)	1 DEC 1996	12	SOLIDARIDAD KU	MEXICO	14.0-14.5/	11.7-12.2	FSS	AR11/A/772/2005	—
224.0 E (136.0 W)	JUN 1985	10	AMIGO-1	MEXICO	17.3-18.1/	12.2-12.7	BSS FSS	RES32/A/1/1560	—
224.0 E (136.0 W)	31 JAN 1990	10	USASAT-16D	USA	14.0-14.5/	11.7-12.2	FSS	AR11/A/225/1687	AR11/C/1000/1772
225.0 E (135.0 W)	1 JUN 1983	10	USGCSS PH3 E PAC USGCSS PH3B E PAC	USA	1.8 / 7.9-8.4/	2.2 7.2-7.7	FSS	SPA-AA/248/1413 SPA-AA/349/1493 AR11/A/668/1960	SPA-AJ/344/1499 AR11/C/405/1629 AR11/C/454/1645
225.0 E (135.0 W)	30 NOV 1996	15	USGCSS PH4 E PAC-3	USA	43.5-45.5/ 1.8 /	20.2-21.2 2.2	FSS MSS	AR11/A/724/1986	—
226.0 E (134.0 W)	31 JAN 1990	10	USASAT-16C	USA	14.0-14.5/	11.7-12.2	FSS	AR11/A/224/1687	AR11/C/1064/1783
227.0 E (133.0 W)	19 APR 1994	12	USASAT-22A GALAXY IR	USA Hughes Communications	5.9-6.4/	3.7-4.2	FSS	AR11/A/536/1903	AR11/C/1777/1954 AR11/C/1778/1954
228.0 E (132.0 W)	15 MAR 1987	10	USASAT-11C WESTAR-B	USA	14.0-14.5/	11.7-12.2	FSS	AR11/A/111/1609	AR11/1063/1782
229.0 E (131.0 W)	1 APR 1996	12	USASAT-23B	USA	14.0-14.5/	11.7-12.2	FSS	AR11/A/640/1946	—
230.0 E (130.0 W)	15 JUN 1987	20	USASAT-10D	USA	14.0-14.5/	11.7-12.2	FSS	AR11/A/108/1609	AR11/C/1057/1781

TABLE 2. PLANNED GEOSTATIONARY COMMUNICATIONS SATELLITES FOR YEAR-END 1992 (CONT'D)

SUBSATELLITE REGISTERED LONGITUDE (°)	PLANNED IN-USE DATE	PERIOD OF VALIDITY (yrs)	SATELLITE DESIGNATION	ITU REGISTERING COUNTRY	FREQUENCY UP/DOWNLINK (GHz)		SERVICE TYPE	ITU SPECIAL SECTION	
								ADVANCED	COORDINATION
230.0 E (130.0 W)	30 NOV 1996	15	USGCSS PH3 E PAC-2 USGCSS PH3B E PAC-2	USA	1.8 / 7.9-8.4/	2.2 7.2-7.7	FSS MSS	AR11/A/407/1806 AR11/A/717/1986	—
230.0 E (130.0 W)	30 NOV 1996	15	USGCSS PH4 E PAC-2	USA	43.5-45.5/ 1.8 /	20.2-21.2 2.2	FSS MSS	AR11/A/723/1986	—
230.0 E (130.0 W)	15 JUN 1992	10	USRDSS WEST	USA	1.6 / 6.5 /	2.5 5.1	FSS MSS	AR11/A/176/1641	—
231.0 E (129.0 W)	18 JUL 1994	10	USASAT-24A	USA	5.9-6.4/ 14.0-14.5/	3.7-4.2 11.7-12.2	FSS	AR11/A/577/1912	AR11/C/1873/1970
233.0 E (127.0 W)	31 AUG 1993	10	USASAT-21B	USA	5.9-6.4/	3.7-4.2	FSS	AR11/A/484/1864	—
234.0 E (126.0 W)	15 SEP 1987	20	USASAT-10C	USA	14.0-14.5/	11.7-12.2	FSS	AR11/A/107/1609	AR11/C/989/1769
236.0 E (124.0 W)	1 NOV 1988	10	USASAT-10B	USA	14.0-14.5/	11.7-12.2	FSS	AR11/A/106/1609	AR11/C/1054/1781
239.0 E (121.0 W)	18 JUL 1994	10	GTE GSTAR 1R USASAT-23C	USA GTE Spacenet	14.0-14.5/	11.7-12.2	FSS	AR11/A/575/1912	AR11/C/1759/1952 AR11/C/1760/1952
240.0 E (120.0 W)	1 NOV 1990	20	MILSTAR-6	USA	29-.32/ 1.8 / 43.5-45.5/	.24-.27 2.2 20.2-21.2	MSS	AR11/A/447/1837	AR11/C/1522/1885 AR11/C/1651/1919
241.0 E (119.0 W)	30 NOV 1991	10	OMRDSS WEST	USA	1.6 / 6.5 /	2.5 5.1	FSS MSS	AR11/A/458/1839	—
247.0 E (113.0 W)	31 JUL 1994	14	SOLIDARIDAD F2 SOLIDARIDAD-2 SOLIDARIDAD 2M SOLIDARIDAD 2MA	MEXICO	1.6 / 14.0-14.5/ 5.9-6.4/	1.5 11.7-12.2 3.7-4.2	FSS MSS	AR11/A/873/2055 AR11/A/28/1539 AR11/A/738/1997	AR11/C/2240/2056
250.8 E (109.2 W)	31 JUL 1994	14	SOLIDARIDAD F1 SOLIDARIDAD-1 SOLIDARIDAD 1M SOLIDARIDAD 1MA	MEXICO	1.6 / 14.0-14.5/ 5.9-6.4/	1.5 11.7-12.2 3.7-4.2	FSS MSS	AR11/A/872/2055 AR11/A/466/1840 AR11/A/735/1996	AR11/C/2190/2039
251.0 E (109.0 W)	19 DEC 1988	15	USGCSS PH4 E PAC-1	USA	1.8 / 43.5-45.5/	2.2 20.2-21.2	FSS MSS	AR11/A/551/1907	AR11/C/1927/1980 AR11/C/1931/1980
251.0 E (109.0 W)	21 MAR 1994	12	SIMON BOLIVAR-3	VENEZUELA ASETA	5.9-6.4/	3.7-4.2	FSS	AR11/A/574/1912	AR11/C/1818/1964
253.5 E (106.5 W)	1 JAN 1997	10	MSAT MSAT-1A	CANADA Telesat Mobile	1.6 / 14.0 / 14.5 /	1.5 11.7 12.2	MSS	AR11/A/56/1563 AR11/A/300/1723 AR11/A/438/1831 AR11/A/806/2022	AR11/C/936/1761 AR11/C/1774/1954
254.0 E (106.0 W)	21 MAR 1994	10	SIMON BOLIVAR-1	VENEZUELA ASETA	5.9-6.4/	3.7-4.2	FSS	AR11/A/422/1817	AR11/C/1816/1964
255.0 E (105.0 W)	30 NOV 1992	20	FLTSATCOM-C E PAC1	USA	.29-.32/ 1.8 / 7.9-8.0/ 43.5-45.5/	.24-.27 2.2 7.2-7.3 20.2-21.2	FSS MSS	AR11/A/697/1973	—
257.0 E (103.0 W)	18 JUL 1994	10	GTE SPACENET 1R USASAT-24B	USA GTE Spacenet	5.9-6.4/ 14.0-14.5/	3.7-4.2 11.7-12.2	FSS	AR11/A/578/1912	AR11/C/1761/1952 AR11/C/1762/1952
257.0 E (103.0 W)	21 MAR 1994		SIMON BOLIVAR-2	VENEZUELA ASETA	5.9-6.4/	3.7-4.2	FSS	AR11/A/573/1912	AR11/C/1817/1964
259.0 E (101.0 W)	30 MAY 1994		MCS-1	USA	1.6 /	1.5	MSS	AR11/A/849/2048	—
259.0 E (101.0 W)	1 JUL 1990	10	USASAT-16B	USA	14.0-14.5/	11.7-12.2	FSS	AR11/A/223/1687	AR11/C/999/1772
259.0 E (101.0 W)	1 JUL 1990	10	USASAT-17A	USA	5.9-6.4/	3.7-4.2	FSS	AR11/A/226/1687	AR11/C/931/1755
260.0 E (100.0 W)	10 SEP 1990	15	AMSC 1 ACS-1	USA American Mobile Satellite	1.6 /	1.5	MSS	AR11/A/301/1723	AR11/C/1106/1792

TABLE 2. PLANNED GEOSTATIONARY COMMUNICATIONS SATELLITES FOR YEAR-END 1992 (CONT'D)

SUBSATELLITE REGISTERED LONGITUDE (°)	PLANNED IN-USE DATE	PERIOD OF VALIDITY (yrs)	SATELLITE DESIGNATION	ITU REGISTERING COUNTRY	FREQUENCY UP/DOWNLINK (GHz)		SERVICE TYPE	ITU SPECIAL SECTION	
								ADVANCED	COORDINATION
260.0 E (100.0 W)	31 AUG 1992	10	ACTS	USA	29.0-30.0/	19.2-20.2	FSS	AR11/A/321/1744	AR11/C/2082/2009
260.0 E (100.0 W)	30 NOV 1992	20	FLTSATCOM-C EPAC2	USA	.29-.32/ 1.8 / 7.9-8.0/ 43.5-45.5/	.24-.27 2.2 7.2-7.3 20.2-21.2	FSS MSS	AR11/A/698/1973	—
260.0 E (100.0 W)	30 SEP 1987	10	USRDSS CENTRAL	USA	1.6 / 6.5 /	2.5 5.1	FSS	AR11/A/175/1641	—
261.0 E (99.0 W)	19 APR 1994	12	GALAXY 4H USASAT-24J	USA Hughes Communications	14.0-14.5/ 5.9-6.4/	11.7-12.2 3.7-4.2	FSS	AR11/A/538/1903 AR11/A/605/1921	AR11/C/2030/2002
263.0 E (97.0 W)	30 APR 1989	10	STSC-2	CUBA	5.9-6.4/	3.7-4.2	FSS	AR11/A/268/1706	—
263.0 E (97.0 W)	1 MAY 1993	10	USASAT-24D TELSTAR 401	USA AT&T	5.9-6.4/ 14.0-14.5/	3.7-4.2 11.7-12.2	FSS	AR11/A/542/1903	AR11/C/2075/2009
265.0 E (95.0 W)	19 APR 1994	12	GALAXY 3H USASAT-22D	USA Hughes Communications	5.9-6.4/ 14.0-14.5/	3.7-4.2 11.7-12.2	FSS	AR11/A/35/1553 AR11/A/539/1903	AR11/C/331/1624 AR11/C/1793/1955
270.0 E (90.0 W)	1 JAN 1998	20	INMARSAT4 GSO-1A	UK Inmarsat	1.6 / 6.4-6.6/	2.5 3.6-3.8	FSS MSS	AR11/A/821/2032	—
270.0 E (90.0 W)	1 JAN 1998	20	INMARSAT4 GSO-2A	UK Inmarsat	1.9 / 6.4-6.7/	2.2 3.6-3.9	FSS MSS	AR11/A/828/2032	—
270.0 E (90.0 W)	1 JUN 1990	20	MILSTAR-1	USA	.29-.32/ 1.8 / 43.5-45.5/	.24-.27 2.2 20.2-21.2	MSS	AR11/A/442/1837	AR11/C/1501/1885 AR11/C/1646/1919
271.0 E (89.0 W)	30 NOV 1991	10	OMRDSS EAST	USA	1.6 / 6.5 /	2.5 5.1	FSS	AR11/A/457/1839	—
271.0 E (89.0 W)	1 MAR 1994	10	USASAT-24E TELSTAR 402	USA AT&T	5.9-6.4/ 14.0-14.5/	3.7-4.2 11.7-12.2	FSS	AR11/A/543/1903	AR11/C/2104/2016
271.0 E (89.0 W)	30 JUN 1990	10	SIMON BOLIVAR-B CONDOR-B	VENEZUELA ASETA	5.9-6.4/	3.7-4.2	FSS	AR11/A/209/1679	—
271.5 E (88.5 W)	SEP 1985	10	USASAT-12D	USA	5.9-6.4/	3.7-4.2	FSS	AR11/A/124/1615	—
273.0 E (87.0 W)	15 JUN 1985	10	USASAT-9B	USA	14.0-14.5/	11.7-12.2	FSS	AR11/A/102/1609	—
275.0 E (85.0 W)	25 JUN 1994	10	NAHUEL-2	ARGENTINA	14.0-14.5/	11.7-12.2	FSS	AR11/A/204/1677	—
277.0 E (83.0 W)	MAR 1988	10	STSC-1	CUBA	5.9-6.4/	3.7-4.2	FSS	AR11/A/58/1578	—
277.0 E (83.0 W)	18 JUL 1994	10	USASAT-24C	USA	5.9-6.4/ 14.0-14.5/	3.7-4.2 11.7-12.2	FSS	AR11/A/579/1912	—
279.0 E (81.0 W)	19 APR 1994	12	USASAT-22F	USA	5.9-6.4/	3.7-4.2	FSS	AR11/A/541/1903	AR11/C/1790/1955
280.0 E (80.0 W)	25 JUN 1994	10	NAHUEL-1	ARGENTINA	14.0-14.5/	11.7-12.2	FSS	AR11/A/203/1677	—
281.0 E (79.0 W)	15 MAR 1987	10	USASAT-11A	USA	14.0-14.5/	11.7-12.2	FSS	AR11/A/109/1609	AR11/C/991/1769
281.0 E (79.0 W)	1 OCT 1987	10	USASAT-12A	USA	5.9-6.4/	3.7-4.2	FSS	AR11/A/121/1615	AR11/C/892/1743
281.0 E (79.0 W)	19 APR 1994	12	GE SATCOM H-1 USASAT-24F	USA GE American Communications	14.0-14.5/ 5.9-6.4/	11.7-12.2 3.7-4.2	FSS	AR11/A/544/1903	AR11/C/1704/1929
282.5 E (77.5 W)	30 JUN 1990	10	SIMON BOLIVAR-A CONDOR-A	VENEZUELA ASETA	5.9-6.4/	3.7-4.2	FSS	AR11/A/208/1679	—
283.0 E (77.0 W)	1 FEB 1989	10	USASAT-11B	USA	14.0-14.5/	11.7-12.2	FSS	AR11/A/110/1609	AR11/C/1060/1782
284.0 E (76.0 W)	15 SEP 1983	7	USASAT-12C	USA	5.9-6.4/	3.7-4.2	FSS	AR11/A/123/1615	AR11/C/907/1748

TABLE 2. PLANNED GEOSTATIONARY COMMUNICATIONS SATELLITES FOR YEAR-END 1992 (CONT'D)

SUBSATELLITE REGISTERED LONGITUDE (°)	PLANNED IN-USE DATE	PERIOD OF VALIDITY (YRS)	SATELLITE DESIGNATION	ITU REGISTERING COUNTRY	FREQUENCY UP/DOWNLINK (GHz)		SERVICE TYPE	ITU SPECIAL SECTION	
								ADVANCED	COORDINATION
284.6 E (75.4 W)	1 MAR 1993	10	COLOMBIA 1A	COLOMBIA	5.8-6.4/	3.6-4.2	FSS	AR11/A/428/1825	—
285.0 E (75.0 W)	1 MAR 1993	10	COLOMBIA 2	COLOMBIA	5.8-6.4/	3.6-4.2	FSS	AR11/A/429/1825	—
285.0 E (75.0 W)	31 JAN 1990	10	USASAT-18A	USA	14.0-14.5/	11.7-12.2	FSS	AR11/A/230/1687	AR11/C/1002/1773
286.0 E (74.0 W)	19 APR 1994	12	USASAT-22E	USA	5.9-6.4/	3.7-4.2	FSS	AR11/A/540/1903	AR11/C/1796/1955
287.0 E (73.0 W)	1 JAN 1990	10	USASAT-18B	USA	14.0-14.5/	11.7-12.2	FSS	AR11/A/231/1687	AR11/C/1004/1773
288.0 E (72.0 W)	15 SEP 1990	15	ACS-2	USA	1.6 /	1.5	MSS	AR11/A/302/1723	AR11/C/1108/1792
288.0 E (72.0 W)	30 JUN 1990	10	SIMON BOLIVAR-C CONDOR-C	VENEZUELA ASETA	5.9-6.4/	3.7-4.2	FSS	AR11/A/210/1679	—
289.0 E (71.0 W)	31 JAN 1990	20	USASAT-18C	USA	14.0-14.5/	11.7-12.2	FSS	AR11/A/232/1687	AR11/C/1005/1773
290.0 E (70.0 W)	31 DEC 1989	7	SATS-1	BRAZIL	5.9-6.4/	3.7-4.2	FSS	AR11/A/399/1802	AR11/C/1461/1874
290.0 E (70.0 W)	30 JUN 1995	15	BRAZILSAT B1 SBTS-B1	BRAZIL	5.8-6.4/	3.6-4.2	FSS	AR11/A/629/1934	—
290.0 E (70.0 W)	30 JUN 1993	15	SISCOMIS-3	BRAZIL	8.0 /	7.3	FSS MSS	AR11/A/499/1882	AR11/C/2161/2033
290.0 E (70.0 W)	15 JUL 1991	10	USRDSS EAST	USA	1.6 / 6.5 /	2.5 5.1	FSS MSS	AR11/A/174/1641	—
291.0 E (69.0 W)	1 APR 1996	10	GTE SPACENET 2R USASAT-24H	USA	5.9-6.4/ 14.0-14.5/	3.7-4.2 11.7-12.2	FSS	AR11/A/643/1947	AR11/C/2038/2004

292.0 E (68.0 W)	1 JAN 1991	20	MILSTAR-8	USA	.29-.32/ 1.8 / 43.5-45.5/	.24-.27 2.2 20.2-21.2	MSS	AR11/A/449 1837	AR11/C/1529/1885 AR11/C/1653/1919
293.0 E (67.0 W)	3 APR 1987	10	USASAT-15D	USA	14.0-14.5/	11.7-12.2	FSS	AR11/A/165/1637	AR11/C/997/1770
295.0 E (65.0 W)	31 DEC 1989	7	SATS-2	BRAZIL	5.9-6.4/	3.7-4.2	FSS	AR11/A/400/1802	AR11/C/1462/1874
295.0 E (65.0 W)	30 JUN 1992	15	BRAZILSAT B2 SBTS B2	BRAZIL	5.8-6.4/	3.6-4.2	FSS	AR11/A/367/1785	—
295.0 E (65.0 W)	30 JUN 1992	15	SBTS C2	BRAZIL	14.0-14.5/	11.7-12.2	FSS	AR11/A/369/1785	—
295.0 E (65.0 W)	30 JUN 1993	15	SISCOMIS 2	BRAZIL	8.0 /	7.3	FSS MSS	AR11/A/498/1882	AR11/C/2157/2033
296.0 E (64.0 W)	30 NOV 1990	10	USASAT-14D	USA	5.9-6.4/	3.7-4.2	FSS	AR11/A/161/1637	AR11/C/930/1755
296.0 E (64.0 W)	30 NOV 1990	10	USASAT-15C	USA	14.0-14.5/	11.7-12.2	FSS	AR11/A/164/1637	AR11/C/996/1770
298.0 E (62.0 W)	1 NOV 1994	15	AMSC 2 ACS-2A	USA American Mobile Satellite	1.6 /	1.5	MSS	AR11/A/603/1920	—
298.0 E (62.0 W)	1 JUL 1992	10	USASAT-14C	USA	5.9-6.4/	3.7-4.2	FSS	AR11/A/160/1637	AR11/C/2215/2041
298.0 E (62.0 W)	9 SEP 1989	10	USASAT-15B	USA	14.0-14.5/	11.7-12.2	FSS	AR11/A/163/1637	AR11/C/993/1770
298.0 E (62.0 W)	1 JUL 1995	—	MCS-2	USA	1.6 /	1.5	MSS	AR11/A/880/2058	—
299.0 E (61.0 W)	30 JUN 1992	15	BRAZILSAT B3 SBTS B3	BRAZIL	5.8-6.4/	3.6-4.2	FSS	AR11/A/368/1785	—
299.0 E (61.0 W)	30 JUN 1992	15	BRAZILSAT C3 SBTS C3	BRAZIL	14.0-14.5/	11.7-12.2	FSS	AR11/A/370/1785	—

TABLE 2. PLANNED GEOSTATIONARY COMMUNICATIONS SATELLITES FOR YEAR-END 1992 (CONT'D)

SUBSATELLITE REGISTERED LONGITUDE (°)	PLANNED IN-USE DATE	PERIOD OF VALIDITY (yrs)	SATELLITE DESIGNATION	ITU REGISTERING COUNTRY	FREQUENCY UP/DOWNLINK (GHz)		SERVICE TYPE	ITU SPECIAL SECTION	
								ADVANCED	COORDINATION
299.0 E (61.0 W)	30 JUN 1993	15	SISCOMIS	BRAZIL	8.0 /	7.3	FSS MSS	AR11/A/497/1882	AR11/C/2153/2033
300.0 E (60.0 W)	1 SEP 1991	8	SATCOM PHASE-3B	BELGIUM NATO	8.0-8.2/	7.2-7.3	FSS	AR11/A/358/1773	AR11/C/2111/2018
300.0 E (60.0 W)	31 DEC 1988	10	USASAT-15A	USA	14.0-14.5/	11.7-12.2	FSS	AR11/A/162/1637	—
300.0 E (60.0 W)	31 DEC 1989	10	USASAT-17D	USA	5.9-6.4/	3.7-4.2	FSS	AR11/A/229/1687	—
300.0 E (60.0 W)	20 MAY 1994	15	USASAT-25H	USA	5.9-6.4/	3.7-4.2	FSS	AR11/A/562/1911	AR11/C/1831/1966
300.0 E (60.0 W)	20 MAY 1994	15	USASAT-26H	USA	14.0-14.5/ or 11.4-11.7 or 11.7-12.2 or 12.5-12.7	10.9-11.2	FSS	AR11/A/570/1911	AR11/C/1839/1967
302.0 E (58.0 W)	15 MAY 1993	10	USASAT-13E	USA	14.0-14.5/	11.7-12.2	FSS	AR11/A/136/1620	AR11/C/702/1670
302.0 E (58.0 W)	20 MAY 1994	15	USASAT-25G	USA	5.9-6.4/	3.7-4.2	FSS	AR11/A/561/1911	AR11/C/1830/1966
302.0 E (58.0 W)	30 JAN 1990	10	USASAT-26G	USA	14.0-14.5/ or 11.4-11.7 or 11.7-12.2 or 12.5-12.7	10.9-11.2	FSS	AR11/A/569/1911	AR11/C/1838/1967
303.0 E (57.0 W)	30 SEP 1987	10	USASAT-13H	USA	5.9-6.9/ or 10.7-11.2	3.7-4.2	FSS	AR11/A/177/1643	—
304.0 E (56.0 W)	30 JUL 1988	10	USASAT-13D	USA	14.0-14.5/ or 12.5-12.7	10.7-10.9	FSS	AR11/A/135/1620	AR11/C/701/1670
304.0 E (56.0 W)	20 MAY 1994	15	USASAT-25F	USA	5.9-6.4/	3.7-4.2	FSS	AR11/A/560/1911	AR11/C/1829/1966
304.0 E (56.0 W)	30 JAN 1996	10	USASAT-26F	USA	14.0-14.5/ or 11.4-11.7 or 11.7-12.2 or 12.5-12.7	10.9-11.2	FSS	AR11/A/568/1911	AR11/C/1837/1967
305.0 E (55.0 W)	31 JUL 1995	20	INMARSAT3 AOR-WEST	UK Inmarsat	1.6 / 6.2 / 6.4 /	1.5 3.9 3.6	FSS MSS	AR11/A/597/1920	AR11/C/1986/1989
305.0 E (55.0 W)	1 JAN 1998	20	INMARSAT4 GSO-1B	UK Inmarsat	1.6 / 6.4-6.6/	2.5 3.6-3.8	FSS MSS	AR11/A/822/2032	—
305.0 E	1 JAN 1998	20	INMARSAT4 GSO-2B	UK Inmarsat	1.9 / 6.4-6.7/	2.2 3.6-3.9	FSS MSS	AR11/A/829/2032	—
305.0 E (55.0 W)	31 DEC 1988	10	USASAT-14B	USA	5.9-6.4/	3.7-4.2	FSS	AR11/A/159/1637	—
306.5 E (53.5 W)	1 JUN 1996	20	INMARSAT3 AOR-WEST-2	UK Inmarsat	1.6 / 6.2 / 6.4 /	1.5 3.9 3.6	FSS MSS	AR11/A/789/2011	AR11/C/2216/2043
307.0 E (53.0 W)	1 MAY 1993	20	INTELSAT 7A F6 INTELSAT7 307E	USA Intelsat	5.9-6.4/ 14.0-14.5/ or 11.4-11.7 or 11.7-11.9 or 12.5-12.7	3.7-4.2 10.9-11.2	FSS	AR11/A/530/1898	AR11/C/1882/1976
307.5 E (52.5 W)	31 MAR 1996	15	USGCSS PH3 W ATL USGCSS PH3B W ATL	USA	1.8 / 7.9-8.4/	2.2 7.2-7.7	FSS MSS	AR11/A/173/1639 AR11/A/667/1960	AR11/C/904/1746 AR11/C/1018/1777 AR11/C/1020/1777
307.5 E (52.5 W)	30 NOV 1996	15	USGCSS PH4 W ATL	USA	1.8 / 43.5-45.5/	2.2 20.2-21.2	FSS MSS	AR11/A/722/1986	—
310.0 E (50.0 W)	1 MAY 1993	10	USASAT-13C	USA	14.0-14.5/ or 11.4-11.7	10.9-11.2	FSS	AR11/A/134/1618	AR11/C/748/1675

TABLE 2. PLANNED GEOSTATIONARY COMMUNICATIONS SATELLITES FOR YEAR-END 1992 (CONT'D)

SUBSATELLITE REGISTERED LONGITUDE (°)	PLANNED IN-USE DATE	PERIOD OF VALIDITY (yrs)	SATELLITE DESIGNATION	ITU REGISTERING COUNTRY	FREQUENCY UP/DOWNLINK (GHz)		SERVICE TYPE	ITU SPECIAL SECTION	
								ADVANCED	COORDINATION
310.0 E (50.0 W)	1 MAR 1996	20	INTELSAT7 310E	USA Intelsat	5.9-6.4/ 14.0-14.5/ or or or	3.7-4.2 10.9-11.2 11.4-11.7 11.7-11.9 12.5-12.7	FSS	AR11/A/581/1914	AR11/C/1883/1976
313.0 E (47.0 W)	1 MAY 1993	10	USASAT-13B ORION-2	USA Orion Satellite	14.0-14.5/ or or or	10.9-11.2 11.4-11.7 11.7-12.2 12.5-12.7	FSS	AR11/A/133/1618	AR11/C/747/1675 AR11/C/1712/1939
313.0 E (47.0 W)	1 AUG 1990	10	USASAT-13J	USA	5.9-6.4/	3.7-4.2	FSS	AR11/A/263/1703	AR11/C/944/1763
313.0 E (47.0 W)	20 MAY 1994	15	USASAT-25E	USA	5.9-6.4/	3.7-4.2	FSS	AR11/A/559/1911	AR11/C/1828/1966
313.0 E (47.0 W)	10 JUN 1994	15	USASAT-26E	USA	14.0-14.5/ or or or	10.9-11.2 11.4-11.7 11.7-12.2 12.5-12.7	FSS	AR11/A/567/1911	AR11/C/1836/1967
315.0 E (45.0 W)	20 MAY 1994	15	USASAT-25D	USA	5.9-6.4/	3.7-4.2	FSS	AR11/A/558/1911	AR11/C/1827/1966
315.0 E (45.0 W)	10 JUN 1994	15	USASAT-26D	USA	14.0-14.5/ or or or	10.9-11.2 11.4-11.7 11.7-12.2 12.5-12.7	FSS	AR11/A/566/1911	AR11/C/1835/1967
316.0 E (44.0 W)	1 APR 1996	15	EDRSS-W	FRANCE ESA	2.0-2.1/ 27.5-30.0/	2.2-2.3 18.1-20.2	FSS	AR11/A/633/1935	—
316.5 E (43.5 W)	1 JAN 1988	10	VIDEOSAT-3	FRANCE	2.0 / 14.0-14.2/ or	2.2 11.7-11.9 12.5-12.7	FSS	AR11/A/148/1631	AR11/C/766/1678
317.0 E (43.0 W)	1 JUN 1988	10	USASAT-13G	USA	14.0-14.5/ or	10.9-11.2 12.5-12.7	FSS	AR11/A/155/1635	AR11/C/756/1676
317.0 E (43.0 W)	10 JUN 1994	15	PANAMSAT II PAS 2 USASAT-25C USASAT-26C	USA Pan American Satellite	5.9-6.4/ 14.0-14.5/ or or or	3.7-4.2 10.9-11.2 11.4-11.7 11.7-12.2 12.5-12.7	FSS	AR11/A/557/1911 AR11/A/565/1911	AR11/C/1826/1966 AR11/C/1834/1967
317.5 E (42.5 W)	30 NOV 1986	15	USGCSS PH3 MID-ATL USGCSS PH3B MID-ATL	USA	1.8 / 7.9-8.4/	2.2 7.2-7.7	FSS MSS	AR11/A/140/1622 AR11/A/716/1986	—
317.5 E (42.5 W)	19 DEC 1998	15	USGCSS PH4 ATL3	USA	1.8 / 43.5-45.5/	2.2 20.2-21.2	FSS MSS	AR11/A/550/1907	AR11/C/1921/1980 AR11/C/1925/1980
319.0 E (41.0 W)	20 MAY 1994	15	USASAT-25B	USA	5.9-6.4/	3.7-4.2	FSS	AR11/A/556/1911	AR11/C/1825/1966
319.0 E (41.0 W)	20 MAY 1994	15	USASAT-26B	USA	14.0-14.5/ or or or	10.9-11.2 11.4-11.7 11.7-12.2 12.5-12.7	FSS	AR11/A/564/1911	AR11/C/1833/1967
319.5 E (40.5 W)	10 MAY 1994	20	INTELSAT7 319.5E	USA Intelsat	5.9-6.4/ 14.0-14.5/ or or or	3.7-4.2 10.9-11.2 11.4-11.7 11.7-11.9 12.5-12.7	FSS	AR11/A/584/1916	AR11/C/1884/1976
321.0 E (39.0 W)	19 DEC 1998	15	USGCSS PH4 ATL2	USA	1.8 / 43.5-45.5/	2.2 20.2-21.2	FSS MSS	AR11/A/549/1907	AR11/C/1915/1980 AR11/C/1919/1980
322.5 E (37.5 W)	31 DEC 1987	10	VIDEOSAT-2	FRANCE	2.0 / 14.0-14.2/ or	2.2 11.7-11.9 12.5-12.7	FSS	AR11/A/86/1598	AR11/C/575/1650 AR11/C/727/1673
322.5 E (37.5 W)	31 DEC 1996	20	EXPRESS 1 EXPRESS-1	USSR	5.7-6.5/ 14.0-14.5/ or	3.4-4.2 10.9-11.2 11.4-11.7	FSS	AR11/A/757/2003	—
322.5 E (37.5 W)	31 DEC 1989	20	RADUGA STATSIONAR-25	USSR	5.7-6.2/	3.4-3.9	FSS	AR11/A/384/1797	AR11/C/1311/1836

TABLE 2. PLANNED GEOSTATIONARY COMMUNICATIONS SATELLITES FOR YEAR-END 1992 (CONT'D)

SUBSATELLITE REGISTERED LONGITUDE (°)	PLANNED IN-USE DATE	PERIOD OF VALIDITY (yrs)	SATELLITE DESIGNATION	ITU REGISTERING COUNTRY	FREQUENCY UP/DOWNLINK (GHz)		SERVICE TYPE	ITU SPECIAL SECTION	
								ADVANCED	COORDINATION
322.5E (37.5 W)	1 MAY 1993	10	USASAT-13A <i>ORION-1</i>	USA Orion Satellite	14.0-14.5/ or 11.4-11.7 or 11.7-12.2 or 12.5-12.7	10.9-11.2	FSS	AR11/A/132/1618	AR11/C/746/1675 AR11/C/1711/1939
322.5 E (37.5 W)	20 MAY 1994	15	USASAT-25A	USA	5.9-6.4/	3.7-4.2	FSS	AR11/A/555/1911	AR11/C/1824/1966
322.5 E (37.5 W)	20 MAY 1994	15	USASAT-26A	USA	14.0-14.5/ or 11.4-11.7 or 11.7-12.2 or 12.5-12.7	10.9-11.2	FSS	AR11/A/563/1911	AR11/C/1832/1967
325.0 E (35.0 W)	19 DEC 1998	15	USGCSS PH4 ATL1	USA	1.8 / 43.5-45.5/	2.2 20.2-21.2	FSS MSS	AR11/A/548/1907	AR11/C/1909/1980 AR11/C/1913/1980
327.0 E (33.0 W)	1 JAN 1994	20	SKYNET-4I	UK	43.5-45.5/	20.2-21.2	FSS MSS	AR11/A/694/1972	—
328.0 E (32.0 W)	1 APR 1996	15	EDRSS-WC	FRANCE ESA	2.0-2.1/ 27.5-30.0/	2.2-2.3 18.1-20.2	FSS	AR11/A/632/1935	—
328.0 E (32.0 W)	31 JUL 1995	20	INMARSAT3 AOR- CENTRAL-2A	UK Inmarsat	1.6 / 6.2 / 6.4 /	1.5 3.9 3.6	FSS MSS	AR11/A/596/1920	AR11/C/1981/1989
329.0 E (31.0 W)	31 MAR 1990	15	EIRESAT-1	IRELAND Atlantic Satellites	12.7-13.2/	10.7-11.2	BSS	AR11/A/182/1656	AR11/C/1349/1850
329.0 E (31.0 W)	1 MAR 1996	20	INTELSAT 7 F5 INTELSAT7 329.0E	USA Intelsat	5.9-6.4/ 14.0-14.5/ or 11.4-11.7 or 11.7-11.9 or 12.5-12.7	3.7-4.2 10.9-11.2	FSS	AR11/A/585/1916	AR11/C/1886/1976
333.5 E (26.5 W)	31 DEC 1987	20	STATSIONAR-17	USSR	5.7-6.3/	3.4-4.0	FSS	AR11/A/219/1686	AR11/C/910/1749

333.5 E (26.5 W)	30 JUN 1988	20	STATSIONAR-D1	USSR	6.4-6.7/	4.5-4.8	FSS	AR11/A/193/1675	AR11/C/1168/1796
333.5 E (26.5 W)	1 AUG 1990	20	TOR-1	USSR	42.5-43.5/ 43.5-45.5/	18.2-20.2 20.2-21.2	FSS MSS	AR11/A/278/1710	AR11/C/1295/1832
333.5 E (26.5 W)	31 DEC 1987	20	VOLNA-13	USSR	1.6 / .27-.28/ .34-.40/	1.5 .24-.29 31-.32	MSS	AR11/A/240/1693	AR11/C/980/1769
335.0 E (25.0 W)	1 AUG 1990	20	TOR-9	USSR	42.5-43.5/ 43.5-45.5/	18.2-20.2 20.2-21.2	FSS MSS	AR11/A/289/1711	AR11/C/1440/1872
335.0 E (25.0 W)	1 MAR 1991	20	VOLNA-1A VOLNA-1M	USSR	1.6 / .27-.28/ .34-.40/	1.5 .24-.29 .31-.32	MSS	AR11/A/291/1712 AR11/A/248/1697	AR11/C/1262/1819 AR11/C/1396/1861
335.6 E (24.4 W)	31 AUG 1987	10	GDL-5	LUXEMBOURG	12.7-13.2/	10.7-11.2	BSS	AR11/A/93/1594	AR11/C/612/1657
337.5 E (22.5 W)	30 NOV 1992	20	FLTSATCOM-C E ATL1	USA	29-.32/ 1.8 / 7.9-8.0/ 43.5-45.5/	.24-.27 2.2 7.2-7.3 20.2-21.2	FSS MSS	AR11/A/695/1973	—
338.5 E (21.5 W)	1 MAR 1996	20	INTELSAT7 338.5E	USA Intelsat	5.9-6.4/ 14.0-14.5/ or 11.4-11.7 or 11.7-11.9 or 12.5-12.7	3.7-4.2 10.9-11.2	FSS	AR11/A/582/1914	AR11/C/1889/1977
340.0 E (20.0 W)	31 JAN 1989	25	GDL-4	LUXEMBOURG	12.7-13.2/	10.7-11.2	BSS	AR11/A/92/1594	AR11/C/610/1657
341.0 E (19.0 W)	31 MAR 1991	7	SARIT	ITALY	12.7-13.2/ 29.5-30.0/ 2.0-2.1/	19.7-20.2 19.7-20.2 2.2-2.3	BSS FSS	SPA-AA/371/1457 AR11/A/294/1716	AR11/C/1334/1839
342.0 E (18.0 W)	1 JAN 1995	20	INTELSAT 7A F7 INTELSAT7 342E	USA Intelsat	5.9-6.4/ 14.0-14.5/ or 11.4-11.7 or 11.7-11.9 or 12.5-12.7	3.7-4.2 10.9-11.2	FSS	AR11/A/533/1898	AR11/C/1890/1977

TABLE 2. PLANNED GEOSTATIONARY COMMUNICATIONS SATELLITES FOR YEAR-END 1992 (CONT'D)

SUBSATELLITE REGISTERED LONGITUDE (°)	PLANNED IN-USE DATE	PERIOD OF VALIDITY (yrs)	SATELLITE DESIGNATION	ITU REGISTERING COUNTRY	FREQUENCY UP/DOWNLINK (GHz)	SERVICE TYPE	ITU SPECIAL SECTION		
							ADVANCED	COORDINATION	
342.2 E (17.8 W)	1 SEP 1990	20	SATCOM-4	BELGIUM NATO	.29-.31/ 7.9-8.0/ 43.5-45.5/	.24-.27 7.2-7.7 7.2-7.7	FSS MSS	AR11/A/342/1762	AR11/C/1288/1832
343.0 E (15.0 W)	1 APR 1996	20	INMARSAT3 AOR-EAST-2	UK Inmarsat	1.6 / 6.2 / 6.4 /	1.5 3.9 3.6	FSS MSS	AR11/A/788/2011	AR11/C/2220/2043
344.0 E (16.0 W)	1 AUG 1992	20	ZSSRD-2	USSR	14.6 / 15.0 /	11.2 12.6 13.5	FSS	AR11/A/189/1672	AR11/C/880/1740
344.0 E (16.0 W)	1 AUG 1990	20	MILSTAR-3	USA	.29-.32/ 1.8 / 43.5-45.5/	.24-.27 2.2 20.2-21.2	MSS	AR11/A/444/1837	AR11/C/1509/1885 AR11/C/1648/1919
344.5 E (15.5 W)	31 JUL 1994	20	INMARSAT3 AOR-EAST	UK Inmarsat	1.6 / 6.2 / 6.4 /	1.5 3.9 3.6	FSS MSS	AR11/A/593/1920	AR11/C/1976/1989
344.5 E (55.0 W)	1 JAN 1998	20	INMARSAT4 GSO-1C	UK Inmarsat	1.6 / 6.4-6.6/	2.5 3.6-3.8	FSS MSS	AR11/A/823/2032	—
344.5 E	1 JAN 1998	20	INMARSAT4 GSO-2C	UK Inmarsat	1.9 / 6.4-6.7/	2.2 3.6-3.9	FSS MSS	AR11/A/830/2032	—
345.0 E (15.0 W)	30 NOV 1992	20	FLTSATCOM-C E ATL2	USA	.29-.32/ 1.8 / 7.9-8.0/ 43.5-45.5/	.24-.27 2.2 7.2-7.3 20.2-21.2	FSS MSS	AR11/A/696/1973	—
346.0 E (14.0 W)	31 DEC 1995	20	EXPRESS 2 EXPRESS-2	USSR	5.7-6.5/ 14.0-14.5/	3.4-4.2 10.9-11.2 11.4-11.7	FSS	AR11/A/758/2003	—
346.0 E (14.0 W)	1 SEP 1990	15	MORE-14	USSR	1.6 / 6.0-6.1/	1.5 3.7-3.8	FSS MSS	AR11/A/183/1662	AR11/C/1086/1791
346.5 E (13.5 W)	1 JUN 1990	10	FOTON-1	USSR	6.5-6.6/	4.6-4.7	FSS	AR11/A/235/1692	—
348.0 E (12.0 W)	31 MAR 1996	15	USGCSS PH3 ATL USGCSS PH3B ATL	USA	1.8 / 7.9-8.4/	2.2 7.2-7.7	FSS MSS	SPA-AA/250/1413 SPA-AA/351/1493 AR11/A/666/1960	SPA-AJ/287/1451 AR11/C/403/1629
348.0 E (12.0 W)	30 NOV 1996	15	USGCSS PH4 ATL-4	USA	1.8 / 43.5-45.5/	2.2 20.2-21.2	FSS MSS	AR11/A/721/1986	—
349.0 E (11.0 W)	31 DEC 1987	10	F-SAT 2	FRANCE	2.0-2.1/ 5.9-6.4/ 29.5-30.0/	2.2-2.3 3.7-4.1 19.7-20.1	FSS	AR11/A/73/1586	AR11/C/466/1647
349.0 E (11.0 W)	31 DEC 1995	20	EXPRESS 3 EXPRESS-3	USSR	5.7-6.5/ 14.0-14.5/	3.4-4.2 10.9-11.2 11.4-11.7	FSS	AR11/A/759/2003	—
349.0 E (11.0 W)	1 AUG 1992	—	VOLNA-11W	USSR	1.6 / 6.1 /	1.5 3.8	FSS MSS	AR11/A/815/2029	—
351.0 E (9.0 W)	1 JUL 1990	20	MILSTAR-2	USA	.29-.32/ 1.8 / 43.5-45.5/	.24-.27 2.2 20.2-21.2	MSS	AR11/A/443/1837	AR11/C/1505/1885 AR11/C/1647/1919
352.0 E (8.0 W)	1 JAN 1998	—	VIDEOSAT-6	FRANCE	2.0-2.1/ 14.0-14.5/	2.2-2.3 10.9-11.2 12.5-12.7	FSS	AR11/A/874/2055	—
352.0 E (8.0 W)	30 APR 1992	10	ZENON-A	FRANCE	2.0 / 1.6-1.7/ 6.4-6.5/	2.2 1.5-1.6 3.6-3.7	FSS MSS	AR11/A/363/1781	—
353.0 E (7.0 W)	25 OCT 1996	10	VIDEOSAT-5	FRANCE	2.0-2.1/ 14.0-14.5/	2.2-2.3 10.9-11.2 11.4-11.7 12.5-12.7	FSS	AR11/A/709/1978	AR11/C/2033/2002
355.0 E (8.0 W)	1 JAN 1998	—	VIDEOSAT-7	FRANCE	2.0-2.1/ 14.0-14.5/	2.2-2.3 10.9-11.2 12.5-12.7	FSS	AR11/A/875/2055	—
356.0 E (4.0 W)	30 DEC 1996	—	AMOS 1-B	ISRAEL	14.0-14.5/	10.9-11.2 11.4-11.7	FSS	AR11/A/804/2019	—

TABLE 2. PLANNED GEOSTATIONARY COMMUNICATIONS SATELLITES FOR YEAR-END 1992 (CONT'D)

SUBSATELLITE REGISTERED LONGITUDE (°)	PLANNED IN-USE DATE	PERIOD OF VALIDITY (yrs)	SATELLITE DESIGNATION	ITU REGISTERING COUNTRY	FREQUENCY UP/DOWNLINK (GHz)	SERVICF. TYPE	ITU SPECIAL SECTION	
							ADVANCED	COORDINATION
357.0 E (3.0 W)	31 DEC 1990	20	TOR-11	USSR	42.5-43.5/ 43.5-45.5/	FSS	AR11/A/308/1736	AR11/C/1408/1862
359.0 E (1.0 W)	1 JAN 1994	20	SKYNET-4F	UK	43.5-45.5/	FSS	AR11/A/691/1972	—
359.0 E (1.0 W)	1 JUN 1995	20	INTELSAT 7 F2 INTELSAT 7 359E	USA inelsat	5.9-6.4/ 14.0-14.5/ or or or	FSS	AR11/A/534/1898	AR11/C/1891/1977
					3.7-4.2 10.9-11.2 11.4-11.7 11.7-11.9 12.5-12.7			

Translations of Abstracts

Architectures des systèmes de télécommunications INTELSAT à l'ère du RNIS

D. M. CHITRE ET W. S. OEI

Sommaire

Cet article présente une série d'architectures pour le système de satellites INTELSAT en vue de l'utilisation du réseau numérique avec intégration des services (RNIS) à large bande et à bande étroite. Ces architectures marquent une évolution du système INTELSAT depuis le rôle traditionnel qui est celui d'un support de transmission physique jusqu'aux fonctions plus complexes de commutation et de signalisation dans le cadre du RNIS. En utilisant l'information contenue dans les messages de signalisation du RNIS et en accomplissant certaines fonctions d'un niveau supérieur au sein du système à satellites en tant que sous-réseau, on peut exploiter les technologies adaptées aux besoins du système et les points forts inhérents pour améliorer le soutien fonctionnel du réseau. Il est en outre possible d'éliminer des insuffisances éventuelles dues au temps de propagation. Pour le RNIS à large bande (RNIS-LB), l'article décrit un trajet de migration distinct parfaitement adapté aux technologies de transmission du réseau optique synchrone et de la hiérarchie numérique synchrone. Cette approche peut éventuellement conduire au traitement à bord des fonctions du RNIS-LB en mode de transfert asynchrone.

Conception et homologation du simulateur de vol de l'AOCS ITALSAT

A. RAMOS, R. L. MINCIOTTI, T. HAMPSCH, G. ALLISON,
E. W. HARE ET J. W. OPIEKUN

Sommaire

Un simulateur du sous-système de commande d'orientation et d'orbite (AOCS) du satellite ITALSAT a été mis au point pour l'Agence spatiale italienne. Ce dispositif, qui fonctionne en temps réel et en boucle, est connu sous le nom de "simulateur de vol de l'AOCS ITALSAT (IAFSIM)." L'Article fait le point sur la conception, l'homologation et les applications de l'IAFSIM, et cite des exemples d'essais d'homologation des modes d'utilisation de l'AOCS au cours des diverses phases de la mission ITALSAT. Des applications futures de l'IAFSIM sont également examinées.

(MPCP) proporciona componentes modulares de software que han sido desarrollados y probados para programar mediciones, interprocesar comunicaciones y compartir recursos e información sobre sistemas. Sus bibliotecas de códigos respaldan interfaces gráficas para el usuario, control de instrumentos, gestión de barra colectora de instrumentos de medición, así como detección y notificación de errores. Sus subsistemas de procesamiento de datos respaldan la gestión de bases de datos, la producción de informes y el análisis interactivo de datos.

Al trabajar en red con el sistema operativo V de UNIX, el software MMS para múltiples usuarios y tareas respalda el funcionamiento en red de zona local o extenso, incluyendo el acceso y control a distancia del equipo de mediciones para pruebas en órbita. Se pone en práctica por medio de una arquitectura de sistema de procesamiento distribuido entre varias estaciones de trabajo diferentes. Con las comunicaciones entre procesos y máquinas que proporciona el sistema de correo MPCP, la interfaz con el usuario y los programas de mediciones separados se pueden ejecutar en máquinas diferentes en momentos distintos, ofreciendo más flexibilidad a las operaciones.

En este artículo se describe el diseño y la implementación del software MMS. Los conceptos y métodos presentados también se pueden aplicar a otros sistemas de mediciones (tales como los utilizados para el monitoreo del sistema de comunicaciones) en los que hay que poner coto al creciente costo del software.

Author Index, CTR 1992

The following is a list of articles that appeared in *COMSAT Technical Review* for 1992. The list is cross-referenced based on COMSAT authors (only). The code number at the end of each entry should be used when ordering reprints from Corporate Records, COMSAT Corporation, 22300 COMSAT Drive, Clarksburg, MD 20871-9475.

- ARNSTEIN, D. S., X. T. Vuong, C. B. Cotner, and H. M. Daryanani. "The IM Microscope: A New Approach to Nonlinear Analysis of Signals in Satellite Communications Systems," *COMSAT Technical Review*, Vol. 22, No. 1, Spring 1992, pp. 93-123 [CTR92/382].
- BEDFORD, R.,** A. Berntzen,** J. A. Lunsford, Y. Ishi,* H. Nakamura,* and T. Kimura,* "The INTELSAT SSTDMA Reference and Monitoring Station," *COMSAT Technical Review*, Vol. 22, No. 2, Fall 1992, pp. 281-325 [CTR92/386].
- BENNETT, S. B.,** "INTELSAT 603 'Reboosted' to Synchronous Orbit," *COMSAT Technical Review*, Vol. 22, No. 1, Spring 1992, pp. 73-91 [CTR92/381].
- BROWN, M. P., Jr.,** F. A. S. Loureiro,** and M. Stojkovic,** "Earth Station Considerations for INTELSAT VI," *COMSAT Technical Review*, Vol. 22, No. 1, Spring 1992, pp. 5-17 [CTR92/378].
- COTNER, C. B., see Arnstein, D. S.
- DARYANANI, H. M., see Arnstein, D. S.
- DIMOLITSAS, S., J. H. Rieser, and H. Feldman,* "Real-Time Transmission of Group 3 Facsimile Over Interconnected Public Switched Digital Mobile Satellite Networks," *COMSAT Technical Review*, Vol. 22, No. 1, Spring 1992, pp. 125-147 [CTR92/383].
- FARIS, F. R., see Poklemba, J. J.
- GUPTA, R. K., see Tamboli, S. P.
- INUKAI, T., see Maranon, C. L.
- KULLMAN, C. L.,** S. J. Smith,** K. P. Chaudhry,** R. Bedford,** P. W. Roach,** P. Nethersole,* and G. J. Burns,* "Deployment, Test, and Transition to Operation of the INTELSAT SSTDMA System," *COMSAT Technical Review*, Vol. 22, No. 2, Fall 1992, pp. 523-548 [CTR92/392].
- LEE, I.-N., and A. K. Sinha,** "Video Transmission and Processing in the INTELSAT VI Era," *COMSAT Technical Review*, Vol. 22, No. 1, Spring 1992, pp. 57-71 [CTR92/380].
- LUNSFORD, J. A., J. F. Phiel,** R. Bedford,** and S. P. Tamboli,** "The INTELSAT SSTDMA System Design," *COMSAT Technical Review*, Vol. 22, No. 2, Fall 1992, pp. 227-279 [CTR92/385].
- LUNSFORD, J. A., see Bedford, R.; Maranon, C. L.; and Mizuike, T.

* Non-COMSAT author.

** INTELSAT author.

- LUZ, F. H.,** D. Sinkfield,** and N. Engelberg,* "The INTELSAT SSTDMA Headquarters Subsystem." *COMSAT Technical Review*, Vol. 22, No. 2, Fall 1992, pp. 367-407 [CTR92/388].
- MARANON, C. L.,** J. A. Lunsford, T. Inukai, and F. H. Luz,** "INTELSAT VI SSTDMA Subsystem Timing Source Oscillator Control," *COMSAT Technical Review*, Vol. 22, No. 2, Fall 1992, pp. 409-446 [CTR92/389].
- MIZUIKE, T.,* L. N. Nguyen,** K. P. Chaudhry,** J. A. Lunsford, and P. A. Trusty, "Generation of Burst Time Plans for the INTELSAT VI SSTDMA System," *COMSAT Technical Review*, Vol. 22, No. 2, Fall 1992, pp. 327-366 [CTR92/387].
- ONUFRY, M., G-P. Forcina,** W. S. Oei,** T. Oishi,** J. F. Phiel,** and J. H. Rieser, "DCME in the INTELSAT VI Era." *COMSAT Technical Review*, Vol. 22, No. 1, Spring 1992, pp. 19-55 [CTR92/379].
- PETTERSSON, B. A.,** A. K. Kwan,** S. B. Sanders,** F. L. Khoo,** and T. J. Duffy,** "The Satellite Control Center and its Role in Testing and Operation of the INTELSAT VI SSTDMA System," *COMSAT Technical Review*, Vol. 22, No. 2, Fall 1992, pp. 485-522 [CTR92/391].
- POKLEMBIA, J. J., and F. R. Faris, "A Digitally Implemented Modem: Theory and Emulation Results," *COMSAT Technical Review*, Vol. 22, No. 1, Spring 1992, pp. 149-195 [CTR92/384].
- RIESER, J. H., see Dimolitsas, S.; and Onufry, M.
- TAMBOLI, S. P.,** X. Zhu,** K. N. Wilkins,** and R. K. Gupta, "The INTELSAT VI SSTDMA Network Diagnostic System," *COMSAT Technical Review*, Vol. 22, No. 2, Fall 1992, pp. 447-483 [CTR92/390].
- TRUSTY, P. A., see Mizuike, T.
- VUONG, X. T., see Arnstein, D. S.

* Non-COMSAT author.

** INTELSAT author.

Index of 1992 Publications by COMSAT Authors

The following is a list of 1992 publications by authors at COMSAT Corporation. The list is cross-referenced based on COMSAT authors (only). Copies of these publications may be obtained by contacting the COMSAT authors at COMSAT Corporation, 22300 COMSAT Drive, Clarksburg, MD 20871-9475.

- AGARWAL, A., see White, L.
- ARNSTEIN, D. S., and J. W. Lee,* "AJ Performance of Smart AGC"™ in MILSATCOM Networks: A Review of Space System Design Principles and Applications," AIAA 14th International Communication Satellite Systems Conference, Washington, DC, March 1992, Session 2, *A Collection of Technical Papers*, Pt. 1, pp. 23-31. AIAA Paper No. 92-1806-CP.
- ARNSTEIN, D., C. Pike,** and G. Estep, "On-Board AJ Enhancement Using Adaptive Nonlinear Processing: Practical Aspects of Smart AGC Implementation," IEEE Military Communications Conference (MILCOM), San Diego, CA, October 1992, *Sec. 7, Conf. Rec.*, pp. 7.5.1-7.5.7.
- ASSAL, F. T., see Gupta, R. K. (two papers); Sorbello, R. M. (three papers); Zaghoul, A. I.; and Mott, R.
- ATIA, A., see Haggag, M.
- ATKIN, G. E.,** and Khalona, R. A., "Steiner System Signal Sets Over the Gaussian Channel," *IEEE Transactions on Information Theory*, Vol. 38, No. 2, March 1992, pp. 469-472.
- BAZ, A., see Haggag, M.
- BHARGAVA, S., see Lee, L-N.
- BHASIN, K. B.,* S. S. Toncich,* C. M. Chorey,* R. R. Bonetti, and A. E. Williams, "Performance of a Y-Ba-Cu-O Superconducting Filter/GaAs Low Noise Amplifier Hybrid Circuit," IEEE MTT-S International Microwave Symposium, Albuquerque, NM, June 1992, *Digest*, Vol. 1, pp. 481-483.
- BHASKAR, B. R. U., "Low Rate Coding of Audio by a Predictive Transform Coder for Efficient Satellite Transmission," AIAA 14th International Communication Satellite Systems Conference, Washington, DC, March 1992, *A Collection of Technical Papers*, Pt. 3, pp. 1400-1410. AIAA Paper No. 92-1994-CP.
- BOHEIM, K. B.,* and R. J. Council, "National Transportable Telecommunications Capability: Commercial Satellite and Cellular Communications for Emergency Preparedness," AIAA 14th International Communication Satellite Systems Conference, Washington, DC, March 1992, *A Collection of Technical Papers*, Pt. 1, pp. 349-352. AIAA Paper No. 92-1848-CP.

* Non-COMSAT author.

** INTELSAT author.